



LUND UNIVERSITY

Evaluation of new active technology for low-energy houses

Davidsson, Henrik

2014

[Link to publication](#)

Citation for published version (APA):

Davidsson, H. (2014). *Evaluation of new active technology for low-energy houses*. [Doctoral Thesis (compilation), Division of Energy and Building Design]. Energy and Building Design, Lund University.

Total number of authors:

1

General rights

Unless other specific re-use rights are stated the following general rights apply:

Copyright and moral rights for the publications made accessible in the public portal are retained by the authors and/or other copyright owners and it is a condition of accessing publications that users recognise and abide by the legal requirements associated with these rights.

- Users may download and print one copy of any publication from the public portal for the purpose of private study or research.
- You may not further distribute the material or use it for any profit-making activity or commercial gain
- You may freely distribute the URL identifying the publication in the public portal

Read more about Creative commons licenses: <https://creativecommons.org/licenses/>

Take down policy

If you believe that this document breaches copyright please contact us providing details, and we will remove access to the work immediately and investigate your claim.

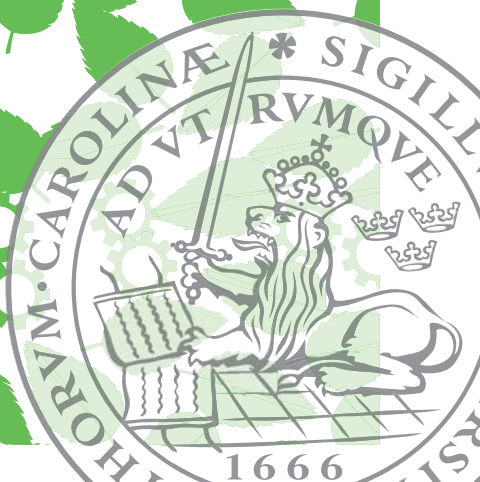
LUND UNIVERSITY

PO Box 117
221 00 Lund
+46 46-222 00 00



Evaluation of new active technology for low-energy houses

Henrik Davidsson | Division of Energy and Building Design | Department of Architecture and
Built Environment | Lund University | Faculty of Engineering LTH, 2014



Lund University

Lund University, with eight faculties and a number of research centres and specialized institutes, is the largest establishment for research and higher education in Scandinavia. The main part of the University is situated in the small city of Lund which has about 112 000 inhabitants. A number of departments for research and education are, however, located in Malmö. Lund University was founded in 1666 and has today a total staff of 6 000 employees and 47 000 students attending 280 degree programmes and 2 300 subject courses offered by 63 departments.

Division of Energy and Building Design

Reducing environmental effects of construction and facility management is a central aim of society. Minimising the energy use is an important aspect of this aim. The recently established division of Energy and Building Design belongs to the department of Architecture and Built Environment at the Lund University, Faculty of Engineering LTH in Sweden. The division has a focus on research in the fields of energy use, passive and active solar design, daylight utilisation and shading of buildings. Effects and requirements of occupants on thermal and visual comfort are an essential part of this work. Energy and Building Design also develops guidelines and methods for the planning process.

Evaluation of new active technology for low-energy houses

Henrik Davidsson

Doctoral Thesis

Keywords

Low-quality heat, hybrid ventilation, heat recovery, active house, solar window, PV/T hybrid, building integration, TRNSYS.

© copyright Henrik Davidsson and Division of Energy and Building Design.
Lund University, Faculty of Engineering, Lund 2014.
The English language corrected by Leslie Walke, CommunicAID.
Layout: Hans Follin, LTH, Lund.
Cover: Henrik Davidsson

Printed by E-huset Tryckeri, Lund 2014

Report No EBD-T--14/18
Evaluation of new active technology for low-energy houses.
Department of Architecture and Built Environment, Division of Energy and Building Design,
Lund University, Lund

ISSN 1651-8136
ISBN 978-91-85147-56-4

Lund University, Faculty of Engineering
Department of Architecture and Built Environment
Division of Energy and Building Design
P.O. Box 118
SE-221 00 LUND
Sweden

Telephone: +46 46 - 222 73 52
Telefax: +46 46 - 222 47 19
E-mail: ebd@ebd.lth.se
Home page: www.ebd.lth.se

Abstract

Using energy at low-quality levels opens up new possibilities for low-energy houses. Low-quality energy can be heat at a temperature that is close to that of its surrounding, and can be used, for example, to pre-heat ventilation air or domestic hot water. Pre-heating the incoming outdoor air reduces the need to heat ventilation and reduces the need for high-quality energy such as electricity or heat from a fire.

This thesis investigates two such possible energy utilizations, the PV/T solar window and the hybrid ventilation system. They are very different in how they reduce the need for auxiliary energy in buildings, and they cover different fields of low-energy building technique. However, what they have in common is the concept of low-quality energy. The solar window produces both electricity and hot water. What the photovoltaic cells cannot utilize at the high-quality energy level is instead used to produce hot water. The hybrid ventilation system pre-heats the incoming ventilation air in the heat recovery system, thereby lowering the need for high-quality energy.

The PV/T solar window comprises PV cells laminated on solar absorbers placed in a window behind the glazing. To reduce the costs of solar electricity, tiltable reflectors were included in the design to concentrate solar radiation onto the solar cells. The reflectors enable control of the amount of solar radiation transmitted into the building. The insulated reflectors also reduce thermal losses through the window. The effects on the light distribution and the architectural implications are discussed in earlier studies (Fieber, 2005; Fieber et al., 2003; Fieber, Nilsson, & Karlsson, 2004) together with effects on the building when different strategies for controlling the reflectors are used.

Long-term measurements were taken of the thermal- and electrical energy output from the solar window. A model was developed to simulate the electricity and hot water production, and the model was calibrated against the measured values from a prototype solar window installed in a laboratory and against a solar window built into a single-family building.

The results from the simulation showed that the solar window produces about 35% more electrical energy per unit cell area than a vertical flat

PV module. However, PV cells placed on the roof of the building would produce approximately 17% more electricity per unit cell area than the solar window. The simulations carried out on system level showed that installing a 16 m² solar window (glazed area) in a single-family building reduces the annual heating need by approximately 600 kWh. However, if the absorbers (5.06 m²) and PV cells (4 m²) from the solar window are installed separately on the roof instead of in the window, the annual heating need is reduced by a further 1100 kWh.

A water-to-air heat exchanger was developed for use in naturally ventilated buildings. This requires that the pressure drop of the air is kept close to zero. The heat exchanger comprises solar collector absorbers soldered onto a manifold. Basic heat transfer equations were used in order to optimize the dimensions of the heat exchanger in terms of heat transfer and pressure drop.

A laboratory measurement showed the temperature heat recovery rate to be 80% at component level. At the same time the pressure drop was 1 Pa for the designed air flow rate.

System simulations were then carried out in order to investigate the impact for a building equipped with natural/hybrid ventilation with heat recovery. A brine-based heat recovery system enables the utilization of other energy sources such as ground collectors or waste water heat recovery units. A waste water heat recovery system was built into a single-family house, and was designed to supply energy to both domestic hot water and the ventilation system. The simulations showed that a typical single-family house can reduce the heating need by approximately 600-800 kWh annually, i.e. roughly 25% of the annual need for hot water, with waste water heat recovery. The simulations showed that using ground collectors for the ventilation system has limited effects on the heating need, so the main benefit is limited to lowering the risk of frost on the heat exchanger surface.

The overall conclusion from an energy perspective is that the solar window performs poorly compared to standard solar energy components. The hybrid ventilation system with the developed heat exchangers has the potential to be an interesting ventilation system when building low-energy houses or when renovating residential buildings to improve energy efficiency.

Contents

Keywords	2
Abstract	3
Contents	5
Nomenclature	9
List of papers	15
List of papers not included in the thesis	16
Structure of the thesis and a short summary of the papers included	19
Open-Access Publishing	21
Acknowledgements	23
Prelude	25
1 Introduction	27
1.1 The alternatives	27
1.2 Saving energy	28
1.2.1 Building skin	28
1.2.2 Ventilation heat recovery	29
1.2.3 Ventilation techniques	29
1.2.4 Natural/hybrid ventilation systems in relation to building regulations	35
1.2.5 Waste water heat recovery	38
1.3 Solar energy	39
1.3.1 Solar electricity	41
1.3.2 Solar thermal energy	41
1.3.3 Hybrid solar collector	43
1.3.4 Building integrated solar energy	44
1.4 Energy as a system, feedback mechanisms, energy flows	45
1.5 Low-quality energy	46
1.6 Solgården	47
1.7 Objectives	49
1.8 Method	50
1.9 Limitations	51
2 TRNSYS	53
3 The solar window	57
3.1 Background	57

3.2	Installations	61
3.3	Measurements	63
3.4	Calculation model	64
3.5	The parameters	67
3.5.1	Radiation, angles, θ	67
3.5.2	Transmission through the glazing, T_{glass}	68
3.5.3	Angular dependence of PV cell, α_{pv}	69
3.5.4	Shading, f_s	70
3.5.5	Reflector contribution, f_{ref}	71
3.5.6	Diffuse solar radiation, C	74
3.5.7	Thermal losses, U	76
3.5.8	Passive gains	81
3.5.9	Control strategies	84
3.6	TRNSYS, the solar window	85
3.7	Evaluation	88
3.8	Results	90
3.8.1	Prototype solar window	91
3.8.2	Solgård solar window	93
3.8.3	Augustenborg solar window	98
3.9	Development	99
3.9.1	Results	101
3.10	Large solar window	102
3.11	Conclusions and discussion	103
3.12	Further development and future work	106
4	The ventilation project	109
4.1	A ventilation system with heat recovery	110
4.2	Design of the heat exchanger	115
4.2.1	Calculations for the heat exchanger	117
4.2.2	Measurement of the heat exchanger	121
4.3	Results	123
4.4	Parametric study of the heat exchanger	129
4.5	Results, parametric study	131
4.6	Discussion and conclusion of the heat exchanger development and the parametric study	134
4.7	Future work, heat exchanger and ventilation	138
5	Waste water heat recovery	139
5.1	The installed test unit	140
5.2	Results	141
5.3	Conclusions, discussion and future work	142
6	Hybrid ventilation: system analysis	143
6.1	Step 1 - method	143
6.2	Step 1 - results	146
6.3	Step 2 - method	150
6.4	Step 2 - results	151

6.5	Step 3 - method and results	153
6.6	Steps 1, 2, 3 – Conclusion and discussion	154
6.7	Future work	156
7	Conclusion and discussion of the thesis	159
	References	163
	Appendix A	171
	Appendix B	177
	Appendix C	179
	Paper I	181
	Paper II	191
	Paper III	201
	Paper IV	225
	Paper V	241
	Paper VI	255

Nomenclature

Solar Window part:

Latin characters

α	absorber width	m
A_{abs}	thermal absorber area	m ²
A_{cell}	PV cell area	m ²
A_{ref}	reflector area	m ²
A_w	window area	m ²
C_1 - C_2	constants to calculate the el. production due to diffuse solar radiation	-
\dot{C}_1 - \dot{C}_2	constants to calculate the heat production due to diffuse solar radiation	-
F	focal point	-
$Flow$	flow to the collector	l/s
f_{ref}	correction factor for the shadow effects on reflector, electrical	-
f'_{ref}	correction factor for the shadow effects on reflector, thermal	-
f_s	shading of the PV cells	-
f'_s	shading of the thermal absorber	-
G	global solar radiation	W/m ²
$G_{b,n}$	beam solar radiation	W/m ²
G_d	diffuse solar radiation	W/m ²
H	height of glazing	m
h	heat losses, total, per glazed area	W/m ² K
h_c	heat losses due to convection	W/m ² K
h_r	heat losses due to radiation	W/m ² K
h_{tot}	heat losses, total, per absorber area	W/m ² K
$m_{c1,c2}$	heat resistance, convection	m ² K/W
m_g	heat resistance, glazing	m ² K/W
m_r	heat resistance, radiation	m ² K/W
m_{tot}	heat resistance, total	m ² K/W
p	focal length	m

P_D	passive gain due to direct solar radiation	W
P_d	passive gain due to diffuse solar radiation	W
P_g	passive gains, total	W
P_t	passive gain due to thermal losses in the absorber	W
P_{diff}	delivered electrical power from diffuse solar radiation	W
P_{dir}	delivered electrical power from direct solar radiation	W
P_{ref}	delivered electrical power from solar radiation via the reflector	W
P_{tot}	total delivered electrical power	W
q	thermal losses	W/m ²
Q_{NS}	angle glazing-projected solar radiation	°
$q_{loss,p}$	thermal losses for the prototype solar window	W/m ² K
$q_{loss,s}$	thermal losses for the Solgård solar window	W/m ² K
Q_{diff}	delivered heat rate from diffuse solar radiation	W
Q_{dir}	delivered heat rate from direct solar radiation	W
Q_{ref}	delivered heat rate from solar radiation via the reflector	W
Q_{tot}	total delivered heat rate	W
r	length	m
R_{ref}	reflectance	-
T_{glass}	transmittance through the glazing	-
T	temperature	K
T_c	temperature, cold	K
T_h	temperature, hot	K
T_m	temperature, mean	K
T_{in}	temperature into collector / heat exchanger	K
T_{out}	temperature out of collector	K
U_p	U -value for the prototype solar window	W/m ² K
$U_{s,out}$	U -value to the outside for the Solgård solar window	W/m ² K
$U_{s,in}$	U -value to the inside for the Solgård solar window	W/m ² K
u	absorber tilt	°
v	optical axis	°
w	angle glazing-absorber plane	°
X	distance	m

Greek characters

α	solar azimuth	°
α_{pv}	angular dependence of the absorbance of the PV	-
γ	solar azimuth	°
ΔT	temperature difference, absorber temperature – ambient temperature	K
ΔT_{in}	temperature difference, absorber temperature – indoor temperature	K
ΔT_{out}	temperature difference, absorber temperature – ambient temperature	K
ε_{eff}	effective emissivity	-
η_{abs}	absorber absorbance	-
η_{pv}	efficiency of PV cell	-
$\theta_1 - \theta_5$	incidence angles	°
θ_z	zenith angle	°
σ	Stefan-Boltzmann constant	W/m ² K ⁴
φ	angle	°

Ventilation part:

Latin characters

A	area	m ²
\hat{C}	heat capacity flow	J/K
C_1	calibration constant	-
C_2	calibration constant	-
C'_1	calibration constant	-
c_p	heat capacity	J/kg/K
d	distance between fins	m
D	diameter	m
D_h	hydraulic diameter	m
f	flow	m ³ /s
f'	friction factor	-
g	gravitational acceleration	m/s ²
Gz	Graetz number	-
h'	height difference	m
l	length	m
Nu_D	Nusselt number	-
P	power	W
Pr	Prandtl number	-
R	resistance	mK/W

Re	Reynolds number	-
S	relative cost	-
T	temperature	K
U	U -value	W/m ² K
u_m	average speed	m/s
v	speed	m/s
V	volume	m ³
w	width	m
x	distance	m
ϕ_i	inner diameter of pipe	m
ϕ_o	outer diameter of pipe	m

Greek characters

Δt_m	LMTD, logarithmic mean temperature difference	K
Δp	pressure difference	Pa
η	efficiency	-
μ	form factor	-
ξ	help variable	-
ρ	density	kg/m ³
Ψ	help variable	-

Index

a	air (only used in the appendix due to long equations)
air	air
Al	aluminium
amb	ambient
$bouyancy$	buoyancy
c	cold
$comp$	component
Cu	copper
h	hot
in	in
$indoor$	indoor
out	out
$pipe$	pipe
$room$	room
tot	total
w	water
$wind$	wind

Abbreviations

ach	air changes per hour
EPS	expanded polystyrene
LCC	life-cycle cost

List of papers

Paper 1

Davidsson H., Perers B., & Karlsson B., Performance of a multifunctional PV/T hybrid solar window. *Solar Energy* 84 Issue 3 (2010) pp 365-372. Co-authors assisted with review and discussions.

Paper 2

Davidsson H., Perers B., & Karlsson B., System analysis of a multifunctional PV/T hybrid solar window. *Solar Energy* 86, Issue 3 (2012) pp 903-910. Co-authors assisted with review and discussions. Perers assisted with TRNSYS simulations.

Paper 3

Davidsson H., Bernardo R., & Hellström B., Theoretical and Experimental Investigation of a Heat Exchanger Suitable for a Hybrid Ventilation System. *Buildings* 2013, 3(1), pp 18-38; doi: 10.3390/buildings3010018; Open access. Co-authors assisted with review and discussions. Hellström assisted with heat transfer calculations.

Paper 4

Davidsson H., Bernardo R., & Hellström B., Hybrid Ventilation with Innovative Heat Recovery-A System Analysis. *Buildings* 2013, 3(1), pp 245-257; doi:10.3390/buildings3010245; Open access. Co-authors assisted with review and discussions.

Paper 5

Davidsson H., Bernardo R., & Hellström B., *Parametric Study of a Heat Exchanger for a Hybrid Ventilation System*. Article number 587. Conference proceedings REHVA World Congress CLIMA 2013, Prague, Czech Republic. Co-authors assisted with review and discussions. Hellström assisted with heat transfer calculations.

Paper 6

Davidsson H., Bernardo R., & Larsson S., Design and Performance of a Hybrid Ventilation System with Heat Recovery for Low Energy Buildings. *Journal of Environment and Engineering* 2011 Vol. 6, No. 2, pp 469-477; doi: 10.1299/jee.6.469 Open access.
Co-authors assisted with review and discussions.

List of papers not included in the thesis

Davidsson H., Perers B. & Karlsson B., Performance of a multifunctional PV/T hybrid solar window. Proceedings *EuroSun 2008* Lisbon, article number 364.
Co-authors assisted with language check and discussions.

Bernardo R., Davidsson H., & Karlsson B., Retrofitting Domestic Hot Water Heaters for Solar Water Heating Systems in Single-Family Houses in a Cold Climate: A Theoretical Analysis. *Energies*, 2012, 5(10), pp 4110-4131, doi:10.3390/en5104110 Open access.
Davidsson assisted with TRNSYS discussions.

Bernardo R., Davidsson H., & Karlsson B., Retrofitting Conventional Electric Domestic Hot Water Heaters to Solar Water Heating Systems in Single-Family Houses — Model Validation and Optimization. *Energies* 2013, 6(2), pp 953-972; doi:10.3390/en6020953 Open access.
Davidsson assisted with TRNSYS discussions.

Gentile N., Davidsson H., Bernardo R., Gomes J., Gruffman C., Chea L., Mumba C., & Karlsson B., Construction of a Small Scale Laboratory for Solar Collectors and Solar Cells in a Developing Country. *Engineering*, 2013, 5, pp 75-80 doi:10.4236/eng.2013.51b014 Open access.
Davidsson assisted with construction of the solar laboratory and evaluation of the equipment.

Bernardo R., Davidsson H., Gentile N., Gomes J., Gruffman C., Chea L., Mumba C., & Karlsson B., Measurements of the Electrical Incidence Angle Modifiers of an Asymmetrical Photovoltaic/Thermal Compound Parabolic Concentrating-Collector. *Engineering*, 2013, 5, pp 37-43 doi:10.4236/eng.2013.51b007 Open access.
Davidsson carried out substantial work on the modeling, the calculations and the illustrations.

Davidsson H., Bernardo R., & Larsson S., Impact of hybrid ventilation and sewage heat recovery on the energy performance of a low energy building; a feasibility study. Conference *EuroSun 2010*, 2010, paper 55.
Co-authors assisted with language check and discussions. Bernardo assisted with TRNSYS simulations.

Structure of the thesis and a short summary of the papers included

The connection between the different papers that form the main part of this thesis is shown in the figure below.

Paper 1 investigates a PV/T hybrid solar window at component level. The solar window, comprising solar absorbers on which PV cells have been laminated, produces both hot water and electricity. Insulated tiltable reflectors were placed behind the absorbers in order to increase the output from the collector. The collector is located on the inside of a window. The paper presents a calculation model to determine thermal and electrical output from the collector. Various factors limiting the performance of the collector are estimated and discussed.

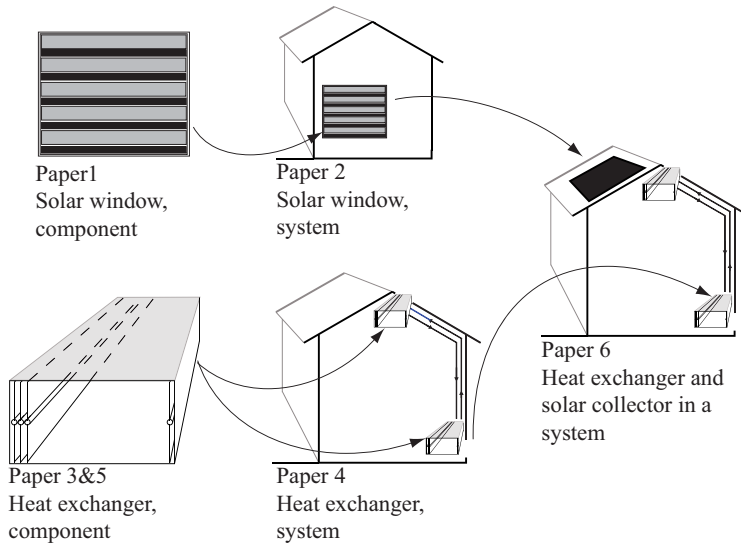
Paper 2 analyses the solar window at system level. Benefits and drawbacks of placing the collector in a window are investigated and discussed. Comparisons are made to improved versions of the solar window and also to buildings equipped with a more traditional solar collector placed on the roof.

Paper 3 and **Paper 5** concern a water-to-air heat exchanger suitable for heat recovery in natural or hybrid ventilation systems. Theoretical calculations and laboratory measurements are presented and discussed. The final result is a heat exchanger with a high heat recovery rate and a low pressure drop. Keeping the pressure drop low is essential to prevent disturbance to the low driving forces related to natural or hybrid ventilation systems.

Paper 4 focuses on the effects of using the heat exchangers discussed in Paper 3 and Paper 5 in a system. Two heat exchangers are connected in series, recovering heat from the outgoing air at the top of the roof and

feeding this energy to the incoming air at the bottom of the building. The ventilation heat recovery system is investigated in combination with a waste water heat recovery system and with a ground source heat exchanger.

Paper 6 investigates a more complex system containing the features from Paper 4, but is also equipped with a solar collector and a heat pump. However, the solar collector that was modelled in the paper is a roof-integrated solar thermal collector and not a solar window collector as discussed in Section 3 and Paper 2. The paper also discusses the effects of combining more than one heat recovery system.



Relationship between the papers on which the thesis is based.

Open-Access Publishing

Publishing papers is of major importance for the research community. The papers can be read by researchers around the world and together they form a platform for shared knowledge in academia. The process of writing, peer reviewing and publishing is a good basis in order to secure high quality published material and findings. However, this is a problem for those who cannot afford to pay for the subscription of the journal in question. This is a major problem for many researchers in developing nations. Furthermore, high costs for research journals are not only a problem for the developing nations, but also for universities in the industrialized nations, as the costs for subscriptions for journals is increasing.

One alternative is to publish the paper in journals that are open to anyone without the need to pay for it. This is known as “open-access publishing”. The open-access journals instead often finance the journal by charging a fee for the publication. Lund University is very active in trying to get the researchers to start publishing in open-access journals. This is why Lund University at present covers 50% of the publication cost. Furthermore, Lund University adopted a new policy for research publications in the end of 2005 (Lund University, 2005). In summary the University recommends the following:

- If possible, researchers should publish research results in journals that are free of charge for the reader.
- A journal that allows for parallel publication should be chosen if a free access journal is not available.
- Copyright release should be avoided. The minimum demand for the author is the right to publish in parallel.
- Lund University is working for a publication model where the papers are made accessible for the reader either directly or through parallel publication.

However, there are many open access journals with varying degrees of professionalism. This is why Lund University runs the Directory of Open Access Journals (DOAJ), a free service that provides a catalogue of quality-controlled open-access journals.

However, the DOAJ catalogue cannot be the only criteria when choosing a journal in which to publish the work. Other factors such as quality of earlier publications in the journal, which people are on the editorial board, and accessibility of the publisher are also very important parameters. Still, in the end, it is the quality of the material that matters.

Acknowledgements

First I would like to thank my four supervisors. The main and co-supervisor from the first half of my studies, Professor Björn Karlsson and Dr. Bengt Perers, and the main and the co-supervisor from the second half, Dr. Åke Blomsterberg and Dr. Bengt Hellström. Naturally, the supervisors have all been very important for me and for the projects. Thank you very much for technical help, project management and personal support over many years.

All my colleagues at EBD deserve big thanks for being helpful, kind, and funny people. Special thanks to Johan Nilsson, Håkan Håkansson, Jouri Kanter, Björn Berggren, Ulla Janson, Maria Wall, Gunilla Kellgren, and to Hans Follin for assistance with a million small things. Johan Nilsson is also acknowledged for the Zemax simulation discusses in chapter 3. Hans Follin is also acknowledged for the layout. Thanks to everybody at the department for pretending to listen when I spoke during coffee breaks.

I would like to thank Professor Bengt Sundén at the Department of Energy Sciences, LTH, Lund University, Dr. Dennis Johansson at the Department of Building and Environmental Technology, Building Services, LTH, Lund University and to Dr. Chris Bales at the Solar Energy Research Centre at Dalarna University in Borlänge. Your comments and help after reading ‘your’ sections were most appreciated. Birgitta Nordquist at the Department of Building and Environmental Technology, Building Services, LTH, Lund University is acknowledged for measurement assistance and discussions.

I’m grateful to the ‘Mozambique group’ for making everything more fun. Working really hard together towards a common goal can be very fulfilling. Thank you, Ricardo Bernardo, Joao Gomes, Luis Chea, Chabo Mumba, Christian Gruffman and Niko Gentile.

Most of all I’m grateful to my kids, Matilda and Albert, for helping me keep the work in perspective and in a context. Working with something is so much pleasanter if it has a meaning. Thank you for providing this. My major thanks go to my wife Eva. She has helped me not only through

moral support, but also by reading and correcting papers and various texts. Eva helped and supported me more than I could ever ask for.

Prelude

Warming of the climate system is unequivocal, as is now evident from observations of increases in global average air and ocean temperatures, widespread melting of snow and ice and rising global average sea level. (IPCC, 2007)

Few scientific reports have caught the general public's interest as much as the IPCC Fourth Assessment Report. In this report, the IPCC, a scientific intergovernmental body set up by the World Meteorological Organization (WMO) and the United Nations Environment Programme (UNEP), concludes that the increase in global temperature is about 0.74°C per 100 years for the 100-year linear trend. IPCC also concludes that sea level is rising by about 3 mm per year and the annual average extent of Arctic sea ice has shrunk by about 2.7% per decade since 1978.

IPCC also reports that most of the observed increase in global average temperatures since the mid-20th century is very probably caused by the observed increase in concentration of anthropogenic greenhouse gases. The concentration of CO₂ and CH₄ in 2005 by far exceeds the natural range over the past 650,000 years. The increase of CO₂ concentration in the atmosphere is due primarily to fossil fuel use. The consequences are immense. By the end of the 21st century average global temperature is expected to rise between 2°C and 4°C depending on simulation used and emission rate of greenhouse gases. This is expected to lead to drought in some areas and increased water availability in other areas. Ecosystems will suffer significant extinction and about 30% of the global coastal wetlands will be lost.

However, not everybody agrees with the conclusions in the IPCC report. Perhaps the most interesting criticism comes from the Peak Oil Theory. Different models show a peak, or a plateau, in world oil production somewhere between 2007 and 2018 (Alekklett, 2007). The exact year depends on model used and increase in oil demand. This shortage of oil will affect the amount of emitted greenhouse gases in more than one way. Of course, the most obvious emission reduction is that, if there is no oil to burn, there will be no emissions from it. However, shortage

of oil will also affect world markets and, if energy prices rise, GNP will very probably grow more slowly. This will slow down the emission rate of greenhouse gases.

We have climbed high on the 'Oil Ladder' and yet we must descend one way or another. It may be too late for a gentle descent, but there may still be time to build a thick crash mat to cushion the fall. (Alekklett, 2007)

1 Introduction

Your standpoint regarding the two theories mentioned in the prelude is down to individual judgement. If you do not believe either of the theories, it is business as usual. If you believe in both of them, or if you only believe in one of them, the conclusion must be that we need to start working to find alternatives to burning fossil fuel. To do this we need to use less energy and ensure that the remaining energy demand is met through renewable energy. Today, buildings account for 40% of the world's primary energy use and 24% of the greenhouse gas emissions (IEA, 2008). That is why new solar energy technology and energy-efficient electrical appliances are important for a greener future.

1.1 The alternatives

Basically there are two ways of reducing the need for energy that produces carbon dioxide – increasing clean energy production or reducing energy use, or preferably both.

There are many renewable alternatives to fossil fuel. Some of the more important renewable sources with greatest potential are wind power, hydro power, geothermal power, bio power and solar power. Nuclear power is not renewable but is an alternative to fossil fuel. All the sources have benefits and drawbacks. The major advantage of renewable energy sources is the low rate of carbon dioxide emissions. On the negative side are appearance and sometimes the high initial costs. Solar power is today an expensive way of producing electricity, but the cost is falling quickly and might soon be competitive in almost any climate. Some people feel that wind power stations ruin unobstructed views over the landscape. Solar energy and wind energy are also unpredictable and difficult to store. A still night provides no renewable energy from wind or solar power. If hydro power stations are built, there will be consequences to wildlife.

The costs of renewable energy have to be compared to the costs of burning fossil fuel and, in the end, we have to decide who is going to pay for the energy we use today. If the answer is ourselves, the fossil fuel

alternative is excluded, since the people living on the planet in the future have to pay with high temperature due to global warming. We are left with the choice of paying through loss of unobstructed views over the landscape, loss of natural values due to construction of dams and hydro power stations, or by investing heavily in producing and installing more solar energy panels.

The alternative to saving energy is less complicated. Building a low-energy house reduces the energy use throughout the year and the day, not just at specific times. This makes saving energy beneficial both from an energy and from a power perspective. Solar cells and wind power are mainly beneficial from an energy perspective as discussed above. Energy can be saved in many ways. One way is to use low-energy components such as water pumps, fans or light bulbs. Another way is to recover energy. This can for instance be done with the ventilation air or the waste water from the house.

1.2 Saving energy

Building low-energy buildings and renovating existing buildings to improve energy efficiency can be done in a number of ways. When aiming to reduce the use of energy in buildings, a five-step strategy for low-energy design has been proposed (Dokka & Hermstad, 2006).

1. Reduce heat losses
2. Reduce electricity use
3. Utilize solar energy
4. Control and display energy use
5. Select energy source

However, the order of the five steps can be questioned, as the price of PV modules is falling. In principle, very cheap PV cells could be a more cost-effective alternative than reducing heat losses.

1.2.1 Building skin

One of the largest energy saving potentials for a residential building is to reduce thermal losses through the building skin. From an energy perspective, modern technology in house building is largely based on constructing a shell that is airtight and that has a low U -value, i.e. thermal losses are low. There are many ways to meet these demands. Almost any material can be used – stone, wood, plastics, and mineral wool – and architec-

tural boundaries are almost limitless. Of course, building site and budget impose restrictions, but the main conclusion is that houses can be built with low thermal losses.

1.2.2 Ventilation heat recovery

Apart from the building skin, one of the parts in the building with the highest thermal losses is the ventilation system. If no attention is paid to ventilation, large quantities of warm air can escape. Modern residential buildings normally recover heat from ventilation air in two main ways. Either a heat pump is used to recover some of the thermal energy from the outgoing ventilation air or some kind of heat exchanger is used to transfer the thermal energy from the outgoing air to the outdoor incoming air. Unless stated otherwise, the efficiency of the heat exchanger discussed in the thesis will be defined according to Equation 1.1:

$$\eta = \frac{T_{in} - T_{amb}}{T_{room} - T_{amb}} \quad \text{Equation 1.1}$$

i.e. efficiency is the ratio of the temperature difference between the incoming air, T_{in} , and the ambient, T_{amb} , air to the indoor air, T_{room} , and the ambient air, T_{amb} .

Ventilation and air movements are a result of pressure difference. Pressure difference can be caused by temperature differences, and air moves because of density differences between air masses, wind, or because of a fan that forces air to move. If the heat recovery is to work properly in a ventilation system, the building needs to be airtight. The flows must be controllable in order to recover thermal energy from the ventilation air. If draughts are present, there is less control of the air masses. Air that passes through the walls in cracks cannot be heat recovered. A high level of airtightness is also important in order to attain a uniform indoor temperature. Wall (2006) shows that the thermal energy use in a low-energy single-family house can increase by approximately 50% if air leakage is increased from 0.05 ach to 0.1 ach (air changes per hour). Consequently, airtightness is a very important factor when building low-energy houses and an airtight building must have a ventilation system to supply outdoor air.

1.2.3 Ventilation techniques

There are many different types and subtypes of ventilation. Some of them are discussed below.

Mechanical ventilation with extraction only

The basic principal of mechanical ventilation is a fan placed somewhere in the house. The air is extracted from the building and outdoor air enters, either through ducts or inlets in the building skin. This type of ventilation normally offers no heat recovery in older residential buildings. One alternative is to have a heat pump connected in series with the outgoing air. The hot air then serves as the heat source for the heat pump. This allows some of the thermal energy to be recovered.

Balanced mechanical ventilation

Mechanical ventilation with heat recovery is a commonly used technique in modern passive houses. Heat can be recovered using recuperative or regenerative rotating heat exchangers (Mardiana-Idayu & Riffat, 2012). This type of ventilation system recovers much of the heat from the outgoing air. The system depends on a fan to run the ventilation.

Natural ventilation

Natural ventilation or, more precisely, passive stack ventilation technique, depends on the weather conditions to operate properly. Either the wind creates under-pressure in the chimney as it passes or there is a temperature difference between the indoor and the ambient air. The wind-induced driving force and the stack effect can also work together to create a ventilation flow. If the driving forces disappear, the ventilation flow will stop. Formulas for calculating the available driving forces can be found in literature, e.g. in Liddament (1996). Equation 1.2 describes the available pressure difference due to the thermal buoyancy caused by the temperature difference between the indoor and the ambient air.

$$\Delta p_{buoyancy} = h' \cdot g \cdot (\rho_{amb} - \rho_{indoor}) \quad \text{Equation 1.2}$$

where h' is the height difference between inlet and intake of the air, g is the gravitational acceleration, and ρ_{amb} and ρ_{indoor} are the densities of the ambient and indoor air masses. This means that for a building with a height difference of 10 m between the inlet and the outlet for the ventilation air, with 20°C inside and 0°C outside, an 8.7 Pa pressure difference is available.

Wind also gives rise to a pressure difference, but it is much more difficult to utilize, partly due to its unpredictability. The wind is affected by local topography, its direction, and the amount of shelter due to surrounding obstacles such as trees and buildings. The pressure related to the wind blowing on the façade can be calculated according to Equation 1.3.

$$\Delta p_{wind} = \mu \frac{\rho_{air} \cdot v_{air}^2}{2} \quad \text{Equation 1.3}$$

where v_{air} is the wind speed, ρ_{air} is the density of the air and μ is the form factor. For $\mu = 0.7$ and $\rho_{air} = 1.2$, Δp_{wind} will be 10.5 Pa if the wind speed is 5 m/s. Simultaneously, $\mu = -0.2$ on the rear of the building (wind direction), giving rise to a pressure of -3 Pa. This gives rise to a considerable pressure difference. However, the wind force is much more unreliable and changes more quickly than in the thermal stack effect. This makes use of the wind-induced forces less attractive. The figures for the form factor above are taken from Liddament (1996), see Table A2.1. These numbers are only used as illustration.

Hybrid ventilation

During periods of low wind speeds and small differences between indoor and outdoor temperatures, the natural ventilation forces will not cover the need. One alternative is then to use hybrid ventilation. In “Principles of Hybrid Ventilation” (Heiselberg, 2002), three different types of hybrid ventilations are discussed. The first of them in the list below will be used as the standard definition of hybrid ventilation in this thesis.

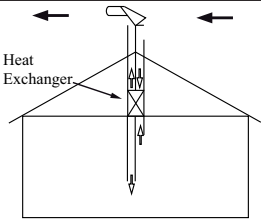
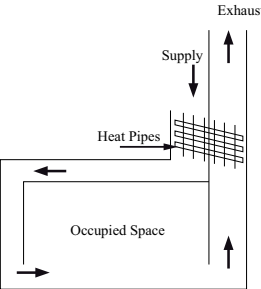
1. Fan-assisted natural ventilation: ventilation that runs on the natural driving forces when they can supply the correct air flow rate and uses a complementary fan when necessary. This minimizes the energy use by the fans in the system.
2. Natural and mechanical ventilation: two autonomous systems with a control strategy that switches between the two.
3. Stack- and wind-assisted mechanical ventilation: mechanical ventilation system that makes optional use of natural driving forces. Low-pressure loss mechanical ventilation system where natural forces can account for much of the necessary pressure.

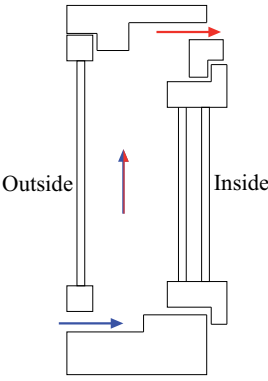
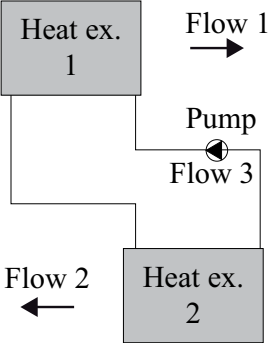
Hybrid ventilation with heat recovery

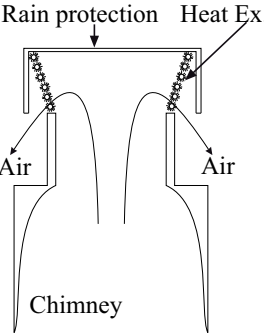
Natural and hybrid ventilation is normally unable to recover heat from the extracted air. This is mainly due to the high pressure drop in the heat exchangers. It is somewhat easier to install heat exchangers for heat recovery in a hybrid ventilation system than in a naturally ventilated system. This is because the fan in the system can be used to compensate for the pressure loss, mainly in the heat exchangers. However, if the pressure drop is too high, the fans will need to be run most of the time and the system will instead be like a mechanical ventilation system. Various ventilation

techniques based on hybrid or even natural driving forces have been presented, including heat recovery. Examples of these ventilation techniques are shown in Table 1.1.

Table 1.1 Various hybrid ventilation systems with heat recovery and heat exchanger arrangements for ventilation.

Description	Illustration	Comment
1. The hybrid ventilation system uses both the stack effect and the wind-induced force to run the system. The system is a simplification from (Skåret, Blom, & Hestad, 1997). An air-to-air heat exchanger recovers some of the heat from the outgoing air. A similar system was tested by Schultz & Saxhof (1994).		In some cases, the system can be difficult to retrofit into existing buildings because of the necessity of installing ducts for both the outdoor air and the outgoing air. However, the system can utilize the wind induces forces rather easily.
2. The passive ventilation system is driven by thermal buoyancy. The heat pipes transfer the heat from the extracted air to the supply air. Heat recovery efficiency of up to 70% has been reported (Riffat & Gan, 1998; Shao, Riffat, & Gan, 1998) . Pressure loss in the heat exchanger can be kept at around 1 Pa for flow speed of 1 m/s.		The system is difficult to retrofit due to the high chimneys needed for the driving force. However, the system is passive, and fans or pumps are not needed.

<p>3. As the air passes through the window, it picks up heat from the window and delivers it to the room. In principle, the U-value of the window is lowered, thereby reducing heat losses. Ventilated window techniques can be used in combination with the exhaust air heat pump to reduce the thermal energy use and to increase the thermal comfort. Thermal comfort is increased since draught is reduced due to increased inlet air temperature (Appelfeld & Svendsen, 2011).</p>		<p>The system is dependent on electricity to recover heat from the extracted air.</p>
<p>4. Run-around heat recovery systems are made up from at least two heat exchangers connected through brine being pumped between them. This type of system can be utilized in buildings if one of the heat exchangers is placed at the air extract and the other is placed at the air intake. The heat extracted from the exhaust air is transferred to the incoming air. This type of heat recovery systems have been investigated and optimized in earlier work, (Emerson, 1984; Forsyth & Besant, 1988; Hatef Madani, 2012; Wallin, Madani, & Claesson, 2009; Zeng, Besant, & Rezkallah, 1992). Most of the work has been carried out on coil heat exchangers, but other types of heat</p>		<p>The system uses two heat exchangers, which lowers the total efficiency of the heat recovery as a system. However, the system is flexible since heat can be transported by water instead of by air. Furthermore, a brine-based heat recovery system could be used to obtain thermal energy from other sources. Brine is quite easy to use in heat exchange, such as in a solar heated tank, a ground collector or even in a waste water heat recovery tank.</p>

<p>exchangers may be used. A variation of the run-around system combining the system with a heat pump was investigated by Madani, Wallin, Claesson, & Lundqvist, (2010).</p>		
<p>5. The “SPARVEN” ventilator was developed in Sweden during the 1980s (Eriksson, Masimov, & Westblom, 1986). The outgoing air passes through the chimney and passes a heat exchanger made up of a spine of finned tubes. The heat exchanger also dampens the ejector force induced by wind. The brine inside the coil heat exchanger is pumped to a heat pump where some of the heat in the ventilation air is recovered. The dampening effect of the ejector force from the wind is considered beneficial since this force often varies strongly with time. Instead the system relies on thermal buoyancy force and an auxiliary fan when needed.</p>	 <p>The diagram illustrates the SPARVEN ventilator system. It shows a cross-section of a building with two chimneys. Air is shown entering from the left and exiting through the left chimney. A heat exchanger (Heat Ex.) is located between the two chimneys, with air flowing through it. Rain protection is shown at the top of the chimneys. The label 'Chimney' points to the left chimney.</p>	<p>The system is easy to retrofit into old buildings. However, the heat recovery system with the heat pump needs electricity in order to work.</p>

The systems described in Table 1.1 have both opportunities and problems. In dwellings, the supply air should be delivered to bedrooms and living rooms and the air extracted from the dirtiest rooms, from an air point of view, i.e. toilets and kitchens. This is illustrated in Figure 1.1. This makes systems 1 and 2 in Table 1.1 less attractive since the air needs to be transported sideways. This is associated with long ducts and a number of bends which will increase pressure drop.

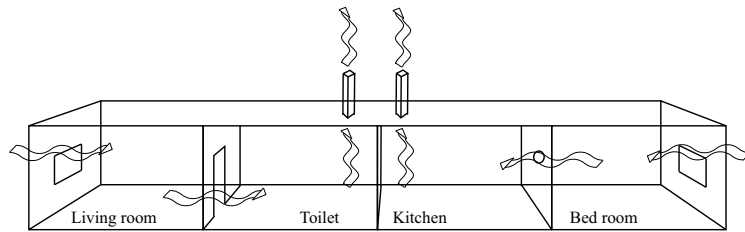


Figure 1.1 The outdoor air enters the building mainly in bedrooms and living rooms. The extract air is removed from the kitchen and the toilets.

Installing a new ventilation system in a building may also have major implications in terms of ducts. For instance, if mechanical ventilation with heat recovery is installed, ducts will need to be installed to or from all the areas. One possibility is to install the ducts on the outside of the building, or better inside the additional insulation when retrofitting the building. This is discussed for example in IEA ECBCS Annex 50 pp15 (Kobler et al., 2011).

1.2.4 Natural/hybrid ventilation systems in relation to building regulations

The following text includes brief extracts from Swedish building regulations, (Boverket, 2011) concerning ventilation. The text in *italics* is taken from the regulations and the plain text that follows comprises comments relating the regulations to the ventilation system discussed in the thesis.

6:21 Common

Buildings and their installations shall be designed to ensure they can provide the conditions for good air quality in rooms where people spend time. The requirements for indoor air quality shall be determined on the basis of the intended use of the room. The air must not contain pollutants in a concentration resulting in negative health effects or unpleasant odours.

6:25 Ventilation

The ventilation system shall be designed to ensure that the required outdoor air flow can be supplied. The system shall also be able to remove harmful substances, moisture, unpleasant odours and emissions from people and building materials, as well as pollutants from activities in the building.

6:251 Ventilation flow

Ventilation systems shall be designed for a minimum outdoor airflow corresponding to 0.35 l/s per m² of floor area. When in use, rooms shall be able to have continuous air exchange. In residential buildings where the ventilation can be controlled separately for each dwelling, the ventilation system may be designed with a control system based on presence and need. However, the air flow rate must not fall below 0.1 l/s per m² of floor area when the dwelling is unoccupied and 0.35 l/s per m² of floor area when the dwelling is occupied. For natural ventilation the Boverket Handbook 'Natural Ventilation' can be used as a guide.

6:252 Distribution of air

- *Supply air shall primarily be supplied to rooms or separable parts of rooms for everyday social interaction and for sleep and rest.*
- *Spread of foul or unhealthy gases or particles from one room to another shall be limited. Intentional air transfer may only be arranged from rooms with more stringent requirements regarding air quality to a room with identical or less stringent requirements.*
- *Extract air shall primarily be taken from rooms with less stringent requirements regarding air quality. Calculation of extract air flow volumes in sanitary rooms and kitchens shall consider the impact of moisture load and the presence of cooking smells. Ventilation in kitchens shall be designed to ensure that a good capture capacity in the cooking area is achieved.*

Comment: The heat recovery for the hybrid ventilation system discussed later in this thesis does not include the air from the kitchen. The strongly polluted air from the kitchen would probably reduce the heat transfer rate on the heat exchangers, thereby reducing the efficiency for the whole building. Instead, the kitchen air, which is strongly polluted with fat and humidity, has to be treated in a different way. Examples are direct evacuation to the outside or use of a carbon filter. However, as humid air is cooled down in a heat exchanger the water can condense on the heat exchanger walls. This enables recovery of the latent heat in the humid air, increasing the total heat recovery efficiency. However, this effect is not considered in this thesis.

6:253 Airing

Room or separable parts of rooms in dwellings for everyday social contact, cooking, sleeping, resting, and rooms for personal hygiene shall have the option of forced ventilation or airing. Airing shall be made possible by use of an openable window or ventilation hatch. These shall be openable to the outside.

6:254 Installations

Ventilation installations shall be located and designed in such a way that they are accessible for maintenance and cleaning purposes. Main and branch ducts shall have fixed points for flow measurement.

Comment: Using short ducts or, if possible, avoiding ducts completely for the incoming outdoor air will reduce the maintenance work. In the ventilation system suggested in this thesis, the outdoor air intake is straight through the outer wall. This considerably reduces maintenance work and installation costs.

6:924 Ventilation

When altering a ventilation system, the way it was originally intended to operate should be considered. Furthermore, the implications for human health and the building's cultural, aesthetic and functional values should be considered. This could lead to choosing an alternative way of ensuring an acceptable air quality than when constructing a new building. It could, for example, be investigated whether it is possible to reconstruct and modify existing ventilation systems.

Comment: The hybrid ventilation system could be used when old ventilation systems are being renovated, such as when natural ventilation systems are being upgraded to enable heat recovery.

The following text is a short extract from the Boverket publication, "Natural Ventilation" (Boverket, 1995) referenced in the Swedish building regulations, (Boverket, 2011).

Under certain circumstances, natural ventilation systems can be installed by suitable design of the air inlets and ducts and through a naturally-ventilated system in order to achieve an acceptable air change rate.

Comment: This section relaxes the requirement for air flow rate never to fall below 0.35 l/s per m² floor area. During short periods, a lower air flow rate can be accepted.

Natural ventilation can be installed and operate if:

- *there are openable windows in all the rooms where people spend time, and in other rooms where increased moisture stress occurs,*
- *specific activities that require larger air volumes than the BBR does not occur,*
- *regulations of thermal need according to BBR are met by using heat recovery or some other means,*
- *devices are installed that automatically prevent excess ventilation,*

- *air velocity and thermal indoor climate according to BBR are maintained.*

Comment: Using a hybrid ventilation system with heat recovery makes it easier to fulfil the energy targets for the building compared to using a standard natural ventilation system without heat recovery.

Chapter 9 Heat recovery

In natural ventilation systems, this type of heat recovery should not be possible due to the increased pressure drop caused by the heat recovery.

Comment: Using a heat exchanger with a very low pressure drop makes it possible to include heat recovery in natural or hybrid ventilation systems.

Chapter 10 Window airing

The possibility of window airing should not form the basis for the function of the natural ventilation system. Window airing is intended for occasional airing, while the ventilation system should be designed in such a way to allow adequate ventilation under normal conditions.

Comment: If open windows are used for ventilating the building, there is less chance of recovering some of the heat in the ventilation air.

1.2.5 Waste water heat recovery

In Table 1.1, it was mentioned that the brine-based heat recovery system could be used to obtain thermal energy from other energy sources. One such heat source could be heat from waste water. Collecting waste water and transferring the heat to the brine can reduce the thermal energy use for air heating. The waste water heat recovery can also be used to lower the heating need for domestic hot water.

On average a Swedish person uses about 800 kWh of thermal energy for domestic hot water annually. This means that a normal family of three to four uses 2400-3200 kWh for hot water (Stengård, 2009). The amount of passing out to sewage is even higher, since a considerable amount of electrical energy used in the house is used to heat cold water in appliances such as washing machine and dish washers, and from cooking. This means that a lot of energy literally just goes down the drain.

The heat recovery market for waste water is not as advanced as building solutions for passive houses or heat recovery systems for ventilation. Various techniques to recover heat from the waste water are available. A

Masters thesis from KTH in Stockholm (Nykqvist, 2012) discusses some of these techniques in more detail. One common technique is to wrap one smaller pipe for fresh water around a part of the sewage pipe. This cross flow heat exchanger is easy to install. This type of sewage heat recovery system has the potential to recover heat from all the waste water. Alternatively the heat recovery takes place where the hot water is being used, for example in direct proximity to the shower. In this case the heat is taken from the drainage of the shower and directly transferred to the incoming cold water. Less hot water from the boiler has to be mixed with cold (or in this case preheated) water from the mains. An alternative method, with many different types of system solutions, is to recover the heat by using a heat pump. Heat can then be recovered from the waste water/sewage and transported to the incoming water.

1.3 Solar energy

Solar energy can be defined as energy used on a higher quality level compared to the zero state. The zero state level is the average temperature of the surroundings.

Throughout this thesis the phrase “thermal energy produced in the absorber” or similar phrases will be used. This does not mean that energy is created out of nothing. As is known from physics, “energy cannot be created or destroyed, only converted into different forms“. The phrase “thermal energy produced in the absorber” therefore means “thermal energy converted from solar radiation to thermal energy in the absorber”. However, this last phrase is too long and the language gets complicated, and so the shorter phrase, although less accurate in terms of physics, will be used.

Knowledge about the sun and the radiation from it is important for the understanding of solar energy. Solar radiation can be divided into four parts, shown in Figure 1.2: direct solar radiation from the sun, diffuse solar radiation from the sky, circumsolar radiation, and ground reflected radiation. The circumsolar radiation comes from angles close to the sun but still outside the solid angle of the sun.

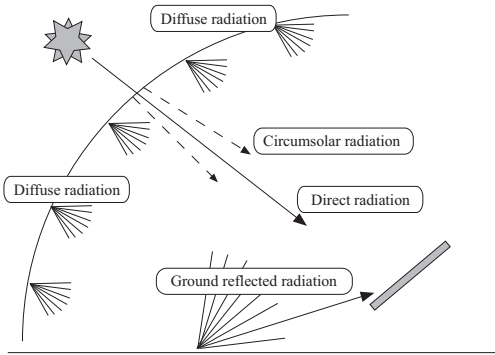


Figure 1.2 Solar radiation divided into direct solar radiation, diffuse solar radiation, circumsolar radiation and ground reflected radiation.

The path of the sun in the sky can be calculated with simple equations. If we know the date and time and the geographic location, the sun's position can be calculated. The position is normally expressed by using the two angles, solar altitude, α and solar azimuth, γ_s . The solar altitude is the angle between the ground and the sun. The solar azimuth is the angle between the sun and the south direction, i.e. the azimuth is zero at noon solar time. The angles are illustrated in Figure 1.3, where the zenith angle, defined as $\theta_z = 90 - \alpha$, is also shown.

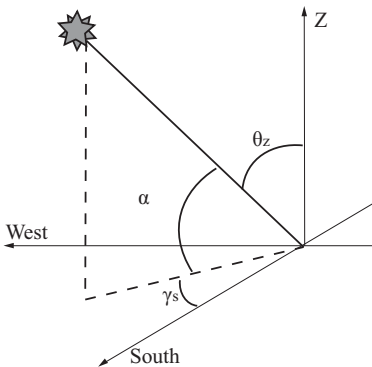


Figure 1.3 The solar angles. γ_s is the solar azimuth. α is the solar altitude and θ_z is the zenith angle.

Solar energy can be used as solar electricity and solar thermal. Solar electricity can be produced in many different ways, but the best-known technique is to use Photo Voltaic cells, commonly known as PV cells. This technique converts photon energy into electrical energy. Alternatively steam can be produced and used to run turbines to produce electricity. PV cells are discussed briefly in section 1.3.1.

The alternative use of solar energy is to produce heat. The heat is most commonly delivered and stored in the form of liquid or a gas. Heat has a lower energy quality and is easier to produce than electricity. Solar thermal energy is discussed in section 1.3.2.

Most solar energy applications carry a high investment cost, so hybrid solar collectors and building integrated solar energy components are particularly interesting since they can potentially reduce the investment costs. Hybrid collectors are discussed in 1.3.3 and building integration in 1.3.4.

1.3.1 Solar electricity

Single PV cells are normally arranged in series or series/parallel in PV modules. Each cell can produce a potential difference of about 0.5 V when irradiated. When placed in series, these potential differences add up to a total potential. If a module has 36 cells, the total maximum potential difference is about 18 V. The PV modules can also be arranged in parallel or in series. The array of PV modules can then be connected to the grid or to a battery. When connected to the grid, an inverter transforms the DC voltage to high AC voltage.

There are many different types of PV cells. They vary in price, appearance and efficiency. The monocrystalline Si cells are the most efficient. These cells are made from one large single crystal. The efficiency of the cells is typically about 14-16%, (Tyagi, Rahim, Rahim, & Selvaraj, 2013). The polycrystalline cells are less efficient, with an efficiency of about 13-15%. The polycrystalline cells consist of many small crystals and thus have a speckled appearance. The third type of cell is the thin film cell. This type of PV cell is much thinner than the mono- or polycrystalline cells. The thickness of the actual cell is as small as 1 μm . Because of their small size, the thin films could become cheap to produce. Today the efficiency of the thin films is about 10%.

1.3.2 Solar thermal energy

The thermal collectors are easy to understand on a component level but difficult to understand when built into a system. The complication arises

due to the losses in the collectors. Investigations of solar collectors on a component level only take the collector itself into account. The inlet temperature to the heat carrier is set to a fixed value. A system analysis on the other hand includes the full system such as storage tanks and consumption profiles. A system analysis uses the temperature of the outgoing heat carrier from the storage tank as incoming temperature for the collector.

The thermal collectors can be divided into three sections, as shown in Figure 1.4. The simplest type of collector is a black-painted surface that heats a liquid or a gas. This can be a black-painted box that preheats the air before it is let into a building or it can be a black-painted sheet of metal that is cooled with water. A pane of glass covers the construction to reduce heat losses. As the fluid runs through the collector, the fluid is heated and pumped away for storage or use. An uncovered solar collector with black-painted sheet of metal will be a poor collector since the losses due to thermal radiation and convection will be large. This limits the use of the collector to a pool heater or similar. To construct a more efficient collector, the thermal losses must be minimized. This is done in a standard flat plate collector which has a selective absorber and cover glass (upper left illustration in Figure 1.4). Anti-reflection treated glazing (Chinyama, Roos, & Karlsson, 1993), (Nostell, Roos, & Karlsson, 1999) maximizes the transmission and the glazing itself limits the convectional losses. In order to minimize the losses due to radiation, the collector is covered with low-emittance coating.

The second type is the vacuum tube, shown in the upper right corner in Figure 1.4. The vacuum tubes are made from low-emittance absorbers placed inside a glass cover. The glass cover is evacuated, hence the name vacuum collector. The low-emittance coating suppresses radiation losses and the vacuum limits the convectional losses. The heat can for instance be transferred to the water pipes in the manifold via a heat pipe.

The third type is the concentrating collector. This type uses reflectors to focus solar radiation onto an absorber. The concentrating collector is illustrated in the lower left corner in Figure 1.4. The small hot absorber area limits thermal losses.

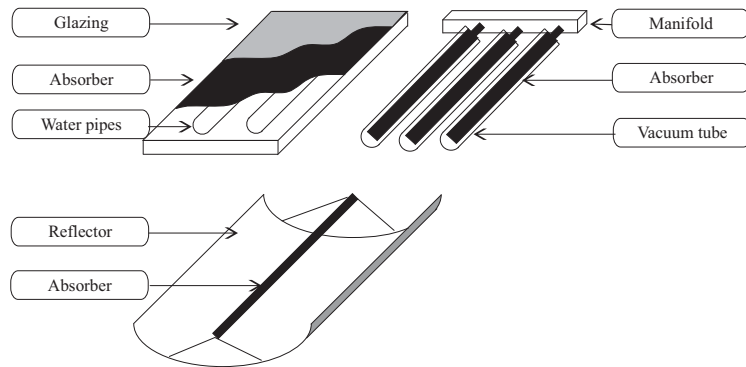


Figure 1.4 Three types of solar collectors. The upper left is a standard flat plate collector. The upper right is a vacuum tube collector and the lower left is a concentrating collector.

1.3.3 Hybrid solar collector

Concentrating systems can also be used for decreasing the cell area in PV installations. Concentrating solar radiation onto the PV cells will lead to high irradiation per cell area and high cell temperatures. Since the PV cells are temperature sensitive, the electrical output will decrease with increasing cell temperatures. Even worse, the cells might be permanently damaged if the temperature becomes too high. To solve this problem, the cells are cooled by water on the reverse side. This results in cool and thereby high-efficiency cells, and the hot water can be used for space heating or domestic use. This multiple production has potential to enable the production of cheap solar energy (Anderson, Duke, Morrison, & Carson, 2009; Kalogirou & Tripanagnostopoulos, 2006; Krauter & Ochs, 2004; Tonui & Tripanagnostopoulos, 2007).

The official homepage of IEA SHC Task 35 PV/Thermal Solar Systems (Sorensen, 2005) gives a good overview of various hybrid technologies. However, there are problems associated with this technique. If PV cells are laminated on top of the absorber, the low-emittance coating will be lost. At the same time, the absorber will produce less heat since some of the photons are used to produce electricity. This is shown in Figure 1.5. At 11:00, the electrical circuit is closed and electrical energy is produced in the hybrid collector. Since the electrical energy is then used elsewhere,

less thermal energy is available for the thermal absorber, hence the dip in thermal energy production. The photons can only be used once.

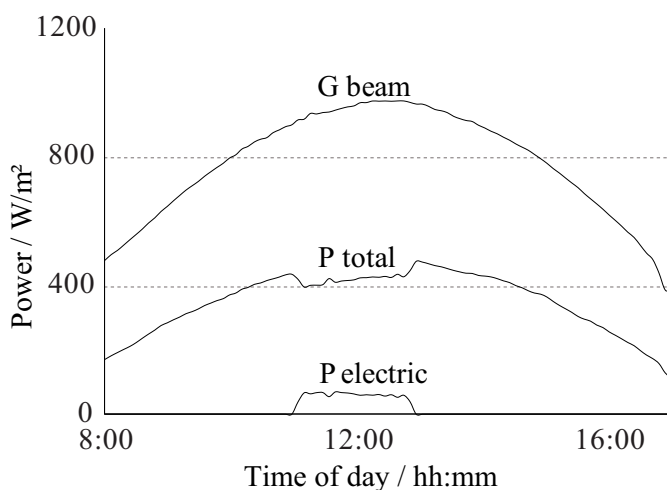


Figure 1.5 The output from a PV/T hybrid collector. At 11:00 the electric load is connected. Measurement performed by Ricardo Bernardo at EBD, LTH Sweden.

1.3.4 Building integrated solar energy

Another way of reducing the price of solar energy is to integrate the collectors and the PV systems in buildings. This saves not only building materials that are replaced by the solar energy systems but also saves work. If the solar collectors or PV modules are introduced into the construction after the building is completed, a significant amount of work has to be performed twice.

The integration can take place in many different ways. Figure 1.6 shows building-integrated PV modules (left figure) and PV modules installed on a wall to work as sunshade (right figure). Using the PV modules as sunshade reduces total costs, since no extra investments are required for solar shading.



Figure 1.6 Left, building-integrated PV modules. Right, PV modules working as a sunshade. Photo: GAIA Solar.

1.4 Energy as a system, feedback mechanisms, energy flows

The energy flows and the energy balance of an entire building are very complex. Some energy aspects are easy to understand, for example a solar collector that transports heated water to a tank is positive to the energy balance as long as the inlet water is warmer than the outgoing water. The energy flow is in one direction only. Introducing an extra pane of glass in the window is more complicated for the energy flow. On the one hand, the U -value, i.e. the thermal loss, is reduced which is beneficial for the energy balance, at least if cooling is not an issue. On the other hand, the extra glazing will reduce the solar transmission through the window, so less solar radiation is let into the building for passive heating. This is negative for the energy balance. Having one positive and one negative effect makes it more complicated to determine the total effect. A building is full of such interactions. Some are more complicated than others. Simulations or measurements might answer the questions raised.

The building envelope is the most important part of a building in cold climates. If the envelope is poorly insulated the thermal losses will be very large. This explains the fast growing market in passive houses (Feist, Schnieders, Dorer, & Haas, 2005). With thick outer insulation and an effective heat recovery unit, a traditional heating system in the building will become redundant. Apart from the free thermal energy from people and electric appliances, the passive house is supplied with extra energy for the ventilation only. The extra costs of thicker insulation and a heat recovery unit are partly compensated for by the lack of ordinary heating system such

as radiators or underfloor heating (Feist et al., 2005). The buildings are also less dependent on solar radiation transmitted through the windows, since they can utilize less solar energy compared to ordinary buildings. This is not a drawback for passive houses; it is simply a consequence of the fact that passive houses need less auxiliary energy and have a shorter heating period compared to ordinary buildings.

Adding all these more or less complicated energy flows together raises a non-trivial question. Are passive houses or active houses preferable? Active houses are houses that actively utilize solar energy. Is it better to have large windows and a heavy building construction to store the solar gain, or is it better to reduce the window size to minimize thermal losses? If the building is equipped with shutters for the doors and the windows, it can be even more active. By opening or closing the shutters, the inhabitants or maybe even the control system can decide how much solar radiation should be let into the building. Opening the shutters to allow the sun to heat the building during the day and closing them at night results in active control over thermal energy losses and gains. The same way of thinking can be applied during summer, when the shutters are closed during the day and opened at night. Using window shutters in a smart way can result in a very different optimum regarding window size in order to minimize energy use for a building. If the losses from the window are reduced by insulated shutters at night, it could be positive for the energy use to have larger windows compared to buildings without the window shutters. Furthermore, is it better to have a heat recovery unit that uses relatively large quantities of electrical energy to save thermal energy than to have natural ventilation with preheating of the air in pipes in the ground? Natural ventilation needs less electrical energy but results in considerably higher thermal energy need. To investigate some of these questions, Solgården located in Älvkarleö in central Sweden was constructed.

1.5 Low-quality energy

As is known from physics, energy cannot be created nor destroyed; it can only be transformed into different forms. A unit of electricity can be transformed into a unit of heat, but a unit of heat cannot be transformed into a unit of electricity. It is not possible to transform to a higher quality level of energy while maintaining quantity. Electricity can be said to be more valuable than heat. If there is an opportunity to choose the order in which to use two different sources of energy, it is better to use the low-quality source first. The following example can be used.

Preheating ventilation air (at for instance -10°C) in the ground (at 5°C), before using energy from waste water (30°C) to heat it further, is more energy efficient than using the waste water first. If the higher energy quality in the waste water heat is used first, it may not be possible to use the low-quality heat in the ground. The high-quality energy in the waste water will then be used quickly.

This reasoning led to the construction of Solgården (see section 1.6), a building equipped with both a solar collector and a hybrid ventilation system with heat recovery. The PV/T hybrid, PhotoVoltaic/Thermal, solar collector in Solgården is discussed in greater detail in Section 3. The PV/T collector produces and saves energy in a wide variety of qualities. Apart from producing high-quality electricity, it produces heat as a by-product from cooling the PV cells, i.e. hot water at 50°C (medium quality). Furthermore it saves heat at 20°C (low quality) in the building as the collector lowers the U -value of the window construction.

Hybrid ventilation recovers parts of the thermal energy that would be lost through the exhaust ventilation duct. In periods of extreme cold, the brine in the hybrid ventilation can be circulated in the ground, at approximately a few degrees above zero, (very low quality) for pre-heating. This has the potential to reduce thermal energy use, while limiting the risk of the heat exchangers freezing.

A waste water heat recovery system is used to preheat (at approximately 20°C , i.e. low quality) the domestic hot water before heat of higher quality from the hot water storage tank is used. All of these measures are to enable the building to use the available thermal energy at the lowest possible level.

1.6 Solgården

Solgården, built in 2005, is a single-family house. The south façade of the building is glazed, as can be seen in Figure 1.7. The building is ventilated by a passive stack system. The idea is to minimize the electrical energy need for ventilation.



Figure 1.7 Parts of the south side showing the heavily glazed façade.

The appliances in Solgården use low energy, so the house benefits less from passive heat gains from electricity use. This is also one of the reasons why Solgården was not built as a passive house. The passive house definition states that the heat supplied to the ventilation air should suffice for the entire building, i.e. there should be no need for another heating system.

The architecture is focused on allowing active control of solar energy. The thick solid brick wall in the centre of the building acts as a storage for the solar radiation absorbed during daytime. The solar radiation allowed into the building can be actively controlled by opening or closing the reflectors in the window. The underfloor heating system also allows the building to utilize the solar thermal energy produced in the solar collector. This means that thermal energy can be stored from one day to another and can be used to heat the building if the weather changes.

The hybrid ventilation can also be used actively. The ground collector and the waste water storage tank can, if beneficial, be used to preheat the ventilation. The waste water heat recovery is described in Section 5. If beneficial, the collector can be used to heat the waste water storage tank. This heat can be used to heat the ventilation air. In other words, Solgården is much more active in controlling the energy balance than a standard passive house. In this way Solgården is intended to be a continuation or an alternative to passive houses, an active house.

1.7 Objectives

PV cells and thermal collectors are well-established technologies. PV/T hybrids are somewhat newer and less investigated. Building-integration of solar energy products has been studied in many projects. However, installing a PV/T hybrid collector equipped with a tiltable reflector in the inside of a window is new. The implication of such an installation on the thermal and electrical performance was unknown, both on a component level and on a system level.

The physics behind a heat exchanger has been known for a long time. Heat transfer and the technology of heat exchangers is a well-established field of technology. The same can be said about ventilation systems, including ventilation equipped with a run-around heat recovery system. However, most work in this area has been carried out on systems based on using a fan for moving the air in the building. Natural ventilation equipped with heat recovery systems is less investigated, especially with run-around heat recovery systems.

The objective of this study was to investigate the energy consequences of installing these two innovative products in a low-energy building. The first product, the solar window is intended to be a key feature when building an active house. In this case, the active component is the tiltable reflectors that enable control of the solar radiation let into the building. The second product is the hybrid ventilation system with heat recovery. Both of the products are designed with the aim of using and producing energy at different energy levels. Using energy at a low quality is advantageous at system level. This will be discussed in the thesis.

The first goal is to identify the important parameters, such as energy efficiency of the solar window and the heat exchanger and the pressure drop for the heat exchanger. The key question for the heat exchanger development was how to design a water-to-air heat exchanger for natural ventilation.

The second goal is to understand the interaction between these products and their surroundings. The objective is to determine both usefulness and possible improvements.

The questions asked are:

- How does the solar window affect the need for heating in a building?
- How does the heat recovery for the ventilation system work in combination with other heat sources?
- Could the products become useful and competitive when building low-energy, passive or even active houses?

- Could the products be developed further? What consequences would this have?

NB: The investigation of the heat exchanger used existing relationships in the field of heat transfer. This knowledge was applied to a specific problem, namely ventilation.

1.8 Method

The first part, the solar window, was first measured and characterized to evaluate the energy performance at component level. The evaluation was carried out using a simple model in Excel, since no simulation program has the mathematical model to simulate the solar window. The final step in the analysis was to use TRNSYS (Transient Systems Simulation Program), i.e. an advanced simulation configuration of different mathematical models describing the physical objects in the system, so that the performance could be tested at system level. TRNSYS 16 and Simulation Studio 2006 were used for the simulations. Simulation Studio is the modern interface for TRNSYS. TRNSYS is described in Section 2.

The second part, the hybrid ventilation system with heat recovery, was carried out differently. At the start of the investigation there was no test facility to deliver data. Instead the first steps were taken using TRNSYS, this time with the newer version TRNSYS 17. The differences between version 16 and 17 are quite small, and have little or no relevance for these investigations. The simulation gave the first indications of how the different systems were to be put together in order to work optimally from an energy point of view. Experiments were then carried out at component level. The new information from these measurements was used to calibrate and to perform more sophisticated TRNSYS simulations.

The question arose of which should come first, experiments on the product or system simulations. It would be pointless to spend time developing a TRNSYS deck to perform simulations on a system that could not be assembled. This could happen if the water-to-air heat exchangers did not work. On the other hand, it would also be pointless to design and produce a product for a system that has no benefits in terms of, for example, energy and economics, compared to already existing products. The question is central and perhaps the answer lies somewhere in between. An iterative process in which the system and the details are developed iteratively might be the best way. This thesis covers the first iteration; the second lies in the future.

1.9 Limitations

- These studies are focused on single-family houses. The solar window would perform differently if it was instead installed in an office building where the need for heat might differ markedly from that of a single-family house.
- The heat exchangers have only been tested in a laboratory. Effects from use in a real situation where there may be uneven air flow or dust on the surfaces have not been investigated.
- All of the simulations were carried out using only weather data from Sweden, and weather data from other parts of the world would have a different effect on both systems. The solar window would be controlled differently if it were placed in a warmer climate. However, the original idea for the solar window was to install it in a single-family house in Sweden. The ventilation system would also be affected by the choice of climate. A warmer climate would affect the natural ventilation, reducing the need for extra heat in the building. This will affect the annual savings, and the optimum design of the system might be different in such climates.
- The investigations/simulations have been carried out with a limited number of storage tanks, pumps, control strategies, consumption profiles etc. The effect from this is assumed to be limited since this is a comparative study.
- No costs analysis was performed for constructing the products. The work is instead focused on finding the consequences for the energy consumption when installing the different products.
- The measurement error was not calculated explicitly. The measurement error regarding the solar window is discussed briefly in Paper 1. The accuracy for the measurements regarding the heat exchanger is discussed in Appendix C.

2 TRNSYS

The thermal performance of a solar thermal collector is dependent on the irradiance to a greater extent than a PV module. Apart from external factors such as temperature, wind and irradiance, the thermal solar collectors are also highly dependent on the load and the storage capacity of the system. The annual output from a collector will vary between high and low domestic water demands. If the load is high for the system, the bottom of the storage tank will be cold due to the fresh water that is let into the tank. If the system has a low water use, the tank will be full of hot water and the inlet temperature to the collector will be high. This will lead to high thermal losses in the collector. The annual output is also dependent on when the water is used. Whether the water is used in the morning or in the evening will affect the system, since the collector will be working at different temperature levels.

In order to analyse such a complex system as a solar window, a flexible simulation tool is required. In this case TRNSYS (Klein) was used. TRNSYS is a dynamic simulation program frequently used in the field of solar energy. It has been commercially available since 1975. It was first developed by the Solar Energy Laboratory at the University of Wisconsin, USA. Since then, the program has been further developed around the world. One of main advantages of TRNSYS is the open structure that allows new components to be constructed. The various mathematical models that are used to describe the different parts in a system, e.g. storage tanks, heat exchangers and buildings, are known as types in TRNSYS. The new types are relatively easy to implement with the standard components. TRNSYS is used to investigate new energy products such as solar collectors, heat exchangers, and PV panels. Apart from products, control strategies and system solutions can also be tested. The program is very flexible.

The modern version of the interface known as Simulation Studio is shown in Figure 2.1. The figure shows how types have been linked to a deck. Each type has parameters, inputs and outputs. The parameters are fixed throughout the simulation while the inputs vary. The inputs are either fixed numbers or calculated from other types. The outputs are calculated in the specific types and then sent as inputs to other types, or as outputs

to a file. The types in TRNSYS are calculated in sub-routines of the main program. All types are calculated separately and in sequential order.

Components are often dependent on each other. For instance, the output of a solar collector depends on the temperature of the storage tank and the temperature of the storage tank depends on the output from the collector. This is solved by iteration in TRNSYS. The iteration continues until a predefined tolerance limit value is reached. If the loop for some reason does not converge, the last calculated value is used and a warning is printed to a file. After a user-defined number of warnings, the simulation is terminated and action has to be taken to solve the problem. Typically this can be to decrease the time step. The time step is the length of each calculation step. A short time step means that the outputs are calculated often. Normally this results in longer computational time but a more stable simulation.

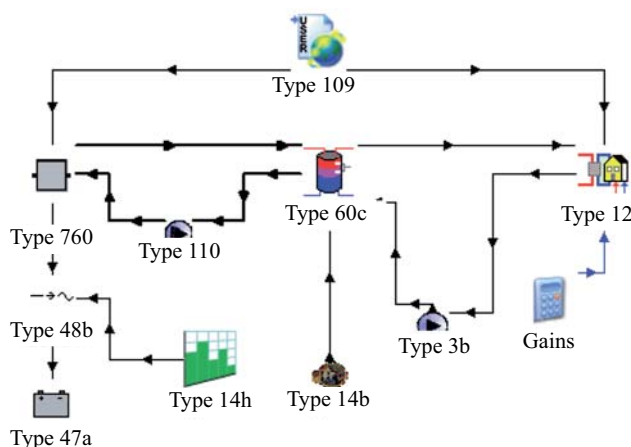


Figure 2.1 The TRNSYS deck. The different flows are marked with arrows.

Most of the different types can be found in the standard library in TRNSYS. This is the case for all the types used in this work except for the solar window. Since the solar window is a new product, a new type had to be developed. The type, given the name type 760, is written in FORTRAN. It is a direct translation from the Excel program discussed in sections 3.4 to 3.6.

The development of simulation programs for predicting energy performance of buildings, ventilation systems, solar energy systems etc. have made it possible for almost anyone to run more or less complex simulations.

While programs that are easy to handle are beneficial, there is also a risk that the results from the simulations are misinterpreted or simply wrong. Running a simulation is one thing, but understanding the limitations in the program, checking whether the results are reasonable, and understanding how to compare results, is completely different.

There are many possible sources of error. The user of the program must understand the range within which the input parameters are defined and tested. The user must understand how to perform tests to check the validity of the program. This question is so central to all simulation work that a short guideline for checking a TRNSYS program is given below. These steps, which have been followed in this report, can probably be applied when checking most simulation programs.

1. Visual. TRNSYS has a built-in function to plot the simulation results as the calculation is running, i.e. while simulating, the program simultaneously plots the results on the screen. Checking this online plot gives a quick check that the simulation is correct, and can detect, for example, whether control functions have been switched off by mistake.
2. Checking each component is also vital. If a specific flow of a certain fluid is sent to a heater delivering a specific power, it should be possible to calculate the increase in temperature. This temperature increase can easily be checked if the increase is the same as that shown on the plot produced by TRNSYS.
3. Another feature in TRNSYS is that it can calculate the energy balance in a component, in a circuit, or in the entire simulation deck. The first step is to check single components. For instance, adding all the energy components that enter to a hot water storage tank and subtracting everything that leaves should result in zero. The balance of the tank depends on energy supplied by the heater, energy taken or given to the tank by different heat exchangers, thermal losses through the shell, thermal energy stored in the tank, and possibly more if present. During a simulation, this should add up to zero, over any time frame. The same is true for a full circuit. The annual energy flow must be equal to zero.
4. Physical objects in the simulation could be connected incorrectly. Types could be run backwards or basically incorrectly, even those that are implausible, so the results must be checked to ensure that they are realistic. For example, does the added solar collector reduce the auxiliary energy need for the building? If not, it is very likely that something is wrong.

At the start of the construction of the TRNSYS deck described in Paper 6, (Davidsson, Bernardo, & Larsson, 2011), for the ventilation study, a hot water storage tank called “type 60” was used. This type was used for three tanks of different sizes in the simulation. However, this proved to be a serious mistake. A small bug in the program code for the type, supplied by the manufacturer, made it impossible to use more than one tank in a single deck. This conflicts with the manufacturer’s instructions for the type, which state that up to 5 tanks can be used simultaneously. This is a very serious problem related to all kind of simulations. In this case, the problem was that the geometry of the tank was only read once and then used for all tanks, even if different tank sizes were used. The problem was solved by using tank type 534 instead.

3 The solar window

3.1 Background

The main purpose of a window is to allow daylight into room. The solar radiation transmitted through the window also heats the building passively, which can sometimes cause an excessively high indoor temperatures unless proper shading is used when needed. A window also causes large net thermal losses during hours of cold and darkness. This means that an ideal window should have the following properties.

- During hours of darkness, it should have low U -value.
- During cold sunny hours, heat losses should still be small, and the window should also effectively transmit solar radiation to the room on the inside, i.e. have a low U -value and high total solar transmittance.
- During warm sunny hours, the solar radiation transmitted through the window should be reduced by, for example, solar shading and/or protective glazing. At the same time the window should transmit daylight into the room.

These properties were all addressed when the solar window was proposed and developed.

One objective of the solar window was to lower the cost of solar energy. There are many different ways of doing this. One example is to use a reflector for focusing solar radiation onto the PV cells, thereby reducing the needed size of PV cells. This often leads to a high cell temperature and consequently low cell efficiency. Active water cooling on the back of the cell increases cell efficiency, and can also provide hot water for domestic use. A further cost reduction is possible if the solar modules can be integrated into the building construction. Integration makes it possible to use existing frames and glazing for the solar modules or, alternatively, to replace roofing material and windows with solar modules. Wall-integrated solar collectors using reflectors have been shown to increase electrical output substantially compared to flat vertical PV modules (Gajbert, Hall, & Karlsson, 2007; Mallick, Eames, Hyde, & Norton, 2004). All these techniques are com-

bined in the solar window, which was proposed and developed by Andreas Fieber, (Fieber, 2005; Fieber et al., 2003; Fieber et al., 2004).

The solar window, see Figure 3.1, comprises solar thermal absorbers on which PV cells have been laminated. The absorbers, marked with (a) in the figure, are integrated with the inside of a standard window, marked with (c) in the figure. This saves frames and glazing of the solar modules, thereby reducing the total cost of the construction. In order to minimize the PV cell area, reflectors, marked with (b) in the figure, have been placed behind the absorbers. When the foldable reflectors are tilted to a vertical position the solar radiation is focused on the absorbers. The reflectors are insulated with EPS, which reduces thermal losses through the window. When the reflectors are tilted to a horizontal position the solar radiation is let into the building to allow passive heating. This means that in a closed position the reflectors increase the solar radiation on the cells, reduce the thermal losses through the window, and also work as a sunshade. The double glazing of the window in front of the absorbers is anti-reflection treated to maximize the solar transmittance (Chinyama et al., 1993; Nostell et al., 1999).

The solar window is not only a solar collector; it is also a sunshade that prevents overheating of the building during the summer. Other innovative solutions for sunshades in buildings have been proposed, such as using thermotropic glass with active dimming (Inoue, Ichinose, & Ichikawa, 2008) and electrochromic windows (Granqvist et al., 1998). The official homepage of IEA SHC Task 21 Daylight in Buildings (IEA) gives a good overview of different solar shading systems.

Apart from the energy aspects, the solar window also affects the daylight distribution. When the reflectors are in open mode, the light will be reflected onto the ceiling. In this way, daylight is transported away from the direct vicinity of the window to the parts further back in the room. However, this thesis is limited to the energy aspects of the solar window. Readers interested in daylight aspects of the solar window are referred to Andreas Fieber's licentiate thesis (Fieber, 2005).

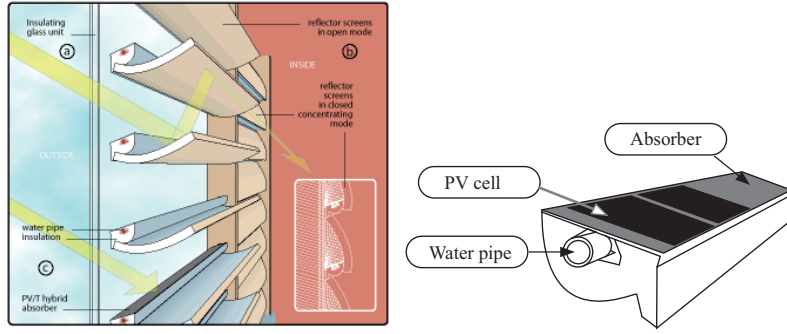


Figure 3.1 *Left: The large figure shows the solar window with the reflectors in an open mode and the inset in the lower right corner shows the solar window in closed mode. Drawings by Andreas Fieber. Right: The absorber on which the PV cells are laminated.*

The geometry of the solar window with the reflector in closed mode is shown in Figure 3.2. The optical axis of the parabolic reflector is directed 15° above the horizon with the focus on the front edge of the absorber, i.e. $v = 15^\circ$. The absorber tilt, u , is 20° . This means that all transmitted solar radiation from 15° and higher projected solar altitudes will directly reach or be reflected onto the absorber between the focal point, F , and the reflector. The focal length is denoted p , the height of the glazing H and the absorber width a . The angle w is the angle between the glazing and the optical axis and q_{NS} is the incident angle of the solar radiation projected in the north-south vertical plane. The reflector parabola is described in Equation 3.1. r is the length from F to a point on the parabola at angle φ .

$$r(\varphi) = p / \cos^2(\varphi/2) \quad \text{Equation 3.1}$$

Both H and a are determined by r and the two angles $w = 105^\circ$ and $u + v = 35^\circ$, respectively for the solar window. The ratio between H and a , which is defined as the geometrical concentration factor, is 2.45 for the construction.

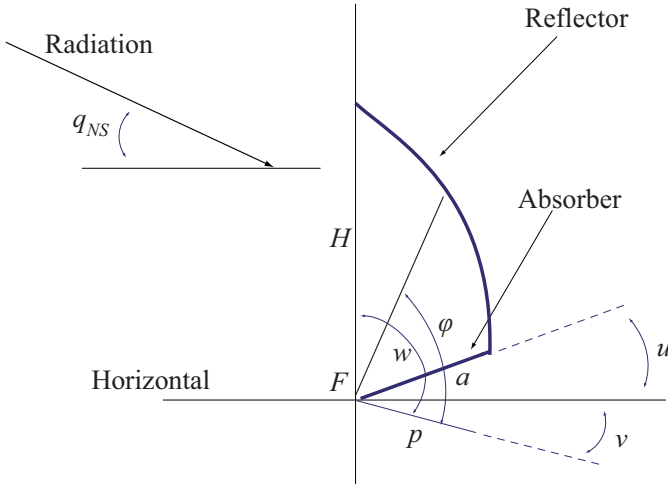


Figure 3.2 Illustration of the parabolic reflector and the absorber.

Figure 3.3 shows how the solar radiation is concentrated on the absorber. If the projected solar height is above 60° , there is no contribution from the reflector. As the projected solar height is lowered, more and more solar radiation is focused via the reflector to the absorber. At 15° solar height, the contribution from the reflector is at a maximum. If the projected solar height is below 15° the reflection will end up outside the absorber, so there will be no contribution from the reflector.

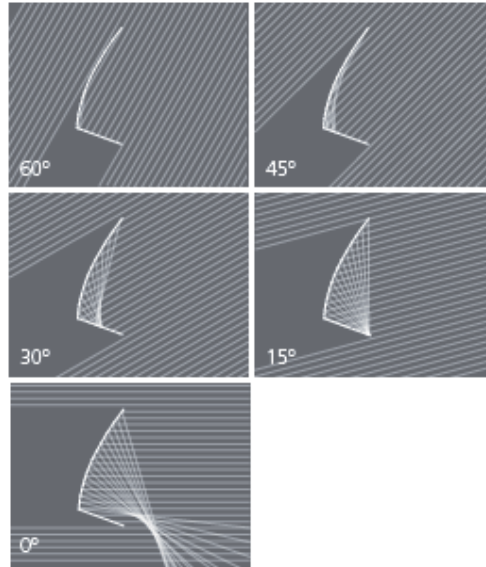


Figure 3.3 The reflection of solar radiation for different projected solar heights. All radiation between 15° and 60° is focused on the absorber. Drawings by Andreas Fieber.

3.2 Installations

Three different versions of the solar window were examined. The first was a prototype shown in Figure 3.4. It was constructed at the Älvkarleby laboratory of Vattenfall Utveckling and later tested at the Solar Laboratory of the Division of Energy and Building Design at Lund University in the south of Sweden (55.7N, 13.1E). In the prototype, consisting of five absorbers and five reflectors, the upper absorber is laminated with PV cells. The glazing of the prototype solar window is about 1.4 m² and was anti-reflection treated to minimize solar transmission losses. The complete construction was placed in an EPS box to minimize the thermal losses from the edges and the back during measurements outdoors. The window was oriented towards south during the measurements.



Figure 3.4 The prototype solar window with five absorbers and five reflectors. The uppermost absorber is laminated with PV cells.

The solar window at Solgården (60.5N, 17.4E), seen in Figure 1.7, which was the second solar window investigated, is planned for a full glazed area of 16 m². Today only 8 m² is in operation. The 8 m² collector is divided into four windows. Each window consists of eight absorbers on which eight PV cells per absorber have been laminated. The insulated reflectors are placed behind the absorbers. The glazing is anti-reflection treated in order to minimize transmission losses.

The third solar window located in Augustenborg in Malmö (55.6N, 13.0E) in the south of Sweden comprises 36 absorbers laminated with PV cells. This solar window differs from the other two in that the reflectors are not insulated and, since it was retrofitted, it has no anti-reflection treated glazing. The existing glazing was kept to minimize the cost of the construction. The absorbers are installed in a staircase in a showroom for green roofs (Scandinavian Green Roof Institute). Since the area around the district of Augustenborg has a distinct environmental profile in Malmö, it was particularly interesting to install the collector here. In this way the solar window is used not only to produce hot water and electricity but also to demonstrate to people this application of solar energy.

3.3 Measurements

The thermal and electrical output from all the three solar windows was measured. An illustration of the measurement setup from the prototype solar window can be seen in Figure 3.5.

The temperatures of the prototype solar window were measured with PT100 sensors. Both T_{in} and T_{out} were measured as close to the solar window as possible to avoid cooling the water. The water flow was measured using an inductive flow meter and the IV-characteristics were monitored simultaneously with an IV-receiver as the calorimetric measurements. The heat carrier flow and its inlet temperature were kept constant throughout each measurement. The diffuse and total solar radiation levels were measured with pyranometers. Measurements were carried out at 10-second intervals. The values were averaged and stored every 6 minutes in a Campbell CR 10 logger. The ambient temperature was monitored with a PT100 sensor.

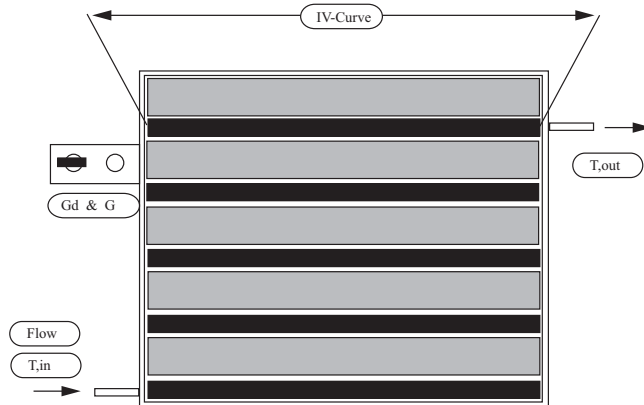


Figure 3.5 The measurement setup for the prototype solar window. T_{in} , T_{out} are the temperatures in and out of the collector. Flow is the mass flow of the circulating water. G is the total solar radiation and G_d is the diffuse radiation. IV-Curve shows where the current and the voltage were monitored.

The measurements from Solgården were carried out in a similar way using similar equipment. No IV curves were monitored and, instead, the current and the voltage given by the maximum power point tracker (MPP tracker) were monitored.

For the Augustenborg solar window, thermocouples were used to measure the temperature. This installation was also equipped with a MPP tracker, so no IV curves were monitored. The electric output was calculated from current and voltage measurements.

The measurements are further discussed in Paper 1 (Davidsson, Perers, & Karlsson, 2010).

3.4 Calculation model

A calculation model was developed in Excel to describe the solar window. The more commonly used method to evaluate a solar collector, described in Perers, (1997) could not be used for this since the amount of data and computing time to process the data would be excessive. The asymmetric concentration and the fact that it is a hybrid collector make this analysis more complicated. The measured data would have to be divided into a matrix of different solar positions. For symmetric collectors, it is enough to divide the measured data into different incidence angles for the solar radiation to the collector plane. There is no difference for different projected solar heights.

This is not the case for a solar collector with concentrating reflectors. If the projected solar height is outside the angle of acceptance, the output due to the reflector will be zero. Furthermore, the method does not allow the removal of different effects, such as shading or transmittance through the glazing. Consequently, a new model was developed for this type of collector, described in Paper 1 (Davidsson, Perers, et al., 2010). The developed Excel model was used to calculate outputs for all of the three solar windows. However, different parameters such as PV cell efficiency and shading due to the frame were used for the different windows, but the calculation model was the same for all three solar windows.

One goal of the calculation was to compare the solar window with a more standardized solar energy system made from separated flat PV modules and flat solar thermal collectors. Another goal was to study whether the solar window could be improved. The developed model was used to calculate the electrical and thermal output from all three windows, but the model could not take any dynamic effects into account. The investigation for the thermal energy production was instead carried out using the developed TRNSYS simulation deck. This is described in section 3.6 and in Paper 2 (Davidsson, Perers, & Karlsson, 2012).

The input parameters for the model are direct and diffuse solar radiation, inlet heat carrier temperature, ambient temperature and. The incidence solar angles are calculated from time, orientation, tilt and location

coordinates. The resulting output parameters are thermal energy rate and electrical power.

In order to simplify the calculations the total electrical power, P_{tot} delivered by the solar window was divided into three components, P_{dir} , P_{ref} and P_{diff} . P_{dir} is power generated by the beam solar radiation that strikes the solar cells directly, P_{ref} is power caused by the beam solar radiation passing via the reflector, and P_{diff} is the power contribution given by the diffuse solar radiation. Figure 3.6 graphically explains the three different components of solar radiation.

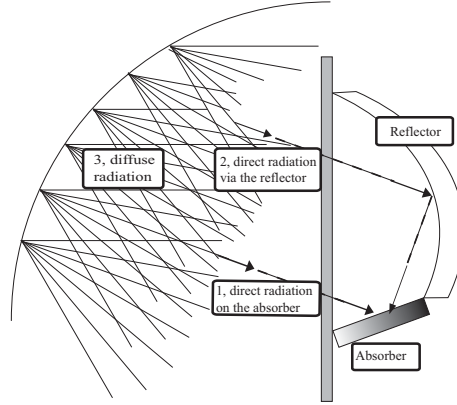


Figure 3.6 Graphical explanation of the calculation method with the three different solar radiation components.

The expression for the electrical output is shown below.

$$P_{dir} = G_{b,n} \cdot T_{glass}(\theta_1) \cdot \alpha_{pv}(\theta_2) \cdot f_s(\theta_3) \cdot A_{cell} \cdot \eta_{pv} \cdot \cos(\theta_2) \quad \text{Equation 3.2}$$

$$P_{ref} = G_{b,n} \cdot T_{glass}(\theta_1) \cdot \alpha_{pv}(\theta_4) \cdot f_{ref}(\theta_3, \theta_5) \cdot A_{ref} \cdot \eta_{pv} \cdot R_{ref} \cdot \cos(\theta_5) \quad \text{Equation 3.3}$$

$$P_{diff} = G_d \cdot C_1 \text{ or } G_d \cdot C_2 \quad \text{Equation 3.4}$$

$$P_{tot} = P_{dir} + P_{ref} + P_{diff} \quad \text{Equation 3.5}$$

$G_{b,n}$ and G_d are the solar beam and diffuse solar radiation against the window. T_{glass} is the angular dependent solar transmittance through the glazing, α_{pv} is the angular dependence of the efficiency of the PV cells, and f_s corrects for the shading of the PV cells caused by the window frame. f_{ref} is a correction factor for the shadow effects of the solar radiation that is reflected. This function includes the shading of the reflector and is

dependent on both the azimuth angle, θ_2 , and the projected solar height to the reflector plane, θ_5 . The angles θ_1 to θ_5 are the incidence angles for the beam towards the components of the solar window. A_{cell} and A_{ref} are the areas of the PV cells and the reflector plane respectively.

The reflector plane is illustrated in Figure 3.7 η_{pv} and R_{ref} are the efficiency of the solar cells and the reflectance of the reflector. C_1 or C_2 are constants to calculate the contribution from the diffuse solar radiation. The constants were obtained from measurements during cloudy days, when the beam solar radiation has negligible influence on the performance. Measurements were performed with the reflector in both horizontal and vertical positions, allowing both constants to be determined. C_1 is for the horizontal reflector position C_2 is for the vertical reflector position.

The transmittance, T_{glass} , through the window was calculated using the Fresnel Equations and Snell's Law. The shading factors f_s and f_{ref} were calculated theoretically from the PV/T window geometry. Measurements determined the angular dependence of the PV cells, α_{pv} . The investigation of the angular dependence for the PV cells is discussed in section 3.5.3.

In order to calculate thermal output from the solar window some of the parameters from the electrical calculations had to be replaced by parameters related to the thermal absorbers.

$$Q_{dir} = G_{b,n} \cdot T_{glass}(\theta_1) \cdot f'_s(\theta_3) \cdot A_{abs} \cdot \eta_{abs} \cdot \cos(\theta_2) \quad \text{Equation 3.6}$$

$$Q_{ref} = G_{b,n} \cdot T_{glass}(\theta_1) \cdot f'_{ref}(\theta_3, \theta_5) \cdot A_{ref} \cdot \eta_{abs} \cdot R_{ref} \cdot \cos(\theta_5) \quad \text{Equation 3.7}$$

$$Q_{diff} = G_d \cdot \dot{C}_1 \text{ or } G_d \cdot \dot{C}_2 \quad \text{Equation 3.8}$$

where A_{abs} and η_{abs} are the area and the absorbance for the thermal absorber; f'_s describes the shading of the thermal absorber caused by the window frame; f'_{ref} is the correction factor for the thermal energy production for the shadow effects of the solar radiation that is reflected; \dot{C}_1 and \dot{C}_2 are the constants to calculate the contribution to the thermal energy production from the diffuse solar radiation.

In order to calculate thermal output, a fourth term must be added to describe the thermal losses in the absorber. The thermal losses $q_{loss,p}$ for the prototype solar window and $q_{loss,s}$ for the Solgården solar window are shown in Equation 3.9 and Equation 3.10. Since the solar window in Solgården experiences thermal losses at two different temperatures, the ambient temperature and the indoor temperature, two different U -values were used. $U_{s,out}$ is the thermal loss to the outside and the $U_{s,in}$ is the thermal loss to the inside. A_w is the total window area. ΔT_{out} is the difference between the average heat carrier temperature and the ambient temperature. ΔT_{in} is the difference between the average heat carrier temperature and

the indoor temperature. The U -values were estimated from heat transfer analyses. This is discussed later in section 3.5.7. U_p is the U -value for the prototype solar window and ΔT is the difference between the average heat carrier temperature and the ambient temperature.

$$q_{loss,s} = U_{s,out} \cdot A_w \cdot \Delta T_{out} + U_{s,in} \cdot A_w \cdot \Delta T_{in} \quad \text{Equation 3.9}$$

$$q_{loss,p} = U_p \cdot A_w \cdot \Delta T \quad \text{Equation 3.10}$$

The total delivered heat rate can be calculated according to Equation 3.11.

$$Q_{tot} = Q_{dir} + Q_{ref} + Q_{diff} + q_{loss} \quad \text{Equation 3.11}$$

where q_{loss} is either $q_{loss,s}$ or $q_{loss,p}$ depending on which solar window being investigated.

The calculations were carried out in six-minute time steps using weather data monitored at the locations for the solar windows.

Calculation methods for the Augustenborg solar window were the same as those for the prototype solar window.

3.5 The parameters

In order to perform the calculations, all the parameters and functions described in Equation 3.2 - 3.10 must be known. Sections 3.5.1 to 3.5.7 explain how these parameters and functions are calculated.

3.5.1 Radiation, angles, θ

Solar radiation was monitored in the plane of the glazing for all installations. However, the calculation model also needed to include the solar radiation on a number of different surfaces as input, so this had to be calculated for each surface. For example, the solar radiation on the absorber is a function of the incidence angle for the absorber, θ_2 . Furthermore, θ_5 needs to be known in order to calculate the solar radiation on the reflectors. The normal to the reflector was approximated with the normal to the reflector plane, which is the plane connecting the endpoints of the curved reflector. An illustration of the different angles of incidence can

be seen to the left in Figure 3.7. To the right is an illustration of how the incidence angles between the solar radiation and the different surfaces change on 5 July.

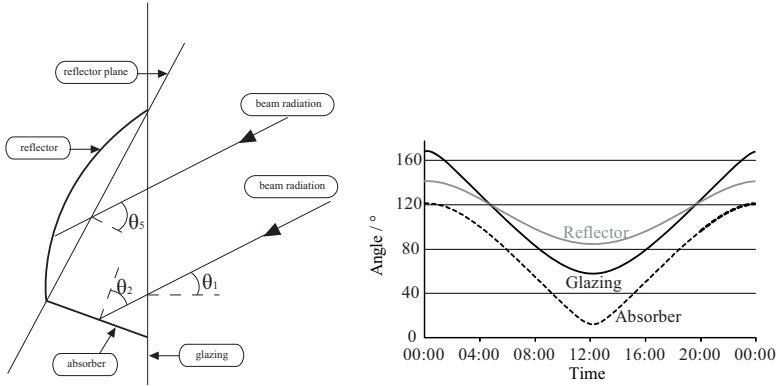


Figure 3.7 Left; angles of incidence for the solar radiation towards the glazing, θ_1 , the absorber, θ_2 , and the reflector plane, θ_5 . Right; example of the incidence angles for the solar radiation against the glazing, in black, the absorber, in dashed line, and the reflector, in grey.

3.5.2 Transmission through the glazing, T_{glass}

Transmission through the glazing was calculated theoretically using the Fresnel Equations and Snell's Law. Figure 3.8 shows transmission through a standard double-glazed window and a double anti-reflection treated window. The glazing of the prototype solar window and the Solgård solar window is anti-reflection treated while the Augustenborg solar window has a standard glass without anti-reflection treatment. The Augustenborg solar window therefore suffers much greater losses due to the low transmission of the glazing.

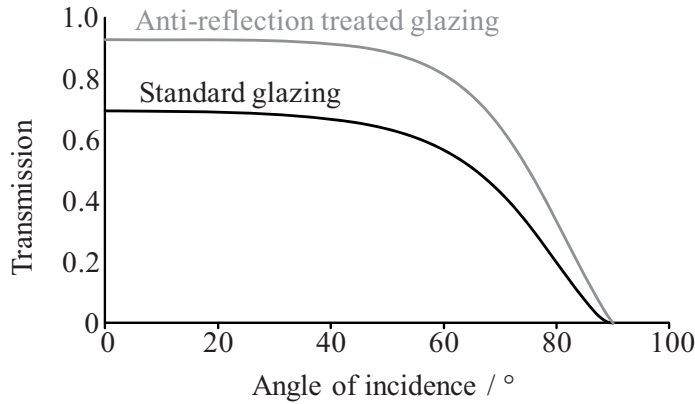


Figure 3.8 Transmission through different types of glazing. Standard double glazing in black and anti-reflection treated double glazing in grey.

3.5.3 Angular dependence of PV cell, α_{PV}

Measurements were performed to determine the angular dependence of a PV cell. The experiment is dependent on parallel solar radiation without disturbing reflections. The experiment could therefore be performed in a box painted black on the inside. The PV cell was attached to a rotatable bar connected to a potentiometer. This can be seen in Figure 3.9. As the bar is turned, the potentiometer monitors the rotation angle. The PV cell and the potentiometer were connected to a logger for easy measurement. The experiment was carried out using a flood light. The hole for the incoming light was large enough for the whole PV cell to be illuminated during all measurements.

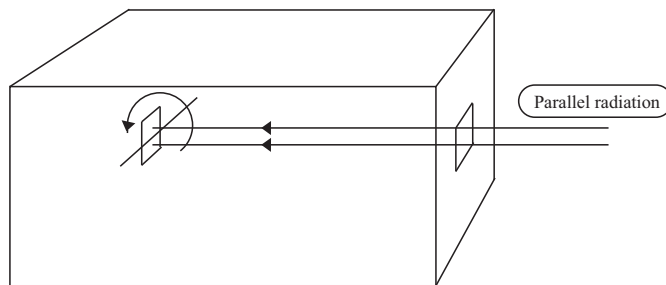


Figure 3.9 Measurement setup to determine the angular dependence of a PV cell. The black-painted box reduces the disturbing reflections in the box. The PV cell is located in the centre of the box. The PV cell and a potentiometer are connected to a logger.

The results from the measurements are presented in Figure 3.10. As can be seen in the figure, the PV cell has a low angular dependence for angles below 60°. Above 60° the output falls quickly. This result was used for all three solar windows.

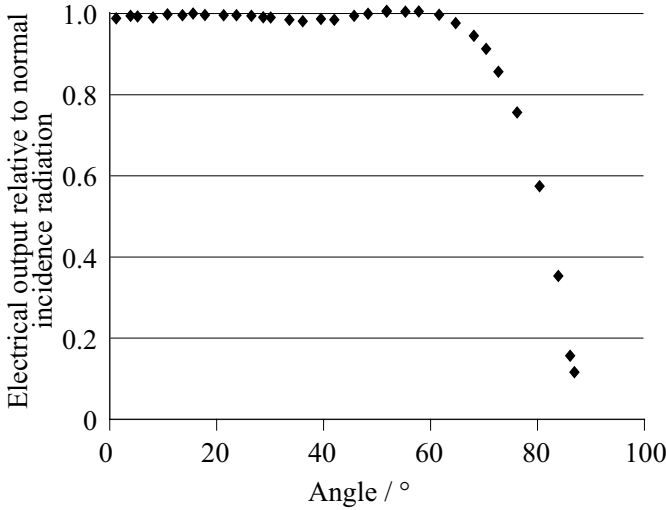


Figure 3.10 Measured angular dependence of a PV cell.

3.5.4 Shading, f_s

Shading is a problem for the solar windows since they are located on the inside of a standard window, and shaded by the window frames and mouldings. A theoretical calculation was performed to determine the amount of shading as a function of the solar azimuth angle. The presented investigation was used for all three windows, both for the electrical and the thermal calculations. Since the most shaded cell determines the electrical output, only the outer cells were investigated. Figure 3.11 shows a sketch of the shading geometry in principle.

As can be seen in Figure 3.12, the PV cells suffer from losses due to shading caused by the window frame from azimuth angles approximately above 30° and below -30° if the window faces south. At noon the shading is zero. The effect of shading the thermal absorber is also shown in the figure. It is clear that the shading will have a much smaller influence on the thermal output than on the electrical output. The impact of shading on the results of the three different solar windows differs slightly due to different geometries. The impact, shown in Figure 3.12, is calculated for the prototype solar window.

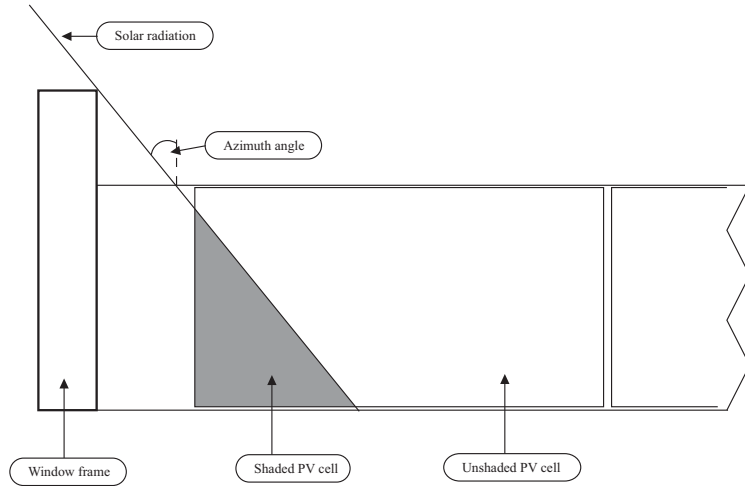


Figure 3.11 Principle sketch of the shading of the absorber with the PV cells due to the frame seen from above. In the sketch about 20% of the outermost cell is shaded.

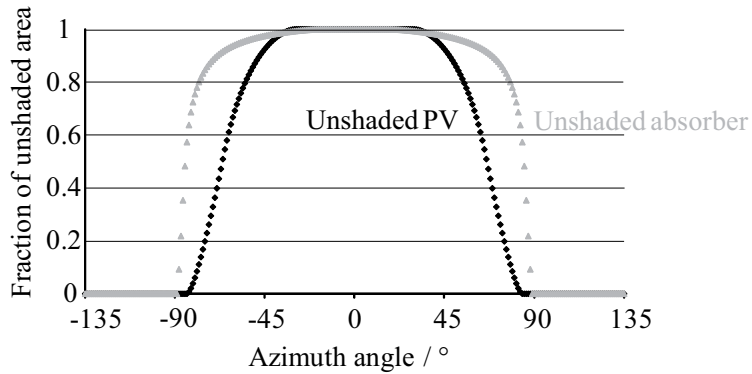


Figure 3.12 Fraction of unshaded area of the PV cell in black and of the thermal absorber in grey. The results are from the prototype solar window facing south.

3.5.5 Reflector contribution, f_{ref}

The contribution of electrical and thermal energy due to the reflectors is diminished by the shading caused by the window frames in. Calculating the contribution of the reflectors to the output is therefore one of the most complicated parts of the model. When the projected solar height is 15° ,

all the solar radiation impinging on the reflector will be reflected onto the focal point at the front edge of the PV cells. If the projected solar height is larger than 15° but less than 60° , the reflected solar radiation will be distributed throughout the absorber. This is illustrated in Figure 3.13 for a projected solar height of 25° .

The data in the figure were calculated using the ray tracing software Zemax (Zemax). As can be seen, most of the reflected solar radiation impinges on the absorber between 20 to 30 mm from the front edge. This is often referred to as the light band. In order to simplify the calculations, the centre of reflection was determined. It is defined as the line on the absorber where 50% of the reflected solar radiation is on either side of the line, see Figure 3.13. For the projected solar height of 25° , the centre of reflection was determined to be 25.9 mm from the front edge. In Figure 3.14 the centre of reflection is shown for different projected solar heights in the same diagram. In the calculations for the contribution from the reflected radiation all this radiation, is assumed to end up on this line.

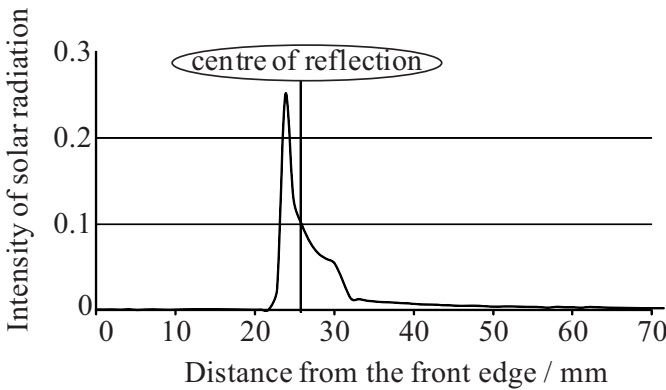


Figure 3.13 The distribution of solar radiation on the absorber from solar radiation with a projected solar height of 25° , which was reflected by the reflector onto the absorber. The centre of reflection, marked with a black line, is 25.9 mm from the front edge.

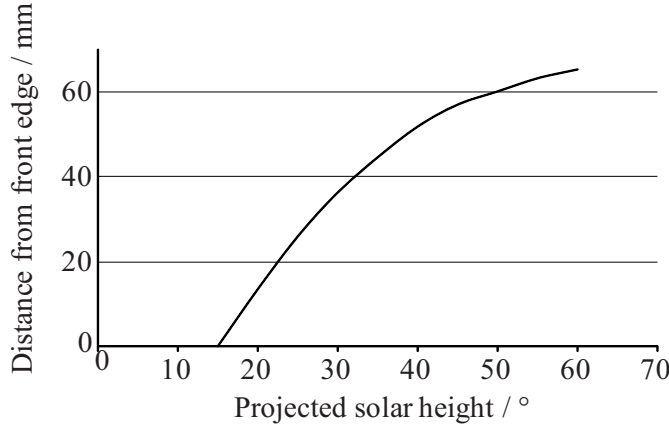


Figure 3.14 The centre of reflection as a function of the projected solar height.

The “centre of reflection” is an approximation of where in the north-south direction the reflected radiation impinges on the absorber. When it is known, together with the solar angles and the geometry of the window, the points A and B in Figure 3.15 can be determined. A is the point where some beam radiation from the reflector is beginning to impinge upon the absorber, coming from only the lower part of the reflector. B is the point where all beam solar radiation is beginning to impinge upon the absorber unshaded, emerging from all parts of the reflector. It is assumed that the increase of solar radiation from A to B is linear, so point B will be fully illuminated and A will be the starting point of solar radiation. Figure 3.15 illustrates the path of the solar radiation to the PV cell via the reflector. The degree of illumination caused by the reflector for the partly shaded PV cell, shown in Figure 3.16 can be calculated using Equation 3.12.

$$f_{ref}(\theta_3, \theta_5) = \frac{0.5 \cdot X_2 + X_3}{X_1 + X_2 + X_3} \quad \text{Equation 3.12}$$

where X_1 is the distance from the beginning of the PV cell to A, which is where reflected beam radiation starts to impinge on the absorber. X_2 is the distance between A and B and X_3 is the distance from B, which is the part that is fully illuminated to the end of the cell. $f_{ref}(\theta_3, \theta_5)$ is the degree of illumination for the total cell. See Figure 3.16 for an explanatory illustration.

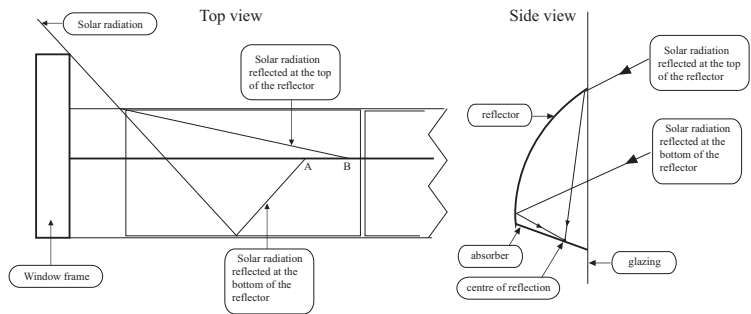


Figure 3.15 The reflection of solar radiation. Left: seen from above, A is where the solar radiation reflected from the lower part of the reflector impinges and B is where the upper part of the reflector impinges. Right: seen from the side, all the solar radiation reflected along the reflector is assumed to end up on the same line, the centre of reflection.

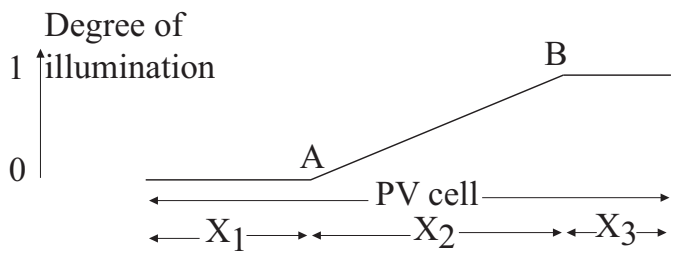


Figure 3.16 The solar radiation distribution on the PV cell as a function of distance from the edge. A is the point where the solar radiation reflected from the lower part of the reflector impinges and B is where the upper part of the reflector impinges.

3.5.6 Diffuse solar radiation, C

Measured data was analysed for the three different solar windows in order to investigate the influence of diffuse solar radiation on the total electric and thermal output. Choosing the cloudiest days and plotting the produced current versus the diffuse solar radiation produces the results shown in Figure 3.17 The constants C_1 and C_2 in Equation 4 for horizontal reflectors were, $C_1=0.002$, and for vertical reflectors, $C_1=0.0026$. C_1 and C_2 are the proportionality constants for the relationship between incident diffuse solar radiation on the solar window and the electrical output. The same

method was used to determine the influence of diffuse solar radiation on the thermal output.

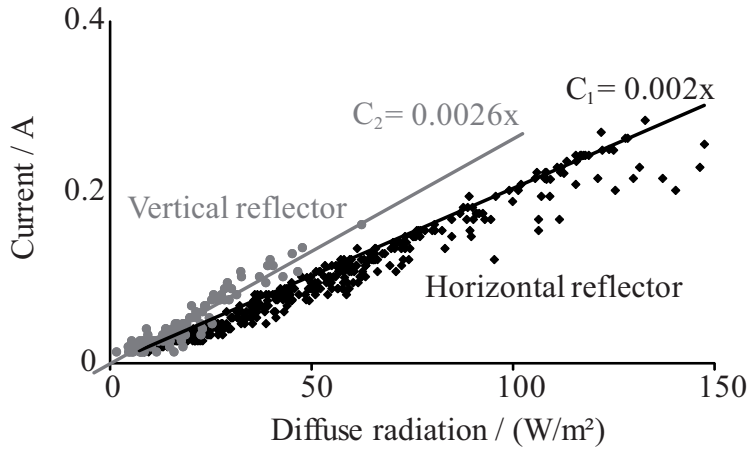


Figure 3.17 The influence of the diffuse solar radiation on the electrical output. Results using horizontal reflectors are in black and vertical reflectors in grey.

A way to validate C_1 and C_2 is to plot the simulated and the measured electrical output on the same graph. The influence of the direct solar radiation is almost zero on the cloudiest days. This is shown in Figure 3.18. This graph indicates that the electrical output due to the diffuse solar radiation is modelled accurately. The periods marked with grey in the graph are periods where the direct solar radiation has little or no influence on the electrical output. The period marked with white shows a period where the direct solar radiation plays a small role in the total output, i.e. a period with both direct and diffuse solar radiation. The model is also accurate during this period.

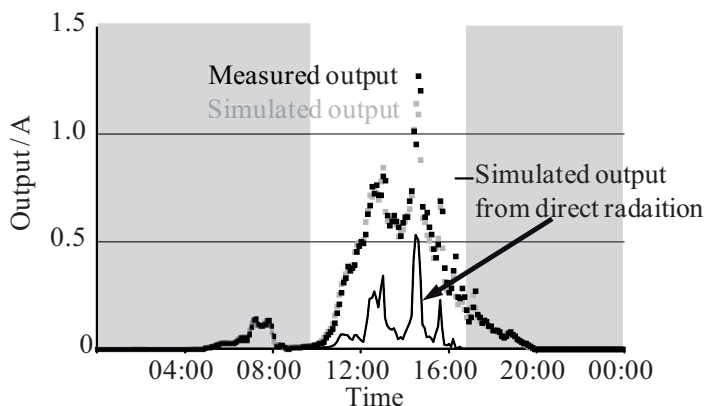


Figure 3.18 Contribution of diffuse solar radiation to the electrical output. The black dots are the results from calculations while the grey dots are from measurements. The black line shows the part of the output that is due to direct solar radiation. The areas marked with grey are periods with little or no influence due to direct solar radiation, and the white area is from a period with a significant contribution from direct solar radiation to electrical output.

3.5.7 Thermal losses, U

Prototype solar window

The thermal measurements were performed using three different inlet temperatures, 30°C, 45°C and 60°C, to the collector. Since the pump was running continuously, the values from the night could be used to determine the thermal losses without impact from the solar radiation. The result can be seen in Figure 3.19.

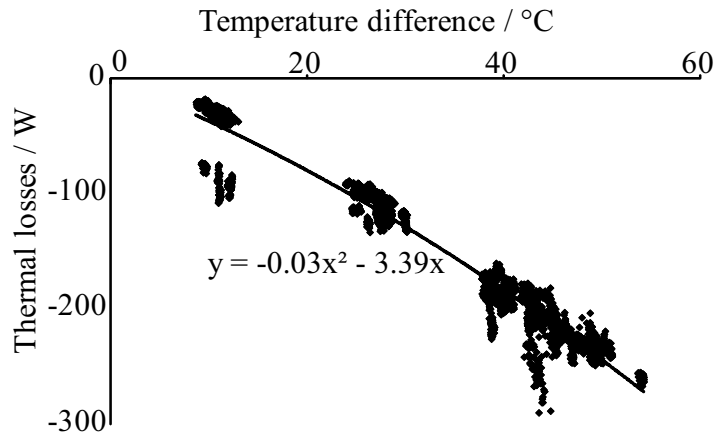


Figure 3.19 Thermal losses from the prototype solar window.

Solgården solar window

Whether the heat is lost backwards or outwards is insignificant for the performance of the prototype solar window. This will not be the case for the Solgård solar window. If the losses are to the front, i.e. to the outside of the window, the heat is lost. If the heat is dissipated backwards, i.e. to the building, the energy is utilized as passive heating in the house. The losses in different directions for the solar window could not be measured, so the U -values of the solar window in the two directions were derived theoretically. Since the total thermal losses from the solar window were measured, the calculations of the total losses could be calibrated. The calculations are presented below.

The calculations are divided into four cases: closed reflectors with heat loss into the building (case 1), closed reflector with heat loss out through the window (case 2), open reflectors with heat loss into the building (case 3), or open reflectors with heat loss through of the window to the outside (case 4). Figure 3.20 shows the different cases.

General

When the measurements and the calculations were performed, the solar window was not completed. The insulation on the back of the reflector was still to be attached. All the calculations are therefore based on the status of the window at the time of measurement.

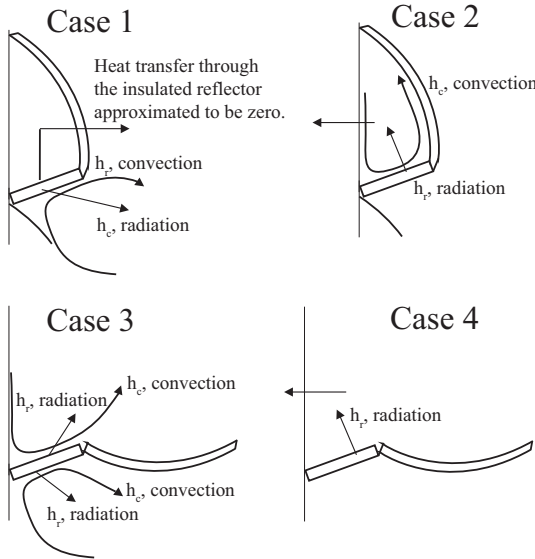


Figure 3.20 Thermal losses from the solar window. Case 1: closed reflectors, losses to the room. Case 2: closed reflectors, losses to the outdoor surroundings. Case 3: open reflectors, losses to the room. Case 4: open reflectors, losses to the outdoor surroundings.

Assumptions

- All cases: the same convection and radiation heat transfer coefficients used.
- Case 1: no losses through the insulated reflector.
- Case 2: $\varepsilon_{eff} = \varepsilon_{abs} = 0.9$ since all the emitted radiation from the absorber is assumed to end up on the glass due to reflections in the reflector. The absorber is small in comparison to the glazing.
- Case 3: all convection losses end up in the room. Half the radiation is radiated towards the glazing and half towards the room.
- Case 4: no contribution from absorber convection to the outside. All the convection losses end up inside the building.

The heat radiation losses for a body can be calculated using the formula $q_r = \varepsilon_{eff} \sigma T^4$, where ε_{eff} is the effective emissivity and $\sigma = 5.67 \cdot 10^{-8}$ is the Stefan-Boltzmann constant. An expression for the heat loss coefficient due to radiation can be derived according to Equation 3.13 to Equation 3.18.

$$q = \varepsilon_{eff} \sigma (T_h^4 - T_c^4) \quad \text{Equation 3.13}$$

$$q = \varepsilon_{eff} \sigma (T_h^2 + T_c^2)(T_h + T_c)(T_h - T_c) \quad \text{Equation 3.14}$$

$$\Delta T = (T_h - T_c) \rightarrow \quad \text{Equation 3.15}$$

$$\rightarrow h_r = \frac{q}{\Delta T} = \varepsilon_{eff} \sigma (T_h^2 + T_c^2)(T_h + T_c) \quad \text{Equation 3.16}$$

$$T_m = \frac{T_h + T_c}{2} \rightarrow \quad \text{Equation 3.17}$$

$$h_r \approx 4\varepsilon_{eff} \sigma \cdot T_m^3 \quad \text{Equation 3.18}$$

T_m is the mean temperature of the absorber and the surrounding colder object, e.g. the inner pane of the glazing. The heat loss coefficient due to convection, h_c , can be calculated for the specific case but values from Swedish and European standards, of 3.6 W/m²K were used instead (EN, 1997; SIS, 2005). In the standard, the value is used for convection heat losses between the room air and the inner glass surface of the window. Since the outdoor air intake for the ventilation of the building is located directly in front of the solar window, this number is assumed to be somewhat higher. The approximate value of $h_c = 4 \text{ W/m}^2\text{K}$ was therefore used in the calculations.

The contribution to the total thermal loss, h_{top} from convection and radiation is summed up in Equation 3.19. In Equation 3.20 this number is divided by the concentration factor, c , of the geometry to obtain the heat transfer coefficient, h , per glazed area instead of per absorber area.

$$h_{tot} = h_c + h_r \quad \text{Equation 3.19}$$

$$h = \frac{h_{tot}}{c} \quad \text{Equation 3.20}$$

Two of the cases described above are calculated in more detail below.

Case 1: closed reflectors, heat losses to the room.

Assuming a mean temperature of 300 K (27°C) and $\varepsilon = 0.9$ results in:

$$h = \frac{h_{tot}}{c} = \frac{h_c + h_r}{c} \approx \frac{4\varepsilon_{eff}\sigma \cdot T_m^3 + h_c}{c} \approx \frac{5.5 + 4}{2.45} \approx 3.9 \text{ W/m}^2\text{K} \quad \text{Equation 3.21}$$

Case 2: closed reflectors, heat losses to the surroundings.

For case 2 a, calculation technique with a thermal network is used for the analysis. The same heat transfer coefficients as in case 1 are used. The convective heat transfer coefficient between the heated air and the inner glass pane is assumed to be $4 \text{ W/m}^2\text{K}$, corresponding to a heat resistance of $0.25 \text{ m}^2\text{K/W}$. The heat resistance is defined as the inverse of the heat transfer coefficient. The full calculation is easier to understand using the analogy of electrical circuits. In Figure 3.21 the total resistance, m_{tot} , is calculated using the thermal resistance between the inner glazing and the outdoor air, m_g , the radiative resistance between the absorber and the inner glazing, m_r , the convective resistances from the absorber to the air pocket, m_{c1} and from the air pocket to the inner glazing, m_{c2} . m_g was calculated as the difference between the full resistance from the inside of the room to the outdoor air and the resistance to the inside of the inner glazing due to radiation and convection. The U -value of double glazing was estimated to be $3.0 \text{ W/m}^2\text{K}$ (Pilkington, 2002), thereby producing a resistance of $1/3 \text{ m}^2\text{K/W}$. The resistance to the inside of the inner glazing was set to $1/8 \text{ m}^2\text{K/W}$ (EN, 1997), so m_g was estimated to be $0.21 \text{ m}^2\text{K/W}$. In Figure 3.21, this formula is displayed. The total resistance is $0.5 \text{ m}^2\text{K/W}$, so the heat transfer coefficient is calculated to be $2.0 \text{ W/m}^2\text{K}$.

Mode 2

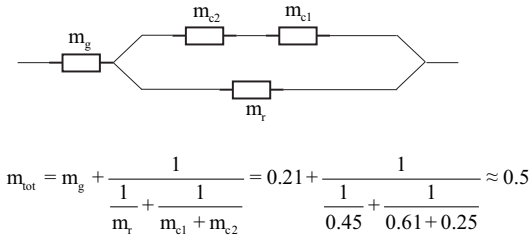


Figure 3.21 The analogy between heat transfer resistance and electrical resistance. m_g is the resistance in the glazing, m_r is the resistance for the radiation, m_{c1} is the resistance for the convection from the absorber to the air and m_{c2} is the resistance for the convection from the air to the glazing.

Performing the same kind of calculations for case 3 and case 4 results in heat transfer coefficients between the absorber and the surrounding, based on glazing area of $5.9 \text{ W/m}^2\text{K}$ (case 3) and $1.3 \text{ W/m}^2\text{K}$ (case 4). The results are summarized in Table 3.1.

Table 3.1 The thermal losses for the solar window.

Heat transfer coefficients / (W/m ² K), Solar window PV/T Collector				
Closed/open case	Closed window		Open window	
Direction of thermal loss	In	Out	In	Out
Standard Window	3.9	2.0	5.9	1.3

Discussion

The calculations described above contain uncertainties. The complex design of the collector creates air pockets between absorber and reflector, resulting in air movements in the space between reflectors and glazing that give rise to a heat transfer that could be difficult to estimate accurately. In addition, the solar window is located in front of a ventilation air exhaust. This also adds uncertainty to the calculations. However, the total thermal losses are included in the validation of the model, see section 3.7. As can be seen in Figure 3.27, there is a high correlation between measurements and calculations. This indicates that the U -values found in the calculations are reasonable. However, in the calculations, when using open reflectors, all the convective heat losses from the solar window are assumed to be utilized as passive heating in the building. This means that the thermal energy gains from the solar window to a building are slightly overestimated.

3.5.8 Passive gains

Placing absorbers in a window will influence the amount of solar radiation transmitted as passive heating to the room. This effect has to be taken into account when evaluating the Solgård solar window. When the reflectors in the solar window are closed, no solar radiation is transmitted into the building. This is both positive and negative for the energy balance. During the summer, this is positive, as the overheating of the building is limited. During the winter, this might be negative, as the free solar energy through the windows contributes to heat the building. Even if the reflectors are open, there will still be large losses of passive heating compared to a standard window, as the absorbers are blocking parts of the incoming solar radiation. This is illustrated in Figure 3.22.

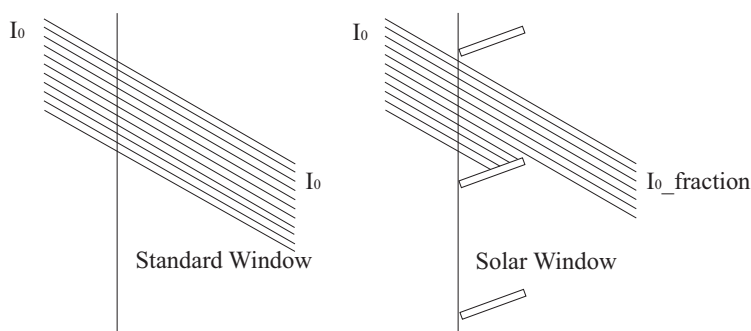


Figure 3.22 Left: transmission through a standard window. Right: transmission through the solar window.

The amount of solar radiation let into the building varies with solar height. This is shown in Figure 3.23. The figure shows that all beam solar radiation above 60° projected solar altitude is transmitted through the glazing impinging on the absorbers, leaving only some thermal losses and a small amount of reflected light. This is mostly positive because radiation from these angles only occurs during the summer when no extra heat is wanted in the building. This is also illustrated in Figure 3.24, which gives the same information as Figure 3.23, but in numerical form. The latter figure shows the fraction of transmitted beam solar radiation to the room compared to the amount of beam solar radiation impinging on the window.

Integration of the diffuse sky radiation results in approximately 35% being transmitted into the building.

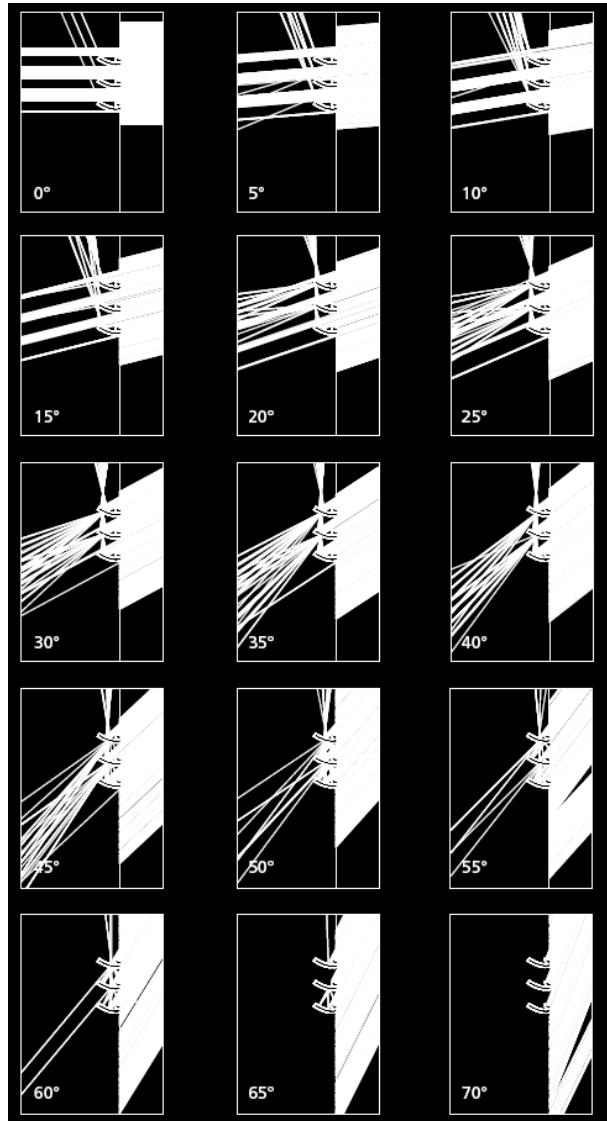


Figure 3.23 The amount of solar radiation transmitted into the building as a function of the projected solar height. Drawings by Andreas Fieber, (Fieber, 2005).

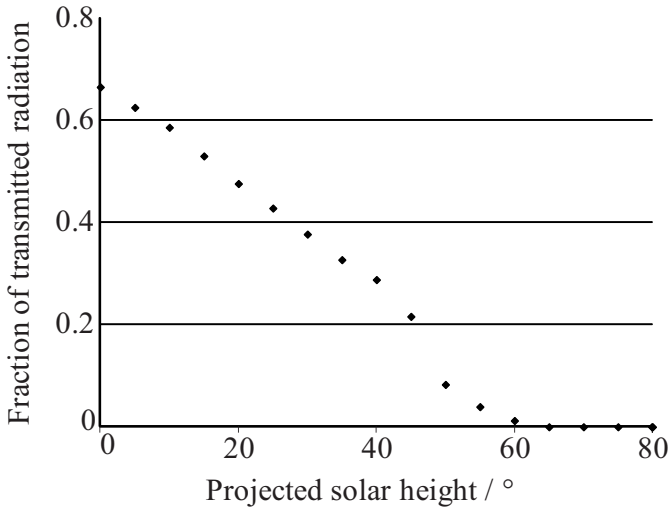


Figure 3.24 The fraction of transmitted solar beam radiation compared to the total solar beam radiation impinging on the window when the reflectors are in the open mode.

3.5.9 Control strategies

The tiltable reflectors can be put in two positions, open (horizontal) or closed (vertical). How to place the reflector is an equation with many parameters. Day lighting, aesthetics, electrical and thermal energy and thermal comfort will all be affected by the choice. How to control the reflectors will be a personal choice of the user. The control strategies discussed in this thesis mainly focus on lowering the thermal energy consumption for the user.

If all energy flows, such as thermal losses, passive heating and electrical energy production from the solar window are known, a decision can be made whether the reflectors are to be closed or open. Different control strategies for opening and closing the reflectors were evaluated. The tiltable reflectors in the solar window were controlled using four different monitoring mechanisms. The control strategies, also discussed in Paper 2 (Davidsson et al., 2012) are listed below.

1. Always open, horizontal reflectors.
2. Always closed, vertical reflectors.
3. The reflectors are open if the solar radiation impinging on the window is between two user-defined values. If the solar radiation falls below

the interval, the reflectors close in order to decrease the U -value of the window and prevent the building from cooling down. If the solar radiation exceeds the interval the reflectors close to avoid overheating of the building.

4. If the temperature in the building falls below a user defined value, the window will be controlled to, if possible, heat the building. This means that the model calculates the energy balance for open reflectors and for closed reflectors and then selects the most favourable alternative in terms of energy. If the indoor temperature exceeds the upper user defined value, the window tries to minimize the thermal energy admitted into the building. This means that during periods with overheating, the reflectors will typically be closed during daytime to hinder the passive heating and open at night in order to increase U -value and thereby ventilate the heat out of the building. If the temperature is between the two stated temperatures, the window will be closed to fill the batteries and the collector tank to a pre-set level. When this condition is fulfilled the reflectors will be opened for aesthetic reasons.

3.6 TRNSYS, the solar window

The thermal part of the solar window is part of a system for a number of reasons. One is that the temperature of the incoming heat carrier is dependent on the temperature and size of the storage tank. Furthermore, the window will block parts of the radiation in the window, so it will lower the amount of passive heating for the building. This is why the evaluation of the thermal properties of the solar window had to be carried out on a system level.

The most important types (models) used in the TRNSYS simulation for the solar window are discussed in Paper 2 (Davidsson et al., 2012). The following complements the paper.

- The inlet heat carrier temperature for the domestic hot water was set continuously to 10°C.
- The heater in the storage tank was set to 60°C with a dead band of 5°C.
- The temperature of the hot water removed from the storage tank for domestic hot water was not regulated apart from the auxiliary heater in the storage tank heating it to 60°C. This means that the delivered water has the temperature equal to the temperature at the top of the tank where the heat exchanger outlet is located.
- The auxiliary energy is added in the upper part of the storage tank.

- The indoor temperature for the building was set to 21°C. No cooling was considered.

Since the solar window is a new product there was no existing type available. The solar window model, given the TRNSYS type number 760, is constructed as a translation from the developed Excel sheet used to evaluate the prototype solar window. Type 760 has the option to choose control strategy for the reflectors as discussed in section 3.5.9.

Before the actual calculation starts in the program, four matrices are read from files that describe the reflectors. These matrices describe the impact of the reflectors on both the thermal and the electrical output from the solar window. Two of the matrices are for thermal calculations and the other two for electrical calculations. The matrices describe the solar radiation on the absorber due to the reflector on 11 different days of the year. Each day is divided into 240 points, i.e. every six minutes. Other days are interpolated from the existing data. The program then calculates all the different limiting factors described in Equation 2-5 in section 3.4. The various limiting factors are described with a polynomial of the 6th degree. Using a polynomial has no physical meaning but makes the calculations easy and fast. After this, P_{dir} , P_{ref} , P_{diff} and so P_{tot} are calculated, see section 3.4. The thermal calculations are carried out in the same way. The only difference is the iteration performed to calculate the temperature of the absorber. The passive gains from the window are also calculated. This calculation is performed for two cases, open or closed reflectors. If the reflectors are open the passive gains are calculated to be

$$P_g = P_D + P_d + P_t \quad \text{Equation 3.22}$$

where P_g is the total passive gains, P_D is the passive gains due to direct solar radiation that goes between the absorbers and is transmitted to the room, P_d is the passive gains due to diffuse solar radiation that goes between the absorber and is transmitted to the rooms, and P_t is the thermal losses from the absorbers that is lost to the room. In the case of closed reflectors, P_D and P_d will be zero and P_t will decrease compared to open reflectors. See Figure 3.25 for an explanatory sketch. The effects of lowering the U -value of the building when the window is closed are added separately outside the type 760. This is possible since one of the outputs from type 760 is whether the reflectors are open or closed.

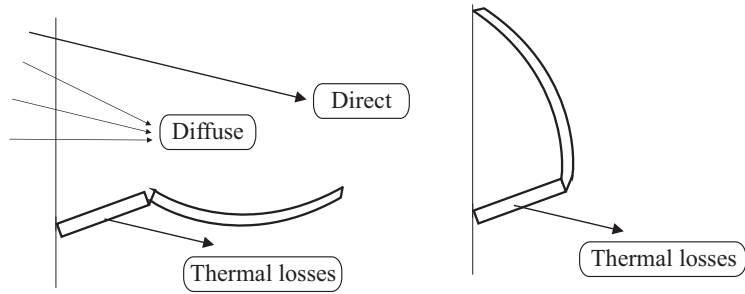


Figure 3.25 *Passive gains to the building. Left: open reflectors allow solar radiation to enter the room. Right: closed reflectors block solar radiation from entering the room.*

The last step in the program is to decide whether the reflectors are to be open or closed. The annual auxiliary energy need for a building including a solar window using control strategies 1 and 2 is simple to calculate, since by definition the reflectors are always open or always closed. The annual auxiliary energy need using control strategy 3 is also simple to calculate, since the reflectors are to be open if the solar radiation is in the interval stated in the parameter list for the type.

Control strategy 4 is more complicated. This control strategy requires that the total energy balance is calculated for open and closed reflectors. The best option is then chosen. If the temperature in the building is below the lower control parameter, the reflectors will be used to maximize the energy flow into the building. If the temperature is above the higher parameter, the opposite will happen, i.e. the reflectors will maximize the energy flow out of the building. If the temperature is between the parameters, the reflectors will be closed to maximize the energy production in the solar window. The energy balance is shown in Figure 3.26. If the reflectors are closed instead of open, the U -value of the building is lowered, less solar radiation is admitted into the building and the thermal energy production is high in the absorbers. Summing up all thermal contributions and comparing them to each other makes it possible to decide whether or not to open the reflectors.

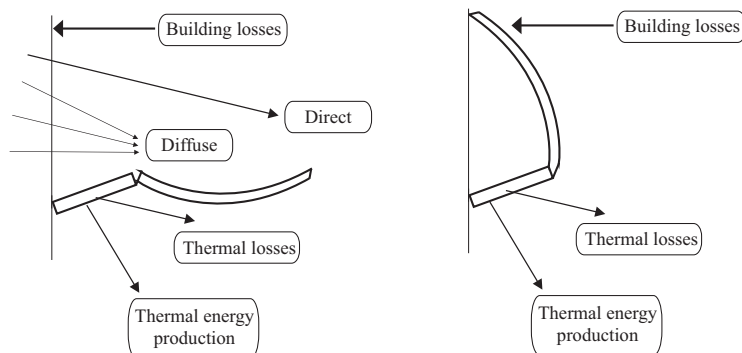


Figure 3.26 The two different situations for the thermal balance calculations. The most favourable in terms of energy is chosen by control strategy 4.

3.7 Evaluation

The results from the Excel model calculations were validated against measured data. This was performed in two different ways. The first was to plot the measured output during one day on the same graph as the simulated output. This was performed for both electrical and thermal output. Figure 3.27 shows the electrical and thermal output validation for both the prototype solar window and the Solgård solar window. The days were chosen to illustrate different weather conditions and different times of the year. The Excel model uses measured temperature differences between the absorber and the ambient air to calculate the thermal losses from the collector. The correlation is high for all four graphs.

In Figure 3.28 the measured electrical output from the solar window is shown in black. The blue and orange lines are the calculated electrical outputs for the cases of the reflector being in a vertical, active, as well as in a horizontal, passive, position. The solar radiation on the window is shown by a dashed line. The area under the output graph is the daily electrical output.

It can be noted that the reflector has greater impact on days with low projected solar height, e.g. winter days for the northern hemisphere. For 12/9, left graph, the reflector accounts for 30% of the total output while it accounts for about 50% of the total output for 3/11, right graph.

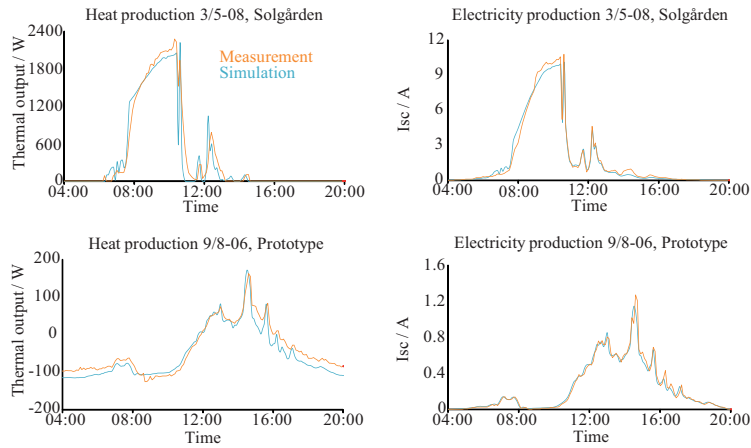


Figure 3.27 Validation of the simulation/calculation model. The upper graphs are from the Solgården solar window and the lower graphs are from the prototype solar window. The graphs on the left side are for thermal output validation and the graphs on the right are for electrical validation. Isc is the short-circuit current.

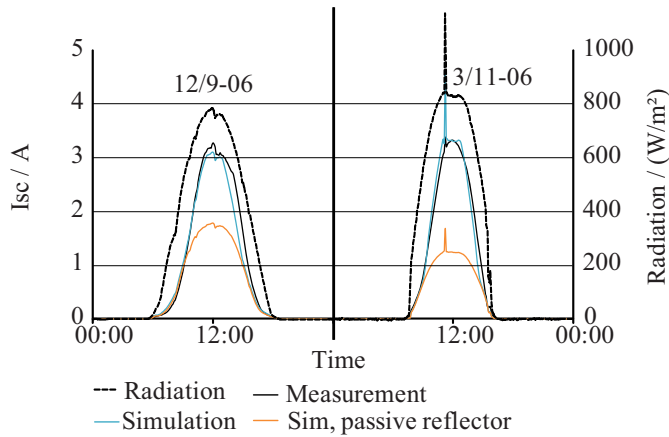


Figure 3.28 Measured and simulated electrical output from the solar window. The peak during 3/11 is probably due to a reflection.

Two different loggers were used for measuring the prototype solar window. One logger was used to register the electrical measurements and the other to register thermal measurements and solar radiation on the wall. During

cloudy weather with sunny intervals, synchronisation problems could arise, since the two loggers were not perfectly synchronised. This means that if the electricity was measured during a cloudless moment and the solar radiation was measured during cloudy conditions, there will be a very poor correlation between measurement and calculation. To overcome this problem the output from the window was integrated day by day, which evened out the irregularity.

The result from this validation is shown in Figure 3.29. The simulated values are plotted on the x -axis and the measured values on the y -axis. A perfect fit between simulation/calculation and experiment would place all the dots on the line $x = y$. The left figure is the validation for the thermal model and the right figure is the validation for the electrical model. The black dots are from the Solgård window and the white dots are from the prototype solar window. The correlation between measurement and simulation/calculation is high for all cases. The data for the prototype solar window is between July and November, and for the Solgård solar window it is between April and July. Consequently, most solar heights throughout the year are included in the validation.

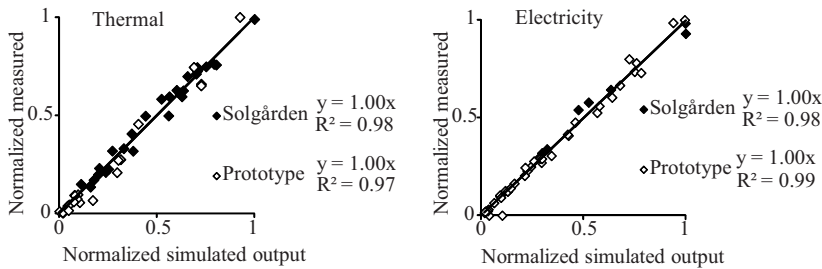


Figure 3.29 Validation of the thermal, left figure, and the electrical, right figure, simulation/calculation. The black dots are from the Solgård solar window and the white dots from the prototype solar window. The simulated/calculated output is on the x -axis and the measured output on the y -axis.

3.8 Results

All the simulations/calculations of the prototype solar window are on component level. The results are obtained from the developed Excel sheet, so the prototype solar window has not been investigated together with a storage tank, different hot water consumption profiles, etc. Instead, the temperature to the prototype solar window was kept constant during

measurements. The results from the Solgården and the Augustenborg solar windows are on system level. All the system results are from the developed TRNSYS-deck. The TRNSYS simulation deck is discussed in section 3.6 and in Paper 2 (Davidsson et al., 2012).

3.8.1 Prototype solar window

Using weather data recorded at the testing facility allowed annual calculations of electrical output from the solar window. However, finding data from one full year without interruptions was not possible. Days where data was corrupted by problems, such as frost on the pyranometer or a displaced diffuse ring, were removed. Exclusion of these days left 46 full weeks. The removed weeks were fairly evenly distributed over the year.

A calculation for the prototype solar window can be seen in Figure 3.30. In this figure the total annual output from the solar window has been plotted together with calculations for two different flat PV-modules. The PV-modules, placed at 20° on a roof and at 90° on a wall, have the same efficiencies and PV cell area as the string module in the solar window, but the PV-modules have no reflectors, are unshaded and they use single glazing instead of the double glazing as in the solar window.

As can be seen in the figure, the electricity from the diffuse solar radiation is heavily suppressed in the solar window. This is mostly due to the vertical position and also to the double glazing of the solar window. The increase of electricity from direct solar radiation for the roof module compared to the solar window, not including the reflector, is due to more favourable solar angles and the single glazing. Also, part of the solar radiation that comes from behind the building can be utilized by the roof-mounted module. This is not possible for the solar window. The total output is 35% greater for the solar window than for a flat solar module placed vertically on a wall. However, the roof-mounted collector produces 17% more than the solar window. All figures have been normalized to the total output from the solar window. The model assumes isotropic diffuse solar radiation.

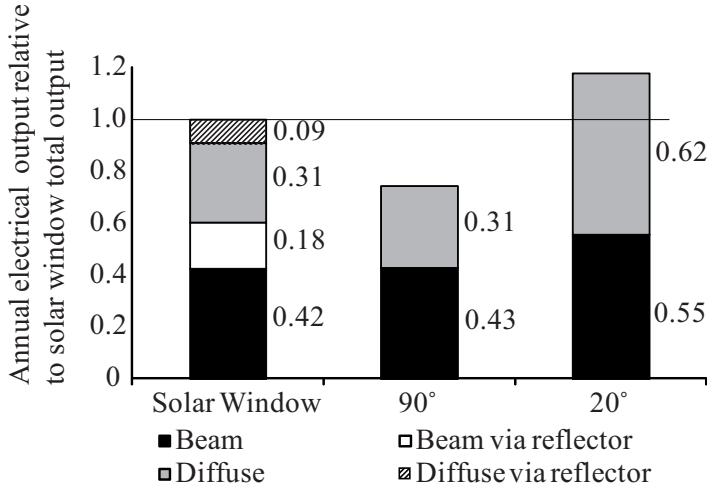


Figure 3.30 The annual electrical output from the prototype solar window and from two flat PV-modules on a wall at 90° tilt and on a roof at 20° tilt. The black part is from beam solar radiation directly impinging on the absorber. The white part is from beam solar radiation that comes via the reflector. The grey part is from the diffuse solar radiation directly on the absorber and the striped part is from the diffuse solar radiation via the reflector. All results have been normalized to the total annual output from the solar window.

Calculations were performed to investigate the influence of the shading factor, $f_s(\theta_3)$, glazing transmission, $T_{glass}(\theta_1)$, and angle dependence of the PV efficiency, $\alpha_{pv}(\theta_2)$. This was done by setting these parameters, one at a time, to unity. The results are shown in Figure 3.31. Even if the angular dependence of the PV cell could be removed, the annual output would only increase by about 1%. The angular dependence of PV cells is apparent only for large solar angles, and large angles are already heavily shaded and affected by the low transmission in the glazing. Consequently, removing the angular dependence of the PV cell will have only small effect. If the shading could be removed, the annual output would increase by almost 20%. The shading of the solar window was described in section 3.5.4. Shading of the PV cells is most apparent at the edges. If the shading is large it might be better to remove one of the cells, thereby creating a larger space between the outer cell and the frame of the window. If the anti-reflection treated double glazing could be removed completely, the annual output would increase by 23%.

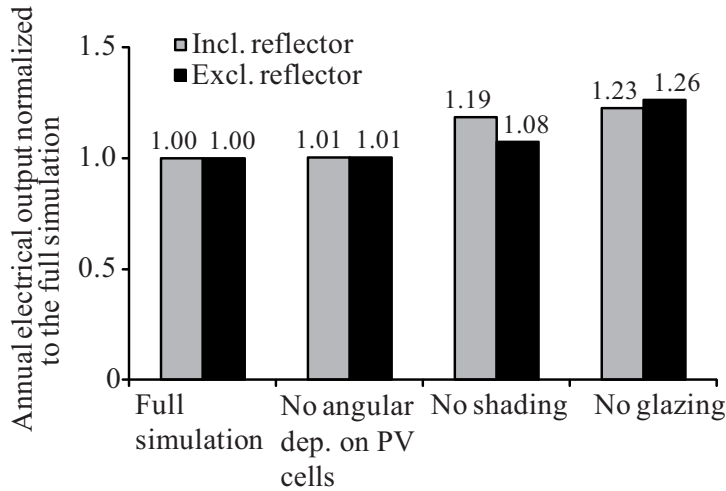


Figure 3.31 Different limiting factors affecting the solar window. The two bars to the left correspond to the original calculation. For the second pair the angular dependence of the PV cells has been removed. For the third pair all shading effects have been removed and, for the last pair, the transmission losses due to the glazing have been removed. The black bars correspond to calculations performed without the influence of the reflector and the grey ones include the reflector contribution.

No thermal simulations were performed for the prototype solar window. The reason is that the thermal output is strongly dependent on the overall system design. The size of the storage tank, the load profile of hot water use, and the surrounding temperature are very important parameters for the solar window. In order to perform such simulations, a more advanced simulation program has to be used. TRNSYS, described in section 2, was chosen as a simulation program suitable for solving simulation tasks for the solar window. The system analysis is discussed in Paper 2 (Davidsson et al., 2012).

3.8.2 Solgård solar window

Electrical results - Solgård

The analysis for the Solgård solar window was carried out using Mete-norm weather data (METEONORM). Results may therefore vary greatly between years with different weather.

Depending on how the reflectors are controlled the electrical energy output will vary. In Figure 3.32 the results from four different control strategies are shown. The second strategy produces the most electrical energy because this strategy has constantly closed reflectors that maximize the output. The maximum production, strategy 2, produces 435 kWh of electrical annually for the weather data used. The total cell area is 4 m² and the efficiency is about 10% for the cells. During the most productive month, i.e. May, the average electrical production is 2 kWh per day.

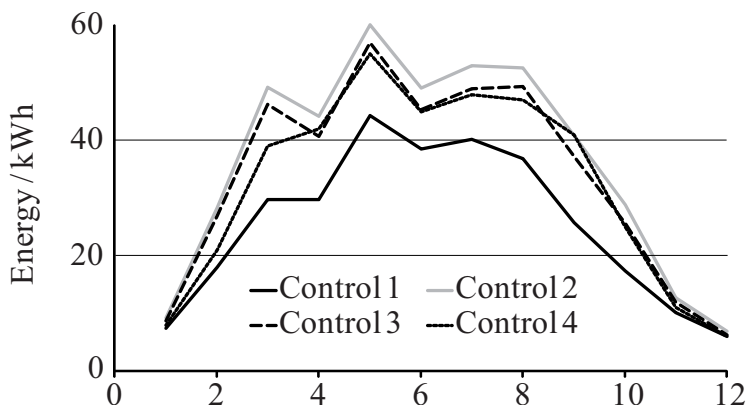


Figure 3.32 The monthly electrical output during one year for different control strategies.

Thermal results - Solgården

The results from the thermal simulations in Solgården are much more complex than from the electrical calculations. The thermal output from the solar window is a function of the indoor temperature, which is a function of the thermal losses from the window, etc. The main goal cannot only be to maximize the energy performance of the building; the comfort demands of the inhabitants must also be taken into account. One such example is control strategy 4, where reflectors are opened to cool the building at night. This is not optimized from an energy point of view since it would be better to overheat the building to maximum temperatures in order to save future heating costs, but of course this is not a strategy that the inhabitants would allow. The consequences of using strategy 3 or strategy 4 were therefore analysed in more detail.

Figure 3.33 shows an analysis of control strategy 3. As can be seen, the best control strategy is to use 100 W/m² as the low parameter. From a thermal energy point of view, the upper parameter is best chosen in the range 600-800 W/m². The results show that the solar window is optimized

for low energy use if the reflectors are tilted backwards to allow passive heating. This is understood since it is more favourable in energy terms to heat the building passively compared to heating it actively through the absorber and the underfloor heating system.

The same analysis for control strategy 4 is shown in Figure 3.34. In this graph it can be seen that the optimized control parameters are 26°C for the lower parameter and 30°C for the upper parameter. Since the upper parameter is used only to lower the temperature in the building, i.e. to lower the energy content, it is always better to have an infinitely large upper parameter.

The situation is more complicated for the lower parameter. If the lower parameter is low, this means that less thermal energy is stored in the building from day to day, since the reflectors will close to maximize energy production in the absorbers. If the lower parameter is set to a high value, the situation will be the opposite. Large amounts of thermal energy will be stored in the building from day to day but energy production in the absorbers will be lower. Which scenario to choose is difficult or even impossible, to answer without simulations. In Figure 3.34, it can be seen that if the upper parameter is fixed to 30°C the optimum low parameter from an energy point of view is 26°C . Both 24°C and 28°C will result in higher thermal energy need.

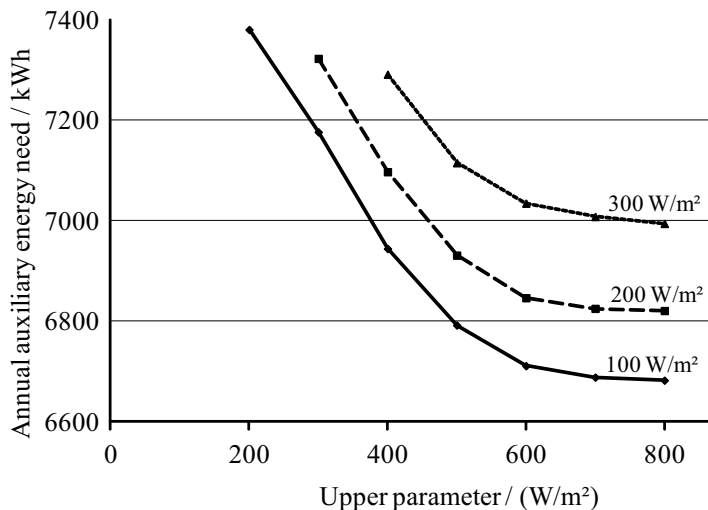


Figure 3.33 The thermal auxiliary energy need for Solgården with a solar window using control strategy 3. The black line is with the lower parameter at 100 W/m^2 . The dashed line is 200 W/m^2 and the broken line is 300 W/m^2 . The upper control parameter is on the x-axis and the annual thermal auxiliary energy need on the y-axis

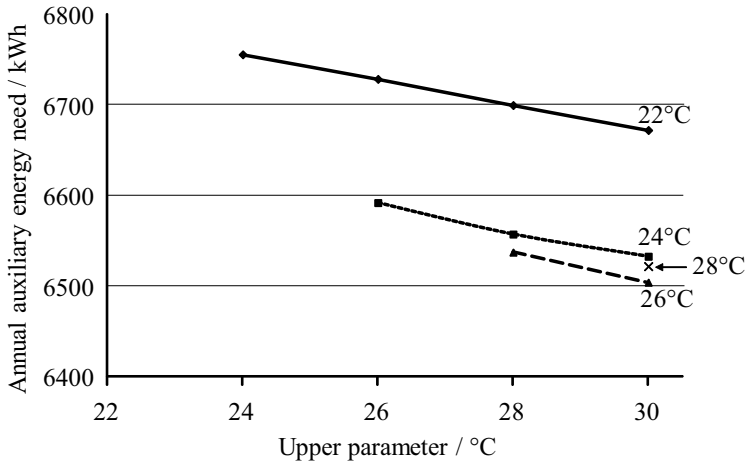


Figure 3.34 The thermal auxiliary energy need for Solgårdén with a solar window using control strategy 4. The black line is with the lower parameter at 22° C. The dashed line is 24° C, the broken line is 26° C and the star is 28° C. The x-axis is the upper control parameter and the y-axis is the annual thermal auxiliary energy need.

In Figure 3.35 it can be seen that control strategy 2 produces most thermal and electrical energy. However, this is not the control strategy that minimizes the thermal auxiliary energy need. As can be seen in Figure 3.35, using control strategy 3 with parameters 100/400 or control strategy 4 with parameters 22/26 results in a lower thermal auxiliary energy need. The reason for this is that no passive heating is utilized if the reflectors are constantly closed. The thermal auxiliary energy need includes space heating, domestic hot water and it covers the losses from the tank. Space heating does not include the hot water use. The domestic hot water use is the same for all simulation cases. Using 9 litres of heated water continuously equates to approximately 4400 kWh of heating need annually. The heat removed from the storage tanks was the same for all control strategies even though no extra control mechanism was used.

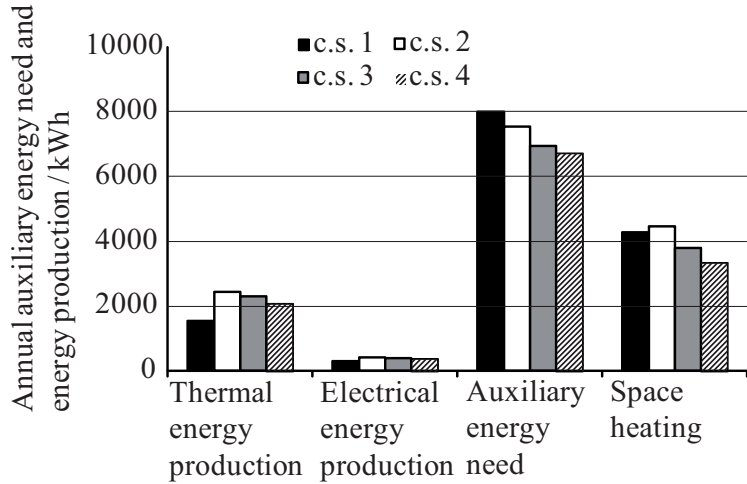


Figure 3.35 Annual energy production and need. Thermal and electrical energy production, thermal auxiliary energy need and space heating need for one full year are on the x-axis. Control strategy 1 is shown in black, 2 in white, 3 in grey and 4 striped. The energy production and need are on the y-axis.

Which control strategy to choose is a more complicated question. Table 3.2 shows control strategies and control parameters. The most interesting parts of the table have been marked with a grey background. As stated before, control strategy 2 produces most thermal and electrical energy, but it will result in a large thermal auxiliary energy need since it fails to utilize passive heating of the building. Instead, control strategy 4 turns out to be the best solution from an energy point of view. Control strategy 4 is also the best way to control the reflectors to avoid overheating of the building. An overheated building is the percentage of the year with temperature above 30°C. Using control strategy 3 with the parameters 100/800 will result in about the same auxiliary thermal energy need as using control strategy 4 with parameters 22/26. However, the building is overheated almost twice as often with control strategy 3. This is discussed further in Paper 2 (Davidsson et al., 2012).

Table 3.2 Parameter study of different control strategies for the reflectors. The parameter row shows the values used for lower and upper parameters for the control strategy. Control strategy 1 & 2 have no parameters. The most optimized control strategies and parameters are marked with grey background.

	Control 1	Control 2	Control 3		Control 4	
Parameters	X	X	100/400	100/800	22/26	26/30
Thermal auxiliary energy need / kWh	8000	7500	6900	6700	6700	6500
Produced ther. energy / kWh	1500	2500	2300	1700	2100	2000
Produced el. energy / kWh	300	430	400	330	390	370
Overheated building / %	27	23	27	33	18	20

3.8.3 Augustenborg solar window

The solar window at Augustenborg in Malmö differs from the other solar windows in several respects. The window is facing approximately 40° west of south. The reflectors behind the absorbers are not insulated, nor is the glazing in front of the absorbers anti-reflection treated. The solar window connected to a storage tank is used to preheat the incoming water before it is heated, so the water temperature in the system can be kept low. This is also one of the reasons why the reflectors are not insulated. The simulations for the solar window in Augustenborg were performed using the Solgård solar window TRNSYS deck. However there are some differences. The water use and the temperature of the water flowing into the tank were set to values that resulted in a temperature profile of the water entering the collector in agreement with the measurements at Augustenborg.

The results presented for the Augustenborg solar window with constantly closed reflectors, i.e. control strategy 2, are for the full year. The results from the calculations show that a flat PV module placed at 20 degrees with an azimuth of 37° to west will produce about 50% more electrical energy than the solar window. The main reason is the effects from the glazing. Since the existing window has standard glazing without anti-reflection treatment, transmission losses will be large. The orientation of the solar window also affects the annual output. At 11.30 at the end of July, half of the outermost cell is still shaded from the sun by the window frame. The cell is partly shaded until after 12.00. This shading is most apparent for the electrical output since the output is limited by the most shaded cell, which is not the case for the thermal output.

The electrical output for the Augustenborg solar window was simulated to be about 110 kWh. The thermal output was calculated to be about 700 kWh annually. The total cell and absorber area for the Augustenborg solar window was 2.25 m² and 2.75 m² respectively. The PV efficiency was 8.2%.

Figure 3.36 shows the electrical output from the solar window over 40 consecutive days. The left side of the graph, in white, is with the reflectors in a closed position and the right side, in grey, is with the reflectors in an open position.

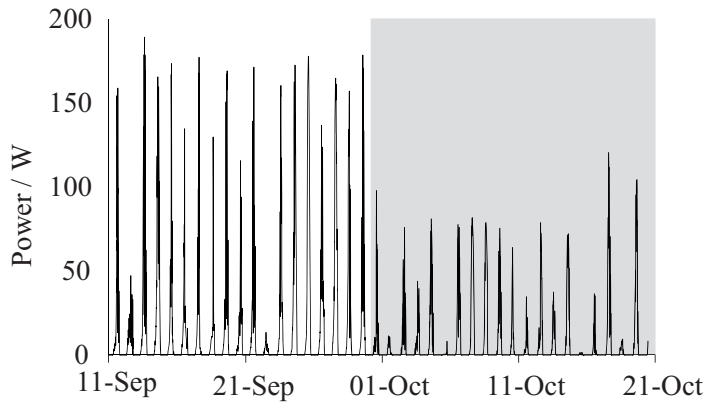


Figure 3.36 *Electrical output from the solar window in Augustenborg. The white part is with closed, active, reflectors and the grey part is with open, passive, reflectors.*

3.9 Development

To maximize the output from the solar window, the glazing was anti-reflection treated. For the same reason no low-e coating was put on the glazing since this coating decreases the solar transmittance. The result is a window with high solar transmittance and a relatively high U -value. In order to investigate the potential for improving the Solgård solar window, a new simulation was performed using a solar window with low-e coated glazing, added insulation on the reflectors, and insulation on the back of the absorbers. The consequences of these potential improvements for the absorber heat transfer coefficients, the U -value, and the solar transmittance of the solar window are shown in Table 3.3. The drastic decrease in the heat transfer coefficient to the inside is due to increased insulation on the back

of the absorber. The table shows the estimated heat transfer coefficients from the absorbers in both directions, in and out of the building, for the standard and the developed solar window with both open and closed reflectors. The solar transmission through the low-e coated glazing is assumed to decrease by 20% compared to the solar window glazing. The U -values for the solar window are lowered to $0.6 \text{ W/m}^2\text{K}$ for closed reflectors and $1.5 \text{ W/m}^2\text{K}$ for the open reflectors. The values for the developed solar window are estimates and serve as a “best case” for a developed product.

Table 3.3 Thermal losses from the absorbers for the open and closed solar window towards the inside and the outside for both the standard and the developed solar window. The solar transmission relative to the standard solar window and the U -values for the thermal losses through the solar window.

PV/T absorber heat transfer coefficient / ($\text{W/m}^2\text{K}$)					Rel. change in window g -value	Win U -value	Win U -value
Reflector mode	Closed		Open			Closed	Open
Direction of heat loss	In	Out	In	Out			
Standard solar window	3.9	2.0	5.9	1.3	1	1.3	2.43
Developed solar window	0.7	1.3	3.5	0.7	0.8	0.6	1.5

The solar window was also compared to a reference case where the 16 m^2 solar window was replaced by an 8 m^2 large standard window with a U -value of $1.1 \text{ W/m}^2\text{K}$. In a third case, this reference case was also equipped with a solar collector and a PV-module of the same size as the solar window constituents and placed separately on the roof. The different systems are shown in Figure 3.37. System 1 is the solar window. The standard and the developed case look the same. System 2 is the reference case with the 8 m^2 standard window. System 3 is the reference system with a solar energy system on the roof. The solar energy system in system 3 is tilted 20° from the horizontal, as is the roof at Solgården. The reference cases will be labelled system 2 and system 3.

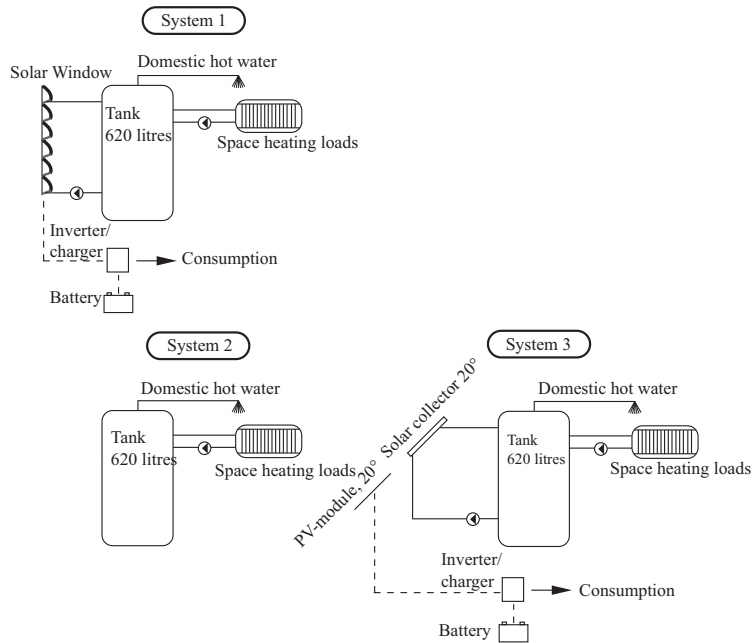


Figure 3.37 System 1 is the solar window. System 2 is the reference case, and system 3 is the reference case including a solar energy system.

3.9.1 Results

All simulations performed for the improved solar window were carried out using the TRNSYS deck developed for the Solgård solar window. The results for the different systems are presented in Figure 3.38. They show that the developed solar window performs better than the original one. This is because it is more important to minimize thermal losses through the solar window than to maximize the thermal output from the collector part.

The developed solar window performs better than the standard solar window. This difference is significant. The standard solar window needs about 600 kWh less thermal energy per year than system 2. However the standard solar window has a poorer performance than system 3, because of the increased UA -value of the building with the solar window. A building equipped with a developed solar window requires about the same amount of thermal energy as a building equipped with system 3. The difference is approximately 200 kWh per year. This analysis is performed with no regard to electric energy production.

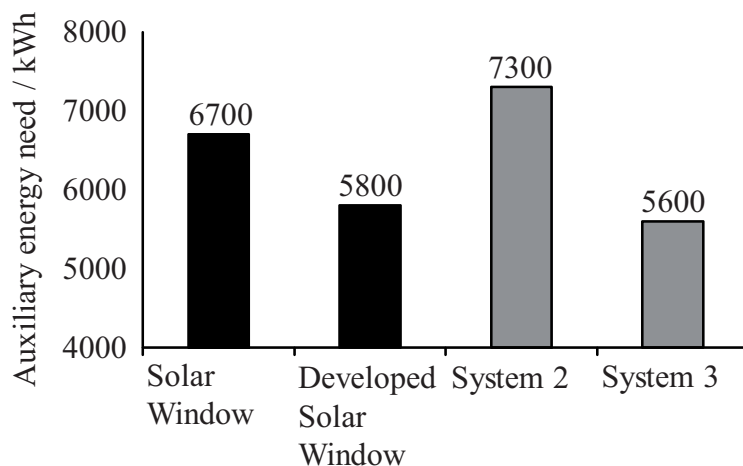


Figure 3.38 The first bar is the solar window using control strategy 4 with parameters 22/26. The second bar is the developed solar window using the same strategy. The third bar is system 2 and the fourth bar is system 3.

3.10 Large solar window

Due to the vertical position of the solar window, the annual distribution of produced thermal and electrical energy is fairly uniform, i.e. there is no sharp peak during the summer. This indicates that it is possible to install a larger solar window to utilize the solar energy more. The simulation performed to investigate this used a solar window that was 50% larger than the standard window. The simulations were carried out using a standard solar window, not the developed version. The simulations were carried out using the TRNSYS deck developed for the Solgård solar window. For comparison the solar collector in system 3 was also increased by 50%. The replacement window in system 3 was kept constant, i.e. 8 m².

The results from these simulations are shown in Figure 3.39. The solar window uses control strategy 4 with parameters 22/26. As can be seen from the results, the need for auxiliary thermal energy increases rather than decreases. This is due to the larger window causing larger thermal losses from the building. The increase in thermal losses from the building is greater than the increase in thermal energy production and passive heating from the increased transmission of solar radiation due to the greater area. Consequently, thermal energy use is larger with a large solar window. For

system 3 the situation is different. Increasing the size of the collector has no negative feedbacks. Much of the increased thermal energy production is utilized by the building, so thermal energy use is lower if the collector area is larger.

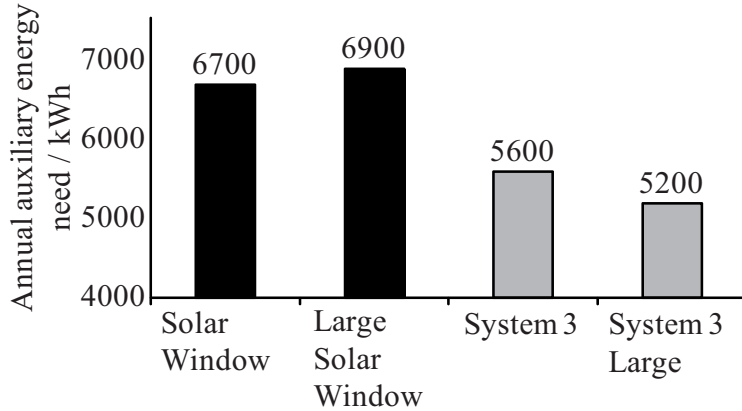


Figure 3.39 Annual thermal auxiliary energy need for the solar window of standard size and increased by 50%, and for system 3 including a solar energy system of standard size, and system 3 with the solar energy system increased by 50%.

3.11 Conclusions and discussion

One of the reasons for the development of the solar window was to lower the total investment cost of a solar energy system. Apart from the energy perspective, the solar window also works as a sunshade and directs daylight to the back of the room. Daylighting and aesthetics are however not investigated in this study. This was covered by Andreas Fieber in his licentiate thesis (Fieber, 2005). This work aims to investigate the energy consequences of the solar window, both on component level and on system level.

The investigation of the solar window was carried out in two steps. First a calculation model was made in Excel to allow characterisation of electrical power production, thermal energy production, heat loss from the absorbers and the influence of reflector placed behind the absorbers. The evaluation showed that the model corresponded well with the measured data. This was true for the prototype solar window and the Solgård solar window, the electrical and the thermal output, and for open and closed reflectors. The second step was to build a TRNSYS simulation deck. This deck was used to investigate the solar window on system level. This investigation

includes effects of a storage tank for the thermal energy production, and thermal energy consumption from the storage tank in the form of hot water use and heating of a building.

The results in Figure 3.30 show that the solar window produces about 35% more electrical energy per PV cell area than a flat PV module placed vertically on the wall, even though it is located on the inside of a window. If space is a limiting factor when PV modules are installed on the roof, the solar window is an interesting product in high-rise houses and staircases. However, if space is not a problem, Figure 3.30 shows that it is better to install the PV modules on the roof. This will result in an additional 17% electrical energy per module area. The complexity is also lower for the roof-mounted installation since no tiltable reflectors are needed. It was shown in Figure 3.31 that the shading of the cells in the solar window lowers the annual output substantially. If the shading effect were eliminated, the output would increase by about 20% annually. Also the solar transmission losses through the glazing are significant, despite the fact that the glazing is anti-reflection treated. If the glazing were to be removed, the annual electrical output would increase by about 25%.

One of the problems is that the performance of PV cells is always limited in some way. During the winter the incidence angle between the sun and the absorber is high, so the sunlight has less access to the absorber.

During the summer the angle between the sun and the absorber is more favourable. However during the summer the incidence angle between the glazing and the solar radiation is high, so transmission losses will be at their highest level during the time when the irradiance is at its maximum. However, the angular dependence of the PV cells is not an important factor.

During the winter the reflector increases the output substantially due to the small angle between the sun and the reflector. However, during the winter there is less need for reflectors since the heat can be utilized directly as passive heating.

In Table 3.2 it was shown how the performance of the solar window depends on the choice of control strategy for the reflectors. Maximizing the annual electrical output using control strategy 2, with reflectors always closed, will result in high thermal auxiliary energy need for a building. This is of course very dependent on the geographical location of the building. If the building is located in the south of Europe the result will be completely different to the results from Sweden.

If the thermal auxiliary energy need is to be minimized, control strategy 4, temperature-dependent control, is preferable. This is also the best strategy from a comfort point of view, resulting in relatively low overheating. The main reason why control strategy 4 is better than control strategy 3, radiation dependent control, is the possibility to utilize high solar irradiance

during the winter. If the solar radiation is high during a cold winter day, it is better to open the reflectors to heat the building passively. If control strategy 3 is used there is a risk that the window will close during hours of high irradiation.

During the tests on the Solgården solar window the absorbers were not insulated. The consequences of improving this and adding a low emission coating on the glazing were studied theoretically. This means that both the U -value and the solar transmittance of the glazing were lowered. The results show that the annual thermal energy use is lowered, so it is more important to lower the heat losses than to maximize the thermal output.

The solar window was also compared to reference systems. In the reference case, labelled case 2, the 16 m² solar window was replaced by an 8 m² standard window. In system 3, a solar energy system of the same size as for the solar window, excluding reflectors, is also included. The reason for choosing to replace the solar window with an 8 m² window and not a 16 m² window is the access to daylight. If the reflectors are open, half the solar radiation transmitted through the glazing in winter ends up on the absorber. This means that the solar window must be twice the size of a standard window in order to have the same amount of daylight reaching the room. As was shown in Figure 3.38 the solar window performs better than system 2.

The heat produced by the solar window is more important than the thermal losses. However, if the solar window is compared to the reference case including the solar energy system, the result is the opposite. System 3 performs better than the solar window. This is one of the most important conclusions. It is more favourable in energy terms to install the thermal absorbers and the PV-cells on the roof than in the window. System 3 was simulated with the solar system at 20° tilt, i.e. the same tilt as the roof in Solgården. This is not an optimal tilt. If the simulation had been performed with the modules at a higher inclination, the difference between the solar window and system 3 would be even larger. Furthermore, the conclusion from Figure 3.30, stating that the roof mounted PV module produces 17% more electricity compared to the solar window, assumes closed reflectors. However, if control system 4 is used with parameters 22/26 the production of electricity will drop another 10% because the reflectors are set in open mode during parts of the year. Consequently, the difference between the solar window and the roof mounted PV-system in a real situation is even greater.

One of the problems with the solar window is that the absorbers and reflectors block the solar radiation from entering the building, thereby reducing passive heating of the building. The problem becomes apparent when the solar window is compared to system 3. A thermal collector can be installed in a window to build something that looks like the solar win-

down or it can be installed on, for instance, the roof. This is illustrated in Figure 3.40. If the collector is installed on the roof as proposed by Corbin & Zhai, (2010), the active area collecting the solar radiation is the sum of the individual areas. In the figure this means $A + B$. If the thermal collector is installed in the window the active area is still just A . The thermal collector is now shading the window. In other words, a photon cannot be used for simultaneously heating the collector and the building.

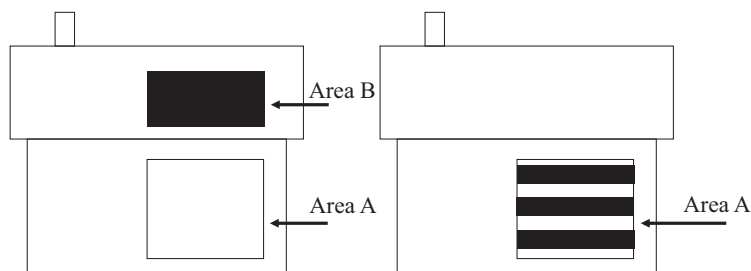


Figure 3.40 Left: Building with a window of size A and a solar collector of size B on the roof. Right: Building with a window of size A in which a solar collector of size B has been placed.

Since the solar window is positioned vertically, annual energy production is distributed rather evenly, i.e. there is no sharp peak during the summer. The simulations suggest that the window area could be increased in order to gain more energy from the sun. This is why the investigation was performed with increased solar window area and increased collector area for system 3. It was shown in Figure 3.39 that increasing the solar window area will lead to higher thermal energy need. This is due to the increased thermal losses caused by the window. The increase in thermal losses is larger than the extra solar thermal energy produced by the window. This is not the case for system 3. If the solar collector is located on the roof, all the extra energy will be used to lower the thermal energy need. There is no negative feedback mechanism that negates the positive effects from the collectors. This is of course a problem for the solar window.

3.12 Further development and future work

Solar radiation and ambient temperature vary considerably at different sites. The weather conditions for a building vary both seasonally and

diurnally. This variation leads to different problems and possibilities. The solar window was designed for the Swedish climate, so at locations around the world with different latitudes and climate, the window would behave differently. Closer to the equator there is less need for solar shading on the south facade. Higher annual temperature will alter the need for passive heating and so alter the control and the benefits of the solar window. Nevertheless, investigating the solar window in other climates would be of interest.

The solar window has to be improved in a number of ways to become an attractive solar energy product. Most important is the U -value. This has to be reduced considerably. If a low-emittance coating is added on the window glazing, the solar transmission through the glazing will be reduced. This is a problem for the window during both summer and winter. During the winter valuable solar radiation for passive heating is lost. The low-emittance coating will also lower the electrical and thermal energy output from the solar window when the transmission is reduced. One way of solving this problem might be to place the collector between the two panes of glass. This would increase transmission and thereby output since the solar radiation only has to pass through one pane of glass. The inner glazing could be single or double and, most importantly, could be low-emittance treated without affecting the collector. The design of the window might become more complicated but that is probably a price that has to be paid.

Another advantage is that the cells will not become dusty. If the collector is placed between the panes the sunshading properties will be improved since less thermal energy will be lost from the absorber to the room. The solar window can also be improved if the shading of the cells is reduced by increasing the distance between the outer cell and the window frame. Furthermore, the shading of the cells could also be reduced if the absorber and PV-cells are placed between the single glazing.

The developed simulation deck could benefit from a more detailed description of the hot water use. This includes both the user profile of the domestic hot water as well as the annual temperature profile for the incoming fresh water. However, the investigation carried out focused on a comparative study. Any choice of parameter such as incoming water temperature will affect all studied systems in a similar manner, so the difference between the systems will be small. One problem with the simplified hot water consumption profile could be the peak power demand. If no peak loads are included in the hot water consumption there is less risk of not being able to meet the power demand. In a real situation the system would have to be sized to meet much higher loads for short periods, but this would not greatly affect the annual performance. It could mean that the storage tank would have to be kept at a somewhat higher temperature,

thereby increasing losses to the surrounding and producing a less preferable heat carrier temperature to the solar collector. Again, since this is a comparative study the effect would be small.

4 The ventilation project

As discussed in section 1.2.4, ventilation of buildings is needed to remove moist air, unpleasant odour and harmful substances. Ventilation can also be an efficient way of controlling the room temperature. However, in cold climates, ventilation uses large amounts of energy because the cold incoming air must be heated. Ventilation heat recovery systems as discussed in section 1.2.2 and 1.2.3 can be used to minimize this energy cost.

Looking at the Swedish market (Energimyndigheten, 2010) for ventilation units with heat recovery, it can be seen that all traditional units use a considerable amount of electrical energy to run the fans in the system. In this discussion it is also important to remember that electricity is more valuable than heat. Exactly how much more valuable is difficult to pinpoint. Electricity is frequently considered to be three times more valuable than heat, at least in terms of primary energy. This potential can be realized by using a heat pump to obtain heat from the electricity, and a heat pump can typically produce three kWh of heat from one kWh of electricity. The exact amount depends on the temperatures of the cold and hot sides of the pump. An investigation by the Swedish Energy Agency showed that the COP of a ground-connected heat pump is typically somewhat higher than 3 (Energimyndigheten, 2012). An example can be used to illustrate the problem of the high electrical energy demand for the fans.

A typical single-family house, approximately 120 m², in the south of Sweden or other cold climate uses approximately 4000 kWh annually to heat the incoming ventilation air. If a heat recovery unit with 75% energy efficiency is used, the heat exchanger reduces the load by 3000 kWh. The electrical energy used to run the air handling unit is about 456 kWh annually (Energimyndigheten, 2010). However, the 456 kWh of electric energy corresponds to about 1370 kWh of primary energy, using a conversion factor of 3. In other words, instead of using 4000 kWh of heat, the use is reduced to 2370 kWh of heat equivalents. Including the electricity use in the calculations greatly reduces the energy savings in the system. Instead of saving 75% the system only saves about 40% of the primary energy when electricity use is included.

This example is by no means a complete analysis; it does not show that heat recovery units should not be used, it merely illustrates a problem, i.e. the high electrical energy use by the fans. More aspects have to be included before more general claims can be made. Vik (2003) compared the LCC of three different ventilation systems: a natural ventilation system with inlets in the façade (NF), a natural ventilation system with embedded ducts (NE), and a “best practice” balanced mechanical ventilation system (MB). Vik concluded that the NE has 5% higher LCC than the MB, but the NF is 8% lower than the MB. This indicates that there are also financial reasons to study natural ventilation in more detail. The case study was based on a three-storey office building in Denmark.

The high level of electrical energy use is the reason behind the attempt to design a ventilation system that uses less electrical energy compared to the standard ventilation systems commonly used today. One way of reducing electrical energy use is to use hybrid ventilation, i.e. using natural forces as far as possible. When the forces are not enough, a complementary fan assists the system. This minimises the electrical energy used to drive the ventilation but, without heat recovery, this type of ventilation would result in a high heating demand during cold periods, and the annual energy need for the building would be high. The ventilation system normally has to recover some of the heat from the outgoing ventilation air in order to meet the energy standards of modern buildings and building regulations. Natural ventilation might also result in cold incoming air, creating cold draughts and reducing indoor comfort. Both of these issues call for a heat exchanger to be used. Traditionally the heat exchangers available on the market have a pressure drop that is too high, or the hybrid ventilation components and systems including heat exchangers are difficult to retrofit into existing buildings or put high demands on the architecture of the building. Installing heat exchangers with high pressure drop in a naturally ventilated building would lower the ventilation rate considerably.

4.1 A ventilation system with heat recovery

One way to construct a hybrid ventilation system with heat recovery is to use two water-to-air heat exchangers connected with a brine system. This was discussed in Table 1.1, case number 4. This type of system, known as a run-around system, is reviewed by (Mardiana-Idayu & Riffat, 2012).

The ventilation air flow in the system can be driven by natural forces, both wind pressure and buoyant forces. The brine in the circuit is driven

by a pump. One of the liquid-to-air heat exchangers is placed as high as possible under the roof, as illustrated in Figure 4.1. This exchanger recovers some of the energy from the outgoing air and transfers it to the brine. The energy is then pumped to the bottom of the building where the other heat exchanger is located. This delivers the recovered heat to the incoming cold outdoor air. The liquid is then pumped back to the roof heat exchangers and the circuit is completed. The heat exchangers in this type of system are preferably placed with a large height difference, since the driving pressure generated from thermal buoyancy is proportional to the height difference between inlet and outlet for the air. This height difference is indicated with h' in Figure 4.1.

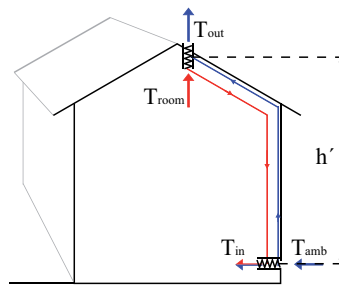


Figure 4.1 The liquid based heat recovery system.

Equation 1.2 in section 1.2.3 showed that a height difference of 10 m and typical conditions of 0°C outside and 20°C inside results in a driving pressure of $\Delta P \approx 8.7$ Pa. It is clear that the pressure losses have to be kept low throughout the system. The available driving pressure has to cover not only the pressure drop in the heat exchangers but also in the ducts, filters, inlets and passes within the building.

Overgaard, Heiselberg, & Hammer (2002) reviewed components for natural ventilation, concluding that there is a clear possibility to develop and use low-positioned inlet components for natural ventilation. Overgaard et al. also concluded that many functions, such as filter, noise reduction, and preheating, can be combined in a single component, without introducing an excessively high pressure drop. Another big advantage is that the duct system can be considered superfluous. One way to reduce the length of ducts in the system is to allow the outdoor supply air to enter directly through the wall to the rooms. In Figure 1.1 this would mean having one heat exchanger on the right side of the building and one heat exchanger on the left side. The brine circuit in the system transporting the recovered heat has to be divided to reach each outdoor air inlet.

At the same time it is beneficial if the heat exchanger surface is easy to clean, enabling installation of a minimal filter or, even better, requiring no filter at all. If these measures are possible, solutions must be investigated from case to case. Wachenfeldt concluded that filters could be used in natural ventilation, but this conclusion was reached from estimating the pressure drop to be as high as 4 Pa. This would limit the possibilities of having natural ventilation for single-family houses with limited driving pressure (Wachenfeldt, 2003, page 325). The local pollution rate, the need for pollen filters, etc. will affect this choice.

If the ambient temperature rises to 10°C, the driving force due to the stack effect, for the example given above with 10 m height difference, will be reduced to 4.4 Pa. Fans for hybrid ventilation systems with a pressure drop less than 2 Pa during inactive periods, i.e. not spinning, are available on the market (Aereco). If the duct work is considered early in the building process, the pressure drop from the ducts can be kept low. If planned correctly, the pressure drop can be limited to less than 1 Pa for a single-family building. This means that designing the ventilation system for running on a thermal stack effect when it is 10°C outside, gives a remaining 2-Pa pressure drop for the two heat exchangers, i.e. the pressure drop for one heat exchanger can be allowed to be approximately 1 Pa. This is of course not an exact figure but it serves as a guideline.

Heat exchangers with very low pressure drop suitable for natural or hybrid ventilation have been reported (Hviid & Svendsen, 2011; Overgaard, Nørgaard, Jensen, & Madsen, 2002). Hviid et al. used plastic pipes to construct the heat exchanger, reaching an efficiency of approximately 70% at system level. Overgaard et al. used oval finned metal pipes to produce a compact heat exchanger, reaching about 43% system efficiency. However, these heat exchangers are difficult to clean, and might require installation of a filter.

The forces created by the wind can also be used. However, these are much more irregular as they change with the wind speed and direction, so wind-induced forces can vary greatly from day to day. The possibility to use the wind as a driving force has to be considered for each specific case, where wind conditions and available pressure from thermal forces, etc. are weighed against each other. Various techniques to enhance the driving forces due to the wind are discussed for example in Khan, Su, & Riffat (2008) and in Vik (2003, pages 29-44).

During extremely cold periods the brine can be cooled to sub-zero degrees if high-efficiency heat exchangers are used. Figure 4.2 shows the ambient temperature entering the building that will result in 0°C outgoing air from the roof heat exchanger, providing the indoor temperature is 20°C. As can be seen for a heat exchanger with 80% temperature efficiency, there is a risk of frost on the heat exchanger already at -10°C ambient air.

All ambient temperatures below this point will lead to negative temperatures for the outgoing ventilation air. These calculations were carried out using the same Excel program as for the calculations presented later in section 6.3.

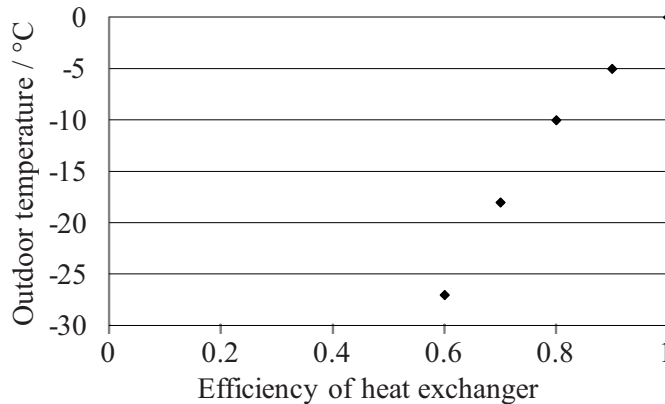


Figure 4.2 The y-axis shows the ambient temperature for which the outgoing air from the building will be 0°C. The x-axis shows the temperature efficiency of the heat exchangers.

The cold brine in the ventilation heat recovery system makes it possible to obtain free energy from the ground. The left illustration in Figure 4.3 shows how the brine is pumped through a plastic tube buried in the ground. This results in a higher lowest temperature for the fluid that enters the roof heat exchanger. This improves the annual performance, while reducing the risk of freezing the outgoing air. Condensation can still occur but this problem is more easily solved. The photograph is taken during the construction of Solgårdén. As can be seen in the figure the tube was placed in a wavy pattern. This “slinky” technique is used to minimize the amount of digging at the same time as the surface area for the hose is kept large. The name for the technique, “slinky”, comes from the old popular toy; see the reference for old memories, (Slinky).

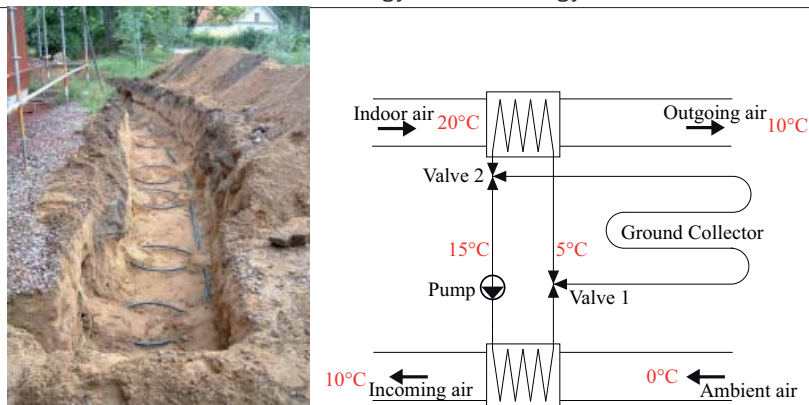


Figure 4.3 Left: The ground collector. Right: A scheme of the heat exchangers with bypass function.

The right illustration in Figure 4.3 shows a bypass valve arrangement for the ground collector in Solgårdén. The figure shows the roof exchanger on the top connected in series with the exchanger at the ground. Valve 1 controls/bypasses the ground collector. During summer, Valve 2 can bypass the roof heat exchanger, so the incoming air can be cooled while the ground is being reheated. Active reheating of the ground was omitted in this work. The interested reader is referred to Rosen, Gabriellsson, Fallsvik, Hellström & Nilsson (2001), in Swedish only. A typical steady-state situation is shown with red text in the right illustration. If the ground temperature is higher than 5°C, it is preferable to allow the brine to pass through the ground collector. If the ground is colder than the brine, it is better to allow the brine to pass directly to the roof heat exchanger. A similar investigation was carried out by Jacobsen et al. In their work a solar air collector was installed to preheat the ventilation air. The case study concluded that installing a solar air heater has the potential to reduce the annual heating demand by 7-10% (Jacobsen, Jensen, Poulsen, & Madsbøll, 1999).

Another technique that could be used in such a system is waste water heat recovery, where heat from the waste water can be used to heat the brine in the system. The systems for waste water heat recovery on the market are mainly for installations in new buildings or for smaller installations, such as for a single shower. In order to install and test a waste water heat recovery system in Solgårdén, a new type of product was tested. The system is described in detail in Chapter 5. The waste water heat recovery system is part of the system simulations carried out in Chapter 6. The investigation presented in Chapter 5 was carried out in order to identify the correct parameters for the component to be used in the system simulation.

The ventilation project was divided into two main steps, the heat exchanger and the system analysis. The heat exchanger was further divided into two smaller steps. The first step, section 4.2, is the development and evaluation of the heat exchanger while the second, section 4.4, is a parametric study of how an optimization of the heat exchanger can be carried out.

4.2 Design of the heat exchanger

The design of the heat exchanger had two main objectives, high heat recovery and low pressure drop simultaneously. For use in a hybrid ventilation system these two factors are more or less equally important. Without heat transfer they are pointless and, with a high pressure drop, the system turns into a mechanical ventilation system with a constant need for electrical power for the fans. The design proposal was to use absorbers for solar collectors as building blocks. Using products already in mass production enables a cheap heat exchanger to be developed. A difference from standard solar collector absorbers is that these absorbers do not need to be treated with low-emittance coating. Low-emittance coating is used to minimize heat transfer from the hot absorber to the surroundings, while absorbing the solar radiation.

The left illustration in Figure 4.4 shows how the absorbers have been placed in two rows to form the heat exchanger. Placement all in one row or dividing them into many rows has no implications for the performance. The most suitable arrangement varies from case to case, but there could be a difference in how easy or difficult the heat exchanger is to clean. One possible cleaning method could be to remove the front of the case, which would be more difficult if the absorbers are placed in multiple rows. This is also a question that is beyond the scope of this investigation and is instead left to product designers. The size of the hole connecting the manifold to the absorbers was limited to 2 mm, to obtain a well-defined pressure drop on the water side. If there were no pressure drop in the heat exchanger pipes, there would be a risk that more water would go into one of the absorbers than in the others. This imbalance would reduce the heat transfer rate.

Insulating material should be placed around the construction to limit the heat transfer from the indoor air to the air inside the exchanger. Even though the energy that was transported from the room to the air in the heat exchanger returns with the outdoor air, it will still limit the heat recovery of the system. If energy passes from the room to the air in the exchanger there will be a smaller temperature difference between the air

and the brine in the heat exchanger, so less energy can be recovered from the roof. In the extreme case, all the energy that comes out from the heat exchanger is taken from the room, so the heating system in the building has to supply this heat. This creates a situation similar to one in which there is no heat recovery system at all.

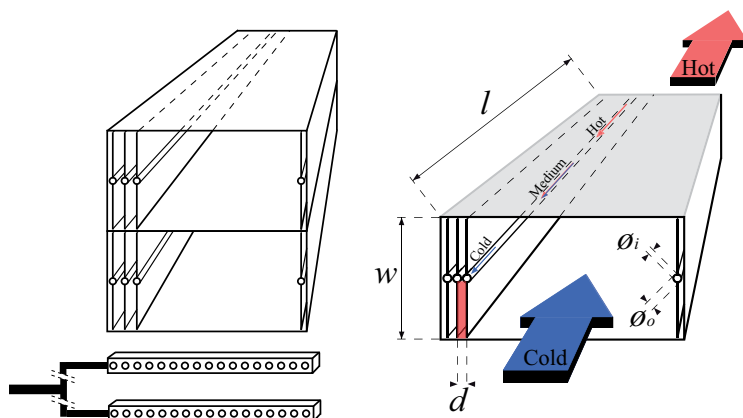


Figure 4.4 Left top: shows the absorbers connected in parallel; bottom illustrates the manifold to which the heat exchangers are connected. Right: Design parameters for the heat exchanger. The red area marks the size of the air flow cell.

Heat transfer rate and pressure drop are calculated for different distances between the absorber, labelled d in the right illustration in Figure 4.4; w in the figure is the width of the absorber, l is the length of the heat exchanger and the absorbers, and ϕ_i and ϕ_o are the inner and outer diameters of the pipes. The red area shows the size of the air flow cell. If the absorbers are less tightly packed, the cell will be twice the height, since the pipes will not cut the cell in the middle.

The absorbers used in the produced prototype and also used as a reference during the calculations are manufactured by S-solar in Sweden (S-solar). S-solar AB also produced the heat exchanger that was tested in the lab. Technical data for the absorbers is given in Table 4.1.

Table 4.1 Technical data for the absorbers in the heat exchanger.

Name	Size	Comment
Width	70, 122, 143 or 167 mm	The 167 mm was used in the prototype
Thickness	0.49-0.53 mm	Calculations was based on 0.5 mm
Material	Copper and aluminium	Copper pipe, aluminium fins

4.2.1 Calculations for the heat exchanger

The design target for the ventilation system was a temperature efficiency of 50%, i.e. 50% of the heat content in the outgoing air will be delivered to the incoming air when there is no condensation. For a standard heat exchanger this means that the temperature efficiency of the heat exchanger must be 50%. This is not the case for a run-around system where the heat transfer process has to be repeated twice, first at the roof for the outgoing air and then for at the air intake for the incoming air. Figure 4.1 and Figure 4.3 serve as examples. Assuming 0°C/20°C outdoor/indoor air temperatures and balanced flows, i.e. the mass flow rate multiplied by the specific heat is the same for the air and the brine, this will produce the same temperature change, but with different signs for the air and the brine. The temperature of the incoming air changes from 0°C to 10°C as it meets the water, of which the temperature falls from 15°C to 5°C. This means that the temperature efficiency of the heat exchanger is 66.67%. However, the temperature efficiency at system level is 50% since the air is heated from 0°C to 10°C when the driving temperature, the room temperature, is 20°C. Figure 4.5 shows the relationship between the component temperature efficiency and the system temperature efficiency. This is discussed in greater detail in Appendix A.

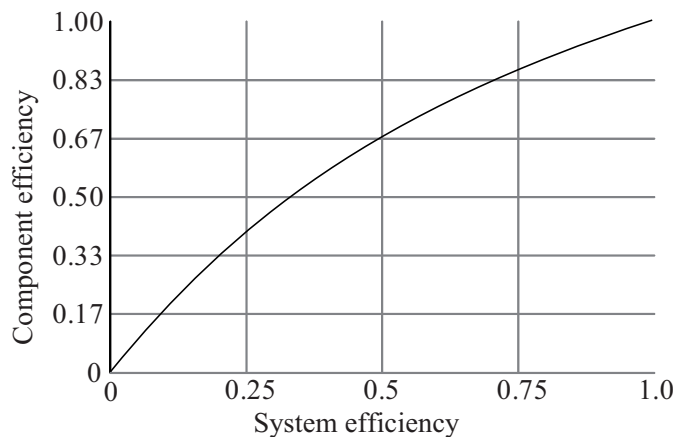


Figure 4.5 The component temperature efficiency as a function of the system temperature efficiency.

The heat transfer calculations were divided into calculating the heat resistance for the heat transfer from the air to the fin, through the pipe, and from the inner wall of the pipe to the water.

Heat transfer calculation, air side

Several assumptions were made for the theoretical calculations:

1. Steady-state conditions
2. One-dimensional conduction
3. Negligible radiation
4. Constant properties, i.e. temperature independent properties.
5. Fully developed flow profile through each cell.

Comments on the assumptions.

1. The indoor and the outdoor conditions change slowly.
2. This is an overestimation for the efficiency of the heat exchanger. In a real situation the heat would be transferred in two dimensions. Figure 4.6 shows an illustration of the problem. If the heat transfer were one-dimensional, the heat would only be transported in the y -direction. Since there is a temperature gradient in the x -direction, the heat will also be transported in this direction. This is indicated with the small arrows in the figure. This will lower the efficiency of the heat exchanger since the exchanger becomes partly short-circuited. There are ways of

improving this. Small strips could be removed from the fins, or parts of the metal in the fin could be replaced with plastic.

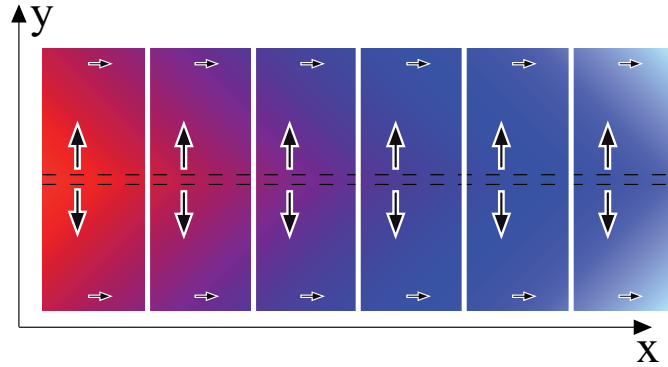


Figure 4.6 *The large vertical arrows illustrate the heat transfer from the pipe in the middle to the fins. The small arrows illustrate the heat transfer in the longitudinal direction.*

3. IR radiation transfers heat from the hotter to the colder part of the fin and is therefore beneficial for the heat transfer and the efficiency in both heat exchangers. However, to some extent it also contributes to the heat transfer lengthwise, which is not beneficial for the efficiency. The truth is probably that IR radiation transfer is not very relevant, since the surface mainly sees other areas with approximately the same temperature. Conductivity and thickness of the fins are probably more important parameters.
4. The physical properties of the water and the air change slightly with temperature in the heat exchanger, but the effects of this are small.

The calculations are described in detail in Paper 3 (Davidsson, Bernardo, & Hellström, 2013c). A short summary of the results are discussed below.

The fin pipes are so densely packed that the copper pipes divide the air flow cells in half. This is illustrated with a red square in the right illustration in Figure 4.4. The width of the cell is therefore $w/2 = 83$ mm. The distance d between the fin pipes was set to 11 mm. If the total air flow is 50 L/s, the velocity of the air can be calculated to be approximately 0.34 m/s. The Reynolds numbers, Re_D , equals 478. This number is far less than the approximately 2300 that is normally considered to mark the onset of turbulence. The air flow is thus assumed to be laminar.

The calculations also take into account the increased heat transfer in the thermal entrance region. This was discussed by Churchill and Ozoe, who developed an expression for Nu_D that covers both the entrance and the fully developed thermal region (Churchill & Ozoe, 1973). This work was reproduced in Bejan, (1993). This is discussed in Appendix B.

Heat transfer calculation, water side

In order to maximize the heat recovery in the system the temperature increase of the air has to equal the temperature drop of the water. In other words, the heat capacity flows should be equal. The heat capacity flow is defined as;

$$\hat{C} = f \cdot \rho \cdot c_p \quad \text{Equation 4.1}$$

If \hat{C} for the hot fluid is equal to \hat{C} for the cold fluid, this gives us:

$\hat{C}_h \cdot \Delta T_h = \hat{C}_c \cdot \Delta T_c$, i.e., $\Delta T_h = \Delta T_c$. This was discussed in London & Kays, (1951) and Holmberg, (1975). This is also discussed in more detail in Appendix A. The basic equations solved to reach this conclusion are shown together with graphs illustrating the energy transport.

This results in a flow of the brine of $1.9 \cdot 10^{-7} \text{ m}^3/\text{s}$, giving a Reynolds number of approximately 23 for the brine. Again this is much smaller than the 2300 and the flow can therefore be considered to be laminar. Including the effects of the thermal entrance region, the Nu_D number is increased by approximately 2%.

The calculations result in a total length of finned pipes of approximately 70 m. If the load is shared between 80 parallel fins (see Figure 4.4 for explanation), it means that each heat exchanger fin needs to have a total length of about 1 m. A 1-m long heat exchanger with the above described geometry would therefore be expected to have a temperature efficiency at system level of 54%, i.e. a component temperature efficiency of 70%.

Calculation pressure drop

One of the key parameters for a heat exchanger in a hybrid ventilation system will be the pressure drop. If it is too large the air will be hindered and the ventilation rate cannot be supplied. The size of the cells in the heat exchanger will greatly affect the pressure drop. Also, the number of cells, and thereby the air speed, will have a major effect on the pressure drop. The pressure drop in the cell is determined by the Darcy friction factor f' . The friction factor varies for different ratios of w/d , see Figure 4.4 for explanation. Equation 4.2 shows the equation from Cornish, Lea and Tadros, reproduced in Knudsen and Katz (1958) for calculation of the

friction factor for rectangular conduits. The equation has been adjusted by a factor of 4 because the Darcy friction factor is 4 times larger than the friction factor defined in Bejan, (1993); Incropera & DeWitt, (2002).

$$f' (d/D_h)^2 \left[1 - \frac{192}{\pi^5 (w/d)} \left(\tanh \frac{\pi w}{2d} - \frac{1}{3^5} \tanh \frac{3\pi w}{2d} + \dots \right) \right] = \frac{6.0}{Re} \cdot 4 \quad \text{Equation 4.2}$$

For the cell shown in Figure 4.4 the friction factor is calculated to 0.171. The pressure drop related to this friction factor can be found using:

$$\Delta p = f' \frac{\rho_{air} u_m^2}{2D_h} l \quad \text{Equation 4.3}$$

where l is the length of the cell, ρ_{air} is the density for the air, u is the average air speed in the cell, and D_h is the hydraulic diameter. The pressure drop for the investigated structure was found to be 0.56 Pa per component, i.e. 1.12 Pa for a system. Using the tabulated value in Incropera & DeWitt (2002) for the friction factor results in almost the same value. The calculations do not include pressure drop from manifolds or any kind of irregularities in the geometry. The pressure drop related to the entrance and the exit of the heat exchanger was estimated to be in the order of 0.01 Pa (Kronvall, 1980).

4.2.2 Measurement of the heat exchanger

The heat exchanger was tested in order to check and calibrate the results from the calculations. The heat exchanger, Figure 4.7, was made 1 m long with 16 parallel connected fin pipes, see Figure 4.4. The total fin area is approximately 5.3 m². This is 1/5 of the size of the supply air heat exchanger for a whole building. The tested heat exchanger can therefore be seen as a heat exchanger used in, for instance, a bedroom. The cross section of the heat exchanger is approximately 0.17 m × 0.17 m. Scaling down the heat exchanger is assumed to have only minor effects on the performance. This is assumed since the width, length, choice of material etc. for the fins is unaltered and the distance between the fins, i.e. the parameter affecting the pressure drop was also the same. Only edge effects are assumed to affect the performance due to the scaling.

The fin pipes could not be soldered to the manifolds in a perfectly straight line due to lack of space between the pipes. Consequently, the fin pipes had to be placed in a zigzag pattern, leaving small gaps between the fins and the wooden sides of the heat exchanger. Any effects on heat exchange and pressure drop from this were disregarded in the calculations.

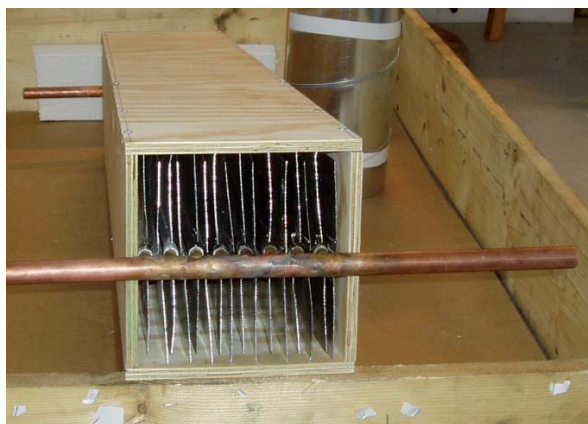


Figure 4.7 *The fin pipes soldered to the manifold in the heat exchanger.*

The wooden box surrounding the heat exchanger was insulated with 50 mm polystyrene and 90 mm glass wool. The test rig, including the heat exchanger, can be seen to the left in Figure 4.8. The controllable fan was installed on top of the heat exchanger to create an under-pressure. Sucking the air through the heat exchanger created a much steadier and a more well-defined air flow compared to blowing air into the exchanger from below.

The air was allowed to pass through a duct of the same size as the surrounding wooden structure of the heat exchanger in order to stabilize the airflow. The measurements follow the standard of measurements presented in Johansson & Svensson (1998). Air at approximately 22°C, i.e. room temperature, was used as inlet air instead of cold ambient air. This simplified the tests significantly. The inlet brine temperature varied between approximately 30°C and 60°C. The measurements were carried out with the following equipment:

- Temperature was measured with a thermocouple for the incoming air. A thermopile was used to create high resolution on the temperature difference for the incoming and outgoing air in the heat exchanger.
- Air flow was measured using an air flow hood, SWEMA Flow 125.
- Water temperatures were measured using PT100 sensors.
- The water flow rate was measured using a MP115 hall sensor from Kamstrup.
- A Campbell CR10 data logger from Campbell Scientific in Logan, USA, was used to collect the measured data.

- A hot wire anemometer, Swema 31, was used to check the air flow profile in the duct. This assured an even distribution of air in the heat exchanger.
- Pressure drop was measured with a Digima Premo. The pressure drop was measured during operation with no heat exchange between the water flow and the air flow. The measurement setup can be seen to the right in Figure 4.8.

The range, accuracy and manufacturers of the measurement devices can be found in Paper 3 (Davidsson et al., 2013c). The calibrations performed for the measurement equipment are discussed in Appendix C.

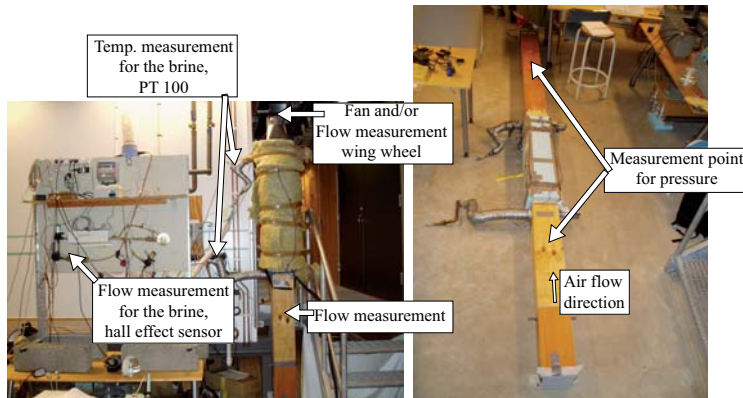


Figure 4.8 Left: The measurement setup. Right: Measurements of the pressure drop.

4.3 Results

Figure 4.9 is a graph showing the brine temperature in and out of the exchanger, the inlet air temperature, the difference between the inlet and the outlet air temperature, and the brine flow rate. The brine flow rate is shown on the right y -axis. The air flow rate was logged manually. This is not shown in the graph. As can be seen, measurements were taken after the temperatures had stabilized. Each dot in the graph is an average of 30 measurements. The measurements were taken every two seconds and were averaged over one minute.

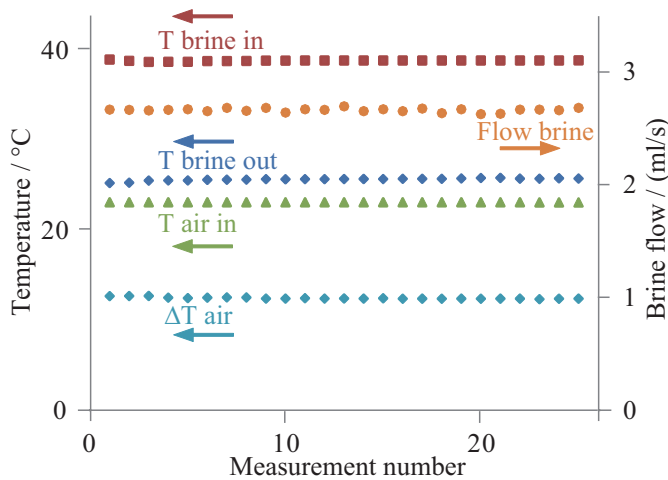


Figure 4.9 Results from a measurement of the heat transfer properties of the heat exchanger. The brine flow uses the right y-axis.

The measurements shown in Figure 4.9 were carried out for five different inlet water temperatures, $T_{w,in}$. The average values over the measurement periods can be seen in Table 4.2. The temperature efficiency, η_{comp} , of the heat exchanger is an average of the temperature efficiency for the water and the air heat recovery. Table 4.2 also shows the power of the heat exchanger, both on the brine side and on the water side. The differences between the two are less than 8% for all measurements, and the average difference is 4%. This is within the estimated error of the air flow measurement alone. Table 4.2 also shows that the temperature efficiency of the heat exchanger appears to drop for high inlet water temperature.

Table 4.2 The performed measurements for the heat transfer rate.

Measurement nr	$T_{w,in}$ /°C	$T_{w,out}$ /°C	ΔT_w /°C	F_w /(mL/s)	T_{amb} /°C	T_{in} /°C	ΔT_{air} /°C	F_{air} /(L/s)	η_{comp}	P_w /W	P_{air} /W
1	31.5	24.6	7.0	2.6	23.3	30.4	7.1	9.1	0.86	76	75
2	38.9	25.7	13.2	2.7	23.3	35.9	12.6	9.5	0.82	146	138
3	42.5	26.7	15.8	2.6	23.3	39.7	16.4	9.0	0.84	173	169
4	61.0	31.0	30.0	2.7	23.2	51.5	28.3	9.8	0.77	336	312
5	61.7	32.1	29.6	2.7	22.2	52.8	30.6	9.5	0.76	327	326

Figure 4.10 is a graph in which both the total length of finned pipes in the heat exchanger and the pressure drop are seen. The continuous lines are calculated values. The length of the heat exchanger was chosen in order to get 67% heat recovery at component level, i.e. 50% at system level. The right y -axis shows the pressure drop for the different spacings and corresponding length. As can be seen in the figure, the pressure drop increases exponentially as the cells becomes smaller. A separation of less than 4 mm would result in a pressure drop higher than the 8.7 Pa discussed in section 1.2.3. Conclusions made from this graph led to the production of the measured heat exchanger with $d = 11$ mm. At this point the pressure drop is still low while the length is reasonably short. If the pressure drop was to be reduced further, the total length of the heat exchanger would be much larger. Alternatively the heat exchanger would have to be made up of a greater number of finned pipes. A decrease in the length of the heat exchanger would increase the pressure drop so much that the system would not work as intended. This is discussed further in section 4.6. The black dot and grey triangle in the diagram are the measured values. Running the heat exchanger according to the conditions described in section 4.2 resulted in a pressure drop approximately double that of the calculated value and 50% total finned pipes length to meet the design target. This is discussed further in section 4.6.

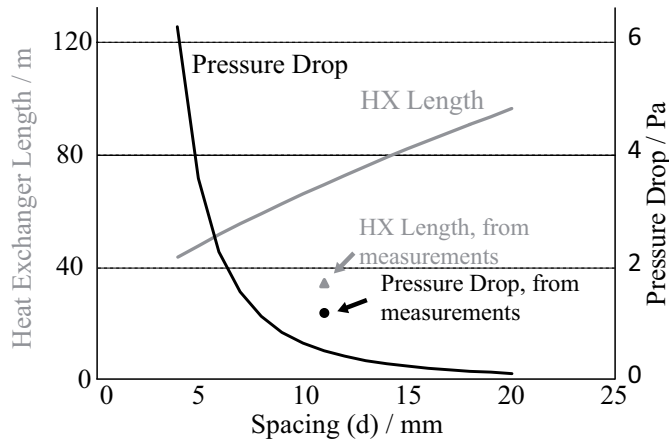


Figure 4.10 Calculated heat exchanger length and pressure drop in order to have 50% system heat recovery temperature efficiency as function of the spacing between the fins. The points show the resulting length and pressure drop for a system of 50% temperature efficiency recalculated from the measurements.

The set up to measure the pressure drop was shown in Figure 4.8, and the results are shown in Figure 4.11. The grey line shows the calculated pressure drop as a function of the air speeds. The calculations were performed assuming no turbulence in the air flow. The figure also shows the measured pressure drop over the heat exchanger (shown in black). As can be seen in the figure, the pressure drop does not increase linearly but there seems to be a quadratic component in the increase of pressure as the air speed is increased. This indicates a turbulent component in the air movement that is apparent even at low air speeds. The pressure drop for normal operation air speed used in a standard single-family house, i.e. approximately 50 l/s, is approximately 1.3-1.4 Pa per heat exchanger, i.e. 2.6-2.8 Pa for both heat exchangers.

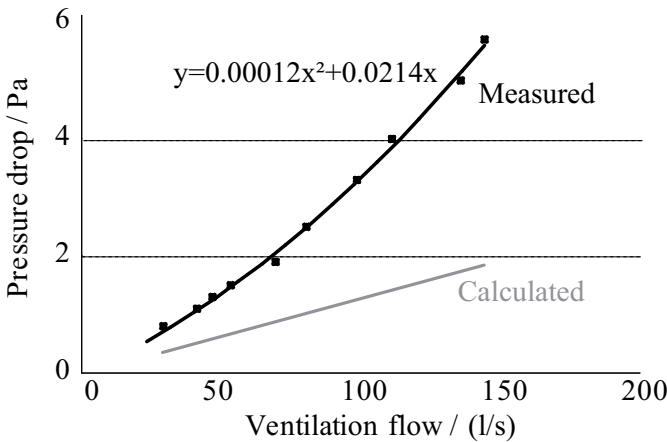


Figure 4.11 Calculated pressure drop for a heat exchanger in grey and measured pressure drop in black.

The discrepancy between the theoretical results, i.e. designing the heat exchanger to have 50% system temperature efficiency and 67% component temperature efficiency, and the experimental results discussed in this section could partly be explained by the finned pipes not being perfectly straight (see Figure 4.12).



Figure 4.12 The heat exchanger. The fin pipes are not straight, resulting in a wavy path for the air through the exchanger. Photo Hans Follin.

Paper 3 introduces scaling factors to account for the discrepancy between the measured and the calculated values (Davidsson et al., 2013c). If the heat transfer resistance is divided by 2 and the pressure drop multiplied by 2.14, the measurements will fit the calculations. This is shown in Equation 4.4 and 4.5.

$$R_{tot} = \frac{R_{air} + R_{pipe} + R_w}{C_1} = \frac{0.55}{C_1} = [C_1 = 2.00] = 0.275 \text{ (W/mK)}^{-1} \quad \text{Equation 4.4}$$

$$\Delta p = f' \frac{\rho_a u_m^2}{2D_h} X \cdot C_2 = 0.647 \cdot C_2 = [C_2 = 2.14] = 1.38 \text{ Pa} \quad \text{Equation 4.5}$$

Equation 4.4 assumes that the error in the calculation is equally distributed between the three different resistances, R_{air} , R_{pipe} and R_w . If, instead, the error is assumed to be completely in the resistance R_{air} , the calibration constant would be $C'_1 = 2.79$. What method to choose is irrelevant for the calibration case, i.e. the 11-mm spacing, but it would affect the rest of the spacings, d , differently. Figure 4.13 shows how the total length of

the finned pipes is affected depending on whether C_1 or C'_1 is used, i.e. assuming the error is equally distributed or fully in the resistance from the air to the pipe. For instance, for $d = 15$ mm, the difference in the total fin pipe length is approximately 4.5%. This is illustrated in Figure 4.13, where the total length of the finned pipes needed to meet the design target is plotted against the spacing between the fins, i.e. d . The grey line is the length assuming calibration constant C_1 and the black line is for calibration constant C'_1 .

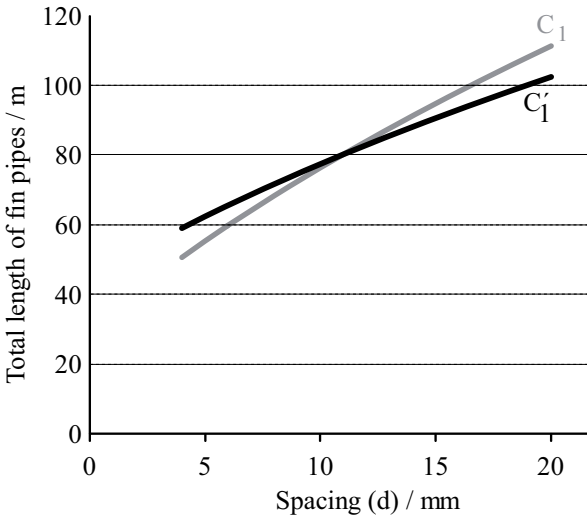


Figure 4.13 Comparison of two alternative calculation assumptions.

Figure 4.14 shows the system performance, i.e. for both the heat exchangers at ground level and the roof heat exchanger. This means that the presented figures are for the sum of the heat exchangers. The temperature efficiency is calculated including the scaling factors C_1 and C_2 . All of the results from this point in the thesis onwards contain the C_1 and C_2 scaling factors. The continuous lines illustrate the total length of finned pipes needed as a function of system temperature efficiency for the ventilation. The blue line is the length needed for a specific temperature efficiency with a maximum pressure drop for the system of 1 Pa, i.e. the pressure drop for both of the heat exchangers at the air intake and the air outlet. The red line shows the same but for 3 Pa, the green line is for 5 Pa and the purple line is for 10 Pa. The dashed lines show the distance between the fin pipes, i.e. the distance d in Figure 4.4, to build those specific heat exchangers. The arrows in the diagram show an example. To obtain 70% system temperature

efficiency with a pressure drop of 1 Pa, the heat exchanger spacing, d , needs to be 18 mm, with a total length of finned pipes of approximately 210 m. The blue dashed line is for the 1 Pa pressure drop heat exchanger, the red, green and purple are for the 3, 5, and 10 Pa pressure drop heat exchangers, respectively.

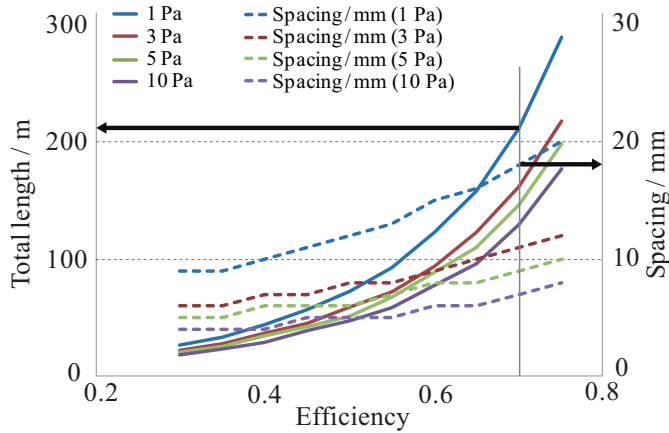


Figure 4.14 Total length of the heat exchanger on the left y-axis and spacing between the fins on the right y-axis as a function of system temperature efficiency for the ventilation for four different total pressure drops, 1, 3, 5 and 10 Pa.

4.4 Parametric study of the heat exchanger

The heat exchanger can be further developed in a number of ways. Changing the geometry or the material of the pipes and fins could result in both more efficient and/or cheaper heat exchangers. The optimization investigation carried out was based on a heat exchanger of 82% temperature efficiency at component level. In order to meet this target, the length of the heat exchanger had to be varied. In the list below all the parametric investigations are presented.

Parametric investigation 1

The geometry of the heat exchanger can be altered to change both heat transfer rate and pressure drop. Two alternatives to the heat exchanger discussed in section 4.2 and 4.3 were investigated. These are shown in Figure 4.15. In Alternative A, the proportions of the fins are changed.

Reducing the width, w , of the heat exchanger by 50% while doubling the number of finned pipes gives the same cross-sectional area for the heat exchanger. Alternative B was to double the size of the heat exchanger. The size of the cells in which the air moves was the same while the number of cells was doubled.

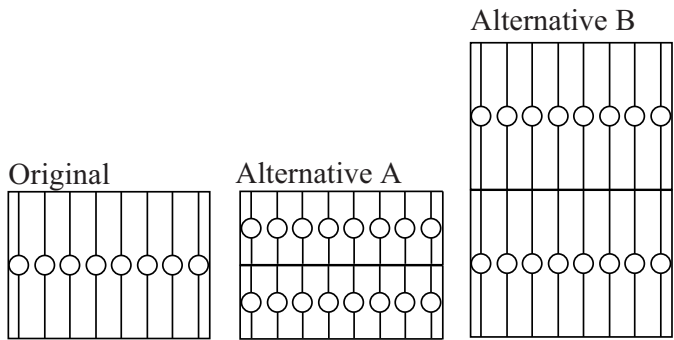


Figure 4.15 The investigated geometries.

Parametric investigation 2

The original heat exchanger was made up of a copper pipe with aluminium fins, but the pipe and fin materials can be altered in a number of ways. Various materials were investigated – aluminium (Al), copper (Cu), plastic (Pla) and stainless steel (Sts). These materials were tested in various combinations for pipe and fin material. The various combinations are listed in Table 4.3.

Table 4.3 Material combinations for the fin pipe.

Material combination	Pipe material	Fin material
1	Cu	Al
2	Cu	Cu
3	Al	Al
4	Pla	Cu
5	Pla	Al
6	Sts	Sts
7	Pla	Pla

It should be noted that the production technique used today by S-solar results in the pipe being fully surrounded by the fin material. Consequently,

material combination 5 in Table 4.3 has a plastic pipe covered by copper, and copper fins attached to it.

Parametric investigation 3

The importance of the thickness and width of the fin was investigated for pipe/fin material combinations 1, 2 and 3. Two fin thicknesses were chosen for the investigation, namely 0.5 mm and 0.1 mm.

4.5 Results, parametric study

Figure 4.16 shows the results from the geometrical study. The length of the finned pipes for the heat exchanger at component level is in black and the pressure drop for the heat exchanger is in grey. The original heat exchanger is made up of 80 m fin pipes and has a pressure drop of approximately 1.4 Pa at component level. In Alternative A the fins are made shorter. This results in longer finned pipes, since the heat exchanger surface per pipe is reduced. However, the pressure drop is reduced since the length of the heat exchanger is reduced. Still, Alternative A has twice as many absorbers as the original. Alternative B has the same number of metres of fin pipes. However, the pressure drop is reduced strongly since the speed of the air is reduced.

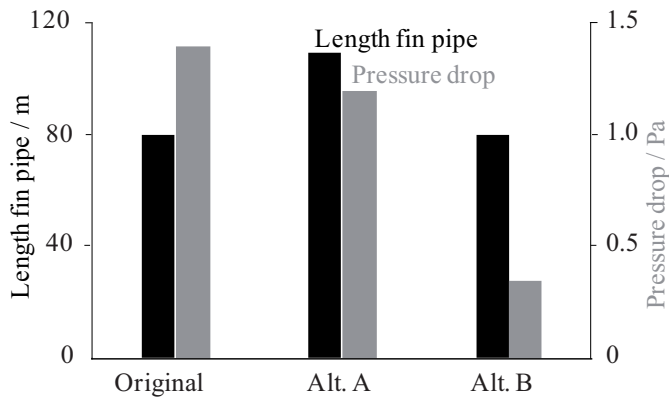


Figure 4.16 Results from the geometrical investigation. The total length of fin pipes is in black and the pressure drop is in grey. Both numbers are at component level.

The investigation of various material combinations for the finned pipes is shown in Figure 4.17. The length of the finned pipes needed to meet the requirement is presented on the y -axis. As can be seen, the difference is not significant, regardless of whether aluminum or copper is used. The fourth and fifth bars show the results when plastic pipes are used. The thickness of the pipe is less than 1 mm. This limits the thermal resistance in the pipe itself, making it possible to use plastic as piping material. However, plastic fins have limited heat transfer, so the total length of finned pipes must be very long. Note that the bar showing the plastic finned pipes has a scale break. Stainless steel also performs poorly.

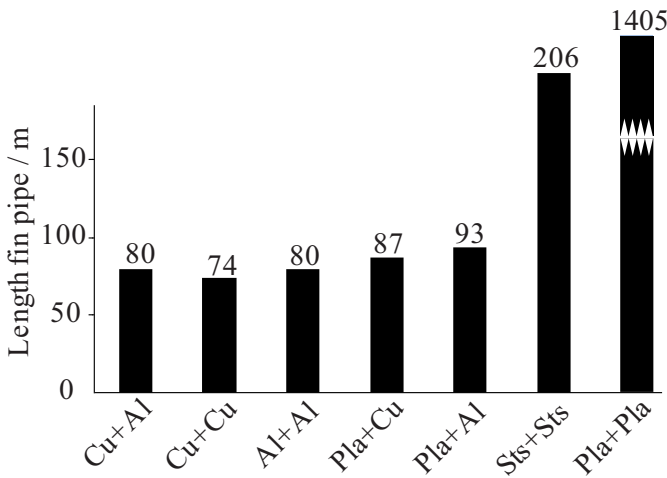


Figure 4.17 Total length of fin pipe for different material combinations.

The effects of varying the thickness and width of the fin are shown in Figure 4.18. The figure shows material combinations 1, 2, and 3. The blue and red lines, using the left y -axis, show the relative material costs. The relative material cost, S , is defined as:

$$S = V_{Al} \cdot 1 + V_{Cu} \cdot 13.9 \quad \text{Equation 4.6}$$

where V_{Al} is the volume of Al and V_{Cu} is the volume of Cu. The multiplication factor for the copper, i.e. 13.9, was determined as the ratio of the price per volume of copper to that of aluminum on 1 November 2012. The green and yellow lines, using the right y -axis, show the total length of finned pipes needed to meet the requirements, i.e. a system temperature efficiency of 70% for the heat exchangers.

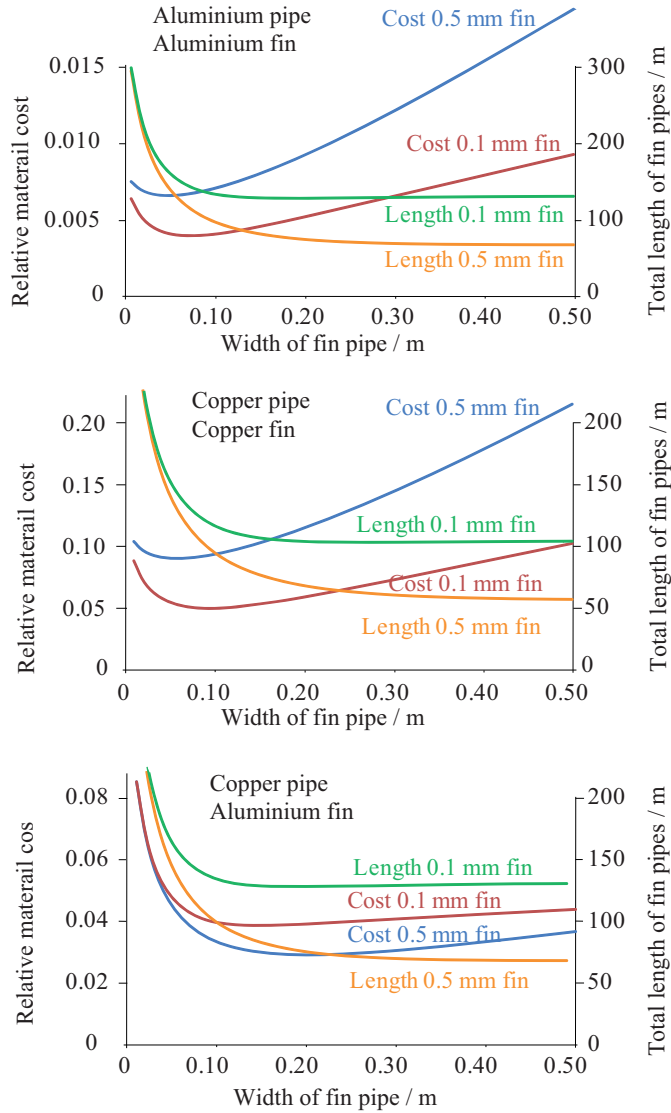


Figure 4.18 Optimization of thickness and width of the fin.

4.6 Discussion and conclusion of the heat exchanger development and the parametric study

A photo of the heat exchanger was shown in Figure 4.12. These non-straight finned pipes and blunt ends of the fins could cause vortices in the air flow. The manifold for the water pipes could also give rise to a disturbed air flow pattern in the entrance region. The disturbed flow will have an increased heat transfer compared to perfectly laminar flow. Simultaneously, it will add resistance to the air, so the pressure drop will increase. This is also seen in the measurements presented in Figure 4.10, where it was shown that the heat transfer rate is increased, and so the required length of fin pipes is reduced. At the same time, the pressure drop is increased. The heat transfer rate and the pressure drop both increase approximately in a similar manner, which is as expected according to the Reynolds analogy (Incropera & DeWitt, 2002). In Figure 4.11, measurements showed that the air flow has a turbulent component already at low air speeds. This leads to the same conclusion.

The effective area is also slightly larger than the theoretical area. The performed calculation does not include the area of the copper pipe, nor does it take heat transfer from the wooden box or the manifold into account. There is also a pressure drop related to the passage into and out of the heat exchanger. This pressure drop was however estimated to be negligible.

Due to the limitations in the project, only one heat exchanger could be tested. This limits the validity of the scaling factors that are presented in Equations 4.4 and 4.5. Strictly speaking, they are only valid for the tested heat exchanger, but Figure 4.13 indicates that the difference in required total length of finned pipes in order to meet the design parameters is limited for the two different approximations. For instance, it was shown that for the 15 mm spacing between the fins the two approximations differ by about 4.5%. These calculations still assume laminar flow, and adding turbulence in the calculations could change this scaling. Measurements for other fin spacings would be useful. If the differences are small between the points where the scaling factors were applied to the new point of interest, the error is limited. This is because the scaling factor was applied for a heat exchanger with 11-mm spacing between the fins, so the equations should also be acceptable for distances close to 11 mm. It is of course very difficult to state the exact range of valid points.

Figure 4.14 shows that the savings in finned pipe length are not very significant, even if the pressure drop is allowed to increase. For instance,

allowing the pressure drop in the system to increase from 3 to 5 Pa for a system temperature efficiency of 70% only reduces the total finned pipe length from 153 m to 138 m, i.e. about 10%. If the pressure drop needs to be even smaller, a larger number of finned pipes could be used. If the heat exchanger is produced with 160 parallel connected finned pipes instead of the 80 discussed in Paper 5 (Davidsson, Bernardo, & Hellström, 2013b), the speed of the air and thereby the pressure drop would be reduced. This was illustrated in Figure 4.16. Basically the heat exchanger can be made up from the greatest possible number of parallel connected finned pipes to keep the pressure drop low. Nevertheless, the total length of finned pipes in the heat exchanger is kept constant, but this is only true to a certain extent. Davidsson et al. (2013c), Paper 3, showed that heat transfer rate is dependent on air speed. Greater air speed increases heat transfer. This means that a greater number of absorbers, and thereby slower moving air, will have a lower heat transfer rate. However, this effect is limited and should be studied in more detail.

Which of the original heat exchanger or Alternatives A or B in Figure 4.16 is preferable will vary according to the situation. If the heat exchanger is to be installed in a renovation project the unit could be installed under or behind a radiator, so a wide and thin unit would be needed. Alternative B or possibly an even wider and shorter alternative could therefore be the best solution. If instead the unit is to be used for the outgoing air in a multi-family building it is more likely that a longer unit has to be used in order to make the cross-sectional area as small as possible. If the unit for the outgoing air has the same area as the sum of all the areas for the incoming air units it might be difficult to install. This could be the case if the one unit for the outgoing air is connected via the brine circuit to many units for incoming air.

For a typical single-family dwelling containing five rooms with fresh air intake, the situation could be the following. In each of the rooms a heat exchanger with the cross-section $17 \times 51 \text{ cm}^2$ is installed. This means that the heat exchanger from Figure 4.7 has been divided in three parallel parts. The length will therefore be approximately 0.33 m. This unit could be installed inside the wall and the air could be let out behind the radiator. The roof unit would then have to be five times larger to have the same heat transfer properties as the total of the five incoming units. However, this would mean a cross-section of $85 \times 51 \text{ cm}^2$ (0.33 m long). It would be difficult to obtain an even air flow through this large unit, so the unit could be made longer. One alternative could be to install a $17 \times 51 \text{ cm}^2$ unit that is five times longer, i.e. 1.67 m long. The figures above serve only as an example. Other cross-sections and lengths of heat exchangers are possible. The installer of such a system must also take into account the piping needed for the brine circuit. One solution could be to install two

branches of pipes, one serving the east side of the building and the other the west. The arrangement will differ between different installations.

The design of this type of heat exchanger with more absorbers, such as Alternative B in Figure 15, would require a large entrance hole in the wall. The large cross-section of the heat exchanger would make it difficult to control the air flow through it. Uneven flow in the heat exchanger will reduce the efficiency. Figure 4.16 also showed that using smaller fins has the potential to result in a more compact heat exchanger, but this would also make it more expensive, since more work is required due to the larger number of finned pipes.

The second parametric investigation presented in Figure 4.17 shows that the choice of material in the pipes is of relatively low sensitivity. For instance, in principle, either plastic or stainless steel pipes could be used. Replacement of the copper pipes in the original heat exchanger by plastic ones only requires an additional 16% of finned pipes, but the use of stainless steel as fins has strong limitations on the performance. The rather low thermal conductivity of the stainless steel greatly limits the performance. As can also be seen in the figure, the use of plastic as fin material is not an option. Which combination of materials is most suitable is a question of both performance and price. The investigation performed here does not consider the technical challenges related to production of the units. Whether for instance the plastic pipe in combination with aluminum fins can be produced is a question for the industry. The performed analysis only explains the drawbacks and benefits of such a product.

Figure 4.18 shows cost optimization based on calculations for different material combinations. The optimization is based solely on material costs. The relative cost of the heat exchanger made of copper is much higher than that of the aluminum, but the total length of the finned pipes is also relevant since it relates to the production costs. Long finned pipes will result in either long heat exchangers or many parallel connected pipes. If the heat exchanger becomes long the pressure drop increases. At the same time the exchanger also becomes difficult to integrate in the building. If, on the other hand, many pipes are connected in parallel the pressure drop will be lower. However, this alternative will very probably increase production costs due to the increased work involved in connecting the many pipes to the manifold. If the cost related to mounting the pipes is high, copper can be motivated, since copper pipes and fins result in shorter heat exchangers. The same could be true for the case with extra thin fins. Figure 4.18 suggests that the 0.1 mm fins appear to be a better choice, but using these thin fins could result in production difficulties. This discussion is beyond the scope of this thesis.

Reducing the size of the heat exchanger or increasing the efficiency could increase pressure drop. This might mean that the system would

not work as intended, i.e. the pressure drop would be so large that the complementary fan would need to be continually operated. However, this could still be a good solution. A few more watts used by a fan could be worthwhile if this increases heat recovery. This is a difficult question and more simulations at building level are needed to answer it.

In the introductory section, it was stated that the mechanical ventilation system recovers only 40% of the primary energy. This does not imply that mechanical ventilation systems should not be used – it is merely an illustration of a problem. The difficulties of drawing conclusions from this are also indicated in Dadoo, Gustavsson, & Sathre (2011), where a number of different investigations are summarized. The energy savings when installing mechanical ventilation with heat recovery vary greatly. Even negative energy savings were found. Furthermore, the energy use from the pumps also has to be included in the calculation. According to one pump manufacturer, the annual energy use for pumping the brine for a single-family house is estimated to be 27 kWh. The recommended pump can be found at the Wilo webpage (Wilo). The fan needed for the system is expected to use approximately 40 kWh annually (Aereco). This figure is much lower than the energy use for running the fans in the mechanical ventilation system.

A pressure drop over the heat exchanger of around 1 Pa with a heat recovery rate of approximately 70% makes it possible to build passive houses using this ventilation technique. However, one problem could be to supply the auxiliary energy needed to keep the building at the desired temperature. This is normally supplied by the air in a passive house. The system could also possibly be used in retrofitting old houses that lack heat recovery for the ventilation system. The alternative to this is otherwise extensive duct work for mechanical ventilation with heat recovery. A clear advantage of the system discussed in this paper is that the effects on the building are small. For instance, the existing exhaust ducts can be used, and the ducts to the incoming air are kept minimal as the incoming air can go straight through the outer wall. The short duct system is beneficial since ducts can be contaminated with dust and dirt (Balvers et al., 2012). This type of ventilation system is also suitable for buildings where cross-contamination is extra sensitive, such as hospitals and research facilities. Cross-contaminations can otherwise occur when the supply air and the exhaust air are located next to each other and meet in the exchanger.

4.7 Future work, heat exchanger and ventilation

Some problems still remain that need to be addressed in future work. Examples are investigating pressure loss in supply air grilles and ducts. Controlling the air flow is also a challenge, not only keeping the air flow high enough to meet the requirements but also to avoid over-ventilating the building during windy conditions. Using automatic dampers to increase pressure drop and thereby reduce the wind-induced air flow or using manually operated supply air grills are two ways of controlling the ventilation rate. However, dampers might also introduce additional pressure drop for the outgoing ventilation air. System design has to take this into account.

The operation of the system is also very important. During periods of overheating in the building, the pump for the water circuit can be turned off or reduced in speed. An unbalanced air/brine flow will lower the amount of recovered heat, thereby reducing the overheating of the building. During the summer when the thermally induced driving forces for the ventilation are low, cross-ventilation by open windows can complement the ventilation system. If this is not possible, the fan in the hybrid ventilation system has to be used.

The ventilation system also needs to be investigated at system level. If the ventilation system is used in a multi-storey building, flows on the different levels must be investigated. Variations in wind pressure at various building heights and varying height differences between incoming air and exhaust air outlet cause uncertainty.

Investigations of the system over a full year would also be very interesting since the ambient temperature can vary greatly. This is not only a question for hybrid ventilation systems but also for mechanically ventilated buildings.

5 Waste water heat recovery

Many of the energy flows relating to a building, such as thermal gains through the windows and from a solar collector on the roof, thermal losses through the building skin, and heat recovery from the ventilation air, are well understood and thoroughly investigated. In most cases, there are also many different solutions on the market. However, this is not the case for recovering heat from waste water. The current market is very small, but the potential market is enormous, i.e. every single dwelling.

One major difference from solar collectors is that waste water heat recovery will save more or less the same amount of energy every month throughout the year. This is not the case for solar thermal collectors, which are dependent on incoming radiation.

A major problem of heat recovery from waste water is that inflow and outflow are not always simultaneous. One of the worst scenarios from this perspective is to recover energy when filling and emptying a bathtub. When water is filling the tub, there might be no water leaving the building, and so no energy can be transferred. The situation is the same when the tub is emptied. The hot water from the tub has no incoming cold water to transfer its energy to, so no heat will be recovered. This problem can be solved partly by storing the waste water in a tank. This type of storage would make it possible to use that energy for other purposes. One idea could be to heat ventilation air with it. If the waste water is somewhere around 30°C, it can be used to heat the ventilation air after the air has been preheated in the heat recovery system. This is discussed in section 6.

A standard waste water heat recovery system could not be installed in Solgårdén. Most systems have to be installed during construction, and retrofitting is more difficult. In order to test the waste water heat recovery system in Solgårdén, a new type of installation was constructed. Measurements of the system were performed after a few months of operation in order to test the heat transfer properties after contact with the waste water. The measurements were used to adjust the heat transfer rate for the TRNSYS type used in the system simulations.

5.1 The installed test unit

Two simple waste water tanks with built-in coil heat exchangers were constructed and installed. This is shown in Figure 5.1. Three coil heat exchangers for different heat carrier flows were placed next to each other inside the tanks. The waste water tanks were constructed and connected in series. The heat exchangers could be utilized by, for instance, solar collectors or heat pumps, or could be used to preheat ventilation air or domestic hot water. The system utilizing two waste water tanks is discussed in Paper 6 (Davidsson et al., 2011). The system investigated in Paper 4 (Davidsson, Bernardo, & Hellström, 2013a) only contains one waste water tank.

During the tests and later in the simulation, only grey water was used, i.e. no water from toilets was included in the system. This was because toilet water could easily clog the system. Toilet water is also cooler and would therefore dilute the warmer grey water.



Figure 5.1 *The heat exchangers inside the waste water tanks.*

5.2 Results

Measurements were carried out for two different heat carrier flow rates, 1.4 l/s and 2.9 l/s. The locations of the different measurement points are shown in Figure 5.2. The measurements were taken after the system was stabilized, i.e. the flow was kept running for a long time so that all temperatures could attain steady state. The results from the 2.9 l/s measurement are presented in Table 5.1. The table also shows the TRNSYS simulations. The presented efficiencies are average values for the waste water heat loss and the fresh water heat gain. During the test only hot water was used, i.e. there was no cold water mixing in any of the taps and so the flow was equal in both directions. The presented values are from simulations carried out with heat transfer rates unaffected by dirt and fat. The results from the measurements and the simulations correspond well.

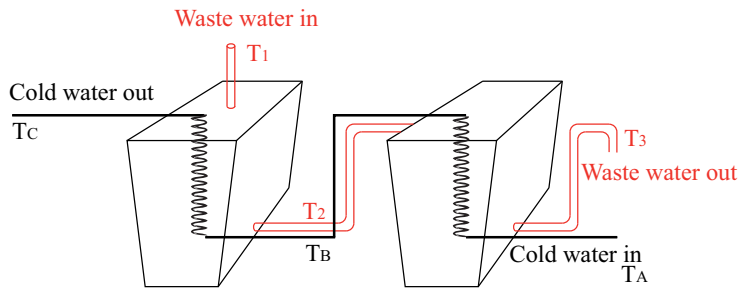


Figure 5.2 Illustration of the measurement setup.

Table 5.1 Validation of simulations of the waste water storage tanks.

Measurement point Flow = 2.9 l/minute	Measurement temp / °C	Simulation temp / °C
T _A	14.1	14.0
T _B	25.5	24.6
T _C	38.5	37.7
T ₃	51	51
T ₂	41	37.9
T ₁	28.5	27.3
	Temperature efficiency = 64%	Temperature efficiency = 64%

5.3 Conclusions, discussion and future work

The main conclusion from the investigation is that the dirt and fat in the waste water have limited effect on the heat transfer rate of the heat exchangers. However, further tests should be carried out in the future to investigate whether this conclusion is still valid for longer test periods.

The limited effect of dirt and fat on the heat exchangers could partly be explained by the installed filter (Avloppscenter). How well this filter protects the heat exchangers was not investigated in this study, but the effect of this filter on the system could be the subject of future study.

6 Hybrid ventilation: system analysis

The hybrid ventilation concept was also investigated on system level using TRNSYS simulations. The aim was to investigate the effects of adding different energy sources such as ground source heat exchangers and waste water heat recovery systems to the ventilation system. The complexity of such flows was discussed briefly in section 1.4. The investigation was carried out in three steps. Step 1 was to investigate the impact of energy use on different configurations of mechanical and hybrid ventilation systems using heat recovery, combined with the waste water heat recovery and a ground source collector. In step 2 a comparison was made between different ways of utilizing the waste water tanks for the preheating of ventilation air. The third step was to also include a solar thermal system.

6.1 Step 1 - method

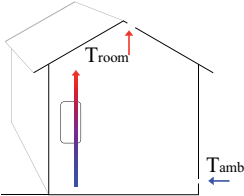
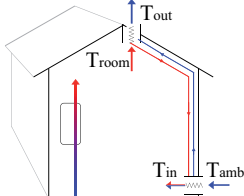
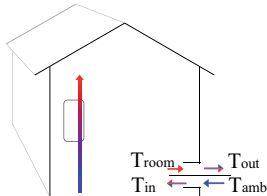
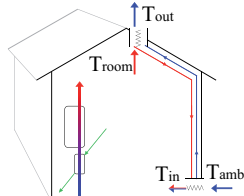
The hybrid ventilation system described in section 4 (see Figure 4.1), with a brine-based heat transport system, enables alternative system solutions. One solution could be to utilize the ground for heating or cooling. The main idea is to preheat the brine in the ground after it has been cooled in the heat exchanger for the incoming air. The brine-based ventilation system also allowed the use of alternative energy sources.

One idea was to make use of the energy from the waste water. The energy content in the waste water is relatively high but the quality of the heat is rather poor due to the low temperature, which makes it difficult to recover. It was also discussed in section 5 that there is a problem with an imbalance between the flows of fresh water and waste water, since they are not always simultaneous nor are they equal in quantity, since the outgoing warm water is larger in quantity than the incoming for heating. This limits the recoverable heat in the system. As discussed, one solution

to these problems could be to use the energy stored in the waste water tanks to heat the incoming ventilation air.

These system solutions were analysed using TRNSYS. The different systems are illustrated and discussed in Table 6.1. The different TRNSYS types and the most relevant parameters used in the simulations are discussed in Paper 4 (Davidsson et al., 2013a).

Table 6.1 The analysed systems

Simulation case	Description	Illustration
Case 1	The baseline case, labelled 1, is a building with natural ventilation with no heat recovery from the ventilation air.	
Case 2a	Case 2a includes heat recovery from natural ventilation. Simulation Case 2a was equipped with the heat recovery system shown in Figure 4.1.	
Case 2b	Case 2 is developed from Case 1. Simulation case 2b was equipped with a mechanical ventilation system with heat recovery.	
Case 3a	Simulation Case 3a had the same ventilation system as Case 2a but it was also equipped with a waste water heat recovery system. The waste water heat recovery system is discussed in section 5. The waste water heat recovery system was used to preheat the domestic hot water.	

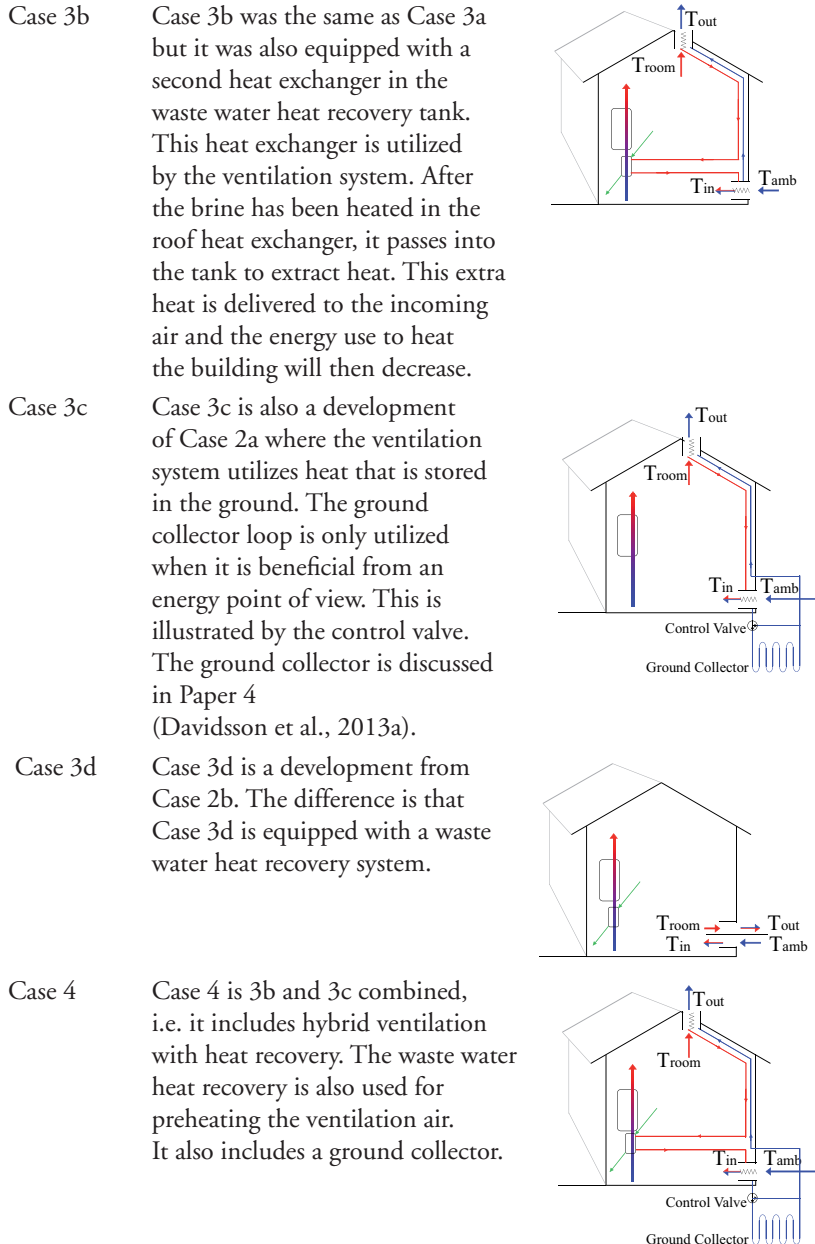


Figure 6.1 shows the daily flow and temperature profiles of the waste water, used in the TRNSYS simulations. The flow profile A is a simplification of the data used by Widén, J., Lundh, M., Vassileva, I., Dahlquist, E., Ellegård, K., & Wäckelgård, E. (2009). Profile A is the parts illustrated in black. Profile B is equal to Profile A, except that it also includes cold water

flushing of the tanks. Flow profile B was introduced in order to investigate the sensitivity of the water flow and temperature profile.

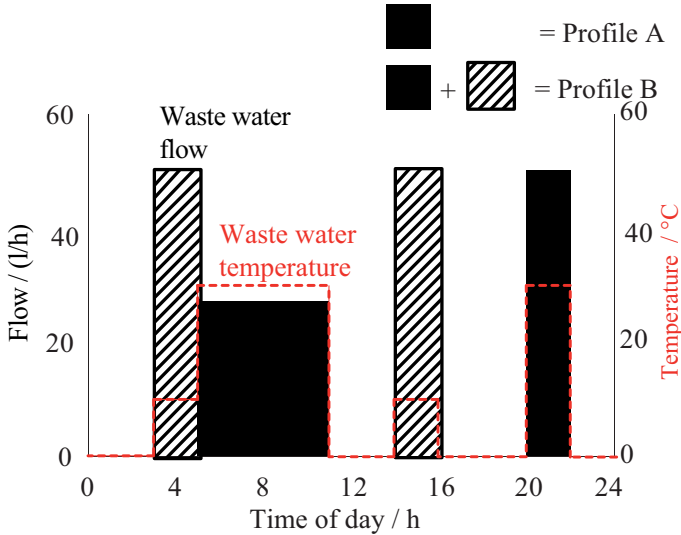


Figure 6.1 The two profiles, A and B, of the flow rate in black and the temperature in red of the waste water used in the simulations.

6.2 Step 1 - results

Figure 6.2 shows the resulting total annual thermal energy demand for space heating and domestic hot water as a function of the temperature efficiency of each of the heat exchangers. The upper figure shows the results for the low-energy building and the lower one for the standard insulated building. The horizontal lines show the resulting annual thermal energy demand for the cases with mechanical ventilation with heat recovery, with and without the waste water heat recovery, cases 2b and 3d. The result does not include the electricity needed to run the ventilation fans. The results are presented as lines since the performance is independent of the temperature efficiency of the heat exchanger for the hybrid ventilation. The results show that installing waste water heat recovery lowers the annual thermal energy need by approximately 600 kWh annually. The simulations were performed using the waste water Profile B, see Figure 6.1. The results also show that the difference in thermal energy performance between system 2a and system 3c is small. The same results are found comparing

system 3a, system 3b, and system 4. The differences in thermal energy performance are small.

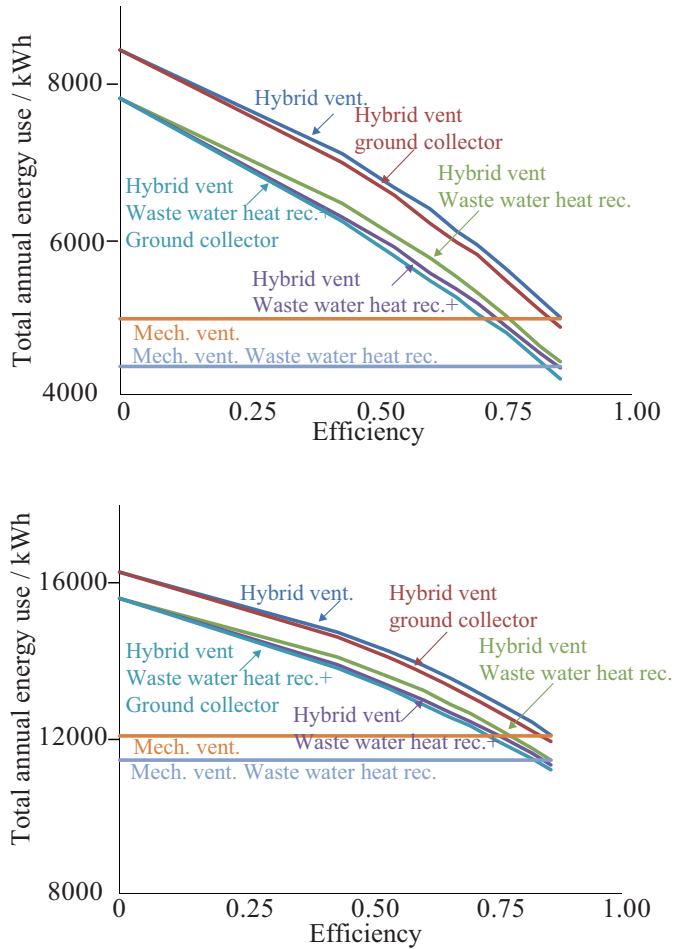


Figure 6.2 Total thermal energy demand, i.e. space and domestic hot water heating, for various simulations as a function of temperature efficiency of each of the heat exchangers for ventilation heat recovery. Upper graph: low-energy building. Lower graph: standard insulated building.

Figure 6.3 illustrates the annual energy flow for a low-energy building. The black bars represent simulation Case 2a and the grey Case 3c. This means that the hybrid ventilation with heat recovery system is compared with an equivalent system, but with the difference that a ground collector has been added.

The first bars show the annual heating needs of the two systems. The difference between the two systems is approximately 150 kWh annually. The second group, with only one bar, is the annual thermal energy transferred from the ground to the brine by the ground collector. This is approximately 1000 kWh annually. The third group is the thermal energy delivered to the incoming air by the heat exchanger located at the bottom of the building. Simulation Case 3c delivered approximately 200 kWh more than simulation Case 2a on an annual basis. The reason why the thermal energy need is only reduced by 150 kWh annually when the heat exchangers deliver 200 kWh is that parts of this energy will not be used to reduce energy use. It will only be used to increase overheating of the building. The fourth group shows the annual thermal energy recovered from the outgoing ventilation air by the roof heat exchanger. The arrows in the figure indicate that what is gained in the ground collector is basically lost in the roof heat exchanger. The simulations are based on using a heat exchanger with a temperature efficiency of approximately 75%.

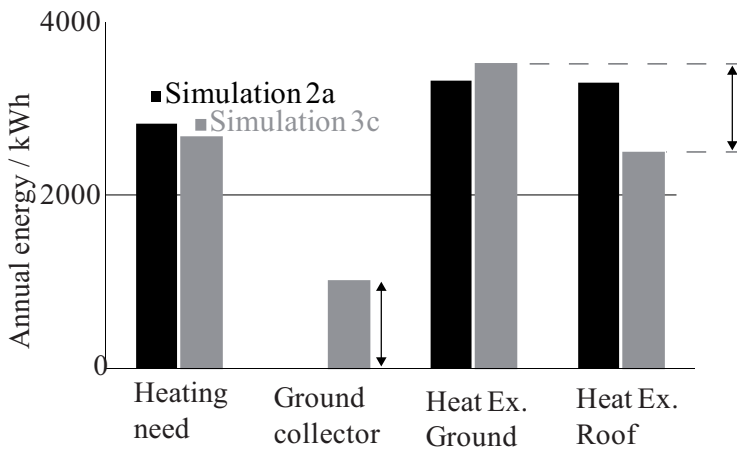


Figure 6.3 The annual thermal energy demand and energy flows for a low energy building for two simulation cases, Case 2a in black and Case 3c in grey.

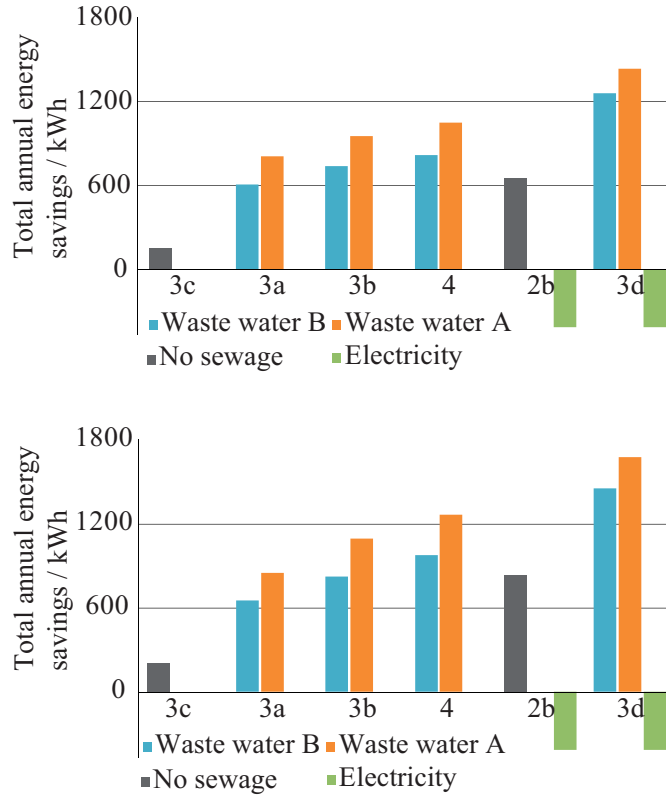


Figure 6.4 Saving potential for the different systems for waste water flow Profiles A and B, see Figure 6.1. Upper graph: results for the low-energy building; lower graph: standard insulated building.

Figure 6.4 shows the potential saving between the different cases. All the simulation cases are based on using heat exchangers with a component temperature efficiency of approximately 75%. The upper figure is for the low-energy building and the lower one for a standard insulated building. The basis for the simulation is case 2a, i.e. a hybrid ventilation system with heat recovery. The first bar shows the achieved annual thermal energy saving by switching to simulation Case 3c. Installation of a ground collector saves about 150 kWh of thermal energy per year. The second group of bars shows the resulting thermal energy saving from simulation Case 3a. The blue bar is for waste water flow Profile B and the orange for Profile A. Installing a waste water heat recovery system reduces the annual thermal energy need by approximately 600-800 kWh. The third group of bars is for System 3b. This case performs slightly better than Case 3a.

The fourth group is for simulation Case 4. The fifth group is for Case 2b, i.e. the mechanical ventilation with heat recovery without waste water heat recovery system. This system will use about 420 kWh more electrical energy compared with the hybrid ventilation systems. This is shown with the green bar.

The electrical energy use for the hybrid ventilation system was estimated from temperature difference data from the simulation, along with information on the fraction of time that the brine was being circulated. The support fan is assumed to have an annual average electrical power use of 4 W (Aereco). The right bars are for Case 3d. This system is assumed to use as much electrical energy as Case 2b. The waste water heat recovery system recovers approximately 700 kWh annually.

6.3 Step 2 - method

The efficiency of the system could be improved if the heat taken from the waste water storage tank delivered to the ventilation system is circulated in a separate circuit instead of in series with the other heat exchangers. This is illustrated in Figure 6.5. To the left are the ventilation systems with one heat exchanger circuit. The right illustrations show the case where the heat recovered from the waste water storage tank is delivered in a separate circuit. The upper illustrations are for systems without a ground collector and the lower are for systems including a ground collector.

The systems shown in Figure 6.5 were investigated both from a steady-state perspective and from an annual thermal energy performance analysis. The annual analysis was carried out with the TRNSYS deck explained in Step 1, see Table 6.1. The steady state analysis was carried out using an Excel sheet program.

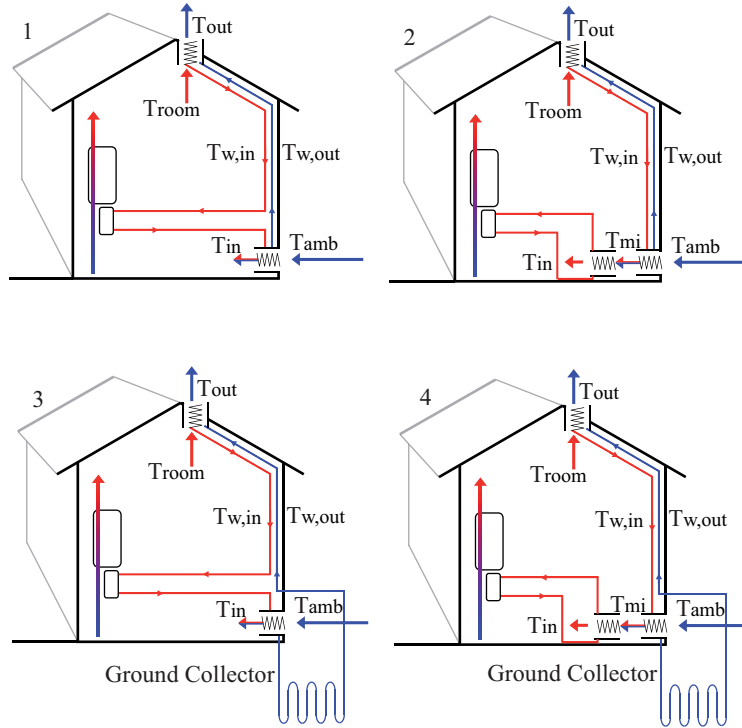


Figure 6.5 The four investigated heat recovery systems.

6.4 Step 2 - results

The results of the steady-state calculations are shown in Figure 6.6. The different systems follow the same numbering as Figure 6.5. The heat exchangers are assumed to have 75% temperature efficiency on a component level. This means having ratio of the UA -value and the $f_a \rho_a c_{pa}$ of 3. At the same time the flows are assumed to be balanced according to $f_a \rho_a c_{pa} = f_w \rho_w c_{pw}$. This is discussed in Appendix A. The ambient temperature is assumed to be -10°C and the outlet brine temperature from the waste water heat recovery system is assumed to be 30°C . The systems with two circuits, illustrated with red lines, perform better than the single-circuit systems. System number 2 lets 24.5°C air into the building while system 1 only reaches 20°C . However the waste water tank is emptied faster in system 2 compared to system 1. The cold brine coming to the waste water tank is 1.5°C colder in system 2. This means that this tank will lose heat

faster. However, this is not a problem since the heat is lost to the incoming air, i.e. the thermal energy is recovered.

The situation is very similar for the systems that include the ground collector. The incoming temperature for the double circuit is approximately 5°C warmer than for the single circuit, i.e. system 3. Furthermore, the ground collector gains more thermal energy in System 4 than in System 3. System 3 has a temperature rise of 8°C when system 4 increases the temperature by approximately 11°C. At warmer ambient temperatures the situation could be more complicated. If the ambient temperature were 10°C, system 3 would have 15°C brine coming into the ground collector. This would mean that the system would lose heat to the ground. This might not be an optimal solution. System 4 would have 12°C warm brine coming to the ground collector.

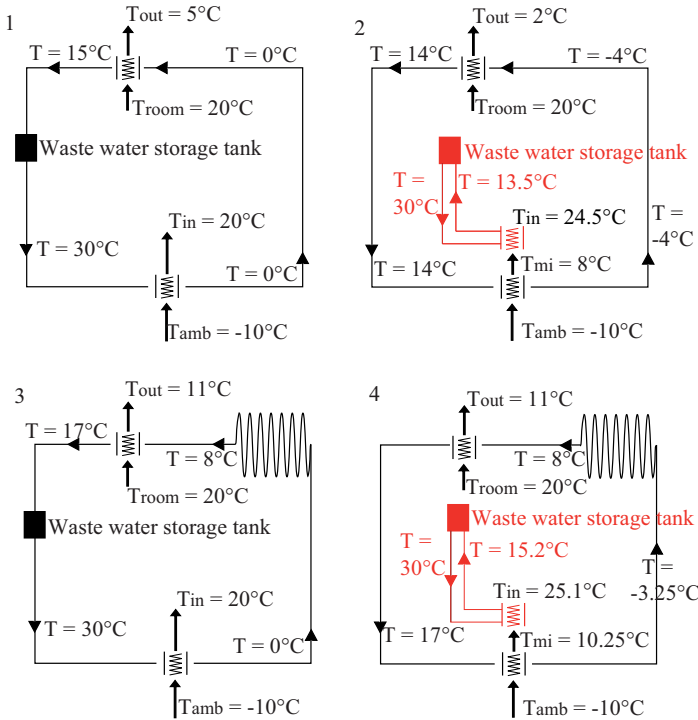


Figure 6.6 Steady-state for the different investigated systems. Red lines illustrate the division into two circuits.

In order to understand the annual consequences, the TRNSYS deck from step 1 was used. The results can be seen in Figure 6.7. The black bars show a reference simulation with no waste water tank. The grey bars

show system 3 in Figure 6.6 and the white bars show system 4, also from Figure 6.6. The system with two circuits performs better than the single circuit. The double-circuit system needs about 200 kWh less auxiliary energy. This is the result even though the heat exchanger at ground level delivers approximately 600 kWh more to the building using the single circuit solution. However, a substantial part of this thermal energy is from the waste water tank. Instead system 4 receives almost 900 kWh from the waste water tank delivered to the building.

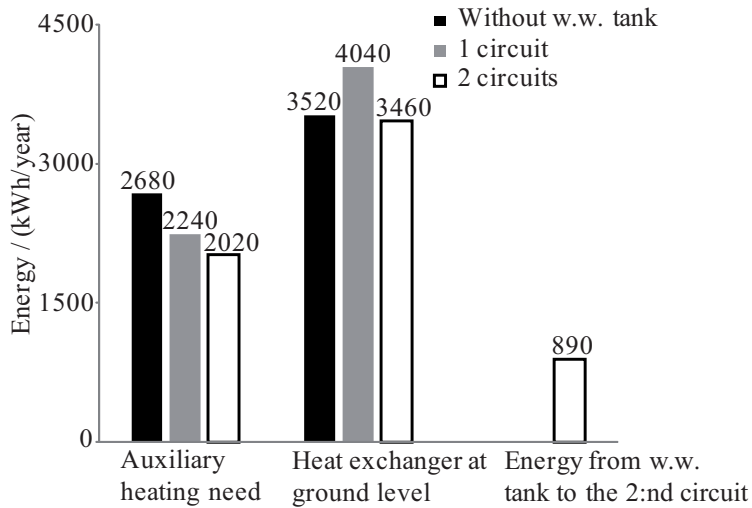


Figure 6.7 Annual thermal energy demand and thermal energy delivered from the ground level heat exchanger and from the waste water tank for different systems.

6.5 Step 3 - method and results

The effects of adding a solar collector to system 2a in Table 6.1 is shown in Figure 6.8. The solar collector is connected to the domestic hot water storage tank. The annual thermal energy demand is reduced by 1000 to 2000 kWh annually, depending on the size of the collector. A somewhat typical size of a collector for a single-family house is 4 m². This collector will reduce the thermal energy use by approximately 1600 kWh/year. This is approximately 100% larger thermal energy saving than when a waste water heat recovery system is installed.

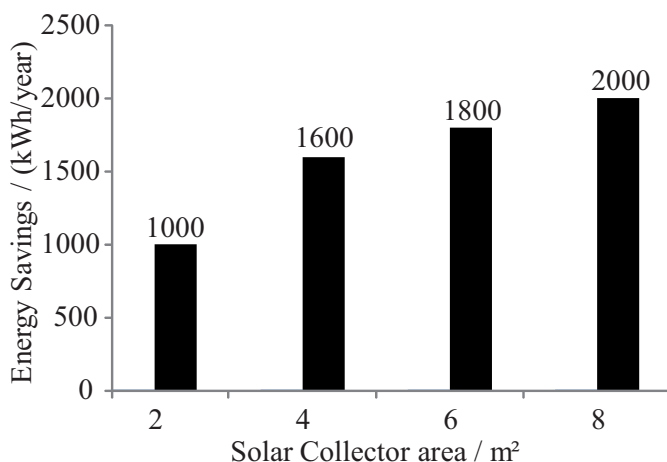


Figure 6.8 Annual thermal energy savings as a function of solar collector size.

6.6 Steps 1, 2, 3 – Conclusion and discussion

The main conclusion from the TRNSYS calculations is that the most important parameter in the investigated systems is the efficiency of the heat exchangers. This is clearly shown by Figure 6.2. This result is also indicated in (Davidsson, Bernardo, & Larsson, 2010), where it was concluded that the heat exchanger must have a temperature efficiency of approximately 70% in order to perform as well as a mechanical ventilation system equipped with heat recovery.

The difference in annual performance between the systems in Table 6.1 for a heat exchanger with a specific temperature efficiency is mostly dependent on using or not using a waste water heat recovery system. The waste water heat recovery system has potential to save somewhere around 600-800 kWh of thermal energy annually for the investigated systems, depending on the water use profile. In real-life measurements, the figure could differ even more, due to huge differences in water use patterns between different users. Using more detailed flow profiles can alter the energy savings but, as the waste water tank stores large quantities of heat over time, this will even out the effects of different user profiles.

Using more accurate profiles is more important for heat recovery systems with instantaneous heat exchange. If larger quantities of heat are used in

the household compared to what was used in the simulations, there is greater potential for energy savings. The variation in domestic hot water use between different households is large (Stengård, 2009). The smallest use in the study was 17 l/day/person while the largest use was 77 l/day/person. The energy savings from a waste water heat recovery system will therefore vary considerably between different users.

Using a ground collector or taking heat from the waste water tanks to use for preheating the ventilation air has only minor effects on the performance from an energy point of view. The reason for this is that, if heat has been collected in the ground collector, there is simply less thermal energy to be recovered in the roof heat exchanger. The energy can only be recovered once.

Figure 6.4 showed that the mechanical ventilation system with heat recovery performed better than the hybrid ventilation system with the brine-based heat recovery system from a thermal energy perspective. It uses approximately 600 kWh less thermal energy per year. However, it also consumes about 400 kWh more electrical energy. Assuming that electricity is worth 3 times more than heat the hybrid ventilation system performs better than the mechanical ventilation.

If a solar collector is installed in system 2a, i.e. to the system equipped only with the hybrid ventilation system with heat recovery, the annual thermal energy use is reduced by approximately 1500 kWh. This is considerably more than if the waste water heat recovery system is installed. However, the solar collector is probably much more expensive to install. Which system to install is a difficult question. Investment price, whether installation is possible, and energy prices will all influence the choice of technology. Davidsson showed in Paper 6 (Davidsson et al., 2011) similar results comparing an installation of a solar collector to a waste water heat recovery system, where the solar collector saved approximately twice the energy saved by the waste water heat recovery system.

The small investigation carried out under Step 2 showed a potential improvement for the ventilation system by separating the heat recovery from the waste water and from the outgoing to the incoming ventilation air into two different circuits. The investigated system reduced annual thermal energy use by approximately 200 kWh. However, using two heat exchangers in series in order to recover the extra energy will increase pressure drop in the system and increase investment cost, due to extra piping and an extra heat exchanger.

Installing a ground collector has the potential to reduce the annual energy demand for the brine-based ventilation heat recovery system. It will also reduce the maximum power need and protect the roof heat exchanger from freezing. These benefits must be included when evaluating the system. The same kind of argument can be applied for the waste water

heat recovery system. This system will work and provide heat throughout the year, regardless of place of installation. This is not the case for a solar collector, which will mainly provide heat during the summer, at least in northern latitudes. The waste water heat recovery system can therefore be used to lower the maximum power need for the system.

The discussed system also has the potential to be retrofitted in old buildings with passive stack ventilation. The commonly used mechanical ventilation with heat recovery system is often difficult to use in old buildings as it is difficult to find acceptable space for the supply duct. One option is to place the ducts on the outside of the building, but this has consequences for the aesthetic characteristics of the building. Installing the heat exchangers discussed in section 4 could, in principle, distort the ventilation air flows, but this effect would probably be small since the pressure drop is very low. Consequently, if the ventilation system in the building works as intended, it will probably continue doing so after installation of the heat recovery system. If it does not work properly, the system can be supplemented with a hybrid fan. While improving the ventilation, this system would allow installation of the heat recovery system.

6.7 Future work

Further investigations regarding the ground collector are recommended. Installation of the ventilation system in colder climates could possibly gain more heat from the ground collector than the findings reported, since the ambient air is colder. Furthermore, in cold climates the ground collector is also extra interesting since frost on the heat exchanger surfaces can be prevented. Heating the brine above 0°C prevents frost. This possibility should be studied using both more detailed simulations and by real installations.

Controlling the flow rate of the brine to alter the degree of heat recovered should be investigated in more detail. Altering the flow rate will have a negative effect on the performance of the system. This is discussed briefly in Appendix A. Moderately cold periods could call for a heat recovery rate less than the system maximum to avoid overheating. This control strategy should be investigated further.

Installations in a real environment would be interesting in order to test how the heat exchanger behaves in a real installation, combined with inlet components, noise reduction units, etc. A real-life installation of the ventilation system would also be highly interesting in order to allow evaluation of the technical problems of the heat exchanger, such as dirt on the heat exchanger surface and pressure drop that limits air flow rate.

One technical challenge is to get an even air flow in the heat exchanger. In a real-life situation there might not be enough space for a long duct to stabilize the flow before entering the heat exchanger. If one side of the heat exchanger has a higher flow than the other, there will be a drop in the total efficiency of the exchanger.

The waste water heat recovery system could be developed further. The measured waste water tanks are prototypes. Long term measurements of the tanks are also important in order to investigate the risk of particles, fat, detergent etc. clogging the heat recovery system.

There are many more energy flow combinations that could be of interest. Using solar energy to heat the ventilation air is an interesting idea that deserves further investigation.

7 Conclusion and discussion of the thesis

A hybrid ventilation system with heat recovery and a solar window for production of electricity and domestic hot water has been investigated. The investigated products are part of the energy system in a single-family building. The building, Solgården, located in Älvkarleö in Sweden was an early attempt to build something that could be called an active house. The building was originally intended as a passive house but, instead of developing this idea fully, alternative measures were taken, such as the solar window and the hybrid ventilation system. An active house, as defined in this project, is not necessarily the opposite of a passive house; it could be something that has been added to the original concept.

The solar window was intended to work as a solar collector for hot water production during warm sunny hours, while reducing solar radiation into the building. During cold sunny hours, the window should transmit the solar radiation for passive heating of the building and, at night, closing the tiltable reflectors should reduce the losses. All this was achieved. Even though the efficiency is somewhat lower compared to a standard installation of solar collectors and PV modules, the hybrid collector produces both heat and electricity. Furthermore, the insulated reflectors lower the U -value of the construction when closed, and the window allows light to enter the building when the reflectors are open.

At the same time the construction creates problems. Since the solar collector is placed in the window it will block parts of the solar radiation that would otherwise light up the room. In order to compensate for this, the window has to be approximately twice the size of a standard window. This will inevitably lead to a high UA -value and thereby large thermal losses. Furthermore, in order to maximize the electrical and thermal output from the collector, there can be no low-emittance coating on the glass in front of the collector, since this will block parts of the solar radiation. This will produce a high U -value that makes the large window even less attractive.

Multiple use of the same space has potential to reduce costs. Putting PV cells on the thermal absorber gives cold, high-producing cells while collecting thermal energy. However, the photons that are used to create electricity cannot also produce heat in the absorber, so thermal output from the collector is reduced when it produces electricity. Like all hybrid collectors, the solar window suffers from this problem. The absorbers in the window collect solar radiation that could allow the entry of daylight and heat the building passively, and reflect this solar radiation to the cells and the absorber. The building will then have lower gains from the sun compared to a case with a standard window and the PV cells and thermal collector placed on the roof. The solar window tries to use the photons not just once or twice but even three times, for PV-cells, thermal absorber and daylighting/passive heating.

However, the investigation of the solar window showed that installing a solar window is better from an energy point of view than doing nothing, i.e. the solar window could be a good solution if the available space on the roof is limited. A more optimal solution though is to place the solar collector and solar cells separately on the roof.

The analysis was performed for a single-family house. Office buildings normally have a lower heating demand per area and lower use of domestic hot water. In some special cases of office buildings the window could show better results. The investigation also shows that there is great potential to improve the solar window. Better insulated absorbers and low-e-coated glass behind the absorbers and the reflectors could improve the energy performance. Even if the solar window is improved, it still has to perform well enough to compensate the increased costs of a complex product. Aesthetics and effects on the day lighting must also be taken into account.

All in all, it is not likely that the solar window can be developed to the point that it becomes an energy-efficient and still reasonably cheap product for a single-family active building.

The brine-based heat exchanger developed in the ventilation project was found to have a temperature efficiency at component level of more than 80%, while pressure drop was limited to just above 1 Pa for the design air flow. There is scope for further development of the heat exchanger. Heat resistance on the water side can be reduced without having any effect on the pressure drop on the air side. This heat exchanger has the potential for use in natural or hybrid ventilation systems with heat recovery. It can be used to retrofit naturally ventilated buildings or exhaust ventilation systems. Installing a heat recovery system has the potential to save energy and increase thermal comfort.

The investigated waste water heat recovery system showed that the thermal energy need for domestic hot water could be reduced by approximately 25%. However, the saving potential is difficult to generalize since it will be

dependent not only on the energy use but also on when the energy is used and the temperature of the water used. Even the cold water use will affect annual performance of the investigated system. The presented analysis also showed that using the low-quality heat from waste water to preheat the ventilation air has the potential to save approximately 200 kWh for a single-family house. This figure can be considerably higher for buildings with greater water needs, such as schools and hospitals.

The brine-based heat recovery system for the ventilation air can be used in an active way, such as to obtain heat from the ground via a ground collector. The analysis showed that the annual saving potential was approximately 150 kWh. This is probably an upper limit of the saving potential since the ground collector was assumed not to be affected by the thermal energy loss to the brine. The relatively low heat gain from the collector was explained by the fact that the roof heat exchanger could recover less energy from the outgoing air, since the brine was preheated. The same energy cannot be saved twice. However, the ground collector can be used to prevent freezing of the heat exchanger. A great risk of frost on a heat exchanger of 80% temperature efficiency was evident already at -10°C . Using a ground collector can solve this problem. This was illustrated in Figure 4.2.

Other solutions, such as actively reducing the heat transfer rate by running the brine in a non-balanced mode, can be used, but this will increase energy use at the very moment when the energy use should be kept low. The investigation also shows that utilizing heat from waste water to heat the ventilation air has a potential to save somewhere around 150-350 kWh annually. The savings depends on the choice of system. The greatest savings are for a system where heat from the waste water is separated from the brine system connecting the two heat exchangers. However, since this system needs three heat exchangers, this will be associated with a higher pressure drop and a higher cost.

Active houses combining the low-energy techniques of passive houses with alternative energy sources can be an attractive solution for future buildings. However, the interaction between the building and the energy supply sources needs to be well understood. Negative energy feedback due to interference between the different energy solutions should be avoided. This was exemplified with the solar window obstructing passive heating through the windows. Furthermore, as building technology improves, the margins for further improvement become smaller. This was exemplified with the ground collector and the utilization of waste water heat being combined to heat the ventilation air. The margins for energy savings are limited after the ventilation heat recovery system has been installed. However, the heat recovery for both the ventilation and from the waste water proved to save considerable amounts of thermal energy. In these

cases low-quality heat was used in order to save energy with a higher quality. This can be electricity, wood or high temperature heat from, for instance, district heating.

References

- Aereco. VBP, *Hybrid assistance fan* Retrieved 2013-05-23, 2013, from <http://www.aereco.com/product/vbp#1>
- Aleklett, K. (2007). *Peak Oil and the Evolving Strategies of Oil Importing and Exporting Countries*. Paper presented at the International Transport Forum, JOINT TRANSPORT RESEARCH CENTRE. Conference paper retrieved from <http://www.internationaltransportforum.org/jtrc/DiscussionPapers/DiscussionPaper17.pdf>
- Anderson, T. N., Duke, M., Morrison, G. L., & Carson, J. K. (2009). Performance of a building integrated photovoltaic/thermal (BIPVT) solar collector. *Solar Energy*, 83(4), 445-455. doi: <http://dx.doi.org/10.1016/j.solener.2008.08.013>
- Appelfeld, D., & Svendsen, S. (2011). Experimental analysis of energy performance of a ventilated window for heat recovery under controlled conditions. *Energy and Buildings*, 43(11), 3200-3207. doi: <http://dx.doi.org/10.1016/j.enbuild.2011.08.018>
- Avloppscenter. *Raita BIO-BOX* Retrieved 2013-10-03, 2013, from <http://www.avloppscenter.se/slamavskiljare/1-hushall/raita-bio-box>
- Balvers, J., Bogers, R., Jongeneel, R., van Kamp, I., Boerstra, A., & van Dijken, F. (2012). Mechanical ventilation in recently built Dutch homes: technical shortcomings, possibilities for improvement, perceived indoor environment and health effects. *Architectural Science Review*, 55(1), 4-14. doi: 10.1080/00038628.2011.641736
- Bejan, A. (1993). *Heat Transfer*. John Wiley and Sons Inc.
- Bernardo, L. R., Davidsson, H., & Karlsson, B. (2011). Performance Evaluation of a High Solar Fraction CPC-Collector System. *Journal of Environment and Engineering*, 6(3), 680-692.

- Boverket. (1995). *Självdagsventilation* Retrieved 2013-09-16, 2013, from <http://www.boverket.se/Global/Webbokhandel/Dokument/1995/Sj%C3%A4lvdragsventilation%20handbok.pdf>
- Boverket. (2011). *BFS 2011:26 - BBR 19* Retrieved 2013-09-16, 2013, from <http://www.boverket.se/Lag-ratt/Boverkets-forfattningssamling/BFS-efter-forkortning/BBR/>
- Chinyama, G. K., Roos, A., & Karlsson, B. (1993). Stability of antireflection coatings for large area glazing. *Solar Energy*, 50(2), 105-111. doi: [http://dx.doi.org/10.1016/0038-092X\(93\)90081-X](http://dx.doi.org/10.1016/0038-092X(93)90081-X)
- Churchill, S. W., & Ozoe, H. (1973). Correlations for forced convection with uniform heating in flow over a plate and in developing and fully developed flow in a tube. *J. Heat Transfer*, 95, 78-84.
- Corbin, C. D., & Zhai, Z. J. (2010). Experimental and numerical investigation on thermal and electrical performance of a building integrated photovoltaic-thermal collector system. *Energy and Buildings*, 42(1), 76-82. doi: <http://dx.doi.org/10.1016/j.enbuild.2009.07.013>
- Davidsson, H., Bernardo, L. R., & Larsson, S. (2011). Design and Performance of a Hybrid Ventilation System with Heat Recovery for Low Energy Buildings. *Journal of Environment and Engineering*, 6(2), 469-477.
- Davidsson, H., Bernardo, R., & Hellström, B. (2013a). Hybrid Ventilation with Innovative Heat Recovery — A System Analysis. *Buildings*, 3(1), 245-257.
- Davidsson, H., Bernardo, R., & Hellström, B. (2013b). *Parametric Study of a Heat Exchanger for a Hybrid Ventilation System*. Paper presented at the REHVA World Congress CLIMA 2013, Prague, Czech Republic.
- Davidsson, H., Bernardo, R., & Hellström, B. (2013c). Theoretical and Experimental Investigation of a Heat Exchanger Suitable for a Hybrid Ventilation System. *Buildings*, 3(1), 18-38.
- Davidsson, H., Bernardo, R., & Larsson, S. (2010). *Impact of hybrid ventilation and sewage heat recovery on the energy performance of a low energy building; a feasibility study*. Paper presented at the EuroSun 2010, Graz.
- Davidsson, H., Perers, B., & Karlsson, B. (2010). Performance of a multifunctional PV/T hybrid solar window. *Solar Energy*, 84(3), 365-372. doi: <http://dx.doi.org/10.1016/j.solener.2009.11.006>

- Davidsson, H., Perers, B., & Karlsson, B. (2012). System analysis of a multifunctional PV/T hybrid solar window. *Solar Energy*, 86(3), 903-910. doi: <http://dx.doi.org/10.1016/j.solener.2011.12.020>
- DOAJ. *Directory of Open Access Journals* Retrieved 2013-09-16, 2013, from www.doaj.org
- Dodoo, A., Gustavsson, L., & Sathre, R. (2011). Primary energy implications of ventilation heat recovery in residential buildings. *Energy and Buildings*, 43(7), 1566-1572. doi: <http://dx.doi.org/10.1016/j.enbuild.2011.02.019>
- Dokka, T. H., & Hermstad, K. (2006). *Energieffektive Boliger for Fremtiden*
- SHC Task 28/ECBCS Annex 38: Sustainable Solar Housing.
- Emerson, W. H. (1984). Making the most of run-around coil systems. *Journal of Heat Recovery Systems*, 4(4), 265-270. doi: [http://dx.doi.org/10.1016/0198-7593\(84\)90065-1](http://dx.doi.org/10.1016/0198-7593(84)90065-1)
- EN. (1997). Glass in building-Determination of thermal transmittance (U-value)-Calculation method (Vol. EN 673, pp. 1-9).
- Energimyndigheten. (2010). *FTX-aggregat hus med 130 m² boyta - Jämförelse* Retrieved 2013-05-23, 2013, from <http://www.energimyndigheten.se/Templates/Public/Pages/ProductGroupPageCompare.aspx?productGroupId=69&productCompareList=412,413,414,415,416,417,418,419&PageID=5552>
- Energimyndigheten. (2012). *Bergvärmepumpar - Jämförelse* Retrieved 2013-05-23, 2013, from <http://energimyndigheten.se/Templates/Public/Pages/ProductGroupPageCompare.aspx?productGroupId=12&productCompareList=98,9,99,97&PageID=5304>
- Eriksson, L., Masimov, T., & Westblom, S. (1986). *Flerbostadshus med styrd ventilation och värmeåtervinning*. Byggforskningsrådet.
- Feist, W., Schnieders, J., Dorer, V., & Haas, A. (2005). Re-inventing air heating: Convenient and comfortable within the frame of the Passive House concept. *Energy and Buildings*, 37(11), 1186-1203. doi: <http://dx.doi.org/10.1016/j.enbuild.2005.06.020>
- Fieber, A. (2005). *Building Integration of Solar Energy*. Lic. Thesis Report, Lund University, Lund University. Retrieved from http://www.ebd.lth.se/fileadmin/energi_byggnadsdesign/images/Publikationer/AvhandlingWEB_alt_Andreas.pdf (EBD-T--05/3)

- Fieber, A., Gajbert, H., Håkansson, H., Nilsson, J., Rosencrantz, T., & Karlsson, B. (2003). *Design, Building integration and performance of a hybrid solar wall element*. Paper presented at the ISES Solar World Congress 2003 Gothenburg, Sweden, Gothenburg, Sweden.
- Fieber, A., Nilsson, J., & Karlsson, B. (2004). *PV performance of a multifunctional PV/T hybrid solar window*. Paper presented at the 19th European photovoltaic solar energy conference and exhibition, Paris, France.
- Forsyth, B. I., & Besant, R. W. (1988). The design of a run-around heat recovery system. *ASHRAE Trans*, 94(2), 20.
- Gajbert, H., Hall, M., & Karlsson, B. (2007). Optimisation of reflector and module geometries for stationary, low-concentrating, façade-integrated photovoltaic systems. *Solar Energy Materials and Solar Cells*, 91(19), 1788-1799. doi: <http://dx.doi.org/10.1016/j.solmat.2007.06.007>
- Granqvist, C. G., Azens, A., Hjelm, A., Kullman, L., Niklasson, G. A., Rönnow, D., . . . Vaivars, G. (1998). Recent advances in electrochromics for smart windows applications. *Solar Energy*, 63(4), 199-216. doi: [http://dx.doi.org/10.1016/S0038-092X\(98\)00074-7](http://dx.doi.org/10.1016/S0038-092X(98)00074-7)
- Heiselberg, P. (2002). *Principles of Hybrid Ventilation*, IEA Annex 35: Hybrid ventilation in New and Retrofitted Office Buildings.
- Holmberg, R. B. (1975). Heat transfer in liquid-coupled indirect heat exchanger systems. *Journal of Heat Transfer*, November, 74, 499-503.
- Hviid, C. A., & Svendsen, S. (2011). Analytical and experimental analysis of a low-pressure heat exchanger suitable for passive ventilation. *Energy and Buildings*, 43(2-3), 275-284. doi: <http://dx.doi.org/10.1016/j.enbuild.2010.08.003>
- IEA. Task 21 *Source Book* Retrieved 2013-09-16, 2013, from http://pubs.iea-shc.org/task21/source_book.html
- IEA. (2008). *Promoting energy efficiency investments* Retrieved 2013-09-16, 2013, from <http://www.iea.org/publications/freepublications/publication/PromotingEE2008.pdf>
- Incropera, F. P., & DeWitt, D. P. (2002). *Fundamentals of Heat and Mass Transfer*: John Wiley & Sons.
- Inoue, T., Ichinose, M., & Ichikawa, N. (2008). Thermotropic glass with active dimming control for solar shading and daylighting. *Energy and Buildings*, 40(3), 385-393. doi: <http://dx.doi.org/10.1016/j.enbuild.2007.03.006>

- IPCC. (2007). *Climate Change 2007: Synthesis Report, Summary for Policymakers*, from http://www.ipcc.ch/pdf/assessment-report/ar4/syr/ar4_syr_spm.pdf
- Jacobsen, T. D., Jensen, S. Ø., Poulsen, C. S., & Madsbøll, H. (1999). *Naturlig ventilation med varmegenvinding og solassistance – forprojekt*.
- Johansson, P., & Svensson, A. (1998). *Metoder för mätning av luftflöden i ventilationsinstallationer*.
- Kalogirou, S. A., & Tripanagnostopoulos, Y. (2006). Hybrid PV/T solar systems for domestic hot water and electricity production. *Energy Conversion and Management*, 47(18–19), 3368–3382. doi: <http://dx.doi.org/10.1016/j.enconman.2006.01.012>
- Kays, W. M., & London, A. L. (1984). *Compact Heat Exchangers* (Harold B. Crawford, Dennis Gleason ed.): McGraw-Hill Book Company.
- Khan, N., Su, Y., & Riffat, S. B. (2008). A review on wind driven ventilation techniques. *Energy and Buildings*, 40(8), 1586–1604. doi: <http://dx.doi.org/10.1016/j.enbuild.2008.02.015>
- Klein, S. A. *A Transient Systems Simulation Program* Retrieved 2013-05-23, 2013, from <http://sel.me.wisc.edu/trnsys/>
- Knudsen, J. G., & Katz, D. L. (1958). *Fluid Dynamics and Heat Transfer*: McGraw-Hill.
- Kobler, R. L., Binz, A., Steinke, G., Höfler, K., Geier, S., Aschauer, J., . . . Almeida, M. (2011). *Retrofit Module Design Guide*.
- Krauter, S., & Ochs, F. (2004). Integrated solar home system. *Renewable Energy*, 29(2), 153–164. doi: [http://dx.doi.org/10.1016/S0960-1481\(03\)00190-3](http://dx.doi.org/10.1016/S0960-1481(03)00190-3)
- Kronvall, J. (1980). *Air Flows in Building Components*. Lund: Lund University. (TVVBH-1002)
- Liddament, M. W. (1996). *A Guide to Energy Efficient Ventilation, International Energy Agency, AIVC*.
- London, A. L., & Kays, W. M. (1951). The Liquid-Coupled Indirect-Transfer Regenerator for Gas-Turbine Plants. *TRANS. ASME*, 73, 14.

- Lund University. (2005, 2005-11-14). *Universitetets forskning ska bli mer tillgänglig*, from http://www.lu.se/nyheter-och-press/pressmeddelanden?visa=pm&pm_id=395
- Madani, H. (2012). *Capacity-controlled Ground Source Heat Pump Systems for Swedish single-family dwellings*. Degree of Doctor in Technology Doctoral thesis, comprehensive summary, KTH, Stockholm, Stockholm. Retrieved from <http://urn.kb.se/resolve?urn=urn:nbn:se:kth:diva-102055> (ISBN-978-91-7501-474-6)
- Madani, H., Wallin, J., Claesson, J., & Lundqvist, P. (2010). *Retrofitting a variable capacity heat pump to a ventilation heat recovery system: modelling and performance analysis*. Paper presented at the International Conference on Applied Energy.
- Mallick, T. K., Eames, P. C., Hyde, T. J., & Norton, B. (2004). The design and experimental characterisation of an asymmetric compound parabolic photovoltaic concentrator for building façade integration in the UK. *Solar Energy*, 77(3), 319-327. doi: <http://dx.doi.org/10.1016/j.solener.2004.05.015>
- Mardiana-Idayu, A., & Riffat, S. B. (2012). Review on heat recovery technologies for building applications. *Renewable and Sustainable Energy Reviews*, 16(2), 1241-1255. doi: <http://dx.doi.org/10.1016/j.rser.2011.09.026>
- METEONORM. *METEONORM 5.0 global meteorological database for solar energy and applied meteorology* Retrieved 2013-05-23, 2013, from <http://www.meteotest.ch/en/>
- Nostell, P., Roos, A., & Karlsson, B. (1999). Optical and mechanical properties of sol-gel antireflective films for solar energy applications. *Thin Solid Films*, 351(1-2), 170-175. doi: [http://dx.doi.org/10.1016/S0040-6090\(99\)00257-6](http://dx.doi.org/10.1016/S0040-6090(99)00257-6)
- Nykvist, A. (2012). *Värmeåtervinning ur spillvatten i befintliga flerbostadshus*. Master thesis, KTH, Stockholm. Retrieved from <http://kth.diva-portal.org/smash/record.jsf?pid=diva2:509810> (119)
- Overgaard, L. L., Heiselberg, P., & Hammer, C. (2002). *Komponenter til naturlig ventilation, Del I – Lavtsiddende indløbsåbninger*.
- Overgaard, L. L., Nørgaard, E., Jensen, S. Ø., & Madsen, K. B. (2002). *Komponenter til naturlig ventilation, Del II – Luft-til-væske varmeveksler*.

- Perers, B. (1997). An improved dynamic solar collector test method for determination of non-linear optical and thermal characteristics with multiple regression. *Solar Energy*, 59(4–6), 163-178. doi: [http://dx.doi.org/10.1016/S0038-092X\(97\)00147-3](http://dx.doi.org/10.1016/S0038-092X(97)00147-3)
- Pilkington. (2002). *Glasfakta* (pp. 18).
- Riffat, S. B., & Gan, G. (1998). Determination of effectiveness of heat-pipe heat recovery for naturally-ventilated buildings. *Applied Thermal Engineering*, 18(3–4), 121-130. doi: [http://dx.doi.org/10.1016/S1359-4311\(97\)00033-1](http://dx.doi.org/10.1016/S1359-4311(97)00033-1)
- Rosen, B., Gabrielsson, A., Fallsvik, J., Hellström, G., & Nilsson, G. (2001). *System för värme och kyla ur mark - En nulägesbeskrivning*: Statens Geotekniska Institut.
- Scandinavian Green Roof Institute. *Augustenborg Botanical Roof Garden* Retrieved 2013-06-16, 2013, from <http://www.greenroof.se/>
- Schultz, J. M., & Saxhof, B. (1994). Natural ventilation with heat recovery. *Air Infiltration Review*, 15(4), 4.
- Shao, L., Riffat, S. B., & Gan, G. (1998). Heat recovery with low pressure loss for natural ventilation. *Energy and Buildings*, 28(2), 179-184. doi: [http://dx.doi.org/10.1016/S0378-7788\(98\)00016-4](http://dx.doi.org/10.1016/S0378-7788(98)00016-4)
- SIS. (2005). Solar protection devices combined with glazing-Calculation of total solar energy transmittance and light transmittance- (Vol. SS-EN 13363-2:2005, pp. 14).
- Skåret, E., Blom, P., & Hestad, T. (1997). *Energy recovery possibilities in natural ventilation of office buildings*. Paper presented at the Cold Climate '97, Reykjavik. <http://www.civil.uwaterloo.ca/beg/archtech/norway%20nat%20vent%20heat%20recovery.pdf>
- Slinky. Retrieved 2013-09-16, 2013, from <http://en.wikipedia.org/wiki/Slinky>
- Sorensen, H. (2005). IEA SHC Task 35 PV/Thermal Solar System.
- Ssolar. Retrieved 2013-05-27, 2013, from <http://www.ssolar.com/>
- Stengård, L. (2009). *Mätning av kall- och varmvattenanvändning i 44 hushåll*: Energimyndigheten.
- Sundén, B. (2006). *Värmeöverföring*: Studentlitteratur.
- Tonui, J. K., & Tripanagnostopoulos, Y. (2007). Improved PV/T solar collectors with heat extraction by forced or natural air circulation.

Renewable Energy, 32(4), 623-637. doi: <http://dx.doi.org/10.1016/j.renene.2006.03.006>

- Tyagi, V. V., Rahim, N. A. A., Rahim, N. A., & Selvaraj, J. A. L. (2013). Progress in solar PV technology: Research and achievement. *Renewable and Sustainable Energy Reviews*, 20(0), 443-461. doi: <http://dx.doi.org/10.1016/j.rser.2012.09.028>
- Wachenfeldt, B. J. (2003). *Natural Ventilation in Buildings*. Doctoral, NTNU Trondheim. (ISBN 82-471-5624-5)
- Wall, M. (2006). Energy-efficient terrace houses in Sweden: Simulations and measurements. *Energy and Buildings*, 38(6), 627-634. doi: <http://dx.doi.org/10.1016/j.enbuild.2005.10.005>
- Wallin, J., Madani, H., & Claesson, J. (2009). *Ventilation heat recovery with run around coil: System analysis and a study on efficiency improvement – Part 1*. Paper presented at the Symposium on "Sustainability and Green Buildings", Kuwait.
- Widén, J., Lundh, M., Vassileva, I., Dahlquist, E., Ellegård, K., & Wäckelgård, E. (2009). Constructing load profiles for household electricity and hot water from time-use data—Modelling approach and validation. *Energy and Buildings*, 41(7), 753-768. doi: <http://dx.doi.org/10.1016/j.enbuild.2009.02.013>
- Vik, T. A. (2003). *Life Cycle Cost Assessment of Natural Ventilation Systems*. Doctoral, NTNU Trondheim. (ISBN 82-471-5561-3)
- Wilo. Wilo-Star-ZNOVA Retrieved 2013-05-27, 2013, from http://productfinder.wilo.com/en/SE/productrange/00000016000393a900020023/fc_range_description
- Zemax. Radiant Zemax Retrieved 2013-09-16, 2013, from <http://www.zemax.com/>
- Zeng, Y. Y., Besant, R. W., & Rezkallah, K. S. (1992). The effect of temperature-dependent properties on the performance of run-around heat recovery systems using aqueous-glycol coupling fluids. *ASHRAE Trans*, 98(1), 12.

Appendix A

Varying the flow rate of the brine or the air in a run-around heat recovery system will alter the efficiency of the system. This has been discussed in earlier work (Holmberg, 1975; London & Kays, 1951), and is also summarized in (Kays & London, 1984).

The upper illustration in Figure A.1 shows the ventilation system. HX2 and HX1 are the roof and inlet heat exchangers. $T_{a,in,1}$ is the temperature of the incoming air to the first heat exchanger. $T_{a,out,1}$ is the temperature of the outgoing air from the first heat exchanger. $T_{w,in,1}$ and $T_{w,out,1}$ are the temperatures of the incoming and outgoing brine, in this case water, in the first heat exchanger. $T_{a,in,2}$, $T_{a,out,2}$, $T_{w,in,2}$, and $T_{w,out,2}$ are the incoming and outgoing air and water temperatures to/from the second heat exchanger.

The lower illustration shows the temperature profile in the system. The temperature of the air increases as it passes through HX1. The outgoing temperature, i.e. $T_{a,out,1}$, mixes with the inside air in the building. This is illustrated by the abrupt increase in temperature. As the air passes through HX2 the temperature is reduced. The temperature in the water increases as it passes through HX2 and is reduced as it passes through HX1. Whatever energy is picked up by the water in HX2 is delivered to the air in HX1.

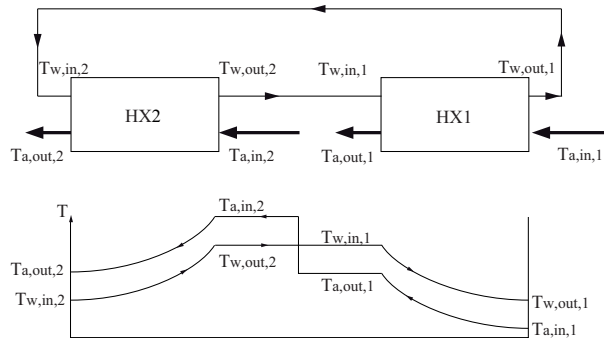


Figure A.1 Upper: Illustration of a run-around ventilation system. HX2 and HX1 illustrate the roof and inlet heat exchangers respectively. Lower: The temperature profile in the system.

For $\xi \neq 1$

$$\frac{AU}{f_a \rho_a C p_a} = \psi \quad \text{Equation A1}$$

$$\frac{f_a \rho_a C p_a}{f_w \rho_w C p_w} = \xi \quad \text{Equation A2}$$

$$\frac{AU}{f_w \rho_w C p_w} = \xi \psi \quad \text{Equation A3}$$

$$T_{w,in,2} = T_{w,out,1} \quad \text{Equation A4}$$

$$T_{w,out,2} = T_{w,in,1} \quad \text{Equation A5}$$

$$\Delta t_m = \frac{(T_{w,out,1} - T_{a,in,1}) - (T_{w,in,1} - T_{a,out,1})}{\ln \left(\frac{T_{w,out,1} - T_{a,in,1}}{T_{w,in,1} - T_{a,out,1}} \right)} \quad \text{Equation A6}$$

$$\Delta t_m = \frac{(T_{a,out,2} - T_{w,in,2}) - (T_{a,in,2} - T_{w,out,2})}{\ln \left(\frac{T_{a,out,2} - T_{w,in,2}}{T_{a,in,2} - T_{w,out,2}} \right)} \quad \text{Equation A7}$$

$$T_{w,out,1} = T_{w,in,1} - \frac{AU \Delta t_m}{f_w \rho_w C p_w} \rightarrow [Eq. A. 3] \rightarrow T_{w,in,1} - \psi \xi \Delta t_m \quad \text{Equation A8}$$

$$T_{a,out,1} = T_{a,in,1} + \frac{AU \Delta t_m}{f_a \rho_a C p_a} \rightarrow [Eq. A. 1] \rightarrow T_{a,in,1} + \psi \Delta t_m \quad \text{Equation A9}$$

$$T_{w,out,2} = T_{w,in,2} - \frac{AU \Delta t_m}{f_w \rho_w C p_w} \rightarrow [Eq. A. 3] \rightarrow T_{w,in,2} + \psi \xi \Delta t_m \quad \text{Equation A10}$$

$$T_{a,out,2} = T_{a,in,2} - \frac{AU \Delta t_m}{f_a \rho_a C p_a} \rightarrow [Eq. A. 1] \rightarrow T_{a,in,2} - \psi \Delta t_m \quad \text{Equation A11}$$

$$Eq. A. 6 \rightarrow [Eq. A. 8, Eq. A. 9] \rightarrow \Delta t_m = \frac{e^{\psi(1-\xi)}(T_{w,in,1} - T_{a,in,1}) - T_{w,in,1} + T_{a,in,1}}{\psi(e^{\psi(1-\xi)} - \xi)} \quad \text{Equation A12}$$

$$Eq. A. 7 \rightarrow [Eq. A. 10, Eq. A. 11] \rightarrow \Delta t_m = \frac{\psi \Delta t_m (\xi - 1)}{\ln \left(1 + \frac{\psi \Delta t_m (\xi - 1)}{T_{a,in,2} - T_{w,in,1}} \right)} \quad \text{Equation A13}$$

$$Eq. A. 12 \& Eq. A. 13 \rightarrow \Delta t_m = \frac{\psi \Delta t_m (\xi - 1)}{\ln \left(1 + \frac{\psi \Delta t_m (\xi - 1)}{T_{a,in,2} - \frac{\psi \Delta t_m (\xi - e^{\psi(1-\xi)} - T_{a,in,1}) - T_{a,in,1}}{1 - e^{\psi(1-\xi)}}} \right)} \quad \text{Equation A14}$$

$$\eta = \frac{T_{a,out,1} - T_{a,in,1}}{T_{a,in,2} - T_{a,in,1}} = \frac{\psi \Delta t_m}{T_{a,in,2} - T_{a,in,1}} \rightarrow [Eq. A. 14] \rightarrow \frac{(1 - e^{\psi(\xi-1)})}{(2 - \xi(1 + e^{\psi(\xi-1)}))} \quad \text{Equation A15}$$

For $\zeta = 1$

$$\Delta t_m = T_{w,in,1} - T_{a,out,1} = T_{w,in,1} - T_{a,in,1} - \psi \Delta t_m \quad \text{Equation A16}$$

$$\Delta t_m = T_{a,in,2} - T_{w,out,2} = T_{a,in,2} - T_{w,in,1} \rightarrow T_{w,in,1} = T_{a,in,2} - \Delta t_m \quad \text{Equation A17}$$

$$[Eq. A1.16 \& Eq. A17] \rightarrow \Delta t_m = T_{a,in,2} - T_{a,in,1} - \Delta t_m - \psi \Delta t_m \quad \text{Equation A18}$$

$$\eta = \frac{\psi \Delta t_m}{T_{a,in,2} - T_{a,in,1}} \rightarrow [Eq. A. 18] \rightarrow \frac{\psi}{\psi + 2} \quad \text{Equation A19}$$

The efficiency of the heat exchanger at component level is

For $\zeta = 1$

$$\Delta t_m = T_{w,out,1} - T_{a,in,1} \quad \text{Equation A20}$$

$$T_{w,out,1} = T_{w,in,1} - \frac{AU \Delta t_m}{\dot{f}_w \rho_w c_{pw}} = T_{w,in,1} - \psi \Delta t_m \quad \text{Equation A21}$$

$$[Eq. A. 20 \& Eq. A. 21] \rightarrow \Delta t_m = T_{w,in,1} - T_{a,in,1} - \psi \Delta t_m \quad \text{Equation A22}$$

$$\eta = \frac{\psi \Delta t_m}{T_{w,in,1} - T_{a,in,1}} \rightarrow [Eq. A. 22] \rightarrow \frac{\psi}{\psi + 1} \quad \text{Equation A23}$$

Equations A.1 and A.3 show the ratio of the heat transfer rate per heat flow capacity for the air and the water in the heat exchanger. The ratio is denoted ψ . The ratio of the heat flow capacity for the air and the water is assumed to be different from unity (Equation A.2). Equations A.4 and A.5 state that the water is unaffected between the heat exchangers, and so the temperature is constant when not passing the heat exchanger, i.e., there are no thermal losses or gains in the pipes.

Equations A.6 and A.7 show the expressions for the logarithmic mean temperature difference for the heat exchangers. The temperature of the outgoing water from HX1 is calculated in Equation A.8. The temperature is reduced by $AU \Delta t_m / \dot{f}_w \rho_w c_{pw}$ from $T_{w,in,1}$ as it passes through the heat exchanger. If Equation A.3 is inserted, the temperature is calculated to be $T_{w,in,1} - \psi \zeta \Delta t_m$. The factor $AU \Delta t_m$ is the delivered power in the heat exchanger. This power loss, P , reduces the temperature in the fluid by $P / \dot{f}_w \rho_w c_{pw}$. In the same way the outlet air and water temperatures are calculated in Equations A.9 to A.11. Equation A.12 is a development from Equation A.6 with Equation A.8 and Equation A.9. Equation A.13 is a development from Equation A.7 with Equation A.10 and Equation A.11. Combining Equation A.12 with Equation A.13 results in Equation A.14. The efficiency of the system is defined by the difference between the inlet

and ambient temperatures, divided by the difference between the indoor and the ambient temperature. This is expressed in Equation A.15.

If the flows are balanced, i.e. $\xi = 1$, Equations A.8 and A.9 become Equations A.16 and A.17. Combining these equations results in Equation A.18. Equation A.19 shows the efficiency of the heat exchanger as a function of ψ .

The investigation for one heat exchanger is shown in Equations A.20 to A.23. In this case the temperature difference is defined as the difference between the incoming water and the incoming air temperature. Equation A.23 shows the efficiency of the heat exchanger as a function of ψ .

Figure A.2 shows an illustration of the efficiency η in Equation A.15. The y-axis is the efficiency and the x-axis is the ratio of the mass flow capacity between the flows, i.e. ξ . The figure illustrates results when ψ is 1, 2, 4, 8 and 16. All of the efficiencies have a maximum for $\xi = 1$. For the low-efficiency heat exchangers the curve is rather flat. For high-efficiency heat exchangers the curve has a clearer maximum around $\xi = 1$. If the ratio of the mass flow capacity for, $\psi = 8$, drops by 35% the efficiency of the heat recovery system will drop by approximately 10%.

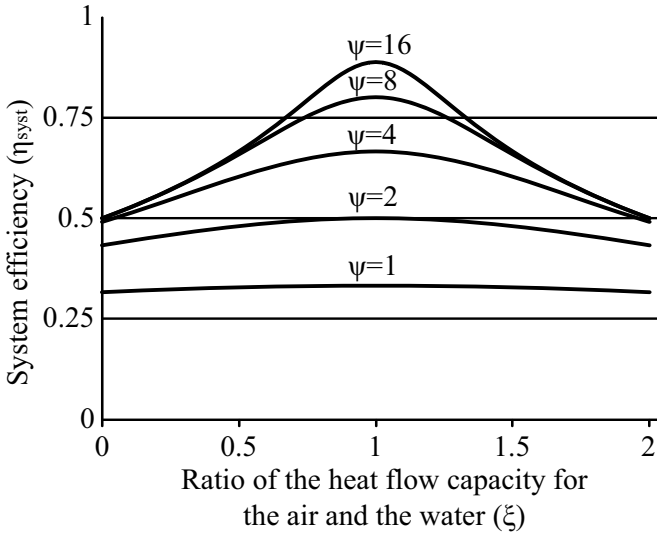


Figure A.2 The efficiency of the heat recovery system as a function of the ratio ξ for different values of ψ . x-axis: Ratio of the heat capacity flow rate of the air to that of the water.

Equations A.19 and A.23 show in a direct way the relationship between the efficiency of the heat exchangers at system level, i.e. two heat exchang-

ers connected in series, and on a component level, i.e. one heat exchanger alone. If $\psi = 2$ the efficiency η for the system becomes 0.5. The efficiency at component level for the heat exchanger becomes $2/3$. This was discussed in section 4.2.1. The investigation is also presented in Figure A.3.

The graphs illustrate the outlet temperatures from the heat exchangers. The ambient temperature, $T_{a,in,1}$, is assumed to be 0°C and the indoor temperature, $T_{a,in,2}$, is assumed to be 20°C . The figure shows the air temperature from heat HX1 and the outlet water temperatures from HX1 and HX2. The left illustration shows the temperatures for $\psi = 2$ and the right illustration for $\psi = 8$. The maximum outlet temperature for the air after passing heat exchanger 1 is reached for $\zeta = 1$, as discussed above.

If the water flow is increased relative to this optimum point, i.e. $0 < \zeta < 1$, the result will be higher temperatures for the water going out from heat exchanger 1 but lower temperatures for the water going out from heat exchanger 2. As already concluded, the total effect is still a lower air temperature from heat exchanger 1. As ζ approaches 0 the outlet temperature from both heat exchangers approaches 10. This is a consequence of the short-circuiting of the water circuit when pumping the water at high speed. If the water flow rate is high there will be little time for the water temperature to fall and rise in the exchangers and so the water temperature will be almost constant throughout the circuit.

If the water flow is instead reduced compared to the optimum point, the water temperature will be higher from HX2 but lower from HX1 compared to the temperatures for the optimum point. This is because the water passes slowly through the heat exchangers. As the water passes slowly through HX2 it has plenty of time to pick up energy and gain in temperature from the outgoing air. The opposite happens in HX1 where the temperature drops considerably in the exchanger. The combined effect is again a lower outlet air temperature from HX1.

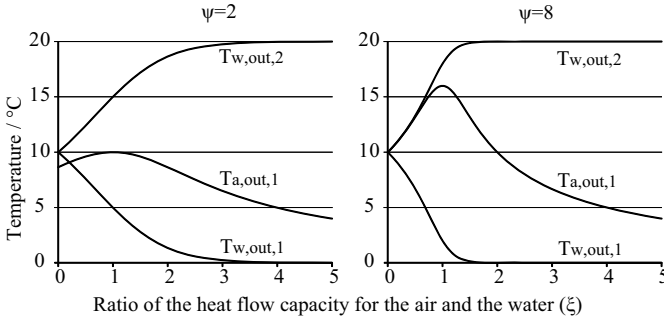


Figure A.3 The outlet temperatures from the heat exchangers. The left illustration shows the temperatures for $\psi = 2$ and the right illustration shows for $\psi = 8$. x-axis: Ratio of the heat capacity flow rate of the air to that of the water (the brine).

The presented results are only valid when there is no heat flux through the pipes between the heat exchangers, i.e. no thermal losses through the pipes and no external heat gains. Heat gains could be heat recovery from waste water or from ground collectors. If these types of arrangements are used the above equations will no longer be valid. If heat is gained or lost, the pump flow rate should in principle be altered in order to maximize the efficiency. This is outside the scope of this discussion.

Appendix B

Nu_D for a circular tube can be calculated as:

$$Nu_D = 4.364 \left(1 + \left(\frac{Gz}{29.6} \right)^2 \right)^{1/6} \cdot \left[1 + \left[\frac{Gz/19.04}{\left[1 + (Pr/0.0207)^{2/3} \right]^{1/2} \cdot \left[1 + (Gz/29.6)^2 \right]^{1/3}} \right]^{3/2} \right]^{1/3}$$

Equation B.1

where Gz is the Graetz number calculated as:

$$Gz = \frac{\pi}{4} \left(\frac{x}{D \cdot Re \cdot Pr} \right)^{-1}$$

Equation B.2

where Pr is the Prandtl number, Re is the Reynolds number, D is the diameter, and x is the distance from the entrance. This means that the average Nu_D number for a one meter tube with parameters corresponding to the air side of the heat exchanger investigated in this article will increase by approximately 15%. All of the investigated geometries for the heat exchanger, *i.e.* different d , were adjusted by 15%. Figure B.1 shows the Nu_D as a function of the distance from the entrance of the heat exchanger for the geometry described in this section. The black graph is the Nu_D number taking the entrance region into account. The grey line is without this effect.

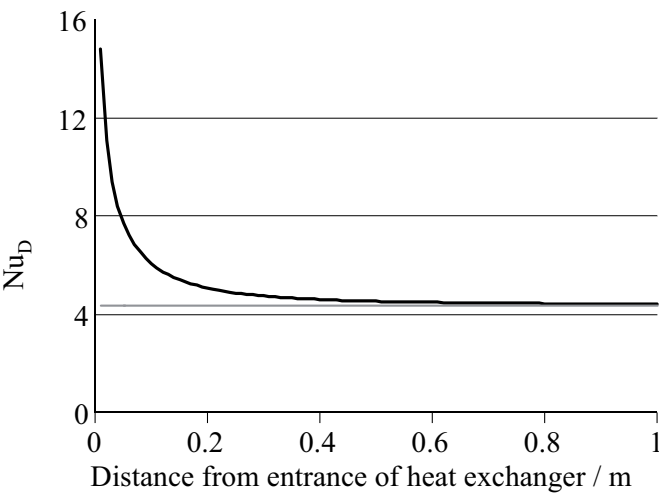


Figure B.1 *The Nu_D as a function of the distance from the entrance of the heat exchanger.*

Appendix C

Air flow was measured with three different techniques. Before the measurements started the hot wire anemometer was calibrated against a wing wheel. The wing wheel has a mechanical integrator that calculates the total volume of air passing the wheel in 1 minute. The maximum deviation was less than 4% and the mean deviation between the two was less than 1%. This small deviation increased confidence in the hot wire anemometer used later.

The air flow was measured by two sensors – a hot wire anemometer placed inside a measurement hood (a Swema 125) and a hot wire anemometer placed on a thin stick (a Swema 31). Each performed measurement during the whole experiment was recorded by both sensors. The Swema 31 was also used to make sure that the flow profile inside the duct was even. If one side of the duct had a higher flow rate than the other side this could be adjusted by adjusting the fan on the top.

The temperature of the air was measured with thermocouples and with a thermopile. The readings from the thermopile were logged and used in the calculations. The thermocouples were used to measure the absolute temperature of the incoming air. The thermocouples were also used to check the thermopile.

The temperature of the brine was measured using PT-100 sensors. The sensors were bought from the manufacturer as a pair, so they showed more or less the same deviation. The sensors were also checked in the lab.

The brine flow meter was calibrated by logging the flow while filling a bottle of known volume. The calibration was carried out three times for different flows. The flow meter was also calibrated outside the standard range for the meter. The maximum deviation was less than 4%.

The pressure drop over the heat exchanger was measured by two different sensors. The sensors showed the same pressure drop as air flow rate varied.

Paper I



Performance of a multifunctional PV/T hybrid solar window

Henrik Davidsson*, Bengt Perers, Björn Karlsson

Energy and Building Design, Lund University, P.O. Box 118, SE 221 00 Lund, Sweden

Received 4 March 2009; received in revised form 18 November 2009; accepted 19 November 2009
Available online 22 December 2009

Communicated by: Associate Editor Matheos Santamouris

Abstract

A building-integrated multifunctional PV/T solar window has been developed and evaluated. It is constructed of PV cells laminated on solar absorbers placed in a window behind the glazing. To reduce the cost of the solar electricity, tiltable reflectors have been introduced in the construction to focus radiation onto the solar cells. The reflectors render the possibility of controlling the amount of radiation transmitted into the building. The insulated reflectors also reduce the thermal losses through the window. A model for simulation of the electric and hot water production was developed. The model can perform yearly energy simulations where different features such as shading of the cells or effects of the glazing can be included or excluded. The simulation can be run with the reflectors in an active, up right, position or in a passive, horizontal, position. The simulation program was calibrated against measurements on a prototype solar window placed in Lund in the south of Sweden and against a solar window built into a single family house, Solgården, in Älvkarleö in the central part of Sweden. The results from the simulation shows that the solar window annually produces about 35% more electric energy per unit cell area compared to a vertical flat PV module.

© 2009 Elsevier Ltd. All rights reserved.

Keywords: Solar window; PV/T; Building integration

1. Introduction

A diversity of technical solutions needs to be applied and developed if solar electricity is to become cheap enough to compete with grid electricity. One technique for reducing the cost of solar electricity is to use a reflector for focusing radiation onto the PV cells, thus allowing expensive PV cells to be replaced by considerably cheaper reflector material. Active water cooling on the back of the cell gives both relatively cool, and thereby high efficient cells, and hot water for domestic use. Photo Voltaic/Thermal (PV/T) hybrid collectors producing electricity and thermal energy simultaneously have been reported earlier as cost effective collectors (Kalogirou and Tripanagnostopoulos, 2006; Krauter and Ochs, 2003; Assoa et al., 2007; Tonui and Tripanagnostopoulos, 2007). The official homepage of IEA SHC Task

35 PV/Thermal Solar Systems (IEA SHC) gives a good overview of different hybrid technologies. Further cost reduction is possible if the solar modules can be integrated into the building construction. Integration makes it possible to use existing frames and glazing for the solar modules or, alternatively, to replace roofing material and windows by using solar modules. Wall integrated solar collectors using reflectors have been shown to increase the electrical output substantially (Gajbert et al., 2007; Mallick et al., 2004) compared to flat vertical PV modules. All technologies mentioned above have been combined in the PV/T hybrid technology that is presented in this work.

A building-integrated multifunctional solar window was proposed and developed by Andreas Fieber (Fieber et al., 2003, 2004). The solar window (Fig. 1) is constructed of solar thermal absorbers on which PV cells have been laminated. The absorbers are building-integrated into the inside of a standard window, thus saving frames and glazing and lowering the total cost of the construction. In order

* Corresponding author. Tel.: +46 46 2224851; fax: +46 46 2224719.
E-mail address: henrik.davidsson@ebd.lth.se (H. Davidsson).

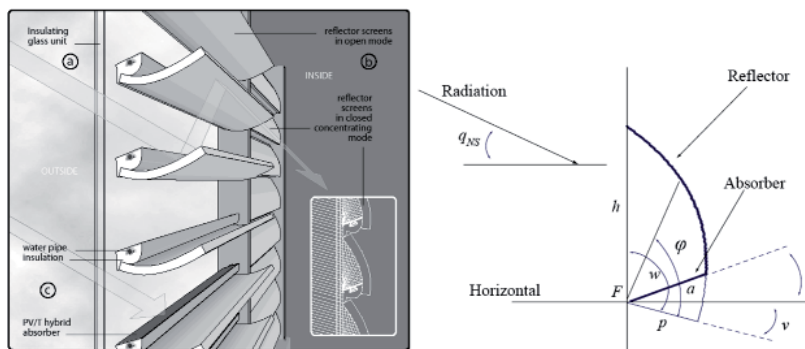


Fig. 1. Left: the solar window. Right: illustration of the parabolic reflector and the absorber.

to minimize the PV cell area, reflectors have been placed behind the absorbers. When tilting the foldable reflectors to a vertical position the solar radiation is focused onto the absorbers. When the reflectors are tilted to a horizontal position the solar radiation is let into the building to allow for passive heating. This means that the reflectors in a closed position increase the radiation on the cells, reduce the thermal losses through the window and also work as a sun shade. The double glazing of the window in front of the absorbers is anti-reflection treated to maximize the transmittance (Chinyama et al., 1993; Nostell et al., 1999; Brogren et al., 2000). Two solar windows have been monitored and characterized, one prototype solar window placed in the solar laboratory at Lund University in the south of Sweden and one solar window integrated into a single family house in Älvkarleö in the central part of Sweden. A detailed construction of the PV/T collector and the architectural implications such as light distribution is presented in Fieber et al. (2003, 2004, 2005). Following this, long term measurements were performed regarding energy production of heat and electricity. This was carried out on both of the solar windows.

In this paper, we describe a model developed to simulate the yearly energy production of the hybrid window system from climatic data. The model uses a combination of both experimentally measured and theoretically derived parameters and functions in the calculations. It takes into account shading caused by the window frames and also includes the transmittance through the glazing and the angular dependence of the efficiency of the PV cells. The model also allows for analyzing different limiting effects such as shading or transmittance through the glazing. This gives an opportunity to study possible improvements for the solar window.

1.1. Geometry

The geometry of the solar window is shown in Fig. 1. The optical axis of the parabolic reflector is directed 15°

above the horizon with focus on the front edge of the absorber, i.e. $v = 15^\circ$. The absorber tilt, u , is 20° . This means that all radiation from 15° and higher projected solar altitudes (Rönnelid and Karlsson, 1997) will hit on the absorber between the focal point, F , and the reflector. The focal length is denoted p , the height of the glazing h and a is the absorber width. The angle w is the angle between the glazing and the absorber plane and q_{NS} is the incident angle of the solar radiation projected in the north–south vertical plane. The absorbers are 113 cm long and 7 cm wide while the PV cells covering the absorber are 12.5 cm by 6.25 cm each. This means that a fraction of 80% of the absorber is covered with solar cells. The solar window in Solgården is constructed of eight absorbers per window unit while the prototype solar window is constructed of five absorbers (Fig. 2). The Solgården solar window has 64 PV cells in series and the prototype solar window has 8 PV cells in series. The total window area is 16 m^2 in Solgården and about 1.2 m^2 in the case of the prototype solar window. The reflectors are made of conventional anodized aluminium from Alanod, Germany, and the anti-reflection treated low iron glazing is from Sunarc, Denmark. The anti-reflection treatment increases the transmittance, weighted by the spectral sensitivity of the PV-cell, by about 5% for each glass pane (Chinyama et al., 1993).

The reflector parabola is described in Eq. (1). r is a vector from F to a point on the parabola at angle φ .

$$r(\varphi) = p / \cos^2(\varphi) \quad (1)$$

Both h and a is determined by r and the two angles $w = 105^\circ$ and $u + v = 35^\circ$, respectively, for the solar window. The ratio between h and a , which is defined as the geometrical concentration factor, is 2.45 for the construction.

2. Methods

Measurements of the performance of the multifunctional PV/T hybrid solar window were carried out during



Fig. 2. Left: the prototype solar window. Right: the solar window in Solgården with closed reflectors.

2006 on a prototype solar window placed in Lund, Sweden (55.44N, 13.12E). A full scale system combining four of these solar windows was installed in a single family home called Solgård in Älvkarleö, Sweden (60.57N, 17.45E) and evaluated during 2006–2008. This window was directed 23° towards east from south. The solar windows can be seen in Fig. 2. The measurements of the generated current and voltage produced by the prototype solar window were carried out using a Campbell CR1000 logger. The radiation, temperatures and water flow through the absorbers were measured using a Campbell CR10 logger. The temperature measurements were carried out using PT100 sensors. All measurements made in Solgården were conducted by using a Campbell CR10.

The water flow was kept at a constant level throughout the measurements for the prototype solar window. The Solgård solar window was equipped with a PV module driven pump. This means that the water flow will vary with the solar radiation. The radiation was monitored using Kipp and Zonen pyranometers for the measurements in Lund and Li-COR pyranometers in Solgård. Measurements were monitored both with the reflectors in a horizontal and in a vertical position. The measurements were carried out with a 10 s sampling interval and the average values were stored every sixth minute. This will determine the resolution. The prototype solar window was supplied with water of constant inlet temperatures and the measurements were carried out during both day and night. Night time data were used for determining the thermal losses of the window. The typical flow in the thermal circuit is 100 liter per hour and the temperature increase is typically 15°. The accuracy in each measurement is around 1% and the accuracy in the thermal measurements adds up to 2–3%. The accuracy of the pyranometer is 3% and the measurements of the current from the solar cells have accuracy below 1%.

A simulation model was developed to describe the solar window. The model uses the direct and diffuse radiation together with the inlet water temperature, the ambient temperature and the time, and thus the solar angles, as inputs. The outputs are thermal and electrical delivered power. In

order to simplify the calculations the total electrical power, P_{tot} , delivered by the solar window was divided into three components, P_{dir} , P_{ref} , and P_{diff} . The first component, P_{dir} , is the power caused by the beam radiation that hits the absorber directly. The second component, P_{ref} , is the power caused by the beam radiation that goes via the reflector. The third component, P_{diff} , is the power contribution given by the diffuse radiation. Fig. 3 explains graphically the three different components of radiation.

The expression for the electrical output is shown below.

$$P_{\text{dir}} = G_{b,n} \cdot T_{\text{glass}}(\Theta_1) \cdot \alpha_{\text{pv}}(\Theta_2) \cdot f_{\text{shading}}(\Theta_3) \cdot A_{\text{cell}} \cdot \eta_{\text{pv}} \cdot \cos(\Theta_2) \quad (2)$$

$$P_{\text{refl}} = G_{b,n} \cdot T_{\text{glass}}(\Theta_1) \cdot \alpha_{\text{pv}}(\Theta_4) \cdot f_{\text{refl}}(\Theta_5) \cdot A_{\text{refl}} \cdot \eta_{\text{pv}} \cdot R_{\text{refl}} \cos(\Theta_5) \quad (3)$$

$$P_{\text{diff}} = G_d \cdot C_{1,2} \quad (4)$$

$$P_{\text{tot}} = P_{\text{dir}} + P_{\text{refl}} + P_{\text{diff}} \quad (5)$$

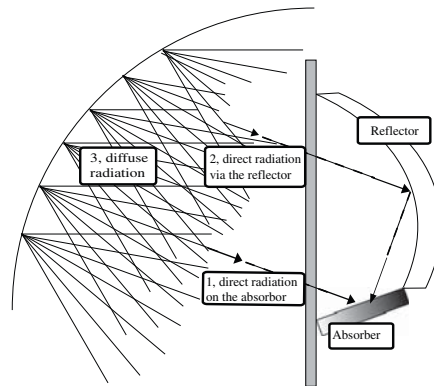


Fig. 3. A graphical explanation of the calculation method with the three different radiation components.

$G_{b,n}$ and G_d are the beam radiation and the diffuse radiation against the window. T_{glass} is the angular dependent transmittance through the glazing; α_{pv} describes the angular dependence of the absorptance of the PV cells, and $f_{shading}$ describes the shading of the PV cells caused by the window frame. f_{ref} is a correction factor for the shadow effects of the radiation which is reflected. This function includes the shading of the reflector. The angles θ_1 to θ_5 are the different incidence angles for the beam towards the components of the solar window. A_{cell} and A_{ref} are the areas of the PV cell and the reflector, respectively. η_{pv} and R_{ref} are the efficiency of the solar cells and the reflectance of the reflector. $C_{1,2}$ is a response function for the diffuse radiation obtained from measurements during cloudy days, when the beam radiation has negligible influence on the performance. Measurements during cloudy days were performed with the reflector in both horizontal and in vertical positions allowing both response functions C_1 , horizontal reflector, and C_2 , vertical reflector, to be determined.

The transmittance, T_{glass} , through the window was calculated using the Fresnel's equations and Snell's law. The shading factors $f_{shading}$ and $f_{reflector}$ were calculated theoretically from the PV/T window geometry. A measurement was performed to determine α_{pv} , the angular dependence of the PV cells. Fig. 4 shows the transmission through the glazing, the angular dependence of the PV cell, the angular impact of shading on the performance of the PV cell and on the optical efficiency of the thermal collector.

In order to calculate the thermal output a fourth term has to be added to describe the thermal losses in the absorber. The thermal losses $P_{loss,p}$ for the prototype solar window and $P_{loss,s}$ for the Solgärden solar window are shown below. The Eqs. (2)–(5) are reused but with parameters and functions for the thermal absorbers instead of the PV-cells.

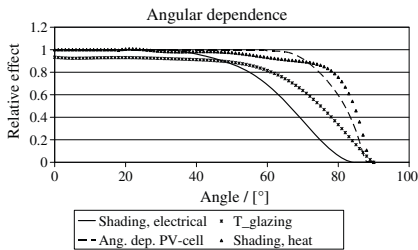


Fig. 4. The angular dependence for the different functions describing the solar window.

Table 1
U-values for the prototype solar window.

Thermal losses/[W/m ² K], solar window PV/T collector				
Closed/open mode	Closed window		Open window	
Direction of thermal loss dissipated from the absorber	In	Out	In	Out
U-value/[W/m ² K]	3.9	2.0	5.9	1.3

$$P_{loss,s} = U_{s,out} \cdot A_{window} \cdot \Delta T_{out} + U_{s,in} \cdot A_{window} \cdot \Delta T_{in} \quad (6)$$

$$P_{loss,p} = U_p \cdot A_{window} \cdot \Delta T \quad (7)$$

Since the solar window in Solgärden experiences thermal losses to two different temperatures, the ambient temperature and the indoor temperature, two different U -values were used. The $U_{s,out}$ represents the thermal loss to the outside and the $U_{s,in}$ the thermal loss to the inside. A_{window} is the total window area. ΔT_{out} is the temperature difference between the average water temperature and the ambient temperature. ΔT_{in} is the temperature difference between the indoor temperature and the average water temperature. The U -values, in Table 1, were estimated from heat transfer analysis. U_p is the U -value for the prototype solar window and ΔT is the temperature difference between the ambient temperature and the average water temperature. The separately measured thermal losses through the solar window are 1.3 W/m²K with reflectors closed and 2.4 W/m²K with reflectors open.

The simulations were carried out with 6 min time steps using weather data monitored at the locations where the solar windows were placed.

3. Results

Two different types of graphs were used to validate the model regarding thermal and electrical output. The first type is shown in Fig. 5, where results from measurements and simulations are compared during a day period. To be able to perform easy and reliable measurements, the short circuit current was monitored and simulated instead of the delivered power. In this way the measurements do not depend on maximum power point tracking. The days were chosen to illustrate different weather conditions, such as different ambient temperatures and cloudy weather with sunny intervals. Results from both the prototype and from Solgärden are shown in Fig. 5. Fig. 5 combined with Fig. 7, discussed later, show that different seasons and thus different solar angles are handled correctly by the model. Fig. 5 illustrates the performance during partly cloudy days.

During the measurements on the prototype solar window, two different, not perfectly synchronized, loggers for monitoring the electrical output and the radiation were used. This means that synchronization problems could arise during partly cloudy days with quickly changing solar irradiance. To solve this problem the simulated and the measured output was integrated daily. Then this irregularity will disappear. The result from this analysis is shown in Fig. 6, where the integrated daily measured output on the

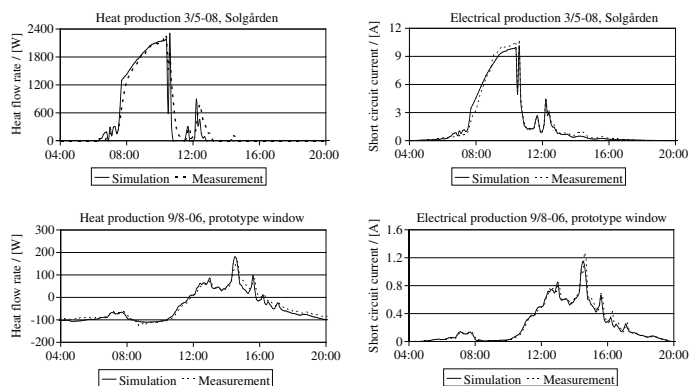


Fig. 5. Measured and simulated thermal and electrical output for 8 m² window in Solgården (upper) and for 1 m² window in the prototype (lower).

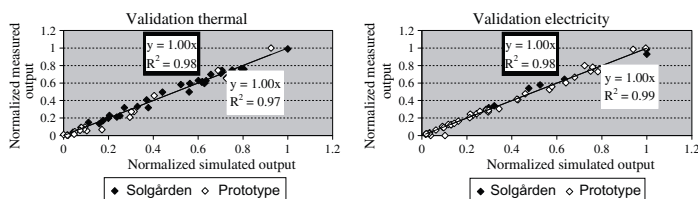


Fig. 6. Comparison of measured and simulated daily thermal and electrical performance of the solar window.

y-axis is plotted versus the integrated daily simulated output on the x-axis. A perfect agreement between simulation and measurement would put all the points on the line, $x = y$. This analysis was performed both for the thermal output, left figure, and the electrical output, right figure. Validation from the Solgården solar window is in filled circles and the validation from the prototype solar window is in empty circles. All values have been normalized to the highest output in each series. The correlation is high for all four validations.

The impact of the reflector on the electrical and thermal output is larger during periods of low solar altitude. This can be seen in Fig. 7 where two simulations have been plotted. The solid black line represents a simulation with active, vertical reflectors, and the dashed black line (the lowest) represents a simulation with passive, horizontal reflectors. The area between the solid black line and the dashed black line is thus the contribution to the electrical output from the reflector. In the left graph dated 12/9-06 the reflector contributes to about 30% of the daily output while the contribution is about 50% in the right graph dated 3/11-06. The filled circles in the figure are from measurements during both days. The correlation is high between measurement and simulation. In the empty squares the irradiance

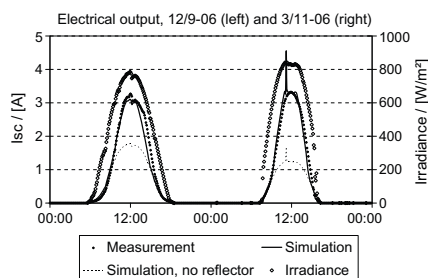


Fig. 7. Measurement and simulation of the electrical output during 12/9-06 (left) and 3/11-06 (right).

during the two days is shown. The right y-axis represents the solar irradiance.

Yearly simulations were made for the prototype solar window and for two flat PV-modules. The PV-modules have the same efficiencies and areas as the string module in the solar window, but they have no reflectors, are unshaded and use single glazing instead of double glazing

as in the solar window. The PV-modules were installed on a wall or on the Solgård roof, tilted 20° . The wall mounted PV module benefits less from the diffuse radiation compared to the solar window due to less favourable view angles between the cells and the sky. The results from the simulation show that the performance of the solar window is suppressed by shadow and transmittance effects. However, annually it delivers about 35% more electric energy per unit cell area compared to a vertical flat PV module.

When the PV module is located on a roof at a low tilt, it receives more diffuse radiation than a wall mounted PV module since the module can see a larger part of the diffuse radiation from the sky. This is clearly visible in Fig. 8. The increase of the electrical output from the direct radiation on the roof mounted PV module compared to the solar window is due to lower losses in the glazing and the possibility for the roof module of utilizing the radiation which comes from directions behind the wall. Note that the increase of the diffuse radiation on the roof mounted module compensates for the reflector contribution on the cells in the solar window. The diffuse irradiation is treated as isotropic.

A similar analysis, in this case using TRNSYS, was performed to investigate the thermal properties of the solar window connected to the thermal system of the house. A TRNSYS-deck including the solar window or flat solar collectors, pumps, a storage tank, etc. and a heating load was constructed. In the simulation all parameters except the areas of the wall collector and the roof collector were kept constant.

The thermal performance of the solar window cannot be compared with a solar collector of the same area, since it will give a substantial over production during the summer period. Therefore a comparison was performed between two solar thermal systems with the same annual energy production. Fig. 9 shows that 8.3 m^2 of wall collectors or 6.0 m^2 of roof collectors tilted 20° annually delivers the same amount of heat as the solar window with 16.0 m^2 glazed area and 5.06 m^2 of absorber areas. The wall and roof collectors are assumed to have $\eta_{\text{direct}} = 0.75$ and $\eta_{\text{diffuse}} = 0.68$. The U -value of the collectors is assumed to

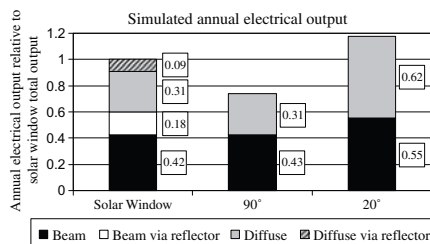


Fig. 8. The annual electrical output from the prototype solar window and from two flat PV-modules on a wall at 90° tilt and on a roof at 20° tilt.

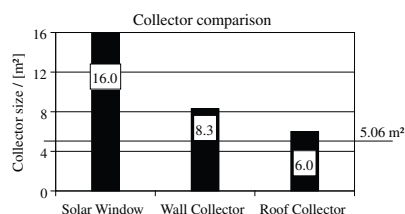


Fig. 9. The required areas of the wall collector and the roof collector to produce an equal annual amount of thermal energy compared to the Solgård solar window. The wall collector is placed vertically and the roof collector is installed at 20° tilt.

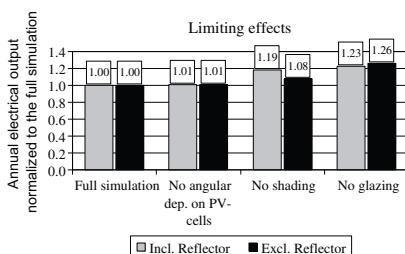


Fig. 10. Limiting factors affecting the performance of the solar window.

be $4 \text{ W/m}^2\text{K}$. All systems are supposed to be oriented 23° from south towards east.

This means that the solar window per absorber area delivers a similar amount of electric and thermal energy as PV-modules and thermal collectors each of the same area as the absorber in the solar window.

To study the limiting factors in the solar window a simulation was carried out where the factors $T_{\text{glass}}(\theta_1)$, $\alpha_{\text{pv}}(\theta_2)$ and $f_{\text{shading}}(\theta_3)$ in Eqs. (2)–(4) were in turn set to 1, see Fig. 10. The impact of setting $\alpha_{\text{pv}}(\theta_2)$ to 1 was small, since the angular dependence of the efficiency of the PV cells is negligible except for such high angles that the shading is already strongly affecting the performance. If the anti-reflection treated glazing were removed the yearly electrical output would increase by about 23% and if the shading effects could be removed completely the increase would be as much as 19%.

4. Discussion

A standard wall gives good insulation but does not utilize the irradiance falling on it. A window uses the solar radiation in an effective way for saving energy for heating. However it has high heat losses during the dark hours and may contribute to overheating during periods of high ambient temperatures and requires a sun shade. A solar

collector uses the high solar intensities for delivering hot water, but its contribution to the heating of the building is limited. A PV-module converts around 10% of the solar radiation to electric energy, while the rest is lost to the ambient as heat. This means that it is a demand for a dynamic façade element that combines the properties of a wall, a window and a solar collector or a PV-module. The ideal façade element should combine the following properties:

- During dark hours it should have low U -value and correspondingly low heat losses like a well-insulated wall.
- During cold sunny hours it should effectively convert the radiation to heat like a window, i.e. have a low U -value and high total solar transmittance.
- During warm sunny hours it should deliver hot water or electricity like a solar collector or a PV cell and simultaneously giving sun shade to the building.

The solar window fulfils to some extent the requirements on an ideal element. A weak point of the solar window is the high U -value, even in a closed position. The large area of the solar window also contributes to the high heat losses. This can be improved by designing the reflector with a thicker insulation and to be tighter in the closed state. The U -value can also be suppressed if the glazing is coated with low emitting films. These films will however also decrease the transmittance with roughly 10%.

Solar cells in concentrating system are principally required to have a lower series resistance due to a high and non-uniform irradiance. The solar window can however be equipped with standard cells since the concentration is relatively low. If the reflectors are flat or have a white diffuse coating, then the irradiance will be uniform. But this also means that the performance will deteriorate significantly.

The reflectors will be closed when there is a demand for production of electricity and heat. During these hours the window will act more like a wall than a window. This is often a disadvantage, even if sometimes a sun shade is demanded. During the summer period, when the projected solar altitude is high, a large fraction of the solar beam goes directly onto the absorber with a low contribution from the reflector. Then the reflector can be partly opened and the window delivers heat, electricity and light. This is probably the ideal use of the solar window. This period will be extended when the window is moved to lower latitudes. However, at lower latitudes the annual irradiation on a vertical wall is decreasing, which means that the solar window will deliver less heat and electricity. Principally also the optical axis of the reflector parabola should be shifted with the latitude. The impact of the optical axis on the annual performance is however not so strong.

The solar window is designed for installation in a south window. However, if the window is designed with a horizontal optical axis it accepts all radiation and it can be installed in all directions. The concentration factor is then

limited to a factor of 2. It is difficult to design external sun shades for standard windows in east and west since the solar altitude is low in the morning and afternoon, respectively. There the solar window has the proper design since it effectively darkens the window in its closed position.

An alternative design of the solar window is to construct it without glazing and thermal circuit on the outside of the wall. Then the electric output will be considerably increased (Gajbert et al., 2007). The long term stability of an unprotected aluminium reflector will however be limited. If the standard solar window does not have a cooling circuit then the cells will be hot and the heat will be delivered to the inside, so the sun shade function will not work.

5. Conclusions

The overall goal of the project presented in this article is to reduce the total costs of the PV and solar thermal systems for a building. An alternative for achieving this goal is to use PV/T hybrid collectors using reflectors which concentrate the irradiance onto the absorbers. Different designs have been proposed (Gajbert et al., 2007; Mallick et al., 2004). But very few geometries, which allows for building integration, have been presented. A multifunctional PV/T hybrid which can be integrated in a window was proposed by Andreas Fieber (Fieber et al., 2003, 2004). This solar window replaces installations of PV-modules, solar thermal collectors and sun shades. The performance of this solar window is analyzed in detail in this paper.

The results from the simulation program developed to evaluate the window, closely match the measured data. The simulated annual electrical energy production clearly shows the importance of utilizing the diffuse radiation. About 40% of the electrical energy produced in the window is due to diffuse radiation. The comparison performed in Fig. 8 shows that the solar window produces about 35% more electrical energy per unit area of PV cells compared to a flat PV module placed on a wall at a 90° tilt. The simulation presented in Fig. 9 shows that the solar window produces more thermal energy per absorber area than a flat plate solar collector placed on the roof of Solgården at 20° tilt. If the flat plate collector is installed at an optimum tilt of 45° the annual output increases by around 5%.

These values were found using weather data from Lund at latitude 55.4° in the south of Sweden. They are representative also for Stockholm at latitude 59.3°. It is important to point out that vertical collectors and windows are more energy effective on high than on low latitudes.

The best method for analyzing the performance of the solar window is to compare it with conventional systems that deliver a comparable amount of heat and electricity. The paper shows that the hybrid absorber in the solar window can be replaced by 8.3 m² of collectors and 5.4 m² of PV-modules installed on the wall. The solar window requires less solar cell-, absorber-, and glazing areas than

the conventional systems. This implies that the materials cost are lower for the solar window. However, the solar window requires a relatively complicated thermal system and tiltable reflectors. The tested solar window is an early prototype, which means that it is difficult to estimate the real cost for a complete installation.

The solar window has a geometrical concentration factor of 2.45, while the real annual concentration is limited to a factor of 1.33 only. The substantial difference is explained by effects of optical axis of the reflector, optical losses in the reflector and glazing, shadow effects and the impact of the diffuse irradiance. The optical axis at 15° means that the beam irradiance vector will be below the optical axis during December and January. If a reflector with a horizontal optical axis is chosen then the geometrical concentration is limited to a factor of 2. Fig. 10 shows that the transmittance of the double glazing decreases the performance by almost 20 percent. The shading is also an important factor that limits the performance of the collector. All of these factors adds up to a total annual concentration factor that is about half of the theoretical value. The low absorbing anti-reflection treated glazing has a very high transmittance and can be improved only marginally. This means that the largest potential for improvement is obtained by minimizing the shadow effects. This can be accomplished by having a sufficient distance between the outer cells and the frame.

As can be seen in Figs. 7 and 8 it is possible to run simulations with the reflectors in either active, vertical, or passive, horizontal, positions. This keeps the simulation realistic by allowing control mechanisms, based on human behaviour, to decide whether or not to have closed reflectors. For instance there is a possibility to cool the building at night by simply opening the reflectors and thus increasing the *U*-value of the window. This is not an option for a standard window with a low *U*-value.

In conclusion, the developed calculation model for the PV/T hybrid solar window is in good agreement with measurements from both the prototype solar window and from the Solgården solar window. The model describes correctly both the electrical and the thermal output from the window. The solar window, placed vertically in a wall, produces about the same amount of electric energy as a roof integrated PV-module per unit cell area. Simultaneously the solar window produces about the same amount of thermal energy per unit absorber area as a solar collector integrated in the same roof tilted 20°.

Acknowledgements

This work was supported by the Swedish Energy Agency through the Program Soler 03-07. B. Hellström and H. Håkansson at Lund University and S. Larsson at Vattenfall Development are acknowledged for assistance during measurements and evaluation.

References

- Assoa, Y.B., Menezes, C., Fraisse, G., Yezou, R., Brau, J., 2007. Study of a new concept of photovoltaic-thermal hybrid collector. *Solar Energy* 81, 1132–1143.
- Brogren, M., Nostell, P., Karlsson, B., 2000. Optical efficiency of a PV-thermal hybrid CPC module for high latitudes. *Solar Energy* 69, 173–185.
- Chinyama, G.K., Roos, A., Karlsson, B., 1993. Stability of antireflection coatings for large area glazing. *Solar Energy* 50, 105–111.
- Fieber, A., Gajbert, H., Håkansson, H., Nilsson, J., Rosencrantz, T., Karlsson, B., 2003. Design, building integration and performance of a hybrid solar wall element. In: *Proceedings of ISES Solar World Congress 2003*, Gothenburg, Sweden.
- Fieber, A., Nilsson, J., Karlsson, B., 2004. PV performance of a multifunctional PV/T hybrid solar window. In: *Proceedings of 19th European Photovoltaic Solar Energy Conference and Exhibition 2004*, Paris, France.
- Fieber, A., 2005. Building Integration of Solar Energy. Lic. Thesis Report, Division of Energy and Building Design, Department of Construction and Architecture, Lund University, Lund Institute of Technology, Report EBD-T – 05/3, pp. 107–192. Available from: <http://www.ebd.lth.se/fileadmin/energi_byggnadsdesign/images/Publikationer/AvhandlingWEB_alt_Andreas.pdf>.
- Gajbert, H., Hall, M., Karlsson, B., 2007. Optimisation of reflector and module geometries for stationary, low-concentrating, façade-integrated photovoltaic systems. *Solar Energy Materials and Solar Cells* 91, 1788–1799.
- IEA SHC Task 35 PV/Thermal Solar System. Available from: <www.iea-shc.org/task35/index.html>.
- Kalogirou, S.A., Tripanagnostopoulos, Y., 2006. Hybrid PV/T solar systems for domestic hot water and electricity production. *Energy Conversion and Management* 47, 3368–3382.
- Krauter, S., Ochs, F., 2003. Integrated solar home system. *Renewable Energy* 29, 153–164.
- Mallick, T.K., Eames, P.C., Hyde, T.J., Norton, B., 2004. The design and experimental characterisation of an asymmetric compound parabolic photovoltaic concentrator for building façade integration in the UK. *Solar Energy* 77, 319–327.
- Nostell, P., Roos, A., Karlsson, B., 1999. Optical and mechanical properties of sol-gel antireflective films for solar energy applications. *Thin Solid Films* 351, 170–175.
- Rönnelid, M., Karlsson, B., 1997. Irradiation distribution diagrams and their use for estimating collectable energy. *Solar Energy* 61, 191–201.
- Tonui, J.K., Tripanagnostopoulos, Y., 2007. Improved PV/T solar collectors with heat extraction by forced or natural air circulation. *Renewable Energy* 32, 623–637.

Paper II

Available online at www.sciencedirect.com

SciVerse ScienceDirect

Solar Energy 86 (2012) 903–910

SOLAR
ENERGYwww.elsevier.com/locate/solener

System analysis of a multifunctional PV/T hybrid solar window

Henrik Davidsson*, Bengt Perers, Björn Karlsson

Energy and Building Design, Lund University, P.O. Box 118, SE 221 00 Lund, Sweden

Received 18 February 2010; received in revised form 23 November 2011; accepted 9 December 2011

Available online 23 January 2012

Communicated by: Associate Editor Yogi Goswami

Abstract

The work presented in this article aims to investigate a PV/T hybrid solar window on a system level. A PV/T hybrid is an absorber on which solar cells have been laminated. The solar window is a PV/T hybrid collector with tilttable insulated reflectors integrated into a window. It simultaneously replaces thermal collectors, PV-modules and sunshade. The building integration lowers the total price of the construction since the collector utilizes the frame and the glazing in the window. When it is placed in the window a complex interaction takes place. On the positive side is the reduction of the thermal losses due to the insulated reflectors. On the negative side is the blocking of solar radiation that would otherwise heat the building passively. This limits the performance of the solar window since a photon can only be used once. To investigate the sum of such complex interaction a system analysis has to be performed. In this paper results are presented from such a system analysis showing both benefits and problems with the product. The building system with individual solar energy components, i.e. solar collector and PV modules, of the same size as the solar window, uses 1100 kW h less auxiliary energy than the system with a solar window. However, the solar window system uses 600 kW h less auxiliary energy than a system with no solar collector.

© 2012 Elsevier Ltd. All rights reserved.

Keywords: PV/T hybrid; Solar window; Building integration; TRNSYS

1. Introduction

If solar electricity is to become cheap enough to compete with electricity from the grid a number of different techniques have to be combined. Examples of these techniques are PV/T technology combining PV cells with solar thermal collectors, the use of reflectors to focus the solar radiation onto the cells, or building integration where building materials can be replaced by the solar thermal collectors and PV modules. All these techniques have the potential for decreasing the costs of utilizing solar energy. However, when a product is used for multiple purposes there is always a risk of complex interactions with the surroundings.

One way of combining different functions is to integrate a PV/T absorber into a window, giving a PV/T hybrid solar

window, in this paper referred to as a solar window. A PV/T hybrid is an absorber on which solar cells have been laminated. The solar window is a PV/T hybrid collector with tilttable insulated reflectors integrated into a window. Such a solar window was suggested and developed by Fieber et al. (2003, 2004) and Fieber (2005). A drawing of the solar window is shown in Fig. 1 to the left. Fig. 1 to the right shows a photo of the solar window with vertical reflectors.

This paper gives an analysis of this solar window on a system level. In a previous paper, an evaluation was made on a component level of the solar window (Davidsson et al., 2009). It showed that the solar window produces 35% more electric energy per cell area compared with a PV module installed vertically on a south wall. Other PV/T hybrid collectors have been reported earlier as cost effective collectors (Anderson et al., 2009; Kalogirou and Tripanagnostopoulos, 2006; Krauter and Ochs, 2003; Tonui and Tripanagnostopoulos, 2007).

* Corresponding author. Tel.: +46 2224851; fax: +46 2224719.

E-mail address: henrik.davidsson@ebd.lth.se (H. Davidsson).



Fig. 1. Left: the solar window with water cooled PV cells, tiltable reflectors and anti-reflection treated glazing. Right: the solar window in Solgården.

1.1. The solar window

The collector part of the solar window is constructed of solar thermal absorbers on which PV cells have been laminated. The absorbers are located on the inside of a window and have tiltable reflectors mounted next to them. In the vertical position the reflectors focus solar radiation, transmitted through the window within the incidence angle acceptance interval of 15–60°, onto the absorbers. Outside of the acceptance interval the irradiation is reflected back. In the horizontal position most of the irradiation is reflected into the building. A secondary effect of the vertical position compared with the horizontal position is that the thermal insulation of the window is increased. The window has two panes that are anti-reflection treated (Nostell et al., 1999), in order to increase the solar transmittance. The window panes do not have a low emittance coating, since this would mean a lower solar transmittance and thus a lower PV-performance. For the construction of the solar window, this anti-reflection treatment of the panes was regarded to be more important than the advantage of a better insulated window. The absorbers and reflectors were put on the inside of the glazing in order to protect the construction from adverse weather. Located in a window, the solar collector will influence the building in both positive and negative ways. When the insulated reflectors are placed vertically the thermal losses through the window are reduced. However, placed in a window, the collector will block some of the radiation that would otherwise heat the building passively. This problem is not shared by PV/T collectors integrated on the envelope of the building (Corbin and Zhai, 2010). In this case all the radiation that is transmitted through the windows is utilized as passive heating. At the same time the roof mounted collector delivers heat to the building.

When the reflectors in the solar window are placed in a vertical position to avoid overheating of the building little or no light is admitted into the building. This has to be compensated for with extra artificial lighting. This effect is however not included in the analysis presented in this

article. This issue of visual comfort was however discussed earlier by Fieber (2005).

The tiltable reflectors work in a similar way as a venetian blind, making it possible to control the intensity of solar radiation transmitted into the building. Other types of mechanisms to control the amount of solar radiation admitted into the buildings have been reported, for instance using thermotropic glass with active dimming (Inoue et al., 2008) or electrochromic smart windows (Granqvist et al., 1998). The official homepage of IEA SHC Task 21 Daylight in Buildings (IEA SHC) gives a good overview of different solar shading systems.

1.2. Solgården, the building

The solar window is installed in a one family building, shown in Fig. 1 to the right, called Solgården in Älvkarleö (60.57N, 17.45E) in the central parts of Sweden. Solgården is a low energy building but does not qualify as a passive house due to the active underfloor heating system.

The solar window is connected to a thermal storage tank of 620 l where thermal energy is stored. The auxiliary thermal energy need is produced with a 9 kW pellet burner. The heating and electrical system is adapted for a future Stirling engine. The produced electrical power from the solar window is stored in a battery bank using a combined regulator, charger and inverter. The 10.6 kWh battery bank ensures that no electric energy is lost due to mismatch between the electricity produced in the PV modules and consumption of electricity in the building. The capacity of the battery bank is far larger than the daily electrical energy usage. A sketch of the system is illustrated in Fig. 2.

2. Method

The work presented in this article aims to investigate the solar window on a system level. The parameters, such as collector absorptance, efficiency on PV-cells, reflectance and shading caused by the window frames used in the simulations were found experimentally (Davidsson et al., 2009).

To make the comparison as fair as possible between the different systems the size of the window glazing in the reference building was chosen to make the windows in the different systems transmit an equal amount of light during an overcast day with only diffuse irradiance. Since the transmittance of diffuse light for the solar window is about 30% and the number for the selected reference window glazing is twice as high, the glazed size of the reference window was chosen to be 50% of that of the solar window glazing.

An analysis was also made to investigate the potential for improving the performance of the solar window. In this improved version, in this article called the “developed solar window”, a low emittance coating was put on the outside of the inner glazing to lower the thermal losses. The absorbers were also better insulated for minimizing the losses. The low emittance coating will not only lower the thermal losses but also lower the transmission through the glazing. The transmission was estimated to be reduced by 20% compared with the glazing in the original solar window. The solar window collector has thermal losses to both the outdoor and the indoor surroundings, which are at different temperature. The losses from the solar window to the inside heat the building passively. Table 1 presents the heat transfer coefficients for heat dissipated from the absorbers. The table shows heat transfer coefficients for both the original solar window and the developed solar window. The heat transfer coefficients are calculated for both vertical and horizontal reflectors and in both directions, in to the building or out to the surrounding. This means that the total heat losses from the collector are calculated by adding the heat loss to the surroundings and the heat loss to the inside. The calculations are described and discussed in more detail by Davidsson (2010). All the numbers in Table 1 are calculated values. The calculated heat transfer coefficients when using the vertical reflectors were verified by comparing simulated with experimental results during a period of 40 days. Since the solar window was

not completed when the measurements took place the reflectors could not be tilted to a horizontal position. However, the theoretical basis for the calculations was the same as in the vertical mode. In the horizontal mode all the convective losses are assumed to be lost to the building. This will slightly overestimate the heat gain to the building. For the developed solar window all the values for the thermal losses have been derived theoretically. The different simulated systems are tabulated in Tables 2 and 3 shows the U-values and the glazing properties for the solar window, the developed solar window and the energy efficient window used in the simulations.

2.1. Reflector control strategies

The solar window was investigated for four different control strategies for the reflector position. The strategies are:

1. Always open, horizontal reflectors.
2. Always closed, vertical reflectors.
3. The reflectors are horizontal if the solar irradiance in the window plane lies between two user defined values. If the irradiance is below the interval the reflectors close to a vertical position in order to lower the U -value of the window. If the irradiance is above the interval the reflectors close to vertical position to avoid overheating of the building.
4. If the temperature in the building falls below a user defined value the window is controlled to give a minimum of heat losses from the building, i.e. the hot water and electricity production is of less importance. This means that the energy balance is calculated for horizontal reflectors and vertical reflectors and that the most energetically favourable alternative is chosen. If the indoor temperature exceeds the upper user defined value, the reflectors are set as to minimize the energy transmitted into the building. This means that during periods

Table 1
Heat transfer coefficients of the solar window collector.

Heat transfer coefficients (W/m ² K), solar window PV/T collector Vertical/Horizontal reflectors	Vertical		Horizontal	
	In	Out	In	Out
Direction of thermal loss dissipated from the absorber				
Solar window	3.9	2.0	5.9	1.3
Developed solar window	0.7	1.3	3.5	0.7

Table 2
The simulated systems.

	System			
	Original solar window system	Developed solar window system	System 2	System 3
16 m ² solar window	X			
16 m ² developed solar window		X		
5.06 m ² solar thermal collector and 4 ² PV-modules				X
8 m ² energy efficient window replacing the solar window			X	X
UA-value, building (W/K)	110	95	80	80

Table 3
U-value and transmittance of the simulated windows and glazings.

Type window	Window and glazing			
	U-value of window (W/K)		U-value (W/K)	Glazing
	Horizontal refl.	Vertical refl.	X	Transmission ^c (%)
Solar window (SW)	2.43 ^a	1.3 ^a	X	0.92
Developed SW	1.5 ^b	0.6 ^b	X	0.74
Energy efficient window	X		1.1	0.6

^a Measured values, (Fieber, 2005).

^b Estimated values.

^c The same value was used for both *g*- and *T*-value.

with overheating the reflectors will typically close to a vertical position during daytime to prevent passive heating and open to a horizontal position during night time for increasing the *U*-value and the heat losses. If the temperature lies between the two stated temperatures the reflectors will be vertical to fill the batteries and the collector tank to a preset level. When this condition is fulfilled the reflectors will be horizontal for daylighting.

Since the solar window was not completed when the measurements took place, the four strategies could only be evaluated with simulations. During the simulations the upper and lower parameters were used throughout the year. The parameters were not changed for different seasons.

2.2. TRNSYS modelling

The analysis of the different systems was performed using TRNSYS. The TRNSYS deck was calibrated against measured consumption of wood pellets and electricity for the building Solgården. Some of the most important model components are:

- **Battery/inverter** and load: TRNSYS types 47 and 48 respectively. A battery bank of 10.6 kW h and a constant electrical load of 375 W throughout the year, i.e. 3285 kW h annually.
- **Tank**: The tank, TRNSYS type 60 (Klein et al., 2000), has a volume of 620 l. The hot water consumption was set to 9 litres per hour throughout the year.
- **Building**: The one zone building, TRNSYS type 12 (Klein et al., 2000), model is a lumped capacitance degree hour model with internal gain. This simplification equates to a building with an open plan layout, which is the case for Solgården. The building has a *U*A-value of 110 W/K and a thermal capacitance of 40 MJ/K. The *U*A-value of the building was lowered to 95 W/K for the developed solar window simulation since its *U*-value was reduced from 2.43 W/m² K to 1.5 W/m² K. The *U*A-value was reduced to 80 W/K for the simulations for system 2 and system 3 since the 16 m² large solar window was replaced with an 8 m² large energy efficient window. The building has

6 m² windows to the west, 2 m² to the east and to the north and about 4 m² to the south apart from the 16 m² solar window also facing south. The building in the deck serves as a load for the hot water consumption.

- **Weather data**: The weather data used for the simulation was derived with meteonorm (Meteonorm) for Gävle, about 20 km from Älvkarleö. Data from a full year was used.
- **Solar window**: A new TRNSYS component for the solar window was constructed.
- The separate PV and collector used to model the solar energy system in system 3 are simplified first order models taking into account solar beam and diffuse radiation, incidence angle, inlet and ambient temperature.
- The thermal losses from the storage tank, the used electricity, the heat produced by the people in the house and the radiation transmitted into the building through the windows were added as internal gains for the building.

The developed TRNSYS deck allowed the electrical and thermal energy production to be simulated. When the control strategies 3 and 4 were simulated the upper and lower set points had to be specified. The choice of set points will affect both energy production and hence the auxiliary energy need and the thermal comfort in the building. If the upper set point for control strategy 3 is set too high, i.e. the reflectors are horizontal during high levels of irradiance; the building is likely to become overheated during hot and sunny summer days. Setting the lower set point too low will result in horizontal reflectors during hours of low irradiance, hence giving large thermal losses.

To investigate the importance and difference in energy production and auxiliary energy need for the building a parametric study was performed for the original solar window using control strategies 3 and 4 with varying upper and lower set points. How to control the reflectors is a highly complex question and there are most likely many answers. The choice of optimizing energy production, thermal comfort or daylight is in many cases a personal preference.

The results of the simulations of the required auxiliary energy need should primarily be used for comparative studies. The building in the TRNSYS deck serves as a load for the

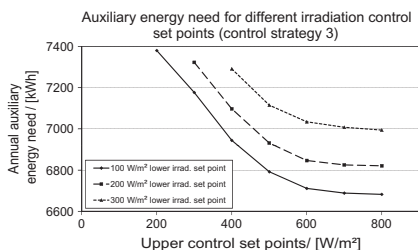


Fig. 4. The annual auxiliary energy need using control strategy 3 for the reflectors as a function of the upper irradiation control set point for different lower set points.

solar energy system. For a complete evaluation of the building itself a more detailed house model than the TRNSYS type 12 has to be used.

3. Results

All the results presented in this article are based on the TRNSYS simulations described in the previous chapter. A parameter study using the 3rd control strategy was performed for different upper and lower set points. The results are shown in Fig. 4. The figure shows simulation results for the lower irradiation set points at 100, 200 and 300 W/m² respectively. The lowest energy consumption was obtained using 100 W/m² as lower set point and 800 W/m² as the upper set point. This means that the reflectors are horizontal during practically all the bright hours. Problems with overheating might arise during hours with strong irradiance. Having the reflectors constantly in the horizontal position can easily overheat the building.

The same kind of analysis was also made for control strategy 4. Simulations were performed, having the lower and the upper temperature set points varying between 22 °C and 30 °C. The results are presented in Fig. 5. As can be seen in the figure the difference in auxiliary energy need is rather small. The lowest energy consumption was obtained using 26 °C as the lower set point and 30 °C as the upper one. However, these are not levels of indoor temperature that are normally preferred by the inhabitants. The solar window is thus not used in an optimal way for the thermal comfort. The preferred levels will be different for different persons and from different location of installation. The strategy might for instance differ between a staircase and an office room.

The choice of control strategy and control set points will not only affect the annual auxiliary energy demand for heating but also the electrical energy production and the thermal comfort in the building. This is illustrated in Table 4. The row “Over heated building” gives the fraction of the year with indoor temperature above 30 °C. The simulations were performed without any increased ventilation

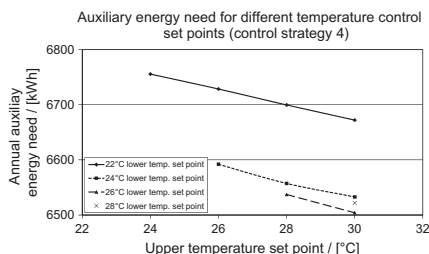


Fig. 5. The annual auxiliary energy need using control strategy 4 for the reflectors as a function of the upper temperature control set point for different lower set points.

regardless of the indoor temperature. A more sophisticated ventilation system, using e.g. night ventilation could bring these numbers down. This would however need a more sophisticated TRNSYS type than type 12. However, the performed simulations serve as a demonstration that the choice of control strategy will affect the thermal comfort and not only the annual auxiliary energy need. The most optimized control strategies and set points are marked with grey background. The solar window was simulated using control strategy 1 and 2 in order to investigate the upper and lower limits of electrical and thermal energy production. These strategies are no option in a real building since the whole idea with the flexible solar window becomes pointless if the reflectors are constantly vertical or horizontal. Since control strategy 4 performs best from an energy point of view as well as from a comfort point of view this strategy was chosen for the analysis presented in Figs. 6–8. In the results presented in Figs. 6–8, the 4th control strategy was used for the solar window with the set points set to 22 °C and 26 °C. If the 4th control strategy is used the PV modules produce electrical energy that covers 12% of the annual use and the thermal absorbers produce 24% of the annual space heating and domestic hot water demand.

The annual distribution of the produced thermal and electrical energy can be seen in Fig. 6. The PV cells have a somewhat more even annual distribution than solar thermal collectors. This is explained by the thermal losses of the collectors which have to be balanced before heat is delivered.

The resulting annual auxiliary energy demand for having the different types of solar energy systems, explained in Fig. 3 and Table 2, are shown in Fig. 7. The first bar shows the annual auxiliary energy need for Solgård with the 16 m² solar window. The second bar shows the same, but with the developed solar window. In the third bar the simulation results for system 2, i.e. when the solar window is replaced by an 8 m energy efficient window, is shown. The last bar shows the results for system 3, i.e. when the solar window is replaced by an 8 m² energy efficient window and a solar collector, and a PV-module of the same size as in the solar window has been placed on the roof with a 20° tilt.

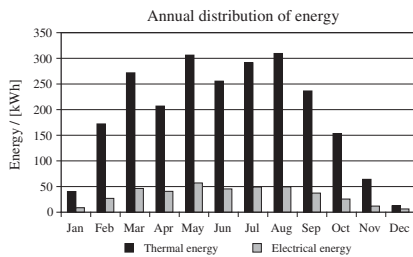


Fig. 6. The annual distribution of delivered solar energy from the window, in black the solar thermal and in grey the solar electricity.

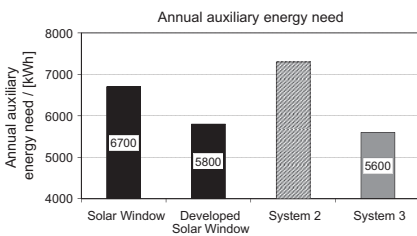


Fig. 7. The annual auxiliary energy need for Solgården using different types of solar collectors.

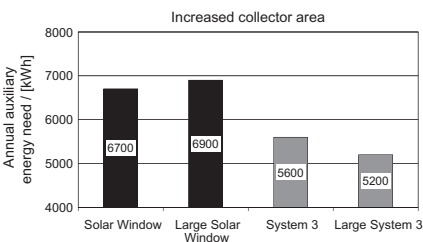


Fig. 8. The annual auxiliary energy need for the solar window in black and the reference in grey. The second and fourth bars labelled large are where the solar window or collector area has been increased by 50%.

A comparison was made between the solar window and the system 3 for the case of increasing the collector area with 50%. For the solar window this means that the entire solar window area is increased, while for system 3 only the roof collector area is increased. The simulation results are shown in Fig. 8. For the solar window case this gave a net negative impact since the thermal energy gain from the collector does not compensate for the increased heating required to balance the heat loss due to the larger glazed area. For the roof mounted collector the situation is different, the increase of the collector area increases the thermal production without increasing the thermal losses of the building.

4. Discussion

In this paper we investigated an improved version of the solar window, labelled the “developed solar window”. The difference from the original solar window is that it was better insulated, partly due to a low emittance coating on one of the panes. The drawback from this is that the thermal and electrical production is also reduced since the solar transmittance is lowered due to the coating. One possibility to further develop the solar window could be to place the absorbers and reflectors behind the outermost anti-reflection treated glazing and to place a low energy double glazing behind the absorbers. This would mean that the irradiation on the PV cells would increase since only one glazing is in front of the absorbers. Simultaneously, the U-value of the solar window would be lowered dramatically with the low energy double glazing plus the external pane. If the double glazing is put behind the absorbers the low emittance coating on the glazing no longer reduces the thermal and electrical output of the PV/T collector. Furthermore, the sunshade function provided by the solar window would be improved since the thermal losses from the absorbers would mainly be lost to the outside. This is beneficial for periods with overheating problems. However, this means that the thermal losses from the absorbers no longer help to heat the building during the winter, which affects the thermal performance during the winter in a negative way.

Apart from the problems with high U-value of the solar window there is also a problem with competition between the solar energy system produced in the absorbers and passive heating and daylighting for the solar radiation. If

Table 4

Parameter study of different control strategies for the reflectors. The parameter row shows what values were used for lower and upper parameters for the control strategy. Control strategy 1 and 2 have no parameters. The row “Over heated building” gives the fraction of the year with indoor temperature above 30 °C.

	Control 1	Control 2	Control 3		Control 4	
Parameters	X	X	100/400	100/800	22/26	26/30
Auxiliary energy need (kWh)	8000	7500	6900	6700	6700	6500
Produced ther. energy (kWh)	1500	2500	2300	1700	2100	2000
Produced el. energy (kWh)	300	430	400	330	390	370
Over heated building (%)	27	23	27	33	18	20

the solar radiation is converted into thermal or electrical energy it can not also be used for passive heating or day-lighting of the building, i.e. a photon can only be used once. This is a drawback of the solar window that should also be considered when a comparison is made with a PV/T system that is separated from the window.

5. Conclusions

TRNSYS simulations were performed on a PV/T hybrid solar window for different control strategies for the position of the tiltable reflectors. The analysis was performed for Swedish climate. The simulations were carried out for different strategies for controlling the position of the reflectors; always horizontal, always vertical, irradiation controlled and controlled by the energy flows to the building and to the collector. The latter strategy, which opened the reflectors to a horizontal position whenever this gave a larger total energy gain, was then chosen for further, more detailed studies.

The building with the solar window was compared to a building with a solar collector on the roof. The roof collector was of the same size as the absorbers of the solar window. The building with the roof collector was equipped with an energy efficient window, half the size of the solar window. The lower size was chosen with the intention of comparing the windows with the same total light transmission. The results show that the auxiliary energy demand of the building was about 1000 kW h less with the solar collector on the roof than for the building with the solar window. This is mainly due to the higher U -value and the larger size of the solar window. However, if the roof collector is taken away from the system the annual auxiliary energy need is 600 kW h larger than for the solar window.

The solar window was originally 16 m². Increasing the solar window by 50% leads to 200 kW h higher annual auxiliary energy need. The increased thermal losses due to the larger glazed area are thus more important than the extra solar thermal energy produced in the PV/T absorbers. If the area of the roof collector is instead increased the annual auxiliary energy need decreases by 400 kW h. In this case the thermal losses of the building do not increase.

Simulations were also made for an improved version of the solar window, in this paper named the “Developed solar window”. In this case the insulation on the reflectors and absorbers was assumed to be increased and a glazing with a lower U -value and a slightly lower solar transmittance was chosen. The simulation results show that the annual auxiliary energy need then dropped by 900 kW h compared with the original solar window. The results are comparable to the case where the solar collector was installed on the roof.

Acknowledgements

This work was supported by the Swedish Energy Agency through the program Solel 03-07. B. Hellström and H. Håkansson at Lund University and S. Larsson at Vattenfall Development are acknowledged for assistance during measurements and evaluation.

References

- Anderson, T.N., Duke, M., Morrison, G.L., Carson, J.K., 2009. Performance of a building integrated photovoltaic/thermal (BIPVT) solar collector. *Solar Energy* 83, 445–455.
- Corbin, C.D., Zhai, Z.J., 2010. Experimental and numerical investigation on thermal and electrical performance of a building integrated photovoltaic-thermal collector system. *Energy and Buildings* 42, 76–82.
- Davidsson, H., 2010. System analysis of a PV/T hybrid solar window. Lic. Thesis Report, Division of Energy and Building Design, Department of Architecture and Built Environment, Lund University, Lund Institute of Technology, report EBD-T—10/11. <http://www.ebd.lth.se/fileadmin/energi_byggnadsdesign/images/Publikationer/Rapportlic_avhandl_HD_Errata.pdf>.
- Davidsson, H., Perers, B., Karlsson, B., 2009. Performance of a multifunctional PV/T hybrid solar window. *Solar Energy* 84, 365–372.
- Fieber, A., 2005. Building Integration of Solar Energy. Lic. Thesis Report, Division of Energy and Building Design, Department of Construction and Architecture, Lund University, Lund Institute of Technology, report EBD-T—05/3. p 107–192. <http://www.ebd.lth.se/fileadmin/energi_byggnadsdesign/images/Publikationer/AvhandlingWEB_alt_Andreas.pdf> visited 2010-02-08.
- Fieber, A., Gajbert, H., Håkansson, H., Nilsson, J., Rosencrantz, T., Karlsson, B., 2003. Design, Building integration and performance of a hybrid solar wall element. In: Proceedings of ISES Solar World Congress 2003 Gothenburg, Sweden.
- Fieber, A., Nilsson, J., Karlsson, B., 2004. PV performance of a multifunctional PV/T hybrid solar window. In: Proceedings of 19th European photovoltaic solar energy conference and exhibition 2004, Paris, France.
- Granqvist, C.G., Azens, A., Hjelm, A., Kullman, L., Niklasson, G.A., Rönnow, D., Strömme Mattsson, M., Veszelei, M., Vaivars, G., 1998. Recent advances in electrochromics for smart windows applications. *Solar Energy* 63, 199–216.
- IEA SHC Task 21 Daylight in Buildings, <<http://www.iea-shc.org/task21/index.html>> visited 2010-02-08.
- Inoue, T., Ichinose, M., Ichikawa, N., 2008. Thermotropic glass with active dimming control for solar shading and daylighting. *Energy and Buildings* 40, 385–393.
- Kalogirou, S.A., Tripanagnostopoulos, Y., 2006. Hybrid PV/T solar systems for domestic hot water and electricity production. *Energy Conversion and Management* 47, 3368–3382.
- Klein, S.A., et al., 2000. TRNSYS program manual.
- Krauter, S., Ochs, F., 2003. Integrated solar home system. *Renewable Energy* 29, 153–164.
- METEONORM 5.0 global meteorological database for solar energy and applied meteorology. <http://www.meteotest.ch> visited 2010-02-08.
- Nostell, P., Roos, A., Karlsson, B., 1999. Optical and mechanical properties of sol-gel antireflective films for solar energy applications. *Thin Solid Films* 351, 170–175.
- Tonui, J.K., Tripanagnostopoulos, Y., 2007. Improved PV/T solar collectors with heat extraction by forced or natural air circulation. *Renewable Energy* 32, 623–637.

Paper III

Buildings **2013**, *3*, 18–38; doi:10.3390/buildings3010018

OPEN ACCESS

buildings

ISSN 2075-5309

www.mdpi.com/journal/buildings/

Article

Theoretical and Experimental Investigation of a Heat Exchanger Suitable for a Hybrid Ventilation System

Henrik Davidsson *, Ricardo Bernardo and Bengt Hellström

Department of Architecture and Built Environment, Division of Energy and Building Design,
Lund University, Box 118, 221 00 Lund, Sweden; E-Mail: ricardo.bernardo@ebd.lth.se (R.B.);
bengt.hellstrom@ebd.lth.se (B.H.)

* Author to whom correspondence should be addressed; E-Mail: henrik.davidsson@ebd.lth.se;
Tel.: +46-46-222-4851; Fax: +46-46-222-4719.

Received: 12 October 2012; in revised form: 21 December 2012 / Accepted: 4 January 2013 /

Published: 14 January 2013

Abstract: A key component in low energy houses is the heat recovery from the ventilation air. Over recent years, the most frequently used ventilation type is the mechanical ventilation with heat recovery. This kind of ventilation results in high heat recovery but does unfortunately consume a considerable amount of electrical energy. Natural or hybrid ventilation has the potential to consume less electricity but normally lacks heat recovery, leading to high-energy consumption for heating, and potentially low comfort. This article describes an investigation of a natural/hybrid ventilation system equipped with heat recovery. One of the key challenges in designing the heat exchanger is to keep the pressure drop low. At the same time the heat recovery rate has to be high. The results from the measurements show that it is possible to design a water-to-air heat exchanger with a temperature efficiency of approximately 80% with a pressure drop of about 1 Pa at air flows corresponding to 0.35 L/(s·m²) building area. This type of ventilation system has the potential to offer a high thermal comfort, high heat recovery rate at the same time as the electrical consumption from fans is kept low. Old buildings with a natural ventilation system without heat recovery could also be retrofitted with this type of ventilation system.

Keywords: hybrid ventilation; heat recovery; low pressure drop

Nomenclature

A_c	cross-sectional area	(m ²)
C_1	scaling factor	(-)
C_2	scaling factor	(-)
C_p	specific heat	(J/kg·K)
d	distance between the fin pipes	(m)
D	diameter	(m)
D_h	hydraulic diameter	(m)
F	friction factor	(-)
f	flow rate	(m ³ /s)
g	gravitational constant	(m/s ²)
G_z	Graetz number	(-)
h'	height difference between ventilation openings	(m)
h	convective heat transfer coefficient	(W/m ² ·K)
k	thermal conductivity	(W/m·K)
l	length of the heat exchanger/fin pipes	(m)
L	total heat exchanger length	(m)
L_c	corrected fin length	(m)
m	help variable	(m ⁻¹)
\tilde{n}	number of fin pipes in the heat exchanger	(-)
N_u	Nusselt number	(-)
N_{uD}	Nusselt number for non circular tube	(-)
P	perimeter	(m)
P_r	Prandtl number	(-)
ΔP	pressure difference	(Pa)
Q	heat transfer rate	(W)
q	heat transfer rate per unit length	(W/m)
R_a	thermal resistance on the air side	(m·K/W)
R_{pipe}	thermal resistance trough the pipe	(m·K/W)
R_{tot}	total thermal resistance	(m·K/W)
R_w	thermal resistance on the water side	(m·K/W)
Re	Reynolds number	(-)
t	thickness of fin	(m)
T_{in}	temperature of inlet ventilation air	(°C)
T_{amb}	temperature of ambient air	(°C)
T_{room}	temperature of indoor air	(°C)
$T_{w,in}$	temperature of incoming water	(°C)
$T_{w,out}$	temperature of outcoming water	(°C)
ΔT	temperature difference	(°C)
u_m	fluid mean velocity	(m/s)
w	width of the fin	(m)

Greek Letters and Other Symbols

η	system efficiency of heat exchanger	(-)
η_{comp}	component efficiency of heat the exchanger	(-)
η_f	fin efficiency	(-)
μ	dynamic viscosity	(N·s/m ²)

ρ_{amb}	density of the ambient air	(kg/m ³)
ρ_{room}	density of the indoor air	(kg/m ³)
ρ_a	density of the air	(kg/m ³)
ϕ_o	outer diameter of copper pipe in fin pipes	(m)
ϕ_i	inner diameter of copper pipe in fin pipes	(m)

Subscripts

a	air
w	water
Cu	copper

1. Introduction

For many years, a commonly used technique for ventilating buildings in Sweden is mechanical ventilation with heat recovery. This technique is also predominant for passive houses and other types of low energy buildings. It offers an efficient recovery of the heat from the exhaust air and results in a high thermal comfort for the residents of the building.

However, the fans needed for the ventilation system often cause noise and consume electrical energy. An investigation by the Swedish Energy Agency showed that the best performing ventilation system in the test consumed 456 kWh of electrical energy annually to run the fans [1]. This number is also in close agreement with data given in [2]. The following example can be used to illustrate a problem. A typical house in the Swedish climate consumes about 4000 kWh to heat the outdoor air. If the system recovers 75% of the heat it means that 3000 kWh is saved annually.

However, the 456 kWh of electric energy corresponds to about 1370 kWh of primary energy, using a conversion factor of three. This strongly reduces the energy savings in the system. Instead of saving 75% the system only saves about 40% of the primary energy including the electricity for the fans in the calculations.

One alternative to this is to use a natural ventilation system, driven by stack effect and wind induced pressure. This kind of technique normally lacks the possibility to recover energy from the outgoing ventilation air. If heat recovery is absent, the consequences will be a high energy demand and a high peak power load for buildings located in cold climates. At the same time, this type of technique easily results in low comfort due to cold draught. Also, the ventilation flow rate is strongly dependent on the wind pressure and the temperature difference between the indoor and the outdoor air. If the wind is absent and the temperature difference is close to zero, the ventilation rate will be unacceptably low. However, between the natural and the mechanical ventilation types, there is a combined technology called hybrid ventilation. This technique uses the natural driving forces when these provide sufficient pressure difference and utilizes a complementary fan otherwise. The hybrid technology combines the low electrical energy consumption for natural ventilation with the high reliability using fans. From an economical point of view hybrid ventilation has the potential for cost savings, especially with regard to installation costs [3]. This reference is also recommended for further reading. The standard heat exchangers used in modern ventilation technique introduces a high pressure drop. These heat exchangers are not possible to use in a system using natural ventilation. Instead, new heat

exchangers with very low pressure drop have to be developed if the hybrid ventilation system is to be equipped with heat recovery.

Many different solutions have been suggested to utilize the hybrid ventilation technology. Schultz *et al.* [4] suggested a system driven solely by the temperature difference between the indoor and the outdoor temperatures, having a heat recovery efficiency of up to 43%. Hviid [5] designed a heat exchanger made of bent plastic tubes reaching a heat recovery of about 75%. Shao [6] presented a system utilizing heat pipes to recover and transport heat from the exhaust air to the fresh incoming air with a heat recovery efficiency of up to 70%.

However, there are problems related to all of the techniques. One main disadvantage is the restrictions imposed on the architecture. Tall chimneys and extensive ducts decrease the flexibility of the system. The size of the heat exchangers is rather large making it difficult to fit in modern buildings. This might introduce problems for the architects. If these heat exchangers are made more compact the pressure drop will increase, making them less suitable for natural or hybrid ventilation.

This paper presents a low pressure drop heat exchanger, suitable for hybrid ventilation systems. The ventilation system is intended to be used in cold climates where heat recovery from the outgoing ventilation air is needed in order to optimize energy consumption and thermal comfort. Heat recovery might not be essential in hot climates or in buildings with large internal gains from electrical appliances. The main focus has been to develop a heat exchanger with a low flow resistance at the same time as the heat recovery efficiency was kept high. Theoretical calculations were performed for different geometries in order to meet these demands. A compact heat exchanger also has the possibility to be used when old houses with natural ventilation systems are renovated in order to lower the energy consumption. These houses normally lack heat recovery making them highly energy consuming or alternatively poorly ventilated. Apart from the economical reasons also the level of discomfort due to cold draught can be reduced if the recovered energy heats the incoming air.

The heat recovery rate from the ventilation air is heavily dependent on the air tightness of the building, regardless of what system is being used. If the building is not airtight the air will enter and leave the building through slats in the envelope. This uncontrolled ventilation decreases the possibilities to recover the heat and thus the total power need will increase. This is for instance discussed in [7]. Uncontrolled ventilation and leakage is also a problem for older houses. The ventilation system discussed in this article offers an alternative to the commonly used mechanical ventilation systems. However, the building skin in old buildings might still need to be renovated in order to achieve high heat recovery with the installed ventilation system. The main benefit with the proposed ventilation system is that no additional ventilation ducts are needed, as is the case when mechanical ventilation with heat recovery is installed. The existing ducts in the building can instead be used for the proposed hybrid ventilation system.

The local climate is also of major importance for the heat recovery system. If the heat exchanger has a high heat recovery rate at the same time as the ambient temperature is very low there is a risk of frost forming on the heat exchanger surface as the water condenses and freezes. This frost can limit or even block the ventilation in the building. This problem can be solved in many different ways. Typical solutions can be to defrost the heat exchanger using an electrical heater or to by-pass the incoming cold air from the heat exchanger and in this way use the heat from the outgoing air to defrost the exchanger. Another solution is to pre heat the air before passing it through the heat exchanger. This pre heating of

the ventilation air can be carried out by letting the air pass through a ground duct before entering the building and the heat exchanger. Different systems addressing solutions to this problem are described in [8].

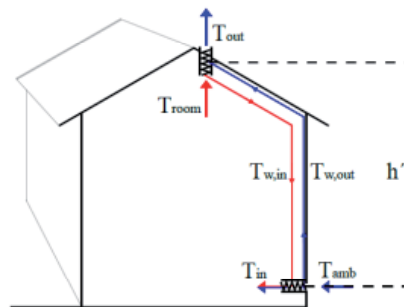
2. Method

The first step in the work was to estimate the heat transfer resistance and pressure drop in the heat exchanger as a function of design. The results from the calculations were used in order to construct a heat exchanger. This exchanger was tested in a test rig and the results from the measurements were finally used to adjust the theoretical findings.

3. Theoretical Considerations for the System

The heat recovery system is built on two fluid-coupled heat exchangers. The air flow is driven by natural forces, due to wind pressure and temperature differences. The brine is circulated by a pump. One of the liquid-to-air heat exchangers is placed as high as possible under the roof, see Figure 1. This exchanger recovers some of the energy from the outgoing air and transfers it to the brine. This energy is then pumped to the bottom of the building where the other heat exchanger is located. This liquid-to-air heat exchanger delivers the recovered heat to the incoming cold fresh air. After this heat exchange the cold liquid is pumped back to the heat exchanger under the roof and the circuit is completed.

Figure 1. The liquid based heat recovery system.



The driving forces for the ventilation system are very limited. The thermal driving pressure can be calculated by:

$$\Delta P = h' \cdot g \cdot (\rho_{amb} - \rho_{room}) \quad (1)$$

where h' is the height difference between the ventilation openings of the building; g is the gravitational constant; and ρ_{amb} and ρ_{room} are the densities of the ambient and the indoor air respectively.

From this it becomes apparent that the heat exchanger at the roof should be located as high as possible to maximize the driving forces for the system. If the height h' of the building is 10 m and the ambient and the room temperature is 0 °C resp. 20 °C the driving force will be:

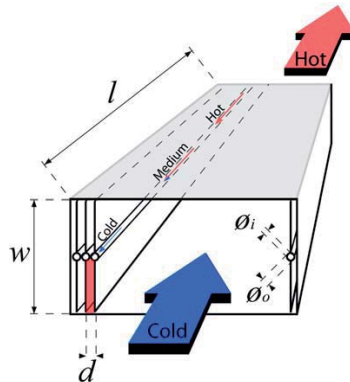
$$\Delta P = 10 \cdot 9.81 \cdot (1.293 - 1.204) \approx 8.7 \text{ Pa}$$

It is clear that the pressure losses have to be kept low in the whole system. The driving pressure created by the temperature difference has to balance not only the losses in the heat exchanger but also losses in the ducts, filters *etc.* It is thus a large advantage if the duct system can be considered superfluous. At the same time it is beneficial if the heat exchanger surface is easy to clean making it possible to install a minimal, or even better, no filter at all. Both of these measures will lower the pressure losses in the system. One way to reduce the amount of ducts in the system is to allow the fresh supply air to go directly through the wall to the rooms. However, the fluid circuit in the system transporting the recovered heat has to be divided to reach every fresh air inlet. Instead of an air supply system, this type of ventilation system instead has a fluid supply system.

If the system is intended to work during periods with lower temperature differences, the pressure drop in the heat exchangers has to be kept low. If the ambient temperature increases to 10 °C at the same time as the indoor temperature is kept constant, the driving force will be reduced to 4.4 Pa. This driving pressure has to match not only the two heat exchangers but also a complementary fan, a small amount of ducts and other ventilation details such as grills, *etc.* Fans for hybrid ventilation systems with a pressure drop less than 2 Pa during inactive periods, *i.e.*, when the blades of the fan are not spinning, can be found on the market [9]. If the duct work is considered early in the building process the pressure drop from it can be kept low. The consideration can for instance be to avoid too many bends and narrow ducts. If planned correctly the pressure drop can be limited to less than 1 Pa. This means that about 2 Pa are left for the two heat exchangers, *i.e.*, the pressure drop for one heat exchanger can be allowed to be approximately 1 Pa. However, the forces created by the wind can also be used. These forces are however much more irregular as they change with the wind which varies a lot. Thus, there can be large differences from the wind induced forces from day to day. If these forces can be used or are to be considered as a disturbing force is left out of this article. This has to be considered for each specific case where wind conditions and available pressure from thermal forces, *etc.*, are weighted together.

4. Theoretical Considerations for the Heat Exchanger

The counter flow liquid-to-air heat exchanger is shown in Figure 2. The heat exchanger is made up from a number of solar collector absorbers. The absorbers are produced by Ssolar in Sweden. The absorbers, from now on referred to as fin pipes, are placed in parallel and connected to a manifold on each side. The copper pipe used as the manifold has 2 mm wide drilled holes connecting it to the fin pipes. The fin pipe is made up of a copper pipe tightly pressed in between aluminum fins. The width, w , of the fin pipe was chosen to be 167 mm and the thickness, t , of the fin is 0.5 mm. This size is a standard component from the supplier. The pipe at the center of the fin pipe has an outer diameter, ϕ_o , of 9.5 mm while the inner diameter, ϕ_i , is 8 mm. The length, l , of the heat exchanger was treated as variable to meet the heat transfer efficiency requirements. The blue and red large arrows in the figure illustrate the air flow while the small arrows at the water pipe illustrate the water flow. This type of fin pipes is mass-produced, resulting in a low price. This is of course essential for the economical considerations for this type of system.

Figure 2. The liquid-to-air heat exchanger.

One clear advantage with this design compared to many other heat exchangers is that it can be cleaned. If the cover is removed the fins can be cleaned. In Figure 2, the top, marked with grey color, can be removed. Furthermore, the heat exchanger can easily be divided into many smaller units. These smaller heat exchangers can be located in every bedroom and living room separately. In this way the air flow rate can be set individually for the different rooms.

The heat exchangers are designed to have a thermal efficiency $\eta = 50\%$ on a system level. The efficiency is defined as the temperature change for the incoming air divided by the difference in temperature between the ambient and the indoor. During the calculation we assume an ambient temperature of $0\text{ }^{\circ}\text{C}$. The efficiency is calculated as:

$$\eta = \frac{T_{in} - T_{amb}}{T_{room} - T_{amb}} \quad (2)$$

A normal ventilation rate for a residential house of approximately 150 m^2 is $180\text{ m}^3/\text{h}$. This corresponds to 50 L/s and results in an air change rate of about 0.5 air changes per hour. If the heat recovery efficiency is 50% and the ambient and the indoor temperatures are $0\text{ }^{\circ}\text{C}$ and $20\text{ }^{\circ}\text{C}$ respectively, the heat exchanger needs to deliver:

$$Q = F_a \rho_a C_{p_a} \Delta T_a = 0.050 \cdot 1.251 \cdot 1007 \cdot 10 = 630\text{ W} \quad (3)$$

where F_a is the air flow rate; ρ_a is the density of the air; C_{p_a} is the specific heat of the air; and ΔT_a is the temperature change for the air that passes through the heat exchanger. If the heat exchanger has an efficiency of 50% and the ambient temperature is $0\text{ }^{\circ}\text{C}$ the inlet air temperature will be $10\text{ }^{\circ}\text{C}$. Assuming that the brine flow rate is adopted to give the same size of temperature change as the ventilation air, i.e., $10\text{ }^{\circ}\text{C}$, the brine temperature will drop from $15\text{ }^{\circ}\text{C}$ to $5\text{ }^{\circ}\text{C}$ as it is cooled in the heat exchanger. In the roof exchanger, the air will be cooled from $20\text{ }^{\circ}\text{C}$ to $10\text{ }^{\circ}\text{C}$ at the same time as the brine temperature is increased from $5\text{ }^{\circ}\text{C}$ to $15\text{ }^{\circ}\text{C}$. This results in a constant temperature difference of $5\text{ }^{\circ}\text{C}$ between the brine and the air. A general formula for calculating this temperature difference, ΔT_{w-a} , can be expressed as:

$$\Delta T_{w-a} = \frac{(1 - \eta)(T_{room} - T_{amb})}{2} \quad (4)$$

In order for a system to be efficient, *i.e.*, for two heat exchangers in series, 50% of the ventilation heat recovery, the efficiency on the component level, *i.e.*, for a single heat exchanger, has to be higher. In the example above, the efficiencies for the individual heat exchangers are:

$$\eta_{comp} = \frac{T_{in} - T_{amb}}{T_{in} + \Delta T_{w-a} - T_{amb}} = \frac{10}{15} \approx 67\% \quad (5)$$

If $\Delta T_{w-a} = 5^\circ\text{C}$, the two heat exchangers needs to have a UA-value of 128 W/K.

Heat transfer calculation, air side: Assumptions made for the theoretical calculations are:

- Steady-state conditions;
- One-dimensional conduction;
- Negligible radiation heat transfer;
- Constant properties;
- Fully developed flow and temperature profile through each cell.

As can be seen in Figure 2, the fin pipes and the walls create small cells in which the air can move. One such cell is illustrated in red transparent color. The number of such parallel cells was kept as a variable during the calculations. The width of the cell, $w/2$, is 83 mm. The distance d between the fin pipes was used as a variable to be able to find a suitable pressure drop and a high heat transfer rate. The performed calculations will be presented using 80 fin pipes connected in parallel and the spacing will be assumed to be 11 mm between the fin pipes. If the total air flow is 50 L/s, the velocity of the air can be calculated to be approximately 0.34 m/s. The hydraulic diameter for the rectangular tube, *i.e.*, the cell indicated with red in Figure 2, is calculated as:

$$D_h = \frac{4A_c}{P} \quad (6)$$

where A_c is the flow cross-sectional area; and P is the perimeter of the cell [10]. The height of the cell is set to 83 mm, half of the fin pipe. This was done since the fin pipes are so densely packed that they divide the cells shown in Figure 2. If the pipes were smaller the width of the cells would instead be 167 mm. This is discussed further in the section labeled “complication”.

The Reynolds number for flow in a circular tube, or noncircular tubes using the hydraulic diameter, is defined in Equation (7). If the density ρ_a of the air is taken at 5°C it is 1.251 kg/m^3 , $u_m \approx 0.34 \text{ m/s}$ is the fluid mean velocity, $D = D_h = 0.019 \text{ m}$ is the diameter of the tube and $\mu = 17.4 \times 10^{-6} \text{ N}\cdot\text{s/m}^2$ is the viscosity:

$$Re_D \equiv \frac{\rho_a u_m D}{\mu} \quad (7)$$

The numbers given above result in a Re_D -number of 478. This number is far less than the approximately 2300 that is normally considered as the onset of turbulence. The air flow can thus be considered to be laminar.

The heat transfer coefficient h_a is calculated from Equation (8):

$$h_a = \frac{Nu_D \cdot k_a}{D_h} \quad (8)$$

In Equation (8) k_a is the thermal conductivity for air; and Nu_D is the Nusselt number. Nu_D for noncircular tubes can be found in reference [10]. The ratio of the sides in the cell, *i.e.*, 83 mm and 11 mm, is approximately 8. The Nusselt number was thus set to 6.49. This is valid for fully developed thermal conditions. The real heat transfer coefficient is higher if thermal entrance effects are present.

Churchill and Ozoe [11] developed an expression for Nu_D that covers both the entrance and the fully developed thermal region. This work was reproduced in [12]. Nu_D for a circular tube can be calculated as:

$$Nu_D = 4.364 \left(1 + \left(\frac{Gz}{29.6} \right)^2 \right)^{1/6} \cdot \left[1 + \left[\frac{Gz/19.04}{\left[1 + (Pr/0.0207)^{2/3} \right]^{1/2} \cdot \left[1 + (Gz/29.6)^2 \right]^{1/3}} \right]^{3/2} \right]^{1/3} \quad (9)$$

where Gz is the Graetz number calculated as:

$$Gz = \frac{\pi}{4} \left(\frac{x}{D \cdot Re \cdot Pr} \right)^{-1} \quad (10)$$

where Pr is the Prandtl number. This means that the average Nu_D number for a one meter long tube with parameters corresponding to the air side of the heat exchanger investigated in this article will increase with approximately 15%. All of the investigated geometries for the heat exchanger, *i.e.*, different d , were adjusted with 15%.

In [10] the fin efficiency is defined as:

$$\eta_f = \frac{\tanh(mL_c)}{(mL_c)} \quad (11)$$

where L_c is the corrected fin length defined as:

$$L_c = w/2 + t/2 \quad (12)$$

and m is defined to be:

$$m = \sqrt{\frac{h_a P}{k A_c}} \quad (13)$$

where P is the fin perimeter. The thermal resistance for one unit length of the fin pipe, R_a , associated with this heat transfer can be calculated by:

$$R_a = \frac{1}{2 \cdot w \cdot h_a \cdot \eta_f} \quad (14)$$

Heat transfer calculation, copper pipe: the thermal resistance for one unit length in the copper pipe can be calculated using:

$$R_{pipe} = \frac{\ln(\phi_o/\phi_i)}{2\pi \cdot k_{Cu}} \quad (15)$$

where k_{Cu} is the thermal conductivity for copper.

Heat transfer calculation, water side: in order to maximize the heat recovery in the system the temperature increase of the air has to be equal to the temperature drop of the water. If the air flow rate and the temperatures are known the water flow rate in each fin pipe can be calculated as:

$$F_w = \frac{\rho_a C_{p_a} F_a}{\rho_w C_{p_w} \tilde{n}} \quad (16)$$

where \tilde{n} is the number of fin pipes the flow has been split into. This results in a velocity of the water of:

$$u_m = \frac{F_w}{\frac{\pi \cdot \phi_i^2}{4}} \quad (17)$$

This low velocity results in a Reynolds number of:

$$Re_D \equiv \frac{\rho u_m D}{\mu} = \frac{1000 \cdot 0.0037 \cdot 0.008}{0.001298} = 23.1$$

This is far smaller than the limit of 2300 for turbulent flow and thus the Nusselt number for the water fluid will be 4.36 [10] assuming laminar, fully developed thermal conditions and uniform surface heat flux. Including the effects from the thermal entrance region, see Equation (9), increases the h_w value by approximately 2%. The heat transfer coefficient h can be calculated with:

$$h_w = \frac{Nu \cdot k_w}{D} \quad (18)$$

where k_w is the thermal conductivity of water. The thermal resistance for one unit length of the pipe is calculated using:

$$R_w = \frac{1}{\pi D \cdot h_w} \quad (19)$$

Heat transfer calculation: The total heat transfer resistance for one unit length, R_{tot} , can finally be calculated by:

$$R_{tot} = R_a + R_{pipe} + R_w \quad (20)$$

The total heat transfer rate for one unit length, with a temperature difference of ΔT is thus:

$$q = \frac{\Delta T}{R_{tot}} \quad (21)$$

This means that the heat exchanger needs a total fin length of:

$$L = \frac{Q}{q} \quad (22)$$

The numbers presented in Appendix shows that the total needed length of heat transfer fins is approximately 70 m. If the load is shared between 80 parallel fins, see Figure 2 for explanation, it means that each heat exchanger fin needs to have a total length of about 1 m. A 1 m long heat exchanger with the above-described geometry would thus be expected to have an efficiency on a system level of 54%. As discussed around Equation 5, the efficiency on the component level differs from the system level. A 54% system efficiency corresponds to 70% efficiency on the component level.

5. Pressure Drop

One of the key parameters for a heat exchanger in a hybrid ventilation system will be the pressure drop. If it is too large the air will be hindered and the ventilation rate cannot be supplied. The size of the cells in the heat exchanger will strongly affect the pressure drop. Also, the number of cells, and thus the air speed will have a major effect on the pressure drop.

The pressure drop in the cell is determined by the Darcy friction factor f . The friction factor varies for different ratios of w/d , see Figure 2 for explanation. Equation (23) shows the equation from Cornish, Lea and Tadros, reproduced in Knudsen and Katz [13] for calculation of the friction factor for rectangular conduits. The equation has been adjusted by a factor 4 because the Darcy friction factor is 4 times larger than the friction factor defined in [12].

$$f(d/D_H)^2 \left[1 - \frac{192}{\pi^5 (w/d)} \left(\tanh \frac{\pi w}{2d} - \frac{1}{3^5} \tanh \frac{3\pi w}{2d} + \dots \right) \right] = \frac{6.0}{Re} \cdot 4 \quad (23)$$

For the cell shown in Figure 2 the friction factor is calculated to be 0.171. The pressure drop related to this friction factor can be found using:

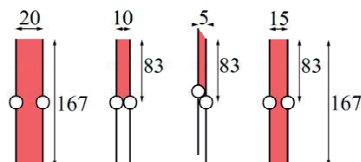
$$\Delta p = f \frac{\rho_a u_m^2}{2D_h} l \quad (24)$$

where l is the length of the cell. The pressure drop for the investigated structure can be found in Appendix A to be 0.56 Pa per component, *i.e.*, 1.12 Pa for a system. Using the tabulated value in [10] for the friction factor results in almost the exact same number. The calculations do not include pressure drop in connections attached to the heat exchanger. Nor is the system with pipes, *etc.*, included.

6. Complications

According to [10] the Nu number differs for different ratio between the width w and the spacing d . The same is true for the friction factor f . Figure 3 shows four different possible geometries for the heat exchanger. In the left figure the ratio is approximately 8. The air flow cell is indicated in red. The same is true for the figure in the middle. This is due to the tightly packed water pipes dividing the air flow cell in two halves. The third figure has approximately the double ratio. This means that the Nu number for the left and the middle heat exchanger is 6.49 while it is higher for the right heat exchanger. Infinitely long fins would result in a Nu number of 8.23. If the distance between the fins is chosen to be somewhere between 10 and 20 mm the cross section of the cell in which the air moves will be two cells partly connected. This is illustrated in the fourth figure. This might affect the Nu number. However, in the calculations performed in this article, a constant Nu number of 6.49 was used. This will underestimate the heat transfer rate slightly for the heat exchangers with a narrow spacing. The difference for the heat transfer rate is less than 10% for any considered geometry compared to heat transfer rates calculated infinitely using the ratio between w and d . In the same way, the friction factor was calculated to be 82 divided by the Re number for the specific heat exchanger.

Figure 3. Experimental setup.



7. Experimental Setup

The performed experiment on the heat exchanger was performed on a 1 m long unit with 16 parallel connected fin pipes, see Figures 2 and 4. This is 1/5 of the size for the supply air heat exchanger for a whole building. The same size of heat exchanger is needed on the roof. The tested heat exchanger can thus be viewed as a heat exchanger used in, for instance, a bedroom. The total fin pipe length is 16 m and the total fin area is approximately 5.3 m². The 16 fin pipes were connected to manifolds. This is shown in Figure 4. The cross section of the heat exchanger is approximately 0.17 m·0.17 m and the length is 1 meter. The soldering of the fin pipes to the manifolds could not be performed in a straight line, due to lack of space between the pipes. Consequently, the fin pipes had to be placed in a zigzag pattern leaving small gaps between the fins and the wooden sides of the heat exchanger. Any effects on heat exchange and pressure drop from this was neglected.

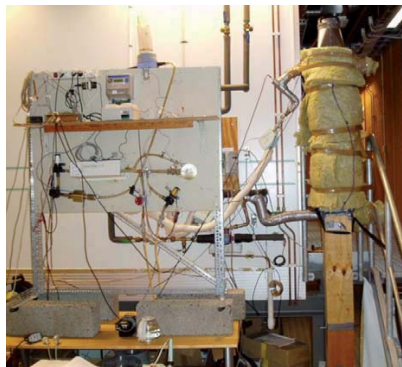
Figure 4. The fin pipes soldered to the manifold in the heat exchanger.



The wooden box surrounding the heat exchanger was insulated with 50 mm polystyrene and 90 mm glass wool. The test rig can be seen in Figure 5. The controllable fan was installed on top of the heat exchanger to create an under-pressure. Sucking the air through the heat exchanger created a much steadier and a more well-defined air flow compared to blowing air into the exchanger from below. The air was allowed to travel through a duct of the same size as the surrounding wooden structure of heat exchanger in order to stabilize the airflow. This can be seen below the insulated heat exchanger in Figure 5. Air at approximately 22 °C, *i.e.*, room temperature, was used as inlet air instead of using cold ambient air. This simplified the performed tests significantly. Furthermore, the inlet brine temperature

was varied between approximately 30 °C to 60 °C. Figure 5 shows the heat exchanger and the heat rack used to keep the inlet brine temperature constant. The rack is equipped with a heater connected in series with a cooler. When operated simultaneously the brine temperature can be kept stable.

Figure 5. The heating rack is shown to the left and the insulated heat exchanger is shown to the right.



The air temperature measurements were carried out with a thermocouple for the incoming air. In order to have a high resolution on the temperature difference for the incoming and outgoing air in the heat exchanger, a thermopile was used. The water temperatures were measured using PT100 sensors. The water flow was measured using a MP115 hall sensor from Kamstrup and the air flow was measured using an air flow hood, SWEMA Flow 125. A Campbell CR10 data logger from Campbell Scientific in Logan, UI, USA, was used to collect the measured data. A hot wire anemometer, Swema 31, was used to check the air flow profile in the duct. This assured an even distribution of air in the heat exchanger. The pressure drop measurements were carried out with a Digima Premo. The pressure drop was measured during operation with no heat exchange between the water flow and the air flow. As can be seen in the table the largest uncertainty is in the flow measurement for the air. The hot wire anemometer, Swema 31, was also used to measure the air flow. The measurement from the Swema 31 confirmed the measurements from the Swema air 125. Since the heat exchanger was thoroughly insulated the energy loss to the sides was limited. Less than 2% of the heat transferred from the water to the air disappears through the sides. This means that what is lost by the water should be gained by the air. This was also the case for all the measurements. This is a good check for the measurements.

Technical data for the measurement devices are shown in Table 1.

Table 1. The sensors used in the experiment.

Product	Range	Accuracy	Comment	Manufacturer
Swema air 125	2 to 125 L/s	10%, not less than 1 L/s	Back pressure measurement. Compensate for the pressure drop from the equipment itself. Manufacturers data.	Swema, Farsta, Sweden
Kamstrup, MP115	0.015 to 3 m ³ /h	Not available from manufacturer	Calibrated outside the standard range. Error < 4% for all ranges.	Kamstrup, Skanderborg, Denmark
PT-100	<200 °C	0.3 °C	0.3 °C accuracy in the used temperature range. Manufacturers data.	Pentronic AB, Gunnebo, Sweden
Thermo pile	<350 °C	2%	Manufacturers data.	Built in Lund University, Energy and Building Design, laboratory
Swema 31	0.1–30 m/s	0.04 m/s	Used to check flow profile. Manufacturers data.	Swema, Farsta, Sweden
Digima Premo	0.1–1999 Pa	0.1 Pa or 0.25%	Manufacturers data.	SI—special instruments GmbH, Nördlingen, Germany

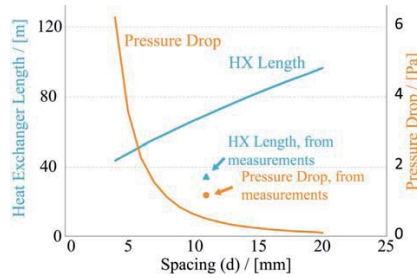
8. Results

All the results from the measurements in this section are from a heat exchanger made up of 16 parallel fin pipes. However, the results were recalculated to numbers for a full heat exchanger with 80 parallel fin pipes. Results for the full size heat exchanger were selected for presentation since this gives the true numbers for a heat exchanger in a normal one-family house.

Results from the theoretical calculations are shown in Figure 6. On the x-axis is the spacing between the fin pipes in mm, see Figure 2 for explanation. The left y-axis shows the total of the 80 parallel connected fin pipes needed in order to have a heat recovery of 50% on a system level, *i.e.*, 66% on component level for the individual heat exchangers. The right y-axis shows the pressure drop for the different spacings. As can be seen in the figure the pressure drop increases exponentially as the cells gets smaller. A separation of less than 4 mm would result in a pressure drop higher than the 8.7 Pa discussed in the section labeled “theoretical considerations for the system”. Conclusions made from the graph led to the production of a heat exchanger with 11 mm spacing between the fin pipes. At this point the pressure drop is still low while the length is reasonably short. If the pressure drop were to be reduced further, the total length of the heat exchanger would be much larger. This would increase the production costs for a future product. Alternatively the heat exchanger has to be made up from a greater number of fin pipes. However, this makes the heat exchanger larger and thus more difficult to use. A decrease in the length of the heat exchanger would results in a higher pressure drop. This would make the pressure drop too high and the system would not work as intended. This is discussed further in the Discussion section.

Also shown in Figure 6 are the resulting length and pressure drop for a system efficiency of 50% recalculated from the measurements.

Figure 6. Heat exchanger length and pressure drop in order to have 50% system heat recovery efficiency as function of the spacing between the fins. The points show the resulting length and pressure drop for a system of 50% recalculated from the measurements.

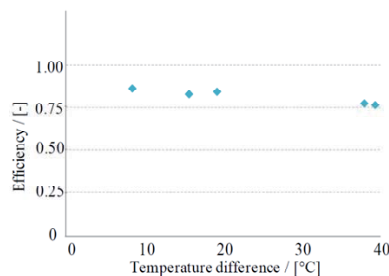


The measurements on the heat transfer rate were performed with different inlet water temperatures. The results from the measurements can be seen in Table 2. See Figure 1 for explanation. The efficiency η_{comp} is the average efficiency for the water side and the air side. All of the results presented in Table 2, except η_{comp} , are measured data. In Figure 7 the component efficiency is plotted as a function of the temperature difference between the incoming water and the incoming air. The results show a tendency for higher efficiencies for lower inlet water temperature. The efficiency is calculated as an average of efficiencies for the water side and the air side.

Table 2. The performed measurements for the heat transfer rate.

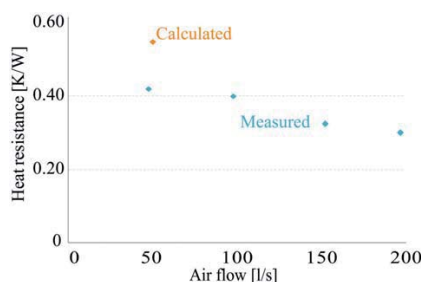
Measure No.	$T_{w,in}$ (°C)	$T_{w,out}$ (°C)	ΔT_w (°C)	F_w (mL/s)	T_{amb} (°C)	T_{in} (°C)	ΔT_a (°C)	F_a (L/s)	η_{comp} (-)
1	31.51	24.56	6.96	2.6	23.32	30.40	7.08	9.1	0.86
2	38.92	25.74	13.17	2.7	23.29	35.86	12.57	9.5	0.82
3	42.50	26.71	15.79	2.6	23.29	39.67	16.38	9.0	0.84
4	61.00	31.00	30.00	2.7	23.15	51.48	28.33	9.8	0.77
5	61.72	32.13	29.59	2.7	22.16	52.79	30.63	9.5	0.76

Figure 7. The measured component efficiency as a function of the difference in temperature between the incoming water and the incoming air.



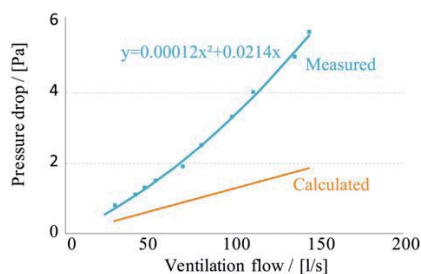
Measurements were also performed for the heat transfer rate for the heat exchanger for different ventilation rates. Figure 8 shows the results. On the x-axis is the air flow rate in L/s and on the y-axis is the heat resistance for the heat exchanger calculated per meter fin pipe per degree difference in Kelvin. In orange is the calculated heat resistance and in blue are the measured values for the different measured ventilation rates. There is a clear trend for reduced heat resistance as the air speed is increased. This indicates a presence of vortices in the airflow, which increase with an increase flow speed.

Figure 8. Heat resistance as a function of the air flow rate. In blue are the measured values and in orange is the calculated value.



The most critical parameter for the heat exchanger is the pressure drop on the air side. If this is too high the ventilation rates will be low. Results from the pressure drop measurements can be seen in Figure 9. In orange is the calculated pressure drop for different air speeds. The calculations were performed assuming no turbulence in the air flow. The figure also shows the measured pressure drop over the heat exchanger. This is shown in blue. The measurements indicate a turbulent component in the air movement. This is apparent even at low air speeds. The pressure drop for normal operation air speed used in a standard one-family house is approximately 1.3–1.4 Pa per heat exchanger, *i.e.*, 2.6–2.8 for both heat exchangers.

Figure 9. Calculated pressure drop for a heat exchanger in red and measured pressure drop in blue.



The discrepancy between the theoretical results, *i.e.*, designing the heat exchanger to have 50% system efficiency, *i.e.*, 66% component efficiency, and the experimental results discussed in this

section could partly be explained by the fin pipes not being perfectly straight. A photo of the heat exchanger is shown in Figure 10. These non-straight fin pipes give rise to a disturbed path for the air through the cells. This wavy movement will increase the heat transfer rate as the air in the cell will be forced to collide with the fin pipes. Simultaneously, it will add resistance for the air; hence the pressure drop will increase. This is also seen in the measurements presented in Figure 6 where it is shown that the heat transfer rate is increased, and thus the needed length of fin pipes is reduced. At the same time the pressure drop is increased. The heat transfer rate and the pressure drop both increases approximately in a similar manner. In Figure 9 it was shown that the air flow has a turbulent component already at low air speeds. This indicates the same conclusion. One other factor that has the potential to increase the heat transfer rate and pressure drop is the turbulence created by the manifold and the blunt ends on the fins. The effective area is also slightly larger than the theoretical area. The performed calculation does not include the area for the copper pipe, nor does it take heat transfer from the wooden box or the manifold into account.

Figure 10. The heat exchanger. The fin pipes are not straight, resulting in a wavy path for the air through the exchanger.



Equations (20) and (24) can be scaled linearly to fit the results from the measurements.

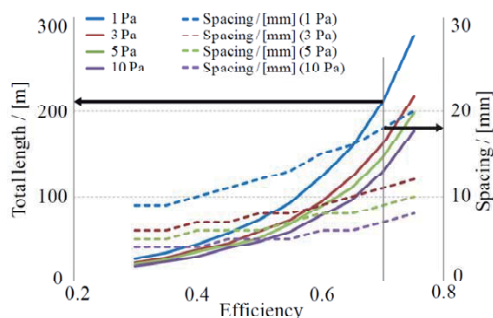
$$\Delta p = f \frac{\rho_a u_m^2}{2D_h} l \quad (25)$$

$$\Delta p = f \frac{\rho_a u_m^2}{2D_h} X \cdot C_2 = 0.172 \frac{1.251 \cdot 0.34^2}{2 \cdot 0.019} 1 \cdot C_2 = 0.647 \cdot C_2 = [C_2 = 2.14] = 1.38 \text{ Pa} \quad (26)$$

Figure 11 shows the system performance, *i.e.*, for both the heat exchangers at ground level and the roof heat exchanger. This means that the presented numbers are for the sum of both of the heat exchangers. The efficiency is calculated including the scaling factors C_1 and C_2 . The full lines illustrate the total length of fin pipes needed as a function of system efficiency for the ventilation. The blue line is the length needed for a specific efficiency with a maximum pressure drop for the system of 1 Pa, *i.e.*,

the pressure drop for both of the heat exchanger at the air intake and the air outlet. The red line shows the same but for 3 Pa, the green line is for 5 Pa and the purple line is for 10 Pa. The dashed lines show the distance between the fin pipes, *i.e.*, the distance d in Figure 2, to build that specific heat exchangers. The arrows in the Figure show an example. To have a 70% system efficiency with a pressure drop of 1 Pa the heat exchanger needs to have a spacing, $d = 18$ mm, and a total length of fin pipes of approximately 210 m. The blue dashed line is for the 1 Pa pressure drop heat exchanger, the red, green and purple are for the 3, 5, and 10 Pa pressure drop heat exchangers, respectively.

Figure 11. Total length of the heat exchanger on the left y-axis and spacing between the fins on the right y-axis as a function of system efficiency for the ventilation for four different total pressure drops, 1, 3, 5 and 10 Pa.



9. Discussion

A reason for the increased pressure drop over the whole range is that the fin pipes fins were not perfectly parallel. This can be seen in Figure 10. The metal fins were all somewhat wavy, giving rise to more narrow passages for the air as it travels through the heat exchanger. This will increase the pressure drop. However, this also has the potential to increase the heat transfer rate. This was also indicated in Figure 6 and in Figure 8 where it was shown that the measured heat transfer rate was higher than the calculated. This led to a shorter, more compact, heat exchanger than expected. The increased heat transfer and pressure drop can also be partly explained by turbulence occurring due to the manifold. This irregularity disturbs the air flow. At the same time it also contributes to the heat transfer. This heat transfer was not included in the theoretical calculations.

Figure 11 shows that the savings in fin pipe length is not very significant even if the pressure drop is allowed to increase. For instance, allowing the pressure drop in the system to increase from 3 to 5 Pa for a system efficiency of 70% only reduces the total fin pipe length from 153 m to 138 m, *i.e.*, about 10%. If the pressure drop needs to be smaller it is better to use the possibility with using more fin pipes. If the heat exchanger is produced with 160 parallel connected fin pipes instead of the 80 discussed in this article the speed of the air and thus the pressure drop would be reduced by 50%. The effects on the heat transfer rate for this new design have to be evaluated experimentally. In Figure 8 it was showed that the heat transfer rate is dependent on the speed of the air. If the heat transfer rate is

affected only slightly the total meter of fin pipes should be the same. Using more fin pipes is however not without problems. As the heat exchanger becomes wider it also becomes more difficult to install it. At the same time there is a greater risk of having uneven flow if the heat exchanger gets too big.

It was mentioned in the result section that if the pressure drop was increased when reducing the length of the heat exchanger the system would not work as intended. Still, this could very well be a good solution. What is needed is then a small fan. This small fan can provide the extra pressure needed to run the system if a smaller spacing of the fin pipes is chosen. It could be a good investment to spend a few Watts on a fan if the heat recovery is increased. This is a difficult question and more simulations on a building level are needed to answer it.

In the introduction section it was stated that the mechanical ventilation system recovers 40% of the primary energy. This does not imply that mechanical ventilation systems should not be used. This is an illustration of a problem. The difficulties of drawing conclusions from this are also indicated in [14] where a number of different investigations are summarized. The energy savings when installing mechanical ventilation with heat recovery differ strongly. Even negative energy savings was found. What transformation factor to use for the electricity is a long discussion with many different answers. However, the energy consumption from the pumps also has to be included in the calculation. According to a manufacturer the annual energy consumption for pumping the brine for a one family house is estimated to 27 kWh. The recommended pump can be found at the Wilo webpage, [15]. This number is much lower than the energy consumption for running the fans in the mechanical ventilation system. Furthermore, the introduction section briefly discussed pre heating of the incoming ventilation air by passing it in the ground before entering the building. The discussed ventilation system can utilize the same kind of pre heating. This can be carried out by passing the brine after being cooled in the heat exchanger at the air intake in the ground outside the building. This has a potential to decrease problems related to frost in the heat exchangers at the same time as energy is gained from the ground.

10. Conclusions

The results found from the measurements show that there is a possibility to develop a ventilation system driven by natural forces including heat recovery. Historically the high-pressure drop in the heat exchangers has limited this kind of system. A low pressure drop over the heat exchanger of around 1 Pa with a heat recovery rate of approximately 70% makes it possible to build passive houses using this ventilation technique. The system could also possibly be used in retrofitting old houses that lack heat recovery for the ventilation system. The alternative to this is otherwise extensive duct work for mechanical ventilation with heat recovery. A clear advantage with the system discussed in this paper is that the effects on the building are small. For instance, the same exhaust ducts can be used and the ducts to the incoming air are kept minimal as the incoming air can go straight through the outer wall. The short duct system is beneficial since ducts often tend to be contaminated with dust and dirt [16]. This type of ventilation system is also suitable for buildings where cross contamination is extra sensitive. This can for instance be hospitals and research facilities. Cross contaminations can otherwise occur when the supply air and the exhaust air are located next to each other and meet in the exchanger.

There are, however, still problems that need to be addressed in future work. This includes investigating pressure loss in supply air valves, and the complementary fan. Controlling the air flow is

also a challenge, not only keeping the air flow rates high enough to meet the requirements but also not over-ventilating the building during windy conditions. Using automatic dampers to reduce the effect from the wind or using manually operated supply air grills are two ways of controlling the ventilation rate. However, dampers will also introduce additional pressure drop for the outgoing ventilation air. This has to be accounted for in the system design. The operation of the system is also of great importance. During periods with overheating in the building the pump for the water circuit can be turned off or alternatively reduced in speed. This will turn off or lower the amount of recovered heat from the outgoing ventilation air. In this way, overheating of the building can be reduced. During the summer when the thermally induced driving forces for the ventilation are low, cross ventilation by open windows can complement the ventilation system. If this is not possible, the fan in the hybrid ventilation system has to be used.

The investigated ventilation system has the potential to have high heat recovery efficiency, low electrical energy need and also to be a quiet system with a minimal number of ducts.

Acknowledgments

Birgitta Nordquist at the Department of Building and Environmental Technology at Lund University along with Niko Gentile and Håkan Håkansson at Energy and Building Design at Lund University are acknowledged for assistance with measurements. Bengt Sundén at the department of Energy Sciences, division of Heat Transfer at Lund University is acknowledged for theoretical discussions.

Appendix

An example of calculation is shown below. The example shows the resulting values of calculations for the investigated heat exchanger:

$d = 0.011$; $w = 0.167$; $\tilde{n} = 80$; $D_h = 0.019$; $Re = 478$; $Nu = 7.45$; $h = 9.4$; $m = 12.6$; $n = 0.74$; $R_{air} = 0.43$; $R_{water} = 0.12$; $R_{pipe} = 0$; $R_{tot} = 0.55$; $L = 69.4$; $f = 0.171$; $\Delta p = 0.56$.

References

1. FTX-Aggregat Hus Med 130 m² Boyta—Jämförelse (in Swedish). Available online: <http://www.energimyndigheten.se/Templates/Public/Pages/ProductGroupPageCompare.aspx?productGroupId=69&productCompareList=412,413,414,415,416,417,418,419&PageID=5552> (accessed on 23 August 2012).
2. Feist, W.; Schieders, J.; Dorer, V.; Haas, A. Re-inventing air heating: Convenient and comfortable within the frame of passive house concept. *Energy Build.* **2005**, *37*, 1186–1203.
3. Principles of Hybrid Ventilation, IEA Energy Conservation in Buildings and Community Systems Programme. Available online: <http://www.hybvent.civil.aau.dk/> (accessed on 27 April 2012).
4. Schultz, J.M.; Saxhof, B. Natural ventilation with heat recovery. *Air Infiltration Rev.* **1994**, *15*, 9–12.
5. Hviid, C.H.; Svendsen, S. Analytical and experimental analysis of a low-pressure heat exchanger suitable for passive ventilation. *Energy Build.* **2011**, *43*, 275–284.

6. Shaw, L.; Riffat, S.B.; Gan, G. Heat recovery with low pressure loss for natural ventilation. *Energy Build.* **1998**, *28*, 179–184.
7. Wall, M. Energy-efficient terrace houses in Sweden simulations and measurements. *Energy Build.* **2006**, *38*, 627–634.
8. Florides, G.; Kalogirou, S. Ground heat exchangers—A review of systems, models and applications. *Renew. Energy* **2007**, *32*, 2461–2478.
9. VBP Hybrid Assistance Fan. Available online: <http://www.aereco.com/product/vbp> (accessed on 23 August 2012).
10. Incropera, F.P.; DeWitt, D.P. *Fundamentals of Heat and Mass Transfer*; John Wiley and Sons Inc.: Hoboken, NJ, USA, 2002.
11. Churchill, S.W.; Ozoe, H. Correlations for forced convection with uniform heating in flow over a plate and in developing and fully developed flow in a tube. *J. Heat Transfer.* **1973**, *95*, 78–84.
12. Bejan, A. *Heat Transfer*; John Wiley and Sons Inc.: Hoboken, NJ, USA, 1993.
13. Knudsen, J.G.; Katz, D.L. *Fluid Dynamics and Heat Transfer*; McGraw-Hill: New York, NY, USA, 1958.
14. Dodoo, A.; Gustavsson, L.; Sathre, R. Primary energy implications of ventilation heat recovery in residential buildings. *Energy Build.* **2011**, *43*, 1566–1572.
15. Wilo-Star-Z NOVA. Available online: http://productfinder.wilo.com/en/SE/productrange/00000016000393a900020023/fc_range_description (accessed on 30 November 2012).
16. Balvers, J.; Bogers, R.; Jongeneel, R.; van Kamp, I.; Boerstra, A.; van Dijken, F. Mechanical ventilation in recently build Dutch homes: Technical shortcomings, possibilities for improvement, perceived indoor environment and health effects. *Archit. Sci. Rev.* **2012**, *55*, 4–14.

© 2013 by the authors; licensee MDPI, Basel, Switzerland. This article is an open access article distributed under the terms and conditions of the Creative Commons Attribution license (<http://creativecommons.org/licenses/by/3.0/>).

Paper IV

Buildings **2013**, *3*, 245–257; doi:10.3390/buildings3010245

OPEN ACCESS

buildings

ISSN 2075-5309

www.mdpi.com/journal/buildings/

Article

Hybrid Ventilation with Innovative Heat Recovery—A System Analysis

Henrik Davidsson *, Ricardo Bernardo and Bengt Hellström

Department of Architecture and Built Environment, Division of Energy and Building Design, Lund University, Box 118, Lund 22100, Sweden; E-Mails: ricardo.bernardo@ebd.lth.se (R.B.); bengt.hellstrom@ebd.lth.se (B.H.)

* Author to whom correspondence should be addressed; E-Mail: henrik.davidsson@ebd.lth.se; Tel.: +46-222-4851, Fax: +46-222-4719.

Received: 11 January 2013 / Accepted: 17 February 2013 / Published: 22 February 2013

Abstract: One of the most important factors when low energy houses are built is to have good heat recovery on the ventilation system. However, standard ventilation units use a considerable amount of electricity. This article discusses the consequences on a system level of using hybrid ventilation with heat recovery. The simulation program TRNSYS was used in order to investigate a ventilation system with heat recovery. The system also includes a ground source storage and waste water heat recovery system. The result of the analysis shows that the annual energy gain from ground source storage is limited. However, this is partly a consequence of the fact that the well functioning hybrid ventilation system leaves little room for improvements. The analysis shows that the hybrid ventilation system has potential to be an attractive solution for low energy buildings with a very low need for electrical energy.

Keywords: hybrid ventilation with heat recovery; waste water heat recovery; system analysis

1. Introduction

Lower energy use and higher comfort in a building can be achieved if the building is allowed to interact with its surrounding in a smart way. This can for instance be to utilize solar radiation, passively through the windows or actively via a solar collector. It can be an efficient day lighting design or it can be the use of natural or hybrid ventilation. The natural ventilation technique is driven

by thermal buoyancy force and wind induced force. The hybrid ventilation technique utilizes these forces to the maximum extent and when it is insufficient, it is complemented with a fan [1]. This, at the same time, results in a high degree of utilization of the natural driving forces and a high reliability. However, these systems normally lack the possibility to recover any of the energy that disappears with the outgoing ventilation air. In cold climates this will result in a high energy need and low comfort due to draughts. One way to solve this is to use so-called mechanical ventilation with heat recovery. This enables a heat recovery efficiency of the outgoing ventilation air of about 75% [2]. At the same time, the air-handling units preheat the incoming air, which results in a reduced draught. However, these types of units use a considerable amount of electrical energy to run the fans in the system. The high energy use by the fans is connected to the high pressure drop in the air-to-air heat exchangers that transfer the energy from the outgoing to the incoming air. At the same time, the units have a risk of creating a disturbing noise from the ventilation system. Recently, there have been reports about heat exchangers designed to work in natural or hybrid ventilation systems [3,4]. The heat exchangers have a very low pressure drop, down to or even less than 1 Pa, and at the same time high heat transfer rates in the units. Heat recovery efficiencies of approximately 70%–80% have been reported. These are instantaneous values. Average values from a full year including frost problems etc. are not available. These heat exchangers may enable a new kind of ventilation systems with heat recovery. If the pressure drop can be kept low, there is a possibility to create natural or hybrid ventilation systems including heat recovery. This also means that it could be possible to build passive houses or other types of low energy buildings with a natural or a hybrid ventilation system. One way to construct a hybrid ventilation system with heat recovery is to use two heat exchangers, one located at the bottom of the building and one at the top of the roof. The energy that is recovered from the roof heat exchanger is pumped in a brine connected system to the heat exchanger at the bottom of the building where the energy is used to preheat the incoming ventilation air. This type of ventilation system, reviewed in [5], is known as run-around heat recovery system. Using such a brine connected system also makes it possible to connect other heat sources such as ground heat storage. Typically, the ground collector is made up of plastic tubes. Different ways of connecting the plastic tube of the collector are discussed in [6].

Other interesting ventilation and heating techniques have been presented. Zhai [7] and Khedari [8] both investigated natural ventilation of buildings induced by roof integrated solar collectors. The aim of this paper is to determine the energy implications of a hybrid ventilation system with heat recovery based on simulations for a low energy and a traditional one-family house.

2. Method

One possible way to build a hybrid ventilation system with heat recovery is to use two water-to-air heat exchangers connected in series. This is illustrated in Figure 1. The temperatures shown in the figure illustrate the principle of the system. Cold outdoor air is heated as it is let through the heat exchanger at the bottom of the building. The temperature of the air is increased from e.g., 0 °C to 10 °C. At the same time, the brine temperature is reduced from 15 °C to 5 °C. When the hot indoor air passes through the roof, it is cooled in the roof heat exchanger. The temperature drops from 20 °C to 10 °C. At the same time, the brine temperature is increased from 5 °C to 15 °C, the circuit is completed

and the process can be repeated. Since the temperatures involved in the processes are low, there is a possibility to use innovative heat sources to improve the system performance. One alternative is to use the ground as a heat source. After the brine has been cooled in the heat exchanger at the bottom of the building, it is run through the ground collector to increase the temperature. During cold periods, the brine can reach sub zero temperatures after passing through the heat exchanger at the bottom of the building. During these periods, the ground can supply the ventilation system with large amounts of energy. Alternatively, the system can utilize energy from the waste water from the building. In order to maximize the potential in such system, the waste water can be stored in a tank. In this way, the energy can be stored and utilized over a large time frame. The waste water heat recovery system is discussed in more detail in Table 1.

However, the interaction between, for instance, the ground collector and the ventilation system is complex. If the ground collector transfers energy from the ground to the brine, and in this way increases the temperature in the brine circuit, there will be less heat recovered from the roof heat exchanger. This will lower the fraction of recovered energy in the ventilation system. The saving potential is thus difficult to estimate without simulations. Mechanical ventilation systems can also be equipped with a ground collector, although this is not usually done. In principle, it is possible to let the air pass into the ground for preheating before it is admitted into the building. Different innovative techniques have been reported to preheat air for different uses. Pinel *et al.* [9] reviewed different types of seasonal storage techniques. These methods are, however, not simulated in this paper. The analysis in this article is based on simulations using the program TRNSYS [10] for a one-family house with a floor area of 150 m². The building is a one and a half storey building with a total volume of 390 m³. The different investigated cases are discussed and illustrated in Table 2. All systems were simulated with two different levels of insulation, this is discussed in more detail in Table 1. The input data for the simulation is also presented in Table 1. All systems are equipped with a hot water storage tank that supplies the domestic hot water. The air flows are assumed to be exactly what is required for both the hybrid ventilation and the mechanical ventilation.

Figure 1. The principle of the proposed hybrid ventilation system with heat recovery.

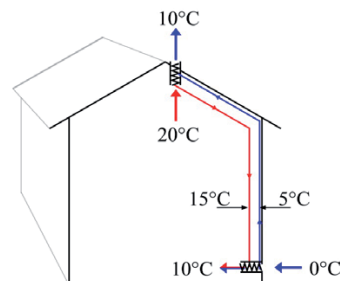


Table 1. Input data for the TRNSYS-deck.

Physical object/control	TRNSYS type	Description
Building	Type 88	The average U-value of the low energy building was 0.215 W/m ² K. This value was chosen to simulate a passive house. The standard insulated building had an average U-value of 0.5 W/m ² K. The thermal capacitance of the buildings was set to 40 MJ/K. This corresponds to approximately 100 m ² concrete floor, 100 m ² brick wall and it includes interior material and the roof.
Internal gains	Equation	Windows facing south (6.5 m ² glazing area), west (6.5 m ²), north (4 m ²) and east (4 m ²) with a g-value of 55% were installed in the building. This gives a glazing to floor area ratio of approximately 14%, which is a typical value. The transmitted solar radiation was treated as internal gains of the building. The thermal losses from the main storage tank and heat from people and electrical equipment were also added as internal gains. The gain from people and electricity was set to 500 W continuously. According to standard [11] the internal gains from people and electricity are 4 W/m ² . 500 W thus corresponds to a 125 m ² building. This is somewhat lower than the actual size of the building. This was chosen in order to include effects of using low energy household appliances.
Main storage tank	Type 4a	The hot water storage tank was set to a volume of 400 l and was assumed to have a heat loss factor of 0.83 W/m ² K, with an area of approximately 1.7 m ² . The heater was set to 60 °C.
Waste water storage tank	Type 534	The waste water heat recovery tank was set to 150 L. The tank is equipped with immersed heat exchangers for the domestic hot water and for the ventilation circuit. The waste water storage tank is assumed to be located outside the building. Hence, the thermal loss from the tank is not utilized by the building. A small test with a waste water heat exchanger was set up in a one family house. The system consists of two series connected waste water tanks with built in heat exchangers. The heat exchangers were made up from corrugated stainless steel pipes with a total length of 17 m. These measurements were used to calibrate the TRNSYS component later used in the simulations presented in this article. The measurements show e.g. that having balanced flow, <i>i.e.</i> , the same flow for the entering waste water as for the hot water at 3L/min results in a heat recovery rate of 66% from the waste water.

Table 1. Cont.

Physical object/control	TRNSYS type	Description
Temperature and flow profiles	Equation	<p>The hot water consumption profile shown in Figure 2 is a simplification of the findings of Widén <i>et al.</i> 2009 [12]. During the morning, the hot water consumption is 20 L/h between 5:00 h and 7:00 h and between 9:00 h and 11:00 h. During 20:00 h–22:00 h, the consumption is 25 L/h. This means that the household consumes 130 L of 60 °C hot water a day. This hot water is mixed with cold water in order to get lukewarm water for the household needs. The inlet water temperature to the storage tank as a function of day number can be seen in the second figure [13]. The numbers are given by the local supplier of fresh water in the southeastern part of Sweden. The third figure to the right shows the waste water. The waste water is assumed to come from showers, sinks and the kitchen, <i>i.e.</i>, the toilets are not included. The waste water flow in L/h is in blue and its temperature in dashed red. The difference between the domestic hot water profile and the waste water flow profile was chosen to include non perfect overlapping. This can for instance be when someone empties a bathtub. This causes a large waste water flow but there might not be a flow in the opposite direction, <i>i.e.</i>, incoming water, thus the difference in simultaneity. Simulations were performed for two different flow profiles, one with only the filled blue squares, labeled Profile A, and one with the filled and the striped squares, labeled B. The simulation that included the striped squares was performed in order to investigate the sensitivity of the flow profile. As can be seen, the difference is that during the periods indicated with striped squares, cold water is let into the waste water tank. This can, for instance, be if cold water is run in the morning to flush the pipes in the building. The total volume of waste water is assumed to be twice the volume of the domestic hot water use for flow Profile A. Flow Profile B is the same as profile A but with an extra volume of 100 L water at 10 °C. The temperature of the waste water is assumed to be a mixture of equal parts of 10 °C and 50 °C water, <i>i.e.</i>, 30 °C.</p>
Ground collector	Equation	<p>The ground collector was simulated using the ground temperature profile shown in Figure 2, the illustration in the middle. The temperature of the outgoing water from the ground collector is assumed to have the ground temperature. This means that the heat transfer is without resistance and that the size of the collector is large enough not to be affected by the energy removed from it. This is a simplification and the results should be viewed as an indication of the impact with ground source heat storage in this type of system.</p>
Weather data	Type 109	<p>The weather data is data from Malmö in the south of Sweden. The weather data was obtained from Meteonorm.</p>
Heat exchangers	Type 5b	<p>The brine in the ventilation circuit was assumed to be water. The heat transfer coefficient was varied resulting in efficiencies between 43% and 86%. The total efficiency of the two in series connected heat exchangers is less than the efficiency of a single unit. For instance, placing two heat exchangers with 86% efficiency as shown in Figure 1 will result in a system efficiency of approximately 75%.</p>
Ventilation system	Equation	<p>The mechanical ventilation with heat recovery was simulated using an “equation” type. It is assumed that the efficiency is always 75%. The ventilation flow rate for all cases was set to 234 kg/h, which is approximately equal to an air change rate of 0.5 changes per hour. This value was chosen in order to meet the requirements of the Swedish Building code [14]. The ventilation flow rate was increased by a factor of two during periods with an indoor temperature that exceeded 27 °C. This was done in order to avoid excessive heat storage in the construction.</p>

Figure 2. The (1) shows the domestic hot water flow profile; (2) shows the ground temperature, *i.e.*, the temperature of the inlet water; (3) shows the flow rate in blue and the temperature of the waste water in red.

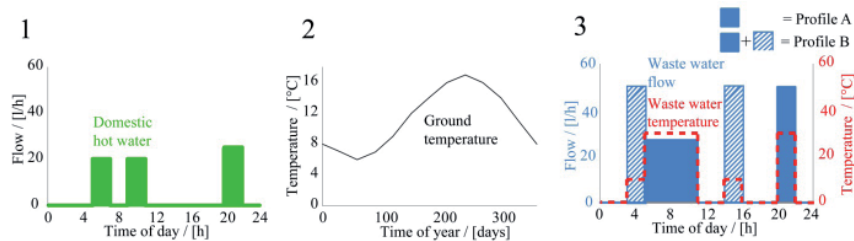


Table 2. The different investigated cases. All systems are equipped with a hot water storage tank that supplies the domestic hot water.

Simulation case	Description	Illustration
Case 1	The baseline case, labeled 1, is a building with mechanical ventilation with no heat recovery from the ventilation air.	
Case 2a	Case 2a includes heat recovery from the ventilation air. Simulation Case 2a was equipped with the heat recovery system shown in Figure 1.	
Case 2b	Case 2 is developed from Case 1. Simulation Case 2b was equipped with a mechanical ventilation system with heat recovery.	
Case 3a	Simulation Case 3a had the same ventilation system as Case 2a but it was also equipped with a waste water heat recovery system. The waste water heat recovery system is discussed in Table 1. The waste water heat recovery system was used to preheat the domestic hot water.	

Table 2. Cont.

Simulation case	Description	Illustration
Case 3b	Case 3b was the same as Case 3a but it was also equipped with a second heat exchanger in the waste water heat recovery tank. The heat exchanger is utilized by the ventilation system. After the brine has been heated in the roof heat exchanger, the brine is passed into the tank to extract energy. This extra heat is delivered to the incoming air and the energy use to heat the building will thus drop. The heat exchanger in the waste water tank used by the ventilation circuit can be bypassed if the extra heat is not needed.	
Case 3c	Case 3c is also a development of Case 2a where the ventilation system utilizes heat that is stored in the ground. The ground collector loop is only utilized when it is beneficial from an energy point of view. The ground collector is discussed in Table 1.	
Case 3d	Case 3d is a development from Case 2b. The difference is that Case 3d is equipped with a waste water heat recovery system.	
Case 4	Case 4 is 3b and 3c combined, i.e., it includes hybrid ventilation with heat recovery, waste water heat recovery where the ventilation is allowed to extract heat from the water tank and it includes a ground collector.	

3. Results

All results in this article are based on TRNSYS simulations. Figure 3 shows the total annual energy need for space heating and domestic hot water as a function of the efficiency of each of the heat exchangers. The left figure shows the results for the low energy building and the right one for the standard insulated building. The dark blue graph, i.e., the uppermost, is for the hybrid ventilation system, i.e., simulation Case 2a. The red graph is simulation Case 3c, i.e., the hybrid ventilation system equipped with a ground collector. The graph shows that the ground collector has almost no effect if the efficiency of the heat exchangers is low. The green line represents the simulation Case 3a, i.e., hybrid ventilation and waste water heat recovery. Installation of waste water heat recovery lowers the annual

energy need by approximately 600 kWh. The simulations were performed using waste water Profile B. The purple line represents simulation Case 3b and the light blue line, *i.e.*, the lowermost one, simulation Case 4. The orange and the light purple horizontal lines show the annual energy need for simulation Cases 2b and 3d, *i.e.*, mechanical ventilation with heat recovery with and without the waste water heat recovery. The result does not include the energy needed to run the fans for the ventilation. The results are presented as lines even though the performance is independent of the efficiency of the heat exchanger for the hybrid ventilation.

Figure 3. The total energy need, *i.e.*, space and domestic hot water heating, for the different simulations as a function of the efficiency of each of the heat exchangers for the ventilation. (a) is the low energy building; and (b) is the standard insulated building.

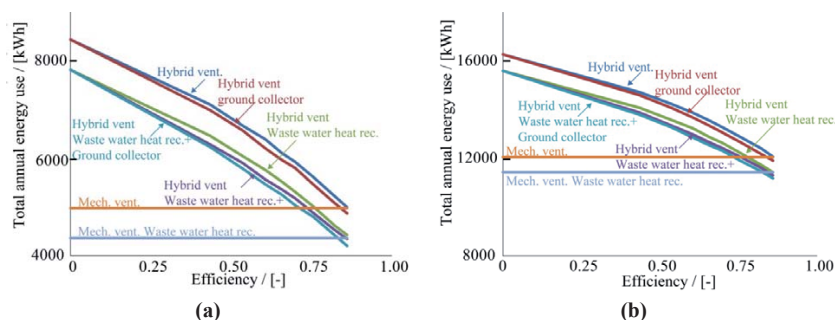


Figure 4 illustrates the annual energy flow for a low energy building. The blue bars represent simulation Case 2a and the red ones simulation Case 3c. This means that the hybrid ventilation with heat recovery system is compared with an equal system, but with the difference that a ground collector has been added. The first bars show the annual heating need for the two systems. The difference between the two systems is approximately 150 kWh annually. The second group, with only one bar, is the annual energy transferred from the ground to the brine by the ground collector. This is approximately 1000 kWh annually. The third group is the energy delivered to the incoming air by the heat exchanger located at the bottom of the building. Simulation Case 3c delivered approximately 200 kWh more than simulation Case 2a on an annual basis. The reason why the energy need is only reduced by 150 kWh annually when the heat exchangers deliver 200 kWh is that parts of this energy will not be used to lower the energy use. It will only be used to increase the overheating of the building. The fourth group shows the annual energy recovered from the outgoing ventilation air by the roof heat exchanger. The simulations are based on using a heat exchanger with an efficiency of approximately 75%.

Figure 5 shows the saving potential between the different cases. All the simulation cases are built on using heat exchangers with a component efficiency of approximately 75%. The left figure is for the low energy building and the right one for a standard insulated building. The basis for the simulation is System 2a, *i.e.*, a hybrid ventilation system with heat recovery. The first bar is for simulation Case 3c. Installation of a ground collector saves about 150 kWh of energy per year. The second group

of bars is for simulation Case 3a. The blue bar is for waste water flow Profile B and the red one for waste water flow Profile A. Installing a waste water heat recovery system lowers the annual energy need by approximately 600–800 kWh. The third group of bars is for System 3b. This case performs slightly better than Case 3a. The fourth group is for simulation Case 4. The fifth group is for Case 2b, *i.e.*, the mechanical ventilation with heat recovery without waste water heat recovery system. This system will use about 420 kWh more electrical energy compared with the hybrid ventilation systems. This is shown with the green bar. The electrical energy consumption for the hybrid ventilation system was estimated from temperature difference data from the simulation along with information on the fraction of time that the brine was being circulated. The support fan is assumed to have an annual average electrical power consumption of 4 W [15]. The right bars are for Case 3d. This system is assumed to spend as much electrical energy as Case 2b. The waste water heat recovery system recovers approximately 700 kWh annually.

Figure 4. The annual energy flows for a low energy building for two simulation cases, Case 2a in blue and Case 3c in red.

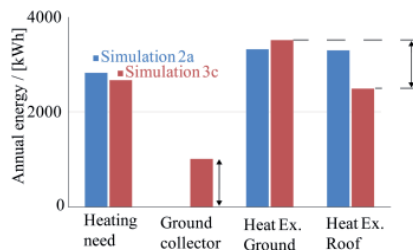
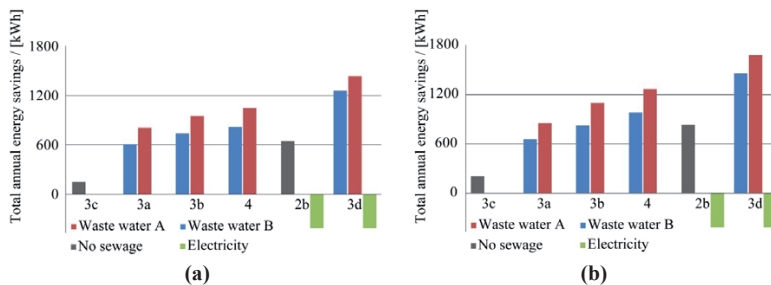


Figure 5. The saving potential for the different systems for waste water flow Profiles A and B, see Figure 2, (a) are the results for the low energy building; and (b) are the results for the standard insulated building.



4. Conclusions

Figure 3 shows that the most important factor in the system is the efficiency of the heat exchangers. Also, there is a possibility to recover about 25% of the energy in the waste water using the kind of

technique presented here. This technique can, however, be developed further for even larger energy savings. Two different waste water flow profiles were tested. This was carried out in order to investigate the sensitivity of different profiles. The waste water heat recovery system annually recovers about 200 kWh more with Profile A compared to Profile B. This is due to the cold water flow in Profile B that flushes the waste water tank, and thus a large amount of energy is lost before it can be recovered.

Figure 3 and Figure 5 show that inclusion of more energy sources in the ventilation heat recovery system, such as the ground collector or utilization of the waste water heat, has only minor effects on the annual performance. In Figure 3 it can be seen that, for the hybrid ventilation system to perform as well as the mechanical ventilation system, the heat exchanger has to have an efficiency of about 86%. A heat recovery efficiency of 86% on a component level equals a system heat recovery rate of 75% [4], *i.e.*, when both the roof and the heat exchanger at the bottom of the building are taken into account. This means that the need for auxiliary energy is the same for both systems. However, the mechanical ventilation system consumes more electrical energy. This is nothing unexpected but well worth pointing out.

In Figure 5 it was shown that the mechanically ventilated system consumes approximately 400 kWh more electrical energy annually compared with the hybrid ventilation system. It should be noted that this energy has to be electrical energy. The energy needed for the heating and the domestic hot water discussed in this article could come from somewhere else, for instance from bio fuels, district heating or heat pumps. The 400 kWh of electrical energy for the fan should thus be considered extra valuable. The primary energy factor to be used can always be discussed. Often a factor of somewhere between 2.5 and 3 is used for electricity. If 2.5 is used, it means that the performance of the hybrid ventilation system can be 1000 kWh of heat worse than that of the mechanical ventilation with heat recovery system and still have the same total annual performance. In other words, a hybrid ventilation system equipped with heat exchangers with an efficiency of 65%–70% performs about the same on an annual basis as the mechanical ventilation system with heat recovery. During hotter periods, it may be possible to reduce or even turn off the ventilation system and instead rely on natural ventilation by means of open windows. This will lower the energy need for the ventilation system. This was, however, not included in any calculations.

One complication that has been left out in this discussion is the heat from the fans in the mechanical ventilation units. The electricity consumed by the fans will, if they are located downstream in the air flow movement, contribute to heating the building. However, far from all of the heat will be beneficial for the building. The heat produced during the summer will only add to overheating. The results in this article assume a mechanical ventilation unit with a 75% heat recovery rate. The electrical energy consumed by the fans is assumed to be included in these 75%.

If the electrical energy consumed by the fans is included in the annual average heat recovery rate for the ventilation unit, it will become beneficial to use inefficient fans. These fans consume and thus create large amounts of energy. This energy, transported to the air, will increase the effective heat recovery rate. Thus, units with high electricity consumption will appear to perform better.

Figure 3 shows that the ground collector had almost no effect if the efficiency of the heat exchangers was low. This can be understood by a more detailed investigation of the temperatures of the brine that is let into the ground collector. If a low efficiency heat exchanger is used for the inlet air,

the brine temperature is not cooled enough to be able to utilize the relatively low temperatures in the ground. The high efficiency heat exchanger cools the brine more efficiently, which leads to the possibility to extract energy from the ground. Since the ground temperature is in the range of 6–8 °C during the winter the brine has to be cooled to temperatures below this in order to be able to gain energy from it. Simultaneously the energy savings are sparse even for higher heat exchanger efficiencies. This is explained by Figure 4, which shows a large drop in the extracted thermal energy from the roof heat exchanger when the ground source was installed. This is explained by the brine already being heated as it arrives at the roof exchanger. There is simply less energy that can be recovered since the temperature has risen already.

One factor that was omitted in this investigation is the risk of having frost on the exchanger. As the outgoing humidified indoor air is let through the heat exchanger at the roof the air is cooled down. When the temperature falls below the dew point, water drops will start to form on the surface. If the temperature continues to drop, water will start dripping from the exchanger. This is a technical issue that needs to be addressed if this system is to be commercialized. If the temperature is lowered even further there is a risk of frost developing on the heat exchanger. This has the potential to completely block the transport of air in the system and severely reduce the heat exchanger efficiency. One possible solution is to use a ground collector. The ground collector has the potential to increase the brine temperature to temperatures above zero. If the brine is above zero, there is no risk of getting frost on the heat exchanger. This means that a ground collector can be motivated even though the benefits from an energy point of view are limited.

Still there are many questions that need to be answered for this hybrid ventilation system.

- Mechanisms to control the hybrid air flow rate. The air flow rate needs to be controlled in both directions, both to ensure that the ventilation is large enough and also to avoid excessive ventilation. The latter can typically occur during windy conditions when the air pressure is higher on one side of the building.
- The heat exchanger surfaces need cleaning. Mechanical ventilation units are normally equipped with a filter. This filter prevents the heat exchanger surfaces from getting dirty. However, the pressure drop over the filter is typically too large for a hybrid ventilation system. One alternative is to construct the heat exchanger in such way that it allows for cleaning. This is possible since the structures in the heat exchanger are in the order of centimeters [4] and not millimeters as in the case of the heat exchangers of mechanical systems.
- The brine flow rate needs to be controlled. The ventilation system could be made up of many heat exchangers located in different rooms. The flow rate to each of these heat exchangers needs to be controlled to assure a balanced flow. One way of designing this type of system is to have one heat exchanger in each room where the ventilation air is intended to come in and one larger heat exchanger at the top of the roof where all the heat is recovered. The heated brine is pumped to the different rooms.
- The design of the ventilation system must be considered to avoid blocking of exhausted air, as this would create a pressure drop and lower ventilation rates for the whole building.

- Noise level. The hard constraints on the pressure drop make it difficult to use a silencer. This will have consequences on the level of noise transmitted from the outside of the building through the fresh air intake. However, at the same time, there will be less noise due to fans running the system.
- Constraints on the architecture. The system might not be suitable for all types of buildings. This has to be investigated from building to building. At the same time, this type of heat recovery system, where the old contaminated air does not meet the fresh incoming air, is suitable when cross contamination has to be avoided. This can for instance be the case for ventilation of laboratories.

In the calculation example of this article the height difference between the air inlet and the outlet is assumed to be 10 m. If the height difference is substantially lower, there might not be enough pressure to run the ventilation system. The complementary fan would have to run more frequently. However, if the height is around 10 m, the investigated ventilation system could be used in future low energy buildings such as passive houses and net zero energy buildings. There are also alternative ways to enhance the ventilation flow rate. Different types of solar chimneys have been suggested. Zhai [16] reviewed the field of solar chimneys and Khan [17] reviewed different wind driven techniques for ventilation. Both of these types of techniques could be used to improve the hybrid ventilation technique.

There is also a possibility to use the ventilation system when old buildings with passive stack ventilation are energy renovated. The question how well this type of ventilation system can work in old buildings is very difficult to answer. If the building is ventilated by opening windows and there are no exhaust air ducts, it will be difficult to implement the ventilation system discussed in this article. However, it can be advantageous with this type of system to renovate old buildings with exhaust ventilation systems where the air flow pattern in the building is unchanged. If the old holes in the outer walls are used for the fresh air supply, the distribution of the air inside the building is not altered. The proposed ventilation system will thus not create places in the building with stagnant air. However, new holes through the exterior wall for the air inlet/outlet will most likely be needed to allow the heat exchanger to be installed. If new holes are introduced in the building in rooms or places previously not ventilated, there is a risk of altering the air movement. This can be a problem, but it can also be a solution for poorly functioning ventilation systems. The roof heat exchanger could be installed in the old ventilation system on the roof. This action would lower the peak power demand, lower the annual energy use and at the same time increase the comfort for the residents as the cold draught is reduced. During summer time when the passive stack effect disappears, the ventilation is carried out either with a complementary fan or with closed/opened windows. Opening windows for ventilation during the winter is still possible after retrofitting the old ventilation system. However, the heat recovery function will not work during the time with open windows.

Acknowledgement

Åke Blomsterberg at the Department of Architecture and Built Environment and Birgitta Nordquist at the Department of Building and Environmental Technology both at Lund University are acknowledged for guidance and valuable discussions.

References

1. Principles of Hybrid Ventilation. IEA Energy Conservation in Buildings and Community Systems Programme. Available online: <http://www.hybvent.civil.aau.dk/> (accessed on 27 April 2012).
2. Feist, W.; Schieders, J.; Dorer, V.; Haas, A. Re-inventing air heating: Convenient and comfortable within the frame of passive house concept. *Energy Build.* **2005**, *37*, 1186–1203.
3. Hviid, C.H.; Svendsen, S. Analytical and experimental analysis of a low-pressure heat exchanger suitable for passive ventilation. *Energy Build.* **2011**, *43*, 275–284.
4. Davidsson, H.; Bernardo, R.; Hellström, B. Theoretical and experimental investigation of a heat exchanger suitable for a hybrid ventilation system. *Buildings* **2013**, *3*, 18–38.
5. Mardiana-Idayu, A.; Riffat, S.B. Review on heat recovery technologies for building applications. *Renew. Sustain. Energy Rev.* **2012**, *16*, 1241–1255.
6. Florides, G.; Kalogirou, S. Ground heat exchangers—A review of systems, models and applications. *Renew. Energy* **2007**, *32*, 2461–2478.
7. Zhai, X.; Dai, Y.; Wang, R. Comparison of heating and natural ventilation in a solar house induced by two roof solar collectors. *Appl. Therm. Eng.* **2005**, *25*, 741–757.
8. Khedari, J.; Hirunlabh, J.; Bunnag, T. Experimental study of a roof solar collector towards the natural ventilation of new houses. *Energy Build.* **1997**, *26*, 159–164.
9. Pinel, P.; Cruickshank, C.A.; Beasusoleil-Morrison, I.; Wills, A. A review of available methods for seasonal storage of thermal energy in residential application. *Renew. Sustain. Energy Rev.* **2011**, *15*, 3341–3359.
10. Klein, S.A. A Transient Systems Simulation Program. Available online: <http://sel.me.wisc.edu/trnsys> (accessed on 21 February 2013).
11. EN (European Standards). *Thermal Performance of Buildings—Calculation of Energy Use for Space Heating*; EN: Brussels, Belgium, 2004.
12. Widén, J.; Lundh, M.; Vassileva, I.; Dahlquist, E.; Ellegård, K.; Wäckelgård, E. Constructing load profiles for household electricity and hot water from time-use data—Modelling approach and validation. *Energy Build.* **2009**, *41*, 753–768.
13. Välkommen till VA SYD. Available online: <http://www.vasyd.se> (accessed on 23 August 2012).
14. Boverkets Byggregler. Available online: <http://www.boverket.se/Global/Webbokhandel/Dokument/2011/Regelsamling-for-byggande-BBR.pdf> (accessed on 23 August 2012).
15. VBP Hybrid Assistance Fan. Available online: <http://www.aereco.com/product/vbp> (accessed on 23 August 2012).
16. Zhai, X.; Song, Z.; Wang, R. A review for the applications of solar chimneys in buildings. *Renew. Sustain. Energy Rev.* **2011**, *15*, 3757–3767.
17. Khan, N.; Su, Y.; Riffat, S.B. A review on wind driven ventilation techniques. *Energy Build.* **2008**, *40*, 1586–1604.

Paper V

Parametric Study of a Heat Exchanger for a Hybrid Ventilation System

Henrik Davidsson, Ricardo Bernardo, Bengt Hellström

Department of Architecture and the Built Environment, Lund University

P.O. Box 118, 221 00 Lund

henrik.davidsson@ebd.lth.se

ricardo.bernardo@ebd.lth.se

bengt.hellstrom@ebd.lth.se

Abstract

Heat recovery from the ventilation air is one of the key components in low energy houses. The energy use in a building would increase considerably without heat recovery on the ventilation air. However, standard mechanical ventilation units with heat recovery use considerable amounts of electricity in order to run the fans. One way to reduce this is to use natural or hybrid ventilation. However, this technology normally has no provision for recovering any heat from the outgoing ventilation air. This results in both a high need for thermal energy and low thermal comfort. This article describes a parametric study of a heat exchanger designed for heat recovery in a natural/hybrid ventilation system. Different materials and different geometries are investigated in order to optimise the performance. The study shows a small potential for the improvement of the heat exchanger.

Keywords - hybrid ventilation; heat recovery; low pressure drop; parametric study

Nomenclature

d	distance between the fin pipes	[m]
g	gravitational constant	[m/s ²]
h'	height of the building	[m]
l	length of the heat exchanger/fin pipes	[m]
ΔP	pressure difference	[Pa]
t	thickness of fin	[m]
T_{in}	temperature of inlet ventilation air	[°C]
T_{amb}	temperature of ambient air	[°C]
T_{room}	temperature of indoor air	[°C]
ΔT	temperature difference	[°C]
ΔT_{w-a}	temperature difference water-air	[°C]
w	width of the fin	[m]
S	Relative cost	[m ³]
V_{al}	Volume of aluminium	[m ³]

V_{cu} Volume of copper [m^3]

Greek letters and other symbols

η system efficiency of heat exchanger [-]

η_{comp} component efficiency of heat exchanger [-]

\varnothing_o outer diameter of copper pipe in fin pipes [m]

\varnothing_i inner diameter of copper pipe in fin pipes [m]

1. Introduction

Many of the ventilation systems installed in newly built houses in Sweden are mechanical units with heat recovery. For low energy houses such as passive houses or Net Zero Energy Buildings, the mechanical ventilation unit with heat recovery is predominant to other techniques. However, the fans needed for the mechanical ventilation systems use a considerable amount of electrical energy. An investigation by the Swedish Energy Agency showed that the best performing ventilation system in the test used 456 kWh of electrical energy annually for the fans [1]. This number is in close agreement with data given by Feist et.al. [2]. The following example can be used to illustrate the problem. A typical house without heat recovery in the Swedish climate requires about 4000 kWh for the heating of the ventilation air. This means that if the heat recovery system recovered 75% of that heat, 3000 kWh could be saved annually.

However, 456 kWh of electric energy corresponds to about 1370 kWh of primary energy, using a conversion factor of three. This greatly reduces the energy savings of the system. Instead of saving 75% the system only saves about 40% of the primary energy, including the electricity for the fans in the calculations.

An alternative to a mechanically ventilated system is a naturally ventilated system. However, this technique normally lacks heat recovery, which may lead to a high energy use and low comfort due to cold draughts. This type of technique must be equipped with a heat recovery in order to be a competitive alternative to mechanical systems. This is unfortunately difficult to achieve. The main reason for this is that the pressure drop has to be kept minimal in order not to block the ventilation. Heat exchangers made for mechanical systems have a pressure drop that is many orders of magnitude larger than the driving forces related to natural ventilation. However, lately there have been reports about heat exchangers suitable for natural or hybrid ventilation. These heat exchangers have been shown to have a heat recovery efficiency of about 80%, while the pressure drop is limited to a few Pa [3-4]. This makes it possible to construct highly efficient ventilation systems based on natural ventilation. Furthermore, there is a technology called hybrid ventilation that combines the natural and mechanical ventilation types. This technique uses the natural driving forces when these provide enough pressure

difference, and otherwise uses a complementary fan. This is typically on days with a low temperature difference between indoor and outdoor air and when the wind is low. The hybrid technology combines the low electrical energy use of natural ventilation with the high reliability of mechanical systems.

Following the work presented in [5], this article investigates and discusses the potential to develop the heat exchangers further. Different geometries and materials are studied and discussed.

The investigated heat exchanger and the presented ventilation system can be used when old houses with natural ventilation systems are renovated in order to reduce their energy use. These houses normally lack heat recovery, making them either high energy users or, alternatively, poorly ventilated. Apart from the economical and environmental reasons for saving energy the level of discomfort due to cold draughts can also be reduced if the recovered energy heats the incoming air.

2. Theoretical Considerations for the System

The investigated heat exchanger is intended to be used in a brine coupled ventilation system made up of two heat exchangers. The air flow is driven by natural forces due to wind pressure and temperature differences. The brine is circulated by a pump. The illustration on the left in Fig. 1 shows the function of the system. One of the liquid-to-air heat exchangers is placed as high as possible under the roof. This exchanger recovers some of the energy from the outgoing air and transfers it to the brine. This energy is then pumped to the bottom of the building where the other heat exchanger is located. This liquid-to-air heat exchanger delivers the recovered heat to the incoming cold fresh air. After this heat exchange the cold liquid is pumped back to the heat exchanger under the roof and the circuit is completed.

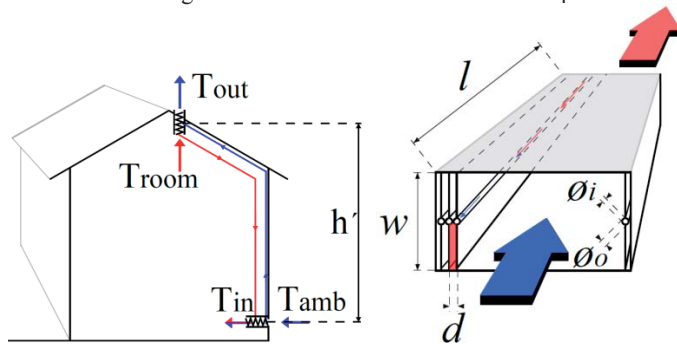


Fig. 1 The brine based heat recovery system to the left and the heat exchanger to the right.

Natural ventilation systems are greatly limited by the driving forces. The thermal driving force ΔP can be calculated by,

$$\Delta P = h' \cdot g \cdot (\rho_{amb} - \rho_{room}) \quad (1)$$

where h' is the height of the building, g is the gravitational constant and ρ_{amb} and ρ_{room} are the densities of the ambient and the indoor air respectively. If the height h' of the building is 10 m and the ambient and room temperature are 0°C and 20°C respectively, the driving force will be $\Delta P = 10 \cdot 9.81 \cdot (1.293 - 1.204) \approx 8.7$ Pa

This shows that the pressure loss in the system has to be limited. The driving pressure created by the temperature difference has to balance the pressure losses not only in the heat exchanger but also in the ducts, filters etc. It is thus a large advantage if the duct system can be considered superfluous. At the same time it is beneficial if the heat exchanger surface is easy to clean, making it possible to install a minimal filter, or even better, no filter at all. Both these measures will lower the pressure losses in the system. One way to reduce the number of ducts in the system is to allow the fresh supply air to go directly through the wall to the rooms. However, the fluid circuit in the system that transports the recovered heat has to be divided to every fresh air inlet. Instead of an air supply system, this type of ventilation system has a fluid supply system. Complementary fans for hybrid ventilation systems with a pressure drop less than 2 Pa during inactive periods, i.e. when the wings of the fan are not spinning, can be found on the market [6].

3. Theoretical Considerations for the Heat Exchanger

The counter flow liquid-to-air heat exchanger investigated in [5] is shown to the right in Fig. 1. The heat exchanger is made up of a number of solar collector fin absorbers produced by the company Ssolar in Sweden. The absorbers, from now on referred to as fin pipes, are placed in parallel and connected to a manifold on each side. The fin pipes are made up of a copper pipe tightly pressed in between aluminium fins. The width, w , of the fin pipe on the tested heat exchanger was chosen to be 167 mm and the thickness, t , of the fin is 0.5 mm. This size is a standard component from the supplier. The pipe at the centre of the fin pipe has an outer diameter, ϕ_o , of 9.5 mm while the inner diameter, ϕ_i , is 8 mm. The length, l , of the heat exchanger was treated as variable to meet the heat transfer efficiency requirements. The blue and red large arrows in the figure illustrate the air flow while the small arrows at the water pipe illustrate the water flow. The distance between the fin pipes, d , was 0.011 m.

The tested heat exchanger was designed to have a thermal efficiency $\eta = 70\%$ on a system level. The efficiency is defined as the temperature change for the incoming air divided by the difference in temperature between

the ambient and indoor air. During the calculation we assume an ambient temperature of 0°C. The efficiency is calculated as:

$$\eta = \frac{T_{in} - T_{amb}}{T_{room} - T_{amb}} \quad (2)$$

See Figure 1 for explanation of the variables. If T_{room} is 20°C, the inlet air temperature, T_{in} , would then be 14°C. In order to have a system efficiency of 70% for the ventilation heat recovery, the efficiency on the component level has to be higher. In the example above the efficiencies for the individual heat exchangers are:

$$\eta_{comp} = \frac{T_{in} - T_{amb}}{T_{in} + T_{w-a} - T_{amb}} = \frac{14}{17} \approx 82\% \quad (3)$$

See Figure 1 for explanation of the variables. ΔT_{w-a} is the temperature difference between the water and the air in the heat exchanger and equals $(T_{room} - T_{in})/2$. In the example above ΔT_{w-a} is 3°C. A normal ventilation rate for a Swedish residential house of approximately 150 m² floor space is around 180 m³/h. This corresponds to 50 l/s and results in an air change rate of about 0.5 air changes per hour.

4. Method

The calculations performed in this article are based on estimations and measurements presented in [5]. The measured heat exchanger also serves as a starting point for all the performed parametric studies.

All the calculations presented here are based on a heat exchanger of 82% efficiency on a component level. In order to meet this target the length of the heat exchanger had to be varied. In the list below all the parametric investigations are presented.

Parametric Investigation 1

The geometry of the heat exchanger can be altered in order to change both the heat transfer rate and the pressure drop. Two alternatives were investigated. These are shown in Fig. 2. In Alternative A, the proportions of the fins are changed. Reducing the width, w , of the heat exchanger by 50% at the same time as the number of fin pipes is doubled gives the same cross section area for the heat exchanger. Alternative B was to double the size of the heat exchanger. The size of the cells in which the air moves was the same while the number of cells was doubled.

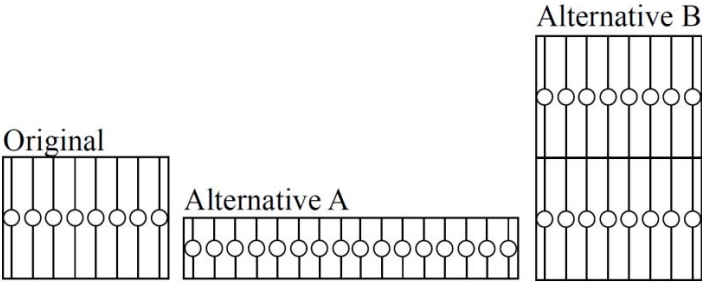


Fig. 2 The investigated geometries.

Parametric Investigation 2

The original heat exchanger was made up of a copper pipe with aluminium fins. The pipe and fin materials can however be altered in many different ways. A number of different materials were investigated. The tested materials were aluminium (Al), copper (Cu), plastic (Pla) and stainless steel (Sts). These materials were tested in different combinations for pipe and fin material. The different combinations are listed in Table 1.

Table 1. Material combinations for the fin pipe.

Material combination	Pipe material	Fin material
1	Cu	Al
2	Cu	Cu
3	Al	Al
4	Pla	Cu
5	Pla	Al
6	Sts	Sts
7	Pla	Pla

Parametric Investigation 3

The importance of the thickness and width of the fin were investigated for pipe/fin material combinations 1, 2 and 3. Two fin thicknesses chosen for the investigation were 0.5 mm and 0.1 mm.

5. Results

Fig. 3 shows the results from the geometrical study. The length of fin pipes for the heat exchanger on a component level is in blue and the pressure drop for the heat exchanger is in red. The original heat exchanger is made up of 80 m fin pipes and has a pressure drop of approximately 1.4 Pa on a component level. In Alternative A the fins are made shorter. This results in longer fin pipes since the heat surface is smaller per pipe. However the pressure drop is reduced since the length of the heat exchanger is reduced. Still, Alternative A has twice as many absorbers as the original. Alternative B has the same number of meters of fin pipes. However, the pressure drop is reduced by 50% since the speed of the air is reduced.

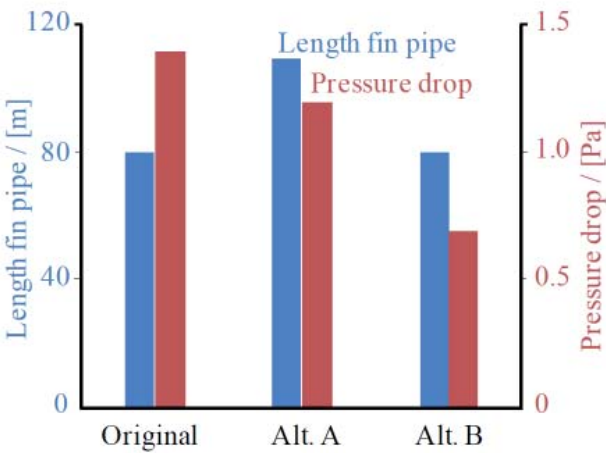


Fig. 3 Results from the geometrical investigation. The total length of fin pipes on a component level is in blue and the pressure drop is in red.

The investigation of different material combinations for the fin pipes is shown in Fig. 4. The length of fin pipes needed to meet the requirement is on the y-axis. As can be seen the difference is not significant whether Aluminium or Copper is used. The fourth and fifth bars are with plastic pipes. The thickness of the pipe is less than 1 mm. This limits the thermal

resistance in the pipe itself. However, plastic fins have limited heat transfer, thus the total length of fin pipes will be very long. Note that the bar showing the plastic fin pipes has been cut. The stainless steel also performs poorly. The continued analysis omits both plastic and stainless steel as options in the heat exchanger.

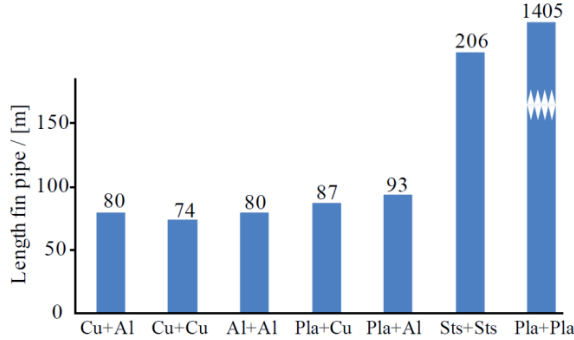


Fig. 4 Total length of fin pipe for different material combinations.

The effects of varying the thickness and width of the fin are shown in Fig. 5. The figure shows material combinations 1, 2, and 3. The red curve shows the result using 0.1 mm thick fins, and the result for 0.5 mm thick fins is in blue. These lines, using the left y-axis, show the relative material costs. The material cost, S , is defined as:

$$S = V_{Al} \cdot 1 + V_{Cu} \cdot 13.9 \quad (4)$$

where V_{Al} is the volume of Al and V_{Cu} is the volume of Cu. The multiplication factor for the copper, i.e. 13.9 was determined as the ratio of the price per volume of copper to that of aluminium. The ratio was taken on the 1st of November 2012. The green and the yellow line, using the right y-axis, show the total length of fin pipes needed to meet the requirements, i.e. a system efficiency of 70% for the heat exchangers with 0.1 mm and 0.5 mm thick fins.

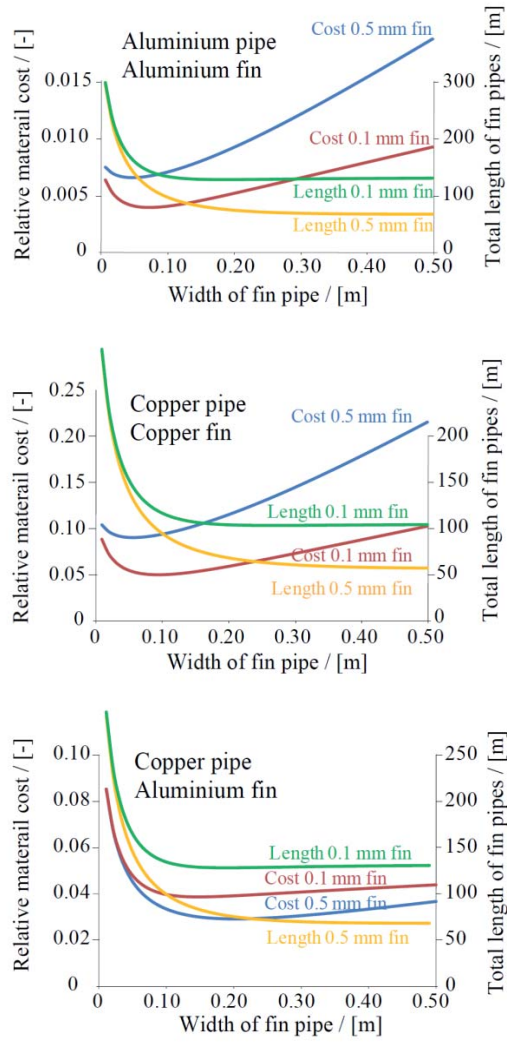


Fig. 5 Optimization of thickness and width of the fin.

6. Discussion

One clear advantage of this design compared to many other heat exchangers is that it can be cleaned. If the cover is removed the fins can be cleaned. The right illustration in Figure 1, the top, marked with grey colour, can be removed. Alternative designs are possible and have been proposed earlier [3-4]. However, these designs are much more difficult to clean. This might be a problem if layers of dust build up on the heat exchanging surface.

The geometrical structure of the original heat exchanger allows for high heat recovery rates, at the same time as the pressure drop is kept low. The results shown in Figure 3 from parametric investigation No 1 showed that for a given heat exchanger, with a specific heat recovery rate, any pressure drop is possible. Basically the heat exchanger can be made up from the greatest possible number of parallel connected finned pipes to get a low pressure drop. Still the total length of finned pipes in the heat exchanger is kept constant. However, the construction of this type of heat exchanger would require a large entrance hole in the wall and the component would not be easy to install in a building. The large cross section of the heat exchanger would also make it difficult to control the air flow through it. Figure 3 also showed that using smaller fins has the potential to result in a more compact heat exchanger. However, this will also make it more expensive since more work is required due to the larger number of finned pipes.

The second parametric investigation presented in Figure 4 showed that the choice of material in the pipes is of low sensitivity. For instance, in principle, plastic pipes could be used. Replacement of the copper pipes in the original heat exchanger by plastic ones only requires an additional 16% of finned pipes. However, the use of stainless steel as pipes and fins has strong limitations on the performance. The rather low thermal conductivity of the stainless steel greatly limits the performance. As can also be seen in the figure, the use of plastic as fin material is not an option. What combination of materials is the most suitable is a question of both performance and price.

Figure 5 showed a cost optimization for different material combinations. The optimization is based on only material costs. The relative cost of the heat exchangers made of copper is much higher than that of the aluminium. However, the total length of the fin pipes is also relevant since it relates to the production costs. Long fin pipes will result in either long heat exchangers or many parallel connected pipes. If the heat exchanger becomes long the pressure drop increases. At the same time the exchanger also becomes difficult to integrate in the building. If, on the other hand, many pipes are connected in parallel the pressure drop will be lower. However, this alternative will most likely result in higher production cost due the increased work related to connecting the many pipes to the manifold. If the cost related to mounting the pipes is high the copper can be motivated since copper pipes and fins result in shorter heat exchangers.

The effects of changing the pressure due to different geometries, different lengths and widths of the fins were omitted throughout this investigation. Instead the pressure drop is assumed to be controlled simply by increasing the number of parallel connected fin pipes. A larger number of pipes results in slower moving air through the heat exchanger and thus a lower pressure drop.

7. Conclusions

The conclusion from this work is that there are some adjustments that can be carried out on the heat exchanger. However, the influence on the costs of the final product has to be investigated. This includes not only the increased or decreased costs of the raw material but also the extra work needed in order to build the exchanger. For instance, increasing the number of finned pipes will lead to a higher price. Also, altering the thickness of the fins, for instance, will have other implications. If the fins are made thinner they will also be more fragile and easily deformed. Longer fins will be more difficult to clean if needed. All of these benefits and drawbacks have to be weighted with respect to the savings or cost increases that the modification will result in.

8. Acknowledgment

The foundation for “Energieffektivt Byggbande” is acknowledged for economic help with this project.

9. References

- [1] Energimyndigheten, “FTX-aggregat hus med 130 m² boyta – Jämförelse”, 2010.
<http://www.energimyndigheten.se/Templates/Public/Pages/ProductGroupPageCompare.aspx?productGroupId=69&productCompareList=412,413,414,415,416,417,418,419&PageID=5552>
Visited 2012-11-06
- [2] W. Feist, J. Schieders, V. Dorer, A. Haas, “Re-inventing air heating: Convenient and comfortable within the frame of passive House concept”, *Energy and Buildings* 37 (2005), pp. 1186-1203
- [3] C.H. Hviid, S. Svendsen, “Analytical and experimental analysis of a low-pressure heat exchanger suitable for passive ventilation”, *Energy and Buildings* 43 (2011), pp. 275-284
- [4] L. Shaw, S.B. Riflat, G. Gan, “Heat recovery with low pressure loss for natural ventilation”, *Energy and Buildings* 28 (1998) pp. 179-184
- [5] H. Davidsson, R. Bernardo, B. Hellström, “Theoretical and Experimental Investigation of a Heat Exchanger Suitable for a Hybrid Ventilation System”, Submitted to *Buildings* (2012)
- [6] “VBP Hybrid assistance fan” <http://www.aereco.com/product/vbp> Visited 2012-11-06

Paper VI

Design and Performance of a Hybrid Ventilation System with Heat Recovery for Low Energy Buildings*

Henrik DAVIDSSON**, Luis Ricardo BERNARDO** and Stefan LARSSON***

**Energy and Building Design Lund University

Box 118, SE-22100 Lund, Sweden

E-mail:henrik.davidsson@ebd.lth.se

***Finsun Inresol AB, Sweden

Bruksgatan 7 Solgården, 81494 Älvkarleö, Sweden

Abstract

A new hybrid ventilation system for low energy buildings has been investigated theoretically using TRNSYS. The system is based on natural ventilation but utilizes a fan during hours when the natural driving forces are not sufficient. Heat from the exhaust air is recovered in an air-to-water heat exchanger. The heated water is pumped to the incoming ventilation air where it is heat exchanged to preheat the fresh air. Energy from solar collectors is used in combination with heat recovered from the sewage system to heat the ventilation air and to preheat the cold water for domestic use. Results from the TRNSYS simulations show that the bought annual auxiliary energy need for the new hybrid ventilation system is lower than for a conventional fan driven ventilation systems using air-to-air heat recovery units combined with an identical solar collector and sewage heat recovery unit. Since the new system is based on natural ventilation it is also more silent compared to standard mechanical ventilation systems.

Key words: TRNSYS, Natural Ventilation, Hybrid Ventilation, NZEB, Low Energy House, Solar Energy, Waste Heat Recovery, System Simulation, Energy Saving, Natural Convection

1. Introduction

During the last years a series of scientific investigations made it clear for a large part of the society that the use of fossil fuel must be drastically reduced. Some of the most important investigations have been reported by IPCC⁽¹⁾. Another topic is the one about the Peak Oil theory⁽²⁾ where the limited fossil fuel supplies, primarily the oil, are discussed. The main conclusion is that the use of fossil fuel must be reduced. This reduction can be achieved in mainly two ways: decreasing the energy consumption and/or increasing the alternative energy production. In this article a possible way to reduce the energy demand for a building is discussed. An investigation was carried out on a ventilation system mainly driven by natural forces. The reason to use hybrid ventilation is to decrease the demand for electrical energy for the ventilation fans.

Low energy houses, such as passive houses or Net Zero Energy Buildings normally use mechanical ventilation with heat recovery. This kind of ventilation system use an electric fan to push the incoming fresh air through a heat exchanger where the outgoing air leaves a fraction of its heat to the incoming air. Typically about 75 percent of the heat is recovered in

this way. However, this doesn't mean that the energy consumption is reduced by 75 percent for the ventilation system. To get a full understanding of the energy flows involved in the ventilation one also has to include the electrical energy consumed by the fans. This issue is better understood by using an example.

A typical one family house in the south of Sweden, or other cold climates, uses roughly 4000 kWh annually to heat the fresh ventilation air. Using a heat pump with a COP of 3 the building consumes 1333 kWh of electrical energy. If a heat recovery unit with 75% efficiency is used the heat exchanger reduces the electrical load with 1000 kWh. However, the fans needed to run the system needs about 466 kWh annually⁽³⁾. This means that about 50% of the recovered energy is needed to run the system. This example is not in any way a complete analysis, it is only used to illustrate a problem. More aspects have to be included before more general claims can be made. The example does not show that heat recovery units should not be used, it just points at a problem, the high electrical energy consumption by the fans.

The ventilation system described in this paper is designed to recover heat from the exhaust air and then deliver the energy to the fresh incoming ventilation air. The system also uses recovered heat from the sewage water of the building and energy from solar collectors.

2. Method

So far the full system, including its components, only exists on the drawing board. Initial measurements on some of the system components have been made in a building called Solgården outside Gävle in the central parts of Sweden. These and other results to come will be used to calibrate the constructed TRNSYS⁽⁴⁾ model. The mathematical models used in this work to describe the different components of the system are all either well documented standard components from the main TRNSYS libraries or well validated by other research. All the results presented in this article are based on TRNSYS simulations. This means that great challenges lay ahead to build a prototype of this new system. In the performed simulations the building is assumed to be a passive house. This means that the building is supplied with energy through the ventilation air, i.e. no radiators are needed to keep the building at the desired temperature. During the simulations the indoor temperature was not allowed to be lower than 19°C. No restrictions were imposed on the relative humidity of the indoor air. However there is nothing that prevents the investigated system to be installed in a building that uses radiators or active floor heating. The six simulated systems are described below.

All the systems are shown in Fig. 1. System 1 is a natural ventilation system without heat recovery. It uses a water-to-air heat exchanger, shown in red in the lower left corner, to heat the ventilation air. The heat is supplied from a tank via a brine circuit, shown with dashed black lines. The tank also supplies the domestic hot water load. The energy to the tank is supplied from a heat pump, illustrated with a red and blue square. The heat pump is connected to a ground collector, illustrated with a blue circuit below the building. System 2 is the same as System 1 but it also includes a solar thermal collector.

The system installed in Solgården is shown in System 3_hyb. The system is based on the concept of natural ventilation. The air is let into the building at the ground floor and escapes through the roof. The heat exchangers circuit is shown with red, for heated, and blue, for cooled, lines. The brine in the circuit is pumped between the cross flow heat exchangers. The heat exchanger at the roof recovers some of the heat from the exhaust air. The heat in the brine is then pumped and delivered in the heat exchanger, located directly on the wall, to the incoming air. The auxiliary energy needed for heating the building is supplied to the ventilation air in the second heat exchanger. System 3_hyb uses the same

tank, heat pump, ground collector and solar collector system as System 1 and 2. As can be seen, the difference from System 3_hyb to System 2 is the heat recovery system.

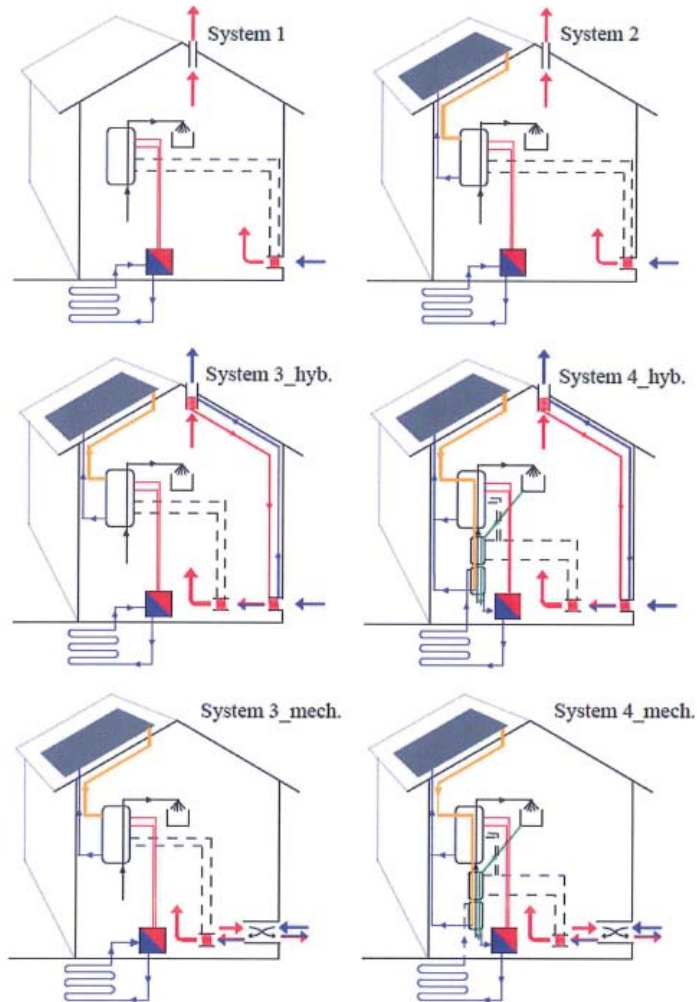


Fig.1 The simulated systems. In orange and blue is the solar thermal circuit. The red and blue square illustrates a heat pump. System 3_mech and 4_mech uses a mechanical ventilation system, the others uses natural ventilation.

The most developed system, System 4_hyb., is shown in the right in the middle row in Fig. 1. It is based on System 3_hyb but it also includes two extra storage tanks located below the

main hot water storage tank. These tanks are grey water sewage tanks where the sewage water from showers, sinks, washing machine etc. is stored temporarily. It is important to note that sewage from the toilets is not included. The sewage water is let into the middle tank. This is indicated with a green arrow in the figure. The sewage is then passed on to the lower tank before it is disposed out of the building. The solar thermal energy is always heat exchanged in the main storage. After this the solar collector loop continues either back to the bottom of the collector or to the sewage tanks. This is illustrated with orange and blue lines. The control strategy for the solar collector loop was chosen as follows: If the temperature in the bottom of the lower tank is below a chosen value the solar heat is exchanged in all of the tanks. If the temperature is above the chosen value the hot water from the solar collector is only heat exchanged in the main tank and then returned to the collector. Alternative control strategies are possible. These strategies could for instance be designed to operate in such way that it aims to minimize the risk of boiling the main tank. This kind of possibilities was however not investigated in this study.

The energy that is stored in the two sewage tanks is used to preheat the incoming cold water and the ventilation air. The first circuit, i.e. the lowest in the figure, goes from the tank to the heat pump connected to the ground collector. This is shown with a blue line. The ground collector ensures that the inlet brine to the tank is not too low, to avoid freezing. The second brine circuit connects the middle tank to the second water-to-air heat exchanger. If the heat is not enough to keep the building on the desired temperature, extra heat can be supplied from the main storage tank. Pumps and controllers used in the TRNSYS model have been left out for visual clarity in the figures. The domestic hot water is preheated by the sewage tanks before reaching its final temperature in main storage tank.

The two systems in the bottom of Fig. 1 shows System 3_mech and System 4_mech. They differ from System 3_hyb and System 4_hyb in the ventilation part. The hybrid ventilation system has been replaced by a mechanical ventilation system with heat recovery. This type of ventilation is common in low energy buildings, e.g. passive houses. In our simulations, the mechanically ventilated systems used the same heating source as the naturally ventilated systems, a heat pump connected to a ground collector. Fig. 2 shows a flow diagram of System 4_hyb. The different energy flows showed in the figure are:

1. Solar thermal energy from collector to storage tank.
2. Domestic hot water.
3. Thermal losses from the building.
4. Heat from electrical appliances, solar radiation transmitted to the building and heat gains from people.
5. Energy from heat pump delivered to the main storage tank.
6. Solar energy from the main storage tank to the sewage tank. Preheating of domestic hot water in the sewage tank before the water is let into the main storage tank.
7. Hot air to heat the building
8. Solar energy from the upper sewage tank to the lower. Preheating of domestic hot water in the lower sewage tank before the water is let into the upper sewage tank.
9. Preheated air from the heat exchanger located in the bottom of the building to the second heater.
10. Energy in the lower sewage tank is used by the heat pump to increase the thermal performance.
11. Energy recovered from the air-to-water heat exchanger on the roof delivered to the air-to-water heat exchanger located on the bottom of the building.

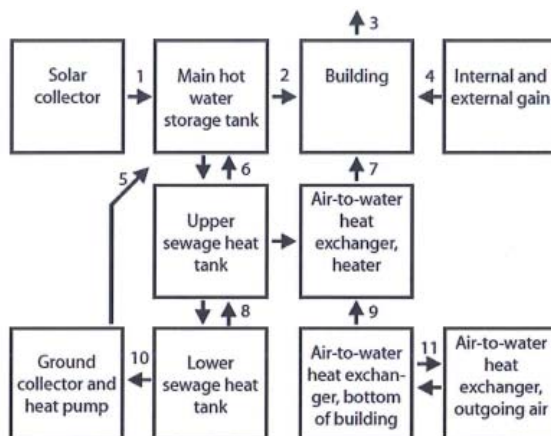


Fig. 2. Energy flow diagram.

The developed TRNSYS deck contains many different mathematical models used to describe the system. Some of the most important TRNSYS components are listed below together with the most important parameters for the specific component.

- Hot water load: 180 litres of 55°C water per day.
- Hot water profile: Simplification from measurements performed in Sweden⁽⁵⁾. The profile is shown in Fig 3.
- Sewage water: Twice the flow of hot water at 30°C. This means that the 55°C hot water was mixed with roughly the same amount of cold water.
- Main storage tank used for domestic hot water: TRNSYS Type 534, size 400 litres.
- Lower and middle tanks in Fig 1 used for sewage in system 4_hyb & 4_mech: TRNSYS Type 534, size 50 litres.
- Solar Collector: TRNSYS Type 832⁽⁶⁾, 12 m², tilt 70°.
- Building: TRNSYS Type 88, U-value 0.19 W/(m²K) i.e. a UA^(*) value of 62.7 W/K for this building, capacitance 40 MJ/K, ventilation rate 180 m³/hr, i.e. 0.5 ach^(**).
- Windows in the building: g-value^(***) 0.55, 6.5 m² glazed area on the south and the on west façades and 3.9 m² on the façades facing north and east.
- Heat Pump: TRNSYS Type 668, SPF (Seasonal performance factor) of 2.5 working between 5°C to 60 °C.
- Air-to-water heat exchangers: TRNSYS Type 5b, effectiveness 0.7.
- Mechanical ventilation: Temperature heat recovery efficiency 0.75, electrical energy use 1.12 W/(l/s).
- Weather data: TRNSYS Type 109, weather data from Malmö (-13.00°,55.58°) in the south of Sweden.
- Gains: The gains from people and electrical use was assumed to be 500 W throughout the year. Gains from the storage tanks and from solar radiation passing through the windows were added to the building.

(*) The UA value is the product of the U-value, i.e. the overall heat transfer coefficient, and the area, A, of the object. The unit for the U-value is W/m²K and the unit for A is m². Hence the unit for the UA value is W/K. The U-value gives the total thermal losses for e.g. a building as a function of the temperature difference between the indoor and the ambient temperature.

(**) The ach is the air change per hour. A value of 0.5 means that half of the air volume in the building is replaced by fresh air every hour.

(***) The g-value of a window is the fraction of incident solar radiation transmitted through a window as heat gain.

The natural ventilated systems are supplemented with a fan during periods with no wind and small heat differences between indoor and ambient temperature, giving a so-called hybrid system. For Systems 3_mech and 4_mech the ventilation fan is assumed to be running the full year. The electrical energy consumption for the fan was set to 1.12 Watts per l/s of air flow. This was the lowest energy consumption used by a mechanical ventilation system with heat recovery in a test performed by the Swedish energy agency⁽³⁾. The natural ventilated systems i.e. Systems 1, 2, 3_hyb and 4_hyb are estimated to run on thermal and wind driven forces 90% of the year. The estimation is built on wind and temperature data from Swedish climate. During the rest of the year a fan assists the ventilation. This fan is assumed to use the same power as the fan used in Systems 3_mech and 4_mech. In the calculation no attention was paid to cooling the building.

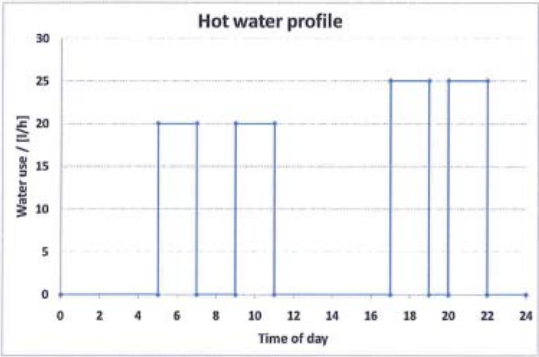


Fig. 3. The domestic hot water profile.

3. Results

Fig. 4 shows the annual auxiliary energy need for all of the systems. In black is the energy needed for the pumps and the fan. In grey is the auxiliary energy supplied to the heat pump. As can be seen the energy need for System 4_hyb is slightly lower compared to System 4_mech. This is largely due to the electricity consumption by the ventilation fan in System 4_mech.

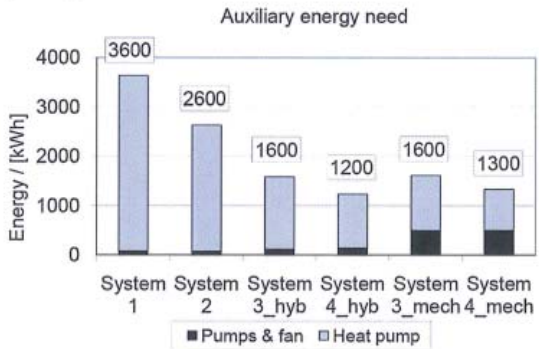


Fig. 4. The annual auxiliary energy need for the Systems.

Fig. 5 shows the monthly distribution of electrical auxiliary energy. The figure clearly shows that the best performing system during the winter months is System 4_mech. However, during the summer period, system 4_hyb consumes less energy compared to the other systems.

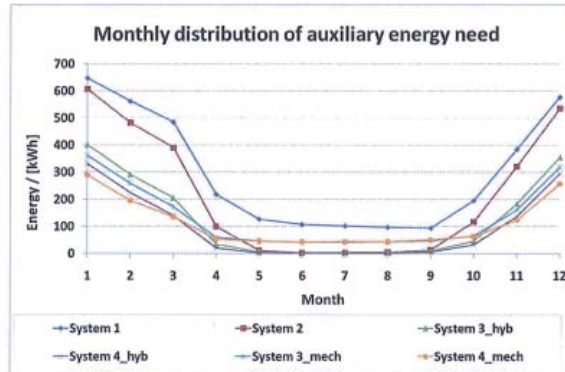


Fig. 5. Monthly distribution of electrical energy need.

Another way to look at the systems is to ask how different installations affect the energy performance. Assuming that System 3_hyb and System 3_mech exist without the solar energy systems, which alternative will save the most energy between an 8 m² solar collector tilted 45° or a sewage heat recovery unit? The results from this analysis can be seen in Fig. 6. Simulations for the naturally ventilated system are shown in grey. If it is supplemented with a solar collector, the annual auxiliary energy need is reduced with about 800 kWh. If it is supplemented with a sewage heat recovery system the annual auxiliary energy need is reduced with about 500 kWh. The figures are the same for the system using mechanical ventilation.

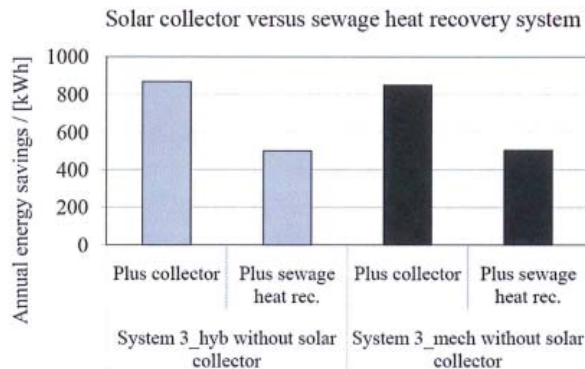


Fig. 6. The energy savings for System 3_hyb without a solar collector, in grey, and System 3_mech without a solar collector, in black.

4. Discussion and Conclusion

The main idea with the project was to study the possibility to construct a ventilation system that runs on the forces supplied by nature, i.e. thermal and wind forces, that compare well to a mechanical system. Such system has benefits apart from the lower electrical energy use. For instance the building can always be supplied with fresh air. This is not the case for a mechanical system that will stop in case of a power failure. At the same time natural ventilation has a low level of disturbing noise. However, naturally ventilated buildings normally result in a high energy consumption since heat recovery from the exhaust air is normally not present. The proposed system shows that it might be possible to construct a naturally ventilated system with a low annual auxiliary energy need. This was shown in Fig. 4. The main reason to this is that the high energy consumption by the electric fan is strongly reduced. Other advantages are that System 4_hyb uses the sewage tank more efficiently than System 4_mech. Heating the cold ventilation air in System 4_hyb lowers the temperature in the sewage tanks more than when the mechanical ventilation is used in System 4_mech. This is not an advantages in itself but it explains why System 4_hyb performs so well. Another advantage with the system is that since the warm humid exhaust air is heat exchanged with the brine, always above 0°C, there is no risk of frost. This is a problem for many mechanical ventilations systems with heat recovery. Of course the warm humid exhaust air can condense but this usually does not cause any problems. The result shown in Fig. 5 suggests that it would be interesting to combine the systems, e.g. using System 4_mech during the colder periods of the year and System 4_hyb during the warmer periods. This would however be costly since double systems would be needed. There is a possibility to use natural ventilation, e.g. by opening windows for cross ventilation, during the summer for System 3 & 4_mech. This alternative was however not investigated since the performance would be highly dependent on the user.

The system that represents the best investment for a new house is not accessed in this article. There are benefits and drawbacks with both systems. If one wants to take a step from System 2 to a more energy efficient building one can choose between mechanical ventilation and natural ventilation. If the mechanical system, System 3_mech, is chosen, the next step, to install a sewage heat recovery system, will lower the auxiliary energy need with around 300 kWh. If the natural ventilation, System 3_hyb, is chosen the energy savings will be around 400 kWh when installing the sewage heat recovery system. For a more complete conclusion from this analysis the economical figures also must be taken into account. Since this is just a prototype it is too early to make this kind of conclusions.

It is important to remember that the savings are carried out on a system supplied with a heat pump. The numbers would be much larger if the auxiliary energy was direct electricity or wood burning. The energy savings would be more evident if the systems were supplied only with electrical heat or wood burning. Since the heat pump in System 4_hyb and System 4_mech is a part of a system it was not possible to compare the different systems using for instance electrical heating.

5. Future work

There are many steps in product development and testing before this system can be improved into a marketable product. Some of the more critical points are the air change rate in the natural ventilated system and the heat exchanger in the sewage tanks. The difficulty with the air flow rate in the system is multi faceted. Not only is it a problem to ensure the required flow during the summer but it is also a challenge to avoid over ventilation during extremely cold or windy periods. An effective control mechanism is a necessity. The IEA Annex 35 on hybrid ventilation⁽⁷⁾ covers some of these questions. Most likely a combination of techniques will be needed to ensure good ventilation levels. This means that the driving

forces for the ventilation has to be both temperature and wind. There is also the possibility to use solar chimneys to enhance the driving force. The wind driven force can be increased with different types of ejectors⁽⁸⁾.

The sewage water tanks also have to be specially designed for the system. If care is not taken, fat from cooking, detergents etc. can stick to the heat exchangers. This will lead to a lower heat transfer rate and thus a lower efficiency in the system. There are however different techniques for cleaning the sewage water. For instance different kind of bio-filters⁽⁹⁾ can be used to clean the water before it is let into the sewage tanks.

In the future other alternatives of systems will be investigated. There are a large number of possible ideas to be tested. For instance, the ground collector can, if installed in such way, be used to provide free cooling of the building, which would then also help to restore heat to the cooled ground.

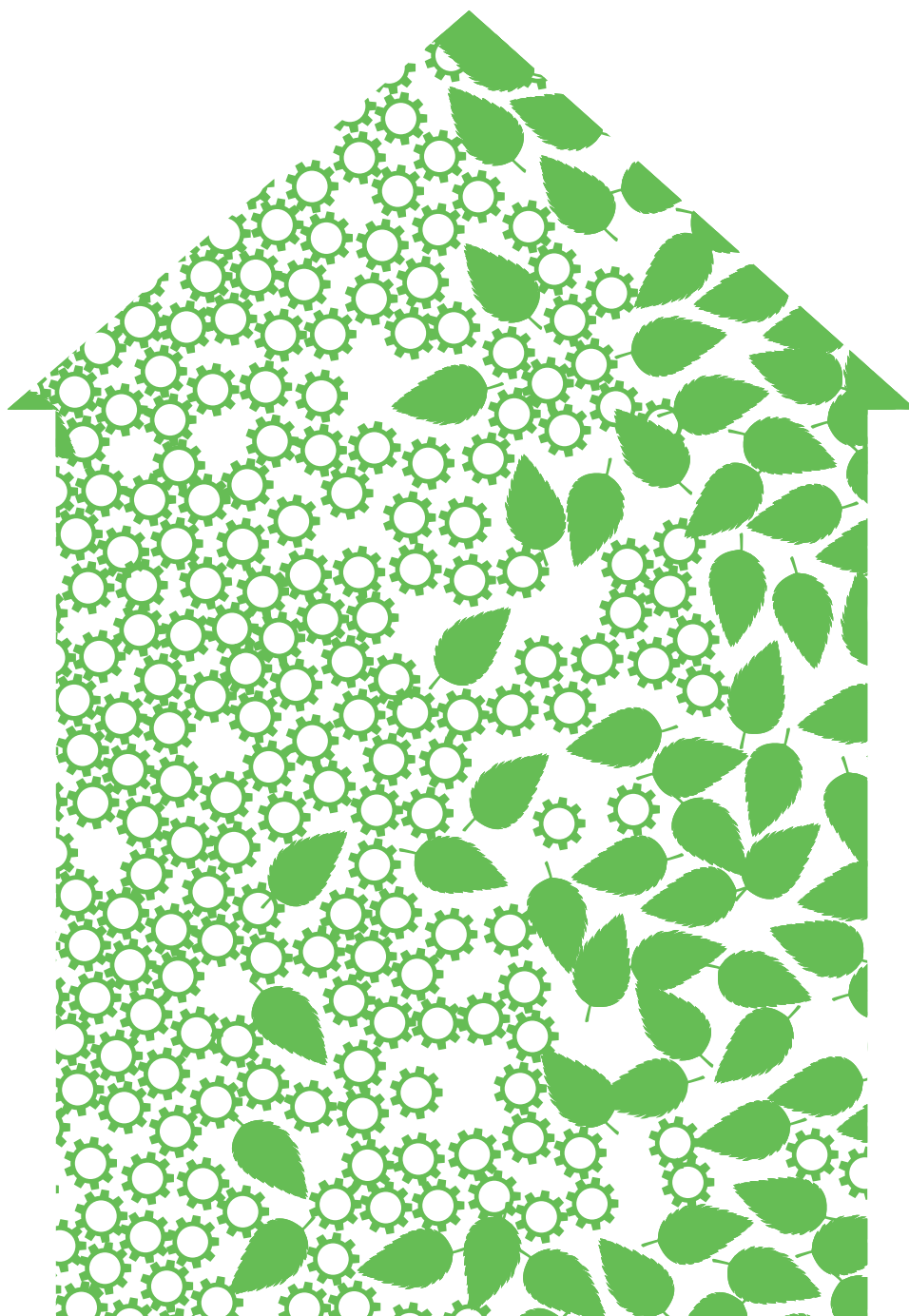
The results from the simulations presented in this article shows that the project is worth to be further investigated. The next step in this project is to construct the different parts needed in the system and proceed with a detailed economic analysis.

Acknowledgement

We acknowledge Bengt Perers at DTU in Lyngby, Denmark and Björn Karlsson and Bengt Hellström and at Energy and Building Design, Lund University in Sweden. This work is the revision and extension of the paper in RE2010 International Conference in Yokohama with the paper number 0347. The opportunity is gratefully acknowledged.

References

- (1) IPCC, Climate Change 2007: Synthesis Report Summary for Policymakers. (online) available from http://www.ipcc.ch/pdf/assessment-report/ar4/syr/ar4_syr_spm.pdf (accessed 2010-11-22)
- (2) Aleklett, K. Peak oil and the evolving strategies of oil importing and exporting countries. Discussion paper No 2007-17. (online) available from international transport forum <http://www.internationaltransportforum.org/jtrc/DiscussionPapers/DiscussionPaper17.pdf> (accessed 2010-11-22)
- (3) Energimyndigheten (Swedish Energy Agency), Test results, (online) available from <http://www.energimyndigheten.se/sv/Hushall/Tester/Testresultat/FTX-aggregat-hus-med-130-m-boyta/?productGroupId=69&productCompareList=412,413,414,415,416,417,419> (accessed 2010-11-29), only in Swedish.
- (4) S.A. Klein, et al. *TRNSYS program manual*, 2000
- (5) M. Lundh et al. Constructing load profiles for household electricity and hot water from time-use data—Modelling approach and validation. *Energy and Buildings* **41**, 7, July 2009, pp 753-768
- (6) Bernardo, L. R., Davidsson, H. and Karlsson, B., Performance Evaluation of a High Solar Fraction CPC-Collector System. Proceedings of Eurosun 2010.
- (7) IEA Annex 35, (online) available from <http://hybvent.civil.auc.dk/> accessed 2010-11-29
- (8) N. Khan et al. A review on wind driven ventilation techniques. *Energy and Buildings* **40** (2008), pp 1586-1604
- (9) Aquatron, Bio-Box, (online) available from <http://www.aquatron.se/BIO-BOX.php>, (accessed 2010-11-29), only in Swedish.



LUND
UNIVERSITY

Report No EBD-T--14/18
ISBN 978-91-85147-56-4
ISSN 1651-8136